National Aeronautics and Space Administration

ARTEMIS II

PRELIMINARY LUNAR SCIENCE REPORT



nasa.gov

Artemis II Lunar Science Leadership Team	
Lunar Science Lead	Dr. Kelsey E. Young[1]
Deputy Lunar Science Leads	Dr. Jacob A. Richardson[1]
	Dr. Marie J.B. Henderson[2,1]
Science Operations Lead	Dr. Kelsey Young[1]
Lunar Science Lead Support	Kiarre Dumes[3]
Data and Software Lead	Dr. Matthew Miller[4,3]
Data Archiving Lead	Dr. David M. H. Baker[1]
Science Themes Lead	Dr. Ariel N. Deutsch[5,6]
Tools/Timeline Lead	Dr. Cherie N. Achilles[1]
Crew Geology Training Lead	Dr. Cynthia Evans[3]
Crew Lunar Observations Lead	Sara E. Schmidt[3]
Science Officers	Dr. Kelsey Young[1]
	Angela Garcia[3]
	Trevor G. Graff[3]

Artemis II Lunar Science Operations Team		
Lunar Science Team	**Crew Lunar Observations**	**Asset Managers**
Dr. Maria Banks[1]	Alex H. Stoken[4,3]	Ryan Bieber (Co-Lead)[4,3]
Dr. Megan Borel[2,1]	Cody Boyer[4,3]	Marco A. Lozano (Co-Lead)[4,3]
Dr. Barbara A. Cohen[1]	David Charney[4,3]	Luke McSherry[4,3]
Dr. Anthony Colaprete[6]	Jared R. Ralleta[5,6]	Michael McLehany[4,3]
Alexandra Constantinou[4,3]	Wilfredo A. García López[4,3]	Pedro Sanchez[4,3]
Dr. Ryan Ewing[3]		Daniel Thomas[4,3]
Ben Feist[4,3]	**Staffing/Logistics Coordinators**	
Dr. Juliane Gross[3]	Andrea Wenzel (Co-Lead)[4,3]	
Dr. Jennifer L. Heldmann[6]	Madeline Walker (Co-Lead)[4,3]	**Communications**
Dr. José Miguel Hurtado, Jr.[4,3]	Abigail Cantoni[4,3]	Molly Wasser (Lead)[12,7]
Dr. Andrew Needham[1]		Rachel Barry[9,3]
Dr. Debra H. Needham[7]		Caela Barry[8,1]
Dr. Noah Petro[1]		Staci Horvath[8,1]
Dr. Aaron B. Regberg[3]		Erin Morton[11,7]
Amber A. Turner[8,1]		Victoria Segovia[3]
Dr. Ryan Watkins[7]		Lonnie Shekhtman[8,1]
Ernest T. Wright[13,1]		Daniel Gallagher[10,1]

[1] NASA's Goddard Space Flight Center
[2] University of Maryland, Baltimore County
[3] NASA's Johnson Space Center
[4] Amentum
[5] Bay Area Environmental Research Institute
[6] NASA's Ames Research Center
[7] NASA Headquarters
[8] ADNET Systems Inc.
[9] Barrios Technology
[10] Abacus Technology Corporation
[11] ASRC Federal
[12] PCI Productions
[13] Science and Technology Corporation

TABLE OF CONTENTS

FOREWORD 8

1.0 MISSION CONTEXT AND LUNAR SCIENCE OPERATIONS OVERVIEW 10
1.1 Lunar Science Objectives 10
1.2 Mission and Science Observation Timelines 12
1.3 Exploration Capability Objectives 14

2.0 CREW PERSPECTIVES 15

3.0 SCIENCE DEVELOPMENT 16
3.1 Lunar Science Team Development 16
3.2 Crew Science Data Collection Plan 16
3.2.1 Crew Imaging Plan 17
3.2.2 Crew Camera Settings 20
3.2.3 Window Quality Observations 21
3.3 Vehicle Science Data Collection Plan 21
3.4 Crew Training in Support of Lunar Science 24
3.5 LST-Developed Crew Flight Products 25
3.6 Pre-Launch Science Planning 26
3.7 In-Flight Science Planning 27

4.0 LUNAR SCIENCE DATA SUMMARY 29
4.1 As-Executed LTP Observations 29
4.2 Types and Volumes of Data Collected 29

5.0 SCIENCE DISCUSSION 32
5.1 Impact Flash Observations 33
5.1.1 Characterizing Impact Events 33
5.1.2 Impact Flash Observations 34
5.2 Color Provinces and Albedo Variations 35
5.2.1 Color/Albedo Associated with Different Physical and Compositional Properties 37
5.2.2 Albedo Anchors Used for Orienteering and Comparisons 39
5.2.3 Color/Albedo Under Earthshine 40
5.2.4 Comparisons of Color/Albedo Between the Earth and the Moon 43
5.3 Photometric Observations 45
5.3.1 Changes in Color/Albedo Variation 45
5.3.2 The Opposition Effect 46
5.3.3 The Evolution of the Crew's Perception of Grimaldi 46
5.4 Impact History 47
5.4.1 Features of Impact Structures 49
5.4.2 Geologic Relationships 49
5.4.3 Features of Young Crater Systems 50
5.4.4 Discussion of Specific Impact Features 51
5.4.4.1 Orientale Basin 51
5.4.4.2 Vavilov Crater 55
5.4.4.3 Glushko Crater 57
5.4.4.4 Sundman J Crater 58

5.4.4.5 Pierazzo and Byrgius A Craters . . . 59
5.4.4.6 Ohm Crater . . . 60
5.4.4.7 Carroll and Integrity Craters . . . 61
5.5 Lunar Environment and Deep Space . . . 61
5.5.1 The Lunar Dust Environment . . . 62
5.5.2 Deep Space . . . 63
5.5.3 Solar Structures . . . 65
5.6 Tectonic History . . . 66
5.6.1 Regional-Scale Fault Complexes . . . 67
5.6.2 Floor-Fractured Craters . . . 69
5.6.3 Massifs of Non-Volcanic Origin . . . 69
5.7 Future Sites and Poles . . . 70
5.7.1 Regional Context of Past Landing Sites . . . 70
5.7.2 Regional Context of Future Landing Sites . . . 70
5.7.2.1 Reiner Gamma . . . 71
5.7.2.2 Aristarchus Plateau . . . 72
5.7.3 The Polar Regions . . . 74
5.8 Limb and Terminator Morphology . . . 75
5.8.1 The Lunar Limb and Horizon . . . 75
5.8.2 The Lunar Terminator . . . 78
5.9 Volcanic History . . . 81
5.9.1 The Variety of Mare Volcanism . . . 82
5.9.2 The Variety of Non-Mare Volcanism . . . 84
5.9.3 Signs of Cryptomaria . . . 87
5.10 Earth Observations from Deep Space . . . 88
5.10.1 Earth's Atmosphere . . . 89
5.10.2 Earth's Surface . . . 93

6.0 COORDINATED OBSERVATIONS . . . 93
6.1 Lunar Reconnaissance Orbiter . . . 93
6.1.1 LRO Data Products of Select Crew-Targeted Features from Pre-Existing LRO Observations . . . 94
6.1.2 LRO Real-Time Imaging of Orion During the Lunar Flyby . . . 94
6.1.3 LRO Observations Acquired During the Time Surrounding the Artemis II Lunar Flyby to Complement Crew Science Observations . . . 96
6.2 Impact Flash Citizen Science Campaign . . . 97
6.3 Additional Coincident Lunar Data Collection . . . 97

7.0 CONSTRAINTS ON SCIENCE IMAGES AND OBSERVATIONS . . . 98
7.1 Window Quality Observations . . . 98
7.2 Effects of the Orion Cabin Environment on Science Observations . . . 99
7.3 Spatial Resolution of Surface Features with Unaided Human Eyes . . . 101
7.4 Comparison of Handheld Cameras as Science Tools . . . 102
7.5 Comparison of Image Quality Between SAW Camera Stills and Video Frames . . . 104
7.6 Photogrammetric Analysis . . . 104

8.0 HUMANS IN LUNAR SCIENCE AND EXPLORATION 105
8.1 Science Synergies of Data Types 106
8.2 Importance of Crew Science Discussions 108

9.0 RECOMMENDATIONS 110
9.1 Science as a Key Mission Component and Outcome 110
9.2 LST-Crew Collaboration 111
9.3 Scientific Crew Training 112
9.4 In-Mission LST to Crew Communications 113
9.5 Science Planning and Preparation 113
9.6 Calibration of Cameras 114
9.7 Instrumentation for Enhanced Science Return 114
9.8 Window Design for Science Observations 115
9.9 Crew-Audio Recording Capabilities and Time Synchronization of Multi-Modal Datasets 116

10.0 CONCLUSIONS 117

ACKNOWLEDGEMENTS 118

REFERENCES 119

APPENDIX 1: LUNAR TARGETING PLAN 127

APPENDIX 2: SCIENCE DATA ARCHIVE AND ACCESS 128

APPENDIX 3: ABBREVIATIONS 129

LIST OF TABLES

Table 1.1: Science Themes, Objective, and Priorities.. 11

Table 3.1: Camera Specifications. 20

Table 4.1: Science Data Summary. 31

Table 5.1: Evolution of Earthshine's Extent 42
Table 5.2: Polar Visibility. 73

Table A.1: PDS Archives. Archive URLs and citations for the PDS-wide search and for individual PDS Nodes. 128

LIST OF FIGURES

Figure 1.1: Artemis II Flight Profile 12
Figure 1.2: Orion Ground Track 13
Figure 1.3: Flyby Point-of-View Details 14
Figure 1.4: Visible Lunar Surface 14

Figure 3.1: Crew Opportunistic Imaging Plan 17
Figure 3.2: Crew Flyby Imaging Plan 18
Figure 3.3: Lunar Mosaics 19
Figure 3.4: Orion Windows. 21

Figure 3.5: Orion Imagery System . . . 22
Figure 3.6: Vehicle Imaging Plan . . . 23
Figure 3.7: The Lunar Targeting Plan . . . 26
Figure 3.8: LTP Targets . . . 28

Figure 4.1: As-Executed Timeline . . . 30
Figure 4.2: Distribution of Image Footprints by Focal Length . . . 32

Figure 5.1: Impact Flash Annotation . . . 35
Figure 5.2: Lunar Color and Albedo Variations . . . 36
Figure 5.3: Orientale Basin Seen By Multiple Instruments . . . 37
Figure 5.4: Earthshine on the Moon . . . 40
Figure 5.5: Tonality of the Moon . . . 41
Figure 5.6: Earthshine Views . . . 42
Figure 5.7: Earthset and Earthrise . . . 44
Figure 5.8: Grimaldi and Orientale Maria . . . 48
Figure 5.9: Orientale Basin. . . . 51
Figure 5.10: Orientale Views from Orion . . . 52
Figure 5.11: Orientale Sketch . . . 52
Figure 5.12: Orientale Ejecta . . . 54
Figure 5.13: Vavilov Crater . . . 55
Figure 5.14: Glushko Crater . . . 57
Figure 5.15: Sundman J and Glushko Craters . . . 59
Figure 5.16: Pierazzo and Byrgius A Craters . . . 60
Figure 5.17: Ohm Crater . . . 61
Figure 5.18: Proposed Carroll and Integrity Craters . . . 62
Figure 5.19: Deep Space . . . 64
Figure 5.20: Vehicle Views of The Eclipse . . . 65
Figure 5.21: The Solar Corona . . . 66
Figure 5.22: Vehicle Views of Sunrise and Sunset . . . 67
Figure 5.23: Iluminated Lunar Disk . . . 67
Figure 5.24: Curvilinear Features . . . 69
Figure 5.25: Rimae Repsold . . . 70
Figure 5.26: Limb Observations . . . 71
Figure 5.27: Past Landing Sites . . . 71
Figure 5.28: Reiner Gamma . . . 72
Figure 5.29: Aristarchus Plateau . . . 73
Figure 5.30: Polar Visibility . . . 73
Figure 5.31: Orientale on the Limb . . . 76
Figure 5.32: Sunset Behind the Limb . . . 77
Figure 5.33: Shadows of Lunar Topography . . . 78
Figure 5.34: The Terminator . . . 78
Figure 5.35: South Polar Terminator. . . . 79
Figure 5.36: Hertzsprung and Vavilov along the Terminator . . . 80
Figure 5.37: Volcanic Targets . . . 81
Figure 5.38: Aristarchus Mineralogy . . . 81
Figure 5.39: Nearside/Farside Transition . . . 84

Figure 5.40: Aristarchus Mineralogy 85
Figure 5.41: Orientale Annular Ring 87
Figure 5.42: Hello, World. 88
Figure 5.43: Earth's Storms 90
Figure 5.44: Saharan Dust 91
Figure 5.45: Cloud Migration 91
Figure 5.46: Earth's Terminator 92

Figure 6.1: LRO Views of Orientale 95
Figure 6.2: Space Station Views of the Moon 98

Figure 7.1: Rimae Sirsalis 102
Figure 7.2: An Apollo and an Artemis Earth 103
Figure 7.3: Vehicle Lunar Views 104
Figure 7.4: Photogrammetry Renders 105

Figure 8.1: Camera Comparisons 107
Figure 8.2: Synergistic Data 108

About the Cover

Earth setting behind the ancient farside terrain of the Moon. As the Artemis II crew flew around the lunar farside, the silver-blue crescent of Earth showing the deep-colored Australian continent came into view before passing behind the terrain of the lunar limb. Shadows from the glancing Sun reveal billions of years of impact cratering in the lunar farside's northern hemisphere, including crater chains (catenae) that permanently scoured the terrain during the Orientale basin impact event.

Report Design by NASA's Goddard Space Flight Center Publication & Design Group
Layout Design: Ruth Jennings
Graphic Artist: Heather Ghannadian
Technical Editor: Chris Fleming

FOREWORD

The *Artemis II Preliminary Lunar Science Report* marks the first report of crewed science activities conducted beyond low Earth orbit in more than half a century. The science investigations enabled by the Artemis II lunar flyby, and executed by its trained crew, are synthesized here, just as was done during the Apollo program and will be done for future Artemis missions. This document is preliminary in nature; while it documents initial science discussions from crew observations, the science return from Artemis II will continue to expand as mission science data become publicly available to the broader community.

The lunar science observations made during Artemis II were accomplished by four crew members, each of whom developed expertise in lunar geography, geology, and observational best practices through rigorous training in classrooms, simulations, and field environments. These four explorers—Commander Reid Wiseman, Pilot Victor Glover, and Mission Specialists Christina Koch and Jeremy Hansen—observed lunar terrains never before seen directly by humans. Like their Apollo 8 and Apollo 10 forebearers, whose missions also primarily focused on orbital observations for lunar science, the Artemis II crew shared new perspectives of the Moon and outer space from viewpoints new to humanity. In flight, the crew became the 25th through 28th people in history to view the Moon from above the lunar farside. This achievement was made possible by a diverse, interdisciplinary team of thousands of people who worked on the development and execution of the mission and helped pave the way for crewed science to be performed on and around the Moon in the twenty-first century.

Team members from multiple NASA Centers staffed the Artemis II Lunar Science Team (LST) in support of the mission's lunar science and exploration capability objectives. With community support, the LST developed training, lunar science planning and implementation processes, and assisted in the development of two new science facilities at NASA's Johnson Space Center—the Science Evaluation Room (SER) in the Mission Control Center (MCC) and the Science Mission Operations Room (SMOR)—as well as development and implementation of the SCIENCE flight controller position, staffed by Science Officers. In flight, the LST developed the crew's scientific observation plan for the lunar flyby, supported crewed science activities, prepared the crew for the lunar flyby, managed science data return from space, and analyzed initial data return. The LST's Science Officers supported real-time activities within the MCC Flight Control Room and communicated directly with the crew in-flight to provide observational guidance during the flyby and lead a post-flyby science discussion.

It should be noted that the LST was not initiated or integrated with the mission until approximately two and a half years prior to launch; this was significantly after the bulk of the mission team had been established. As opposed to traditional science teams working on missions led by NASA's Science Mission Directorate (SMD), SMD tasked the LST with weaving lunar science around an existing mission and its pre-defined trajectory and hardware constraints. The central priority of the Artemis II mission was testing life support systems and spacecraft performance during the first crewed flight of the Orion vehicle and returning the crew safely home. This report explains the integration of science into Artemis II, and how the LST took advantage of the mission parameters established well before the LST existed to maximize lunar science return from this historic test flight. Despite the mission not being developed and flown solely for science, the dedication and commitment of the crew, the Flight Control Team (FCT), the Orion team, and the LST yielded a dataset that can complement existing lunar datasets. This important expansion is another tool in the toolbox for planetary scientists seeking to unravel the mysteries and history of our closest celestial neighbor. This report's companion document, the *Artemis II Lunar Science Operations Report*, describes how the LST was structured, how lunar science was woven into the fabric of mission operations, and provides recommendations on how future human spaceflight mission science teams can maximize science return and efficiency.

The primary purpose of this *Artemis II Preliminary Lunar Science Report* is to document the planning process and execution of lunar science observations, as well as provide initial discussion of the mission's science data. This report is one of four publications required from the LST by NASA Headquarters within six months post-mission, alongside an archive of mission science data in the NASA Planetary

Data System (PDS). The other three publications are the (1) *Artemis II Lunar Science Operations Report*, (2) *Artemis II Open Science Data Management Plan (OSDMP)*, and (3) *Artemis II Lunar Science Data User Guide*. Together, these four publications provide a scientific overview of Artemis II mission data and activities, and a technical summary of how the science plan was developed and implemented. LST responsibilities for science integration pre- and post-mission included developing the lunar science objectives, maximizing opportunities through mission planning and execution to collect data to address these objectives, and then providing an assessment and initial discussion, via this document, of the science data related to these objectives. By providing these data and reports, the LST hopes to provide a foundation from which the broader scientific community can access and utilize the data for a wealth of science investigations. The term *Preliminary Science Report* follows the nomenclature established during the Apollo program, when NASA published mission-specific reports after each flight to document initial scientific observations and findings (NASA, 1969, 1970, 1971, 1972a, 1972b, 1973). For Artemis II, the term "preliminary" similarly describes the timing and nature of results presented, recognizing that further analysis and scientific publications will continue independently.

This report begins with an overview of lunar science objectives (**Section 1**) and perspectives penned by the Artemis II crew (**Section 2**). Next, the report includes details about how the Artemis II LST planned the execution of lunar science objectives (**Section 3**) and a summary of collected lunar science data (**Section 4**). Preliminary discussions of lunar science data and findings are presented in **Section 5**, guided by the Artemis II lunar science objectives. These discussions vary in level of detail, reflecting the variety of data collected within the constraints of the Artemis II mission profile (e.g., what portions of the lunar surface were illuminated during the lunar flyby). By documenting (1) the science intent that drove the development of the observation plan, (2) the nature of the data acquired, and (3) the operational context in which those data were collected, this report is intended to support transparency and enable the broader science community to continue scientific analysis of Artemis II data. The report then includes discussions of cross-mission observation coordination (**Section 6**), constraints on science imaging and observations (**Section 7**), and the value of humans in lunar science and exploration (**Section 8**). Finally, the report includes recommendations developed by the LST to improve and support science investigations in future Artemis missions (**Section 9**), followed by conclusions (**Section 10**). Appendices provide a summary of the flyby science plan (**Appendix 1**), an inventory of the science data for the mission (**Appendix 2**), and a list of abbreviations used in this report (**Appendix 3**).

Artemis II has been a mission defined by historic firsts, remarkable achievements, and a global connection to the Moon. As we venture forward to the Moon together, we—as members of this first Artemis Lunar Science Team—hope that the inspiration and Moon joy of Artemis II endures. As new analyses of Artemis II data are undertaken, we challenge the next generation of scientists and explorers to build upon the early discoveries presented here and to expand our understanding of the Moon and our place within the broader universe.

1.0 MISSION CONTEXT AND LUNAR SCIENCE OPERATIONS OVERVIEW

Artemis II marked humanity's return to lunar space in more than 50 years, heralding the beginning of a new era of crewed planetary exploration. First and foremost, Artemis II was a test flight, designed to launch humans on the Space Launch System (SLS) rocket for the first time, test the crewed performance of the Orion spacecraft (named *Integrity* by the Artemis II crew), and return the crew safely home through splashdown in the Pacific Ocean. The mission scope is analogous to that of Apollo 8, in that Artemis II marked the first mission in a new human spaceflight campaign to send astronauts around the Moon to prepare for future lunar landed missions. In the decades since Apollo 8, our knowledge of the Moon has substantially expanded, thanks to the Apollo missions and the decades of orbital and landed missions that followed. Accordingly, the Artemis II lunar science objectives and observational plan ultimately executed by the crew, FCT, and LST were developed and prioritized to take advantage of the unique profile of the Artemis II mission, while being responsive to the priorities of the lunar and planetary science community (National Research Council, 2007; LEAG, 2016; NASA, 2020, 2022; National Academies, 2022).

The LST designed the mission's science campaign to leverage the unique capabilities of human observation and complement the extensive lunar and planetary science datasets acquired over decades of instrumentation-driven exploration, while simultaneously designing processes, protocols, procedures, and structures for integrating lunar science into the Artemis operational framework (see the companion *Artemis II Lunar Science Operations Report* for details). Human visual systems can offer a substantially greater dynamic range, enhanced depth perception, and more nuanced color discernment than previously flown, robotic camera systems. When paired with the cognitive abilities of the human brain, including intuitive spatial judgment, pattern recognition, and rapid comparative assessment, human visual observations become a powerful tool for interpreting other worlds and guiding scientific inquiry. As a result, crew observations provide valuable contextual insight that enriches the existing wealth of robotically acquired datasets that help inform science questions for future missions.

Artemis II also flew separate investigations led by the Human Spaceflight Mission Directorate (HSMD) Human Research Program (HRP) and SMD's Biological and Physical Sciences (BPS) division. Three HRP investigations examined the crew's' physiology and behavioral responses to deep spaceflight; results will help NASA keep crews safe and healthy on future deep space missions. The BPS investigation leveraged Orion's microgravity and space radiation environment to study human biology and cellular responses in deep space through flying microfluidic devices containing living human cells. The Johnson Space Radiation Analysis Group (SRAG) flew a radiation monitor within the Orion vehicle. The radiation data will be used to address deep space environmental science objectives of SMD's Heliophysics Division (HPD). These investigations were managed independently of the LST's campaign and are outside the scope of this report.

1.1 Lunar Science Objectives

Artemis II lunar science plans were developed by the LST and anchored by a science traceability matrix (STM) approved by NASA's SMD in October 2024. The STM has ten themes and 22 supporting objectives (**Table 1.1**) that address overarching agency and community lunar science goals (National Research Council, 2007; LEAG, 2016; NASA, 2020, 2022; National Academies, 2022). The Artemis II STM was built on the principle that a unique human perspective of observing the entire lunar disk from a distance will complement existing lunar data. The science themes were prioritized based on the science achievable in the unique mission architecture of Artemis II.

- **Priority 1:** Science objectives that humans can uniquely contribute to at the Moon (Themes: Impact Flashes, Color Provinces and Albedo Variations).
- **Priority 2:** Science objectives accomplishable under a wide range of illumination conditions (Themes: Photometric Observations, Impact History, Lunar Environment and Deep Space, Tectonic History, Future Sites and Poles).

- **Priority 3:** Science objectives accomplishable under specific, favorable viewing conditions (Themes: Limb and Terminatory Morphology, Volcanic History, Earth Observations).

The STM was the guiding document used in the creation of the lunar targeting plan (LTP) (**Sections 3.5**, **3.6**), which provided the crew with multiple continuous hours of science activities. These activities focused on lunar, Earth, and deep space targets that traced to the STM themes and objectives, as the crew were asked to image and discuss several targets while addressing questions about scale, color, albedo, texture, patterns, and geologic relationships. The LTP was designed to achieve a balance of STM broad coverage (with at least one target to address each objective, if possible, given the trajectory) and STM depth (with multiple targets to emphasize high-priority and/or cross-cutting themes). LTP targets (**Appendix 1**) included the whole Moon as a system, as well as specific lunar surface targets and targets selected by the crew live during the flyby.

Table 1.1: Science Themes, Objectives, and Priorities. The ten lunar science themes and their accompanying science objectives, which built the foundation of the Artemis II STM. Theme priorities were developed by the LST and approved by NASA's SMD in response to the Artemis II mission profile. The complete Artemis II STM also included observables, data types (observations, images, annotations), crew observational and imaging activities, observational requirements (e.g., illumination constraints), and traces to high-priority science goals identified in NASA's Moon to Mars Objectives (NASA, 2022), the Decadal Strategy for Planetary Science and Astrobiology 2023–2032 (National Academies, 2022), and the Artemis III* Science Definition Team Report (NASA, 2020). *Note: At the time this report was produced, Artemis III referred to the first planned landed mission, but mission numbering has since been revised.

Science Theme	Science Objectives	Priority
Impact Flashes	• Characterize impact events observed by the crew.	1
Color Provinces and Albedo Variations	• Characterize color/albedo associated with different physical properties. • Characterize color/albedo associated with different geochemical/compositional properties.	1
Photometric Observations	• Describe changes in spatial and temporal scales of color/albedo variations.	2
Impact History	• Characterize features of impact structures. • Characterize features of young crater systems. • Characterize ejecta interactions with surrounding features.	2
Lunar Environment and Deep Space	• Determine whether lofted lunar dust is identifiable from lunar orbit that would allow for the characterization of the lunar exosphere environment. • Characterize deep space.	2
Tectonic History	• Characterize region-scale fault complexes including relationships (e.g., cross-cutting) with surrounding features. • Characterize floor-fractured craters. • Characterize massifs.	2
Future Sites and Poles	• Characterize the regional context for past landing sites. • Characterize the regional context for potential future landing sites. • Characterize polar regions.	2
Limb and Terminatory Morphology	• Characterize the lunar limb, surface features along the limb, and the horizon. • Characterize surface features at the lunar terminator.	3
Volcanic History	• Characterize the variety of mare volcanism. • Characterize the variety of non-mare volcanism. • Determine if cryptomaria are identifiable from orbital data.	3
Earth Observations	• Characterize Earth's atmosphere. • Characterize Earth's surface.	3

1.2 Mission and Science Observation Timelines

Artemis II launched at 22:35 UTC on April 1, 2026, arrived at lunar pericynthion at 23:01 UTC on April 6, and splashed down in the Pacific Ocean at 00:07 UTC on April 11 (**Figure 1.1**). During the 10-day mission, the crew made scientific observations of Earth, the Moon, the Sun, and other features in outer space at scheduled and serendipitous times. Scheduled lunar science observations were made during the 6.75-hour lunar flyby and during 15- to 30-minute opportunistic lunar imaging events, when Orion windows were purposefully pointed at the Moon within 72 hours of the lunar flyby, before and after the flyby. Serendipitous science observations were made throughout the 10-day mission, when the Earth, the Moon, or the Milky Way were visible to the crew from the Orion windows, whether observation-enabling spacecraft pointing was intentional for science or not.

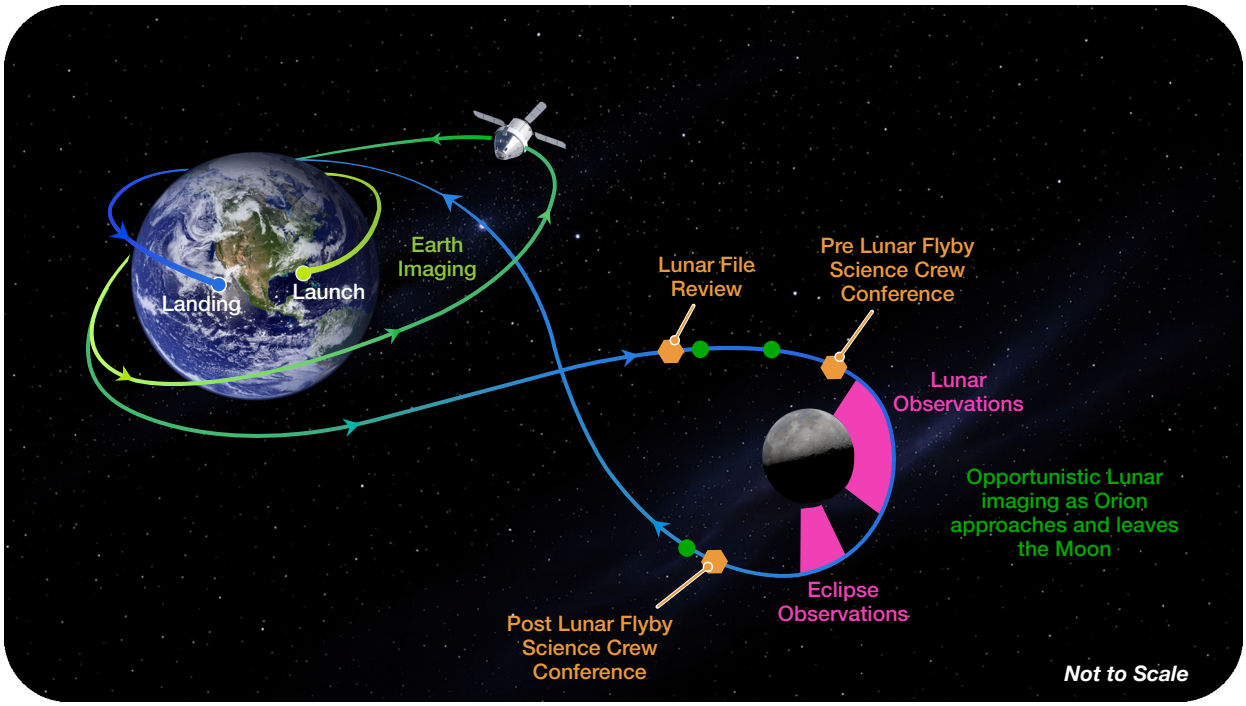


Figure 1.1: Artemis II Flight Profile. Schematic of the Artemis II mission flight profile, annotated with LST mission milestones. The green trajectory indicates the time period prior to the trans-lunar injection burn, while the blue trajectory indicates the flight path after.

Lunar flyby observations started at 18:45 UTC on April 6, 2026, and concluded at 01:30 UTC on April 7 (**Figure 1.2**). Due to the April 1 launch date, the crew had an opportunity to view an eclipse of the Sun by the Moon during the lunar pass. To optimize spacecraft performance while maximizing science impact during this hour-long eclipse, the flyby was segmented into two observation periods. The first observation period included observations and data collection of Sun-illuminated regions of the Moon (**Figure 1.3**) and a 40-minute lunar farside closest-approach pass bookended by earthset (22:43 UTC) and earthrise (23:22 UTC). During this farside pass, Orion arrived at a pericynthion distance of 6,544 km (23:01 UTC), where the lunar disk appeared to be 24.2° in diameter to the crew, about 2,300 times larger by area than its size as viewed from Earth. Immediately after earthrise, the spacecraft was reoriented to a tail-to-Sun posture for about one hour during which the Moon was not visible outside the Orion windows to optimize thermal and power performance of the spacecraft.

The second observation period started when the Orion spacecraft was reoriented to enable lunar viewing during a period when the Moon passed in front of the Sun. This eclipse period occurred between 00:34 and 01:30 UTC on April 7, 2026, and included opportunities to view phenomena in

the Solar System, as well as a nearside Moon that, from the crew's perspective, was in a waxing phase and illuminated only by earthshine. Sunrise at 01:30 UTC concluded the science observation period of the lunar flyby.

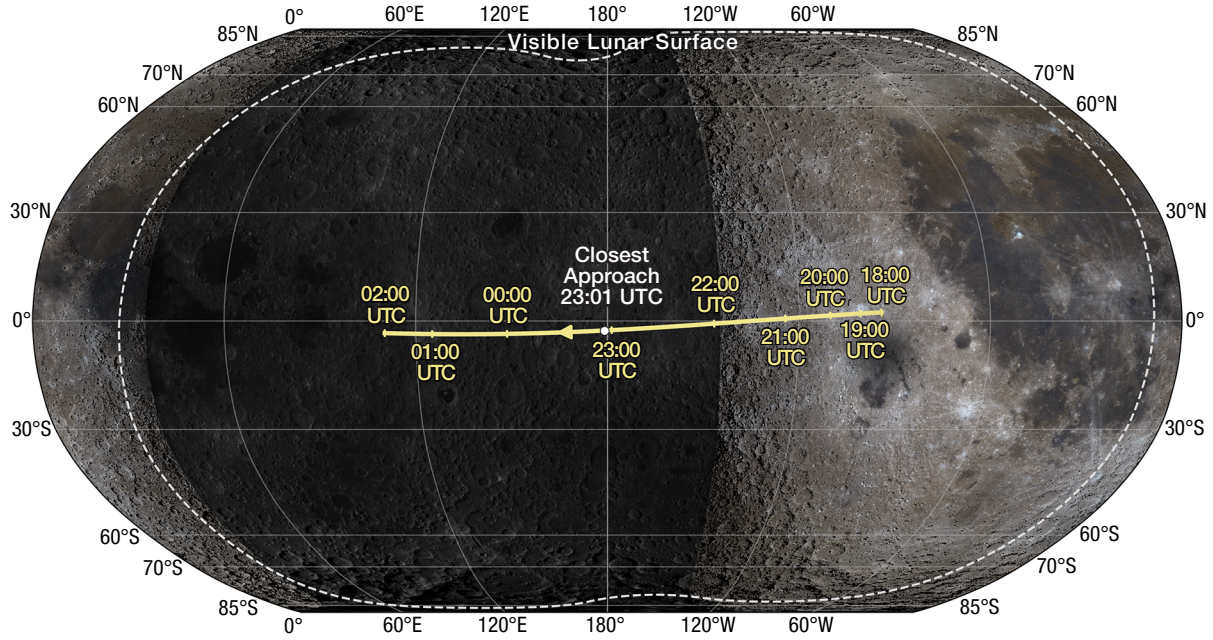


Figure 1.2: Orion Ground Track. The spacecraft moved (see arrow direction) from west (right) to east (left) during the course of the flyby, and had a slightly southernly trending groundtrack, such that more northern latitudes were visible at the beginning of the flyby and more southern latitudes were visible toward the end (illumination agnostic). The area within the white dashed line was visible to the Artemis II crew during the lunar flyby period, based on the position of the Orion spacecraft. The darkened area (bounded between ~35°E and ~145°W) indicates the non-sunlit area at 22:00 UTC, the approximate midpoint of the flyby. The white dot indicates sub-spacecraft point at closest approach. Map uses Robinson projection and simulated illumination conditions for a hillshaded terrain at center of flyby (22:00 UTC).

The Artemis II mission trajectory enabled the crew to observe virtually the entire lunar disk in a single view—a rare perspective of the lunar surface seen briefly by Apollo crews near the Moon but not in orbit. Observing the entire lunar disk provides body-wide spatial context that enables instantaneous regional comparisons and interpretation of large-scale geologic patterns and relationships. During the more than six-hour lunar flyby, the Orion spacecraft was oriented so its forward windows were facing the lunar surface. The altitude of Orion ranged between 17,040 km at 18:45 UTC (start of flyby observations) and 6,544 km at 23:01 UTC (closest approach).

Lighting conditions during the Apollo missions and Artemis II varied significantly, which affected the lunar surface features visible to each mission's crew. The Apollo landed missions required optimal lighting of the lunar surface for navigation on approach to landing sites. Thus, Apollo mission illumination constraints dictated that the Sun be between 5° and 20° above the eastern horizon (behind the lander at the time of landing). As a result, all Apollo landings took place during local early morning at each landing site; therefore, significant areas of the Moon's western hemisphere, including Orientale basin and other features at a similar longitude, were never seen in sunlight by human eyes at any time during those missions (**Figure 1.4**). In contrast, illumination of the lunar farside was not a requirement for the Artemis II launch window. At the start of the lunar flyby on Flight Day 06, 18.6% of the lunar farside was illuminated. This progressively increased during the flyby, and 20.3% of the lunar farside was illuminated at closest approach. The sunlit area fortuitously included nearly all of the longitude gap in Apollo's visibility of the surface (**Figure 1.4**).

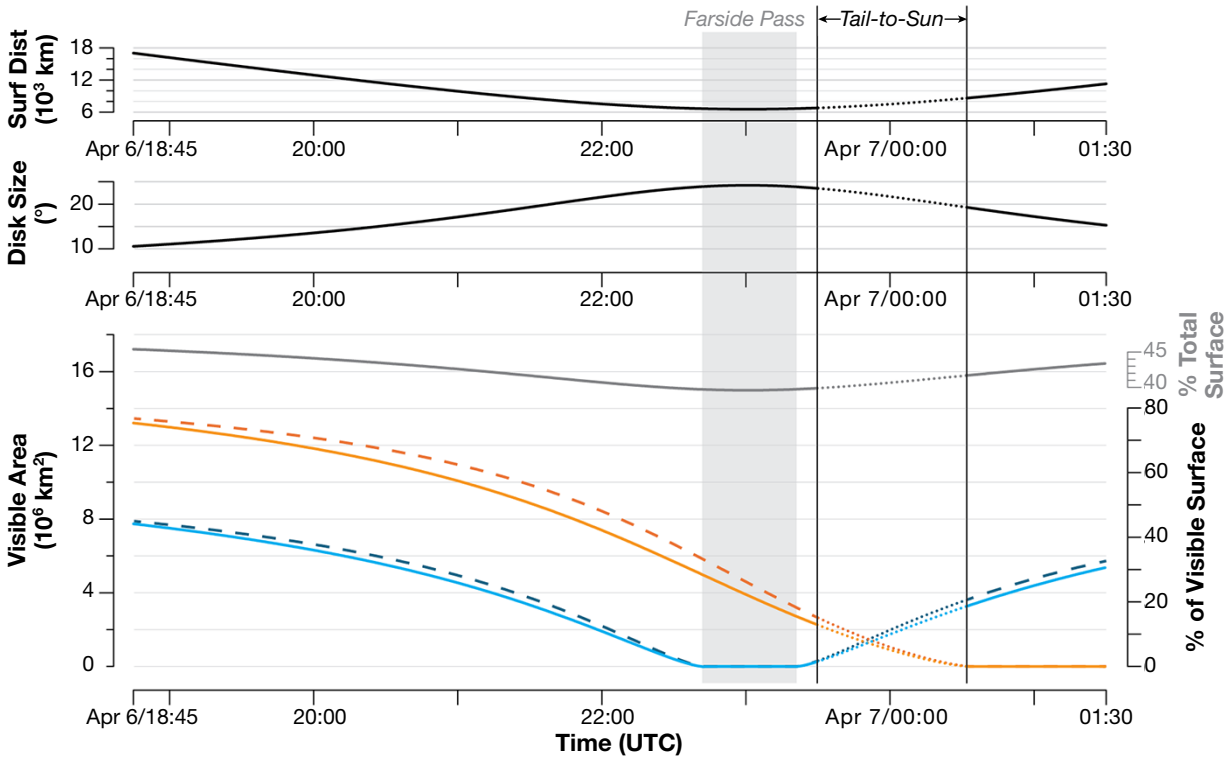


Figure 1.3: Flyby Point-of-View Details. Artemis II lunar point-of-view details during the flyby of April 6–7, 2026, (days 96–97 of 2026). (**A** top) Distance from Orion to the lunar surface (17,000 to 6,543 km). (**B** middle) Size of the visible lunar disk from the crew's perspective (10.5–24.2º). (**C** bottom) Visible areas of the whole Moon (gray), of regions illuminated by the Sun (orange), and of regions illuminated by the Earth (blue). Solid lines correspond to area in kilometers; dashed lines correspond to percent of visible surface. During the flyby, the crew were able to observe nearly an entire hemisphere (79–92% of the hemisphere, or 39.5–46% of the entire lunar surface, gray right y-axis). Visibility curves are represented by dotted lines for the hour where the spacecraft was pointed away from the Moon. The shaded vertical bar indicates the farside pass, when loss of signal occurred as the Moon occulted Earth.

1.3 Exploration Capability Objectives

In addition to developing lunar science objectives (**Table 1.1**), the LST established four exploration capability objectives to support the development and integration of science into human exploration operations for future missions. The exploration capability objectives, which received approval from NASA's SMD, are to:

- Exercise crew lunar imagery and observation product and execution development;
- Exercise science flight team support;
- Exercise science data capture methods; and
- Exercise science data archiving methods.

Details of these objectives are provided in this report's companion document, the *Artemis II Lunar Science Operations Report*.

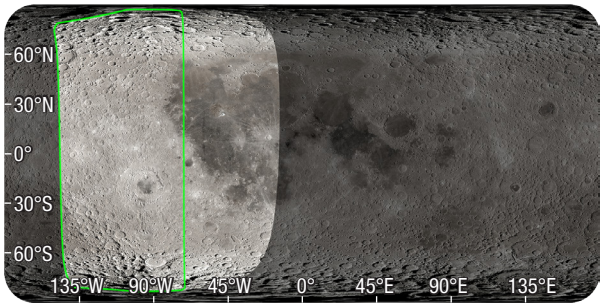


Figure 1.4: Visible Lunar Surface. Sunlit areas of the lunar surface visible to the Artemis II crew during the flyby. The brighter part of the map is the area of the Moon in sunlight and within the field of view of the crew from April 6 at 18:45 UTC until the end of the eclipse. The green outline is the portion within this area that was never in sunlight when any of the Apollo crews were near the Moon.

2.0 CREW PERSPECTIVES

This section was written by Commander Reid Wiseman, Pilot Victor Glover, and Mission Specialists Christina Koch and Jeremy Hansen.

When Gene Cernan and Dr. Harrison Schmitt left the lunar surface in 1972, Gene said, "We leave as we came, and God willing, we shall return, with peace and hope for all mankind." After journeying 252,756 miles from home, it was easy for our crew to relate to words like peace, hope, joy, and all humanity. Seeing the vastness of space, we felt lucky to be from Earth, and we yearned to be safely reunited with our friends and family. It is impossible to adequately cover the emotional response we felt to being this close to the Moon, to seeing tiny Earth so far beyond in the black of space, and to being immersed in the heavens.

As we awoke on lunar flyby day to the pre-recorded voice of Jim Lovell welcoming us to "the old neighborhood," the lunar surface was roughly 20,000 miles away and closing. The Moon was large out Window 3, and what a magnificent view it was. We could see the entire disk illuminated with most of the view being the familiar nearside with portions of the farside easily distinguishable to the left. Despite only having 18% farside illumination, we could easily make out our primary science objectives. It was hard to pull ourselves away from the windows for the next 6.75 hours.

Unlike during the Apollo program, the entire Moon is now mapped with myriad sensors. In preflight, we had total command and understanding of what the Moon would look like, the topography, the gravitational composition, and the spectral analysis. Twelve men have walked on the lunar surface and decades of studying their samples and observations have left us with a solid fundamental understanding of the nearside surface. Even so, there is nothing that compares to the creative nature of human eyes and brains putting the entire puzzle together. We saw features on the far side of the Moon that were not seen in Apollo. We could see fine variation in color across the near and far sides. We could see meteors hitting the eclipsed portions on the Moon. We looked with curiosity and wonder as we described the epic features of Orientale, Ohm, Vavilov, Hertzsprung, and many others. It was also interesting to note the things that fascinated all of us—the terminator with its black shadows and the extreme detail of crater walls. Having lived our entire lives on a planet with an atmosphere, looking from 4,000 miles down onto the lunar surface with no atmosphere seemed impossibly clear and detailed. More contrast, more dimensionality, in such crisp and vivid detail. All four of us remarked how simple it would be to pop down to the surface and go for a walk. We were so close, it felt clearly within our reach.

After hours of scientific observations, we were exhausted but also felt very at home. We looked at the Moon now as a part of us, a friend, a partner in this epic journey. Our nearest celestial neighbor had one last magnificent surprise in store for us. A solar eclipse. Watching the Sun eclipse behind the Moon was something that caught all of us off guard. As the Sun eclipsed, we were deep in scientific reporting on coronal structures, but then the view turned to something completely unexpected. The Moon became a three-dimensional, matte-black sphere ominously lit by the eclipsed Sun with the zodiacal light, stars, planets all forming a backdrop of wonder and awe. It was truly impossible to adequately describe the view and the emotion of this moment, and all four of us felt similarly about the experience.

As we said farewell to the Moon and began the journey towards home, we were thankful to have had a fully committed science team who trained us and kept us curious about the Sun, the Earth, and the Moon. Their passion and motivation adequately prepared us for the primary science objectives of the mission. Their expertise enabled us to advance our understanding of how viewing geometry shapes human perception of different lunar surface materials. We were able to reveal subtle color and albedo variations that inform hypotheses about material origin and composition. We witnessed and documented the active, dynamic impact environment surrounding the Moon. We provided new context about how impact-structure properties vary as a function of age, geologic history, and mode of formation. And most of all, we used our human curiosity to describe what we saw, often correctly identifying well-known

processes, sometimes highlighting new features and providing new questions to be analyzed, and occasionally developing erroneous theories that science teams quickly debunked.

We were thankful to have had a diverse crew who each brought our own rich life experiences into our observations. Working in pairs allowed us to discuss our observations in real time. It also enabled the two off-duty crew members to provide administrative support to the on-duty crew in addition to providing science situation reports to Mission Control. We were thankful to have had options in our recording devices, and we optimized for each. We had various cameras, including the Nikon D5 with an optical viewfinder and the Z9 with a digital viewfinder, as well as iPhones and GoPros for photo and video. The optical viewfinder on the D5 was more realistic and gave us a greater degree of observational ability whereas the Z9's digital viewfinder provided higher contrast and greater detail but muted the minute color variations. We were also thankful to have had audio recording capability although it was not optimized for scientific observations. We cannot overemphasize the criticality of recording the senses in real time. Recording what we saw, what we thought, and how it felt was critical to the teams on the ground and also critical to rebuilding our data post flight.

Our crew were the first to fly on Orion, and our mission was as much about science and inspiration as it was about testing this spacecraft in deep space. There is no doubt humanity was again united by a journey to the Moon. An entire new generation of humans now look at the Moon with renewed curiosity and excitement. As we have traveled the world in post flight, we are overwhelmed by the outpouring of support in every country on every continent. We must keep it going. For All, by All.

3.0 SCIENCE DEVELOPMENT

The lunar flyby served as the capstone science activity of the mission, with more than six hours of dedicated science observation time scheduled for the Artemis II crew. Crew and vehicle observations during the flyby were intentionally designed to address the mission's lunar science objectives (**Section 1.1**; **Table 1.1**) through a coordinated science plan developed by the LST. This section includes discussions of the development of the LST (**Section 3.1**), of the lunar science data that were acquired by the crew (**Section 3.2**) and the vehicle (**Section 3.3**), of crew training activities (**Section 3.4**) and LST-developed flight products (**Section 3.5**) in support of lunar science, and of the science planning processes that occurred pre-launch (**Section 3.6**) and in-flight (**Section 3.7**).

3.1 Lunar Science Team Development

The LST members have broad expertise in a wide range of scientific backgrounds, including terrestrial and planetary field geology, lunar and planetary science, data science, space science, data visualization, and science operations. Having a diverse set of scientific and technical backgrounds on the LST was critical in developing the science themes, objectives, observation actions, and imaging requests incorporated into the LTP to maximize the potential for interdisciplinary science return.

3.2 Crew Science Data Collection Plan

The science observation data collected by the crew during the mission fall into three categories: verbal descriptions, images, and annotations. The crew's verbal descriptions and other commentary were either directly transmitted to Earth on voice loops between the Orion spacecraft and MCC or were recorded on their portable computing devices (PCDs) using 3M PELTOR headsets. Crew-collected images and video were collected with an array of cameras that included two Nikon D5s, one Nikon Z9, and four iPhone 17 Pro Max cameras. The crew also made annotations (e.g., drawings, notes) digitally on their PCDs using Microsoft OneNote and manually on their kneeboards with flight pens. All three types of science data that the crew collected were downlinked from Orion during flight and also retrieved from Orion after it returned to Earth.

During the lunar flyby, two crew members were stationed at the windows to make observations, while the other two crew members monitored the vehicle and assisted those at the windows with timekeeping

and orienteering guidance. Additionally, the assisting crew members provided periodic verbal reports to the ground via science situation reports (SitReps), which provided situational awareness to the LST about which targets the observing crew members were currently describing and imaging. The crew members at the windows observed the Moon from two different perspectives: (1) with a Nikon D5 equipped with an 80–400mm lens; and (2) with the unaided eye. The crew member with and the crew member without the camera also recorded verbal observations on their PCDs when stationed at the windows. The crew recorded verbal observations guided by LTP actions, which were written by the LST for each target, taking into account science objectives, the tool each crew member was using (camera or unaided eye), and the viewing and illumination geometries (and, therefore, defining the target's planned observation time). For each target, additional crew notes and sketches were enabled by digital OneNote pages that included to-scale computer visualizations of each target rendered in illumination geometries realistic to what the crew was seeing at the time of each scheduled target.

Detailed descriptions of crew datasets are provided in the *Artemis II OSDMP* and the *Artemis II Lunar Science Data User Guide*, and details of how crew activities were structured to support this data collection are available in the *Artemis II Lunar Science Operations Report*.

3.2.1 Crew Imaging Plan

As discussed in **Section 1.2**, science observations were made during periods of opportunistic imaging and during the lunar flyby and eclipse period. Opportunistic imaging periods were coordinated with other FCT consoles to identify times where either the Moon or other scientific targets happened to be visible because of existing vehicle-pointing attitudes or because vehicle resources permitted a short attitude excursion to enable scientific observations. Before the flyby, opportunistic imaging occurred on Flight Days 04 and 05, as the crew imaged the Moon on approach with the 80–400mm lens on the Nikon D5 and Nikon Z9 (**Figure 3.1**). Images with both cameras were requested to enable comparisons between the imaging systems (further discussed in **Section 7.4**). These pre-flyby opportunistic imaging events allowed the crew to orient themselves to the Moon from their vantage point in Orion and to begin making lunar observations, marking the first time the spacecraft attitude was adjusted to bring the Moon into view through the forward windows. During the lunar flyby observations, the crew took images using the Nikon D5 and Nikon Z9 (**Figure 3.2**). Finally, during post-flyby opportunistic imaging on Flight Day 07, the crew imaged the nearside of the Moon during their return journey with the Nikon D5.

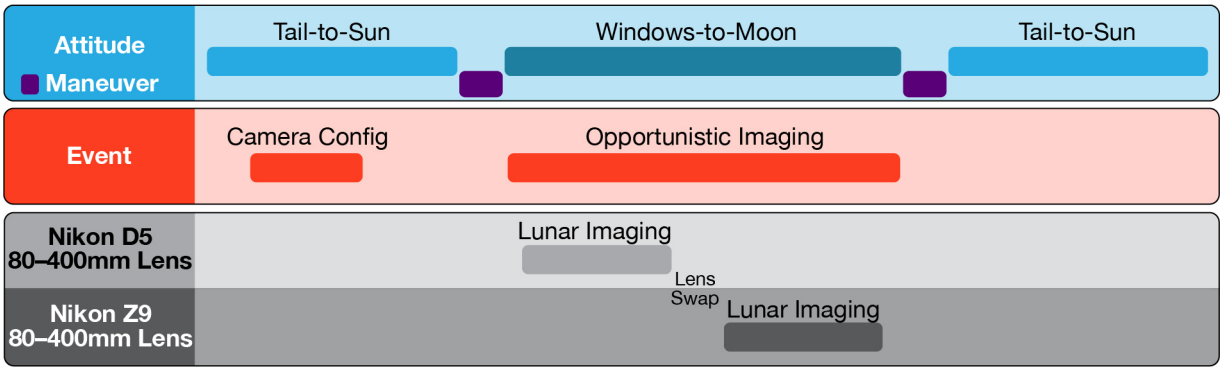


Figure 3.1: Crew Opportunistic Imaging Plan. Schematic showing the crew camera imaging plan during opportunistic imaging events on Flight Days 04 and 05, utilizing the Nikon D5 and Nikon Z9 cameras with the same lens. The lens swap in the figure denotes when the 80–400mm lens was taken off the Nikon D5 and attached with an adapter to the Nikon Z9. Tail-to-Sun is the Orion attitude with its X-axis to the Sun, which allows solar charging. Maneuvers (purple boxes) indicate spacecraft attitude changes.

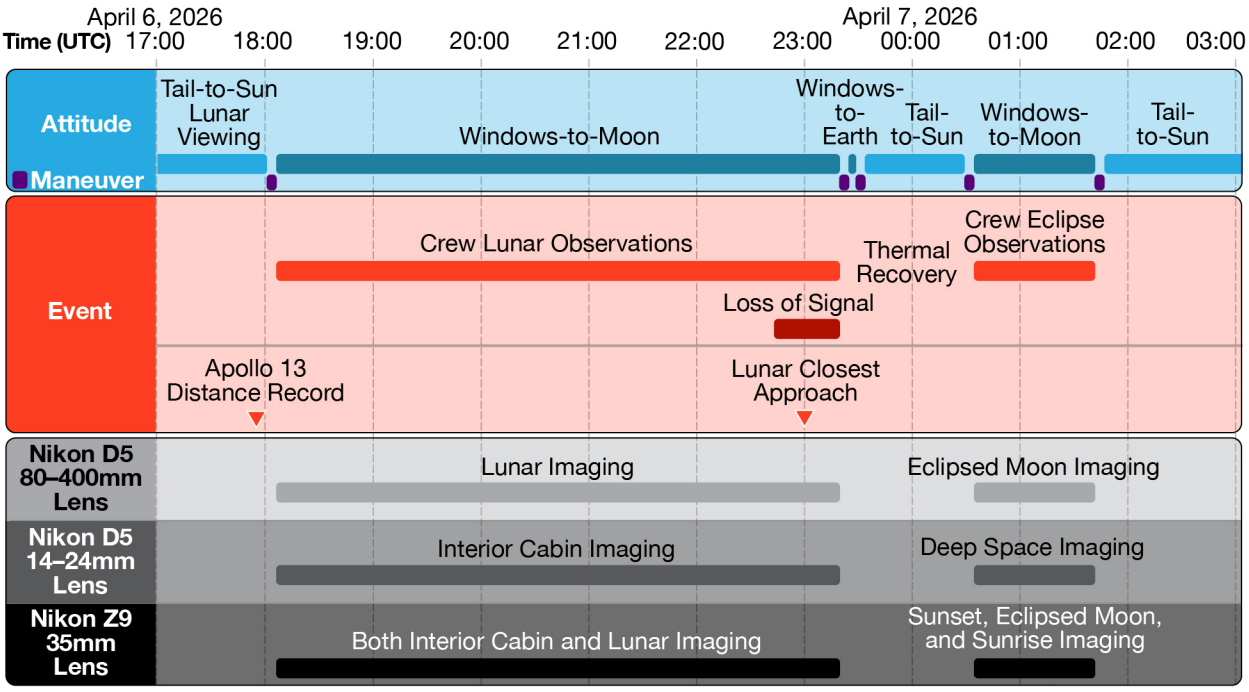


Figure 3.2: Crew Flyby Imaging Plan. The timeline shows the crew camera imaging plan during lunar flyby observations, utilizing the Nikon D5 and Nikon Z9 cameras and an array of lenses. Tail-to-Sun is the Orion attitude with its X-axis to the Sun, which allows solar charging. Maneuvers (purple boxes) indicate spacecraft attitude changes.

The crew imaging plan included multiple strategies to capture scientific features of interest. Small features were imaged at multiple zoom levels, up to the maximum suggested focal length based on the imaging that was conducted to assess window quality on Flight Day 03 (**Sections 3.2.3**, **7.4.1**). Larger targets were captured either by zooming out or through planned mosaics at full or moderate zoom levels. Zoom levels of crew-acquired images varied according to the intention of the image, following crew expertise and views. The entire Moon and the lunar terminator were selected multiple times for mosaic imaging (**Figure 3.3**), where sequential images overlapped >30%. As the eastward lunar limb was always effectively rotating out of view of the spacecraft, for mosaicking purposes, the crew were instructed to obtain successive mosaic images from east to west. For all lunar imaging, the window used for imaging was shrouded to limit cabin-light effects and the camera lens was intended to be flush to the cabin window to minimize glare and reflections.

Images are science data and are therefore best captured when taken with intent, while also considering the capabilities of the camera system and the characteristics of the physical environment (e.g., target properties, illumination and viewing geometries). For Artemis II, crew training, operation of the cameras by the crew, downlink, and delivery to the LST of the acquired image data required close collaboration between the LST, the Flight Operations Directorate (FOD), the FOD Intravehicular Activity (IVA) Photo/Television team (Photo/TV), Image Science and Analysis Group (ISAG), and Orion Electronic Still Camera group (OESC) at NASA's Johnson Space Center. This close coordination was imperative to maximizing science return. For example, downlink collaboration facilitated timely downlink of data needed to assess window quality to best position flyby imaging, as well as by providing data from crew flyby observations to the LST shortly after flyby to inform LST questions for the following day's crew conference. Through collaboration among these groups, Artemis II demonstrated how image data intentionally captured by humans can yield valuable science data and spectacular images that inspire the world, adding new context to decades of lunar imaging science enabled by robotic spacecraft.

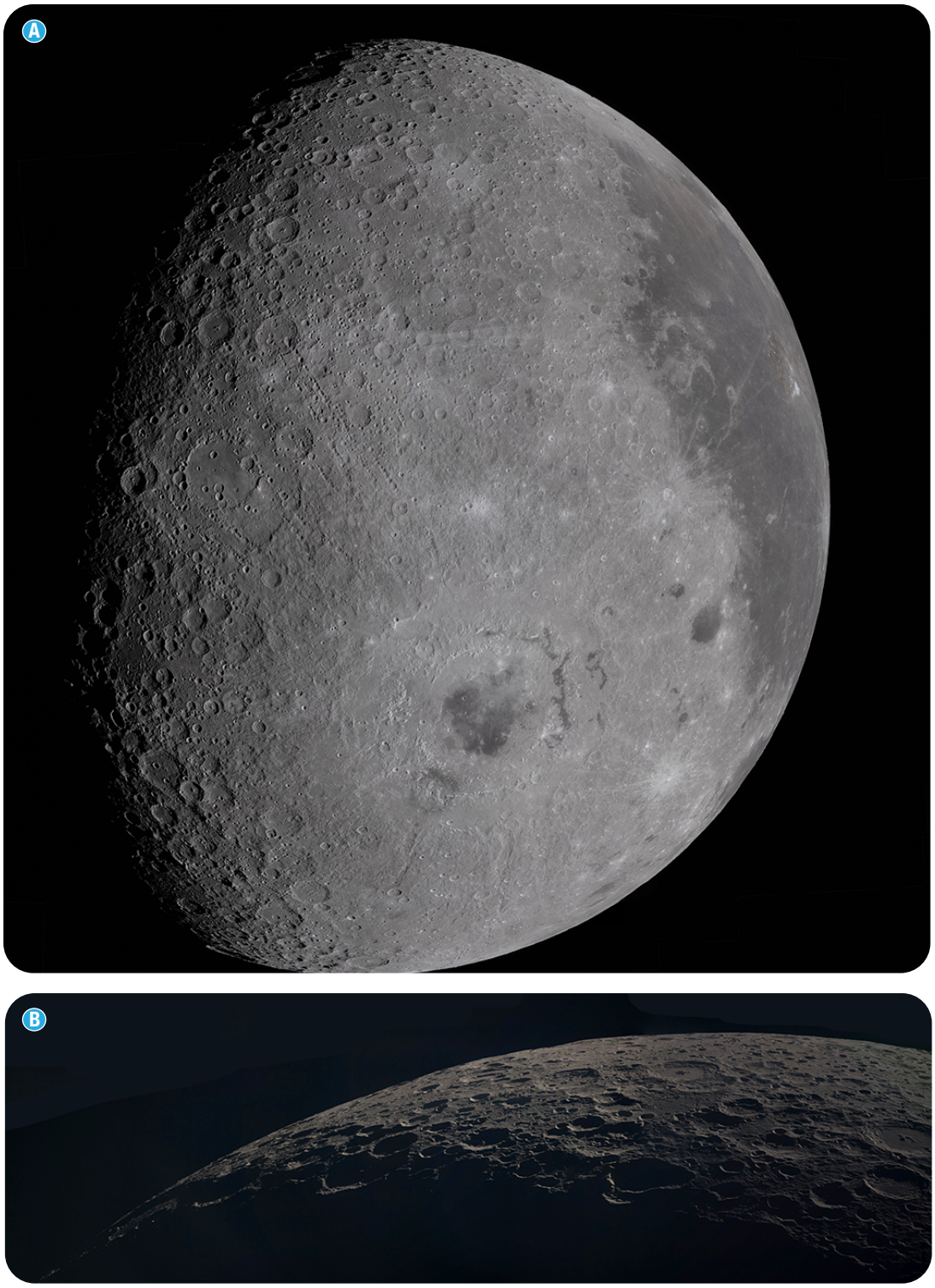


Figure 3.3: Lunar Mosaics. (**A**) Full Moon mosaic created using images taken with the Nikon D5 camera using a 400mm focal length, captured at the beginning of the lunar flyby, and mosaicked by the LST (mosaic created from multiple crew images within art002e019950 to art002e020127). (**B**) Mosaic of the limb with the terminator, created using images taken with the Nikon D5 camera using a 400mm focal length, captured between 23:09:15 and 23:09:34 UTC, and mosaicked by the LST (mosaic created with art002e014040, art002e014042, art002e014045, art002e014050, art002e014055, art002e014057, art002e014060).

3.2.2 Crew Camera Settings

The crew cameras were commercial off-the-shelf (COTS) instruments: the Nikon D5, which is a full-frame digital single lens reflex (DSLR) camera, and the Nikon Z9, which is a full-frame digital mirrorless camera. Both cameras have been used on the International Space Station for Earth observation and other imaging (e.g., deep space imaging, interior space station imaging). A modified Nikon Z9, known as the handheld universal lunar camera (HULC), is planned for future Artemis missions, including for extravehicular activities (EVAs) on the lunar surface.

Table 3.1 presents a summary of key features of the D5 and Z9 camera systems used during Artemis II, and additional hardware details can be found in the *Artemis II OSDMP* and *Artemis II Lunar Science Data User Guide*. In comparison to the D5, the Z9 has the advantage of having a sensor with more megapixels (45.7 megapixels for the D5 vs. 20.8 megapixels for the Z9) that can acquire images at a relatively higher spatial resolution. The Z9, however, has an electronic viewfinder (vs. the D5's optical viewfinder) and a lower international organization for standardization (ISO) film-speed equivalent range that were less advantageous to science observations on the Artemis II mission, as discussed more completely in **Section 7.4**.

Table 3.1: Camera Specifications. A comparison of specifications relevant to Artemis II science for the Nikon D5 and Nikon Z9 cameras.

Feature	Nikon D5	Nikon Z9
Camera Type	DSLR	Mirrorless
Sensor Resolution	20.8 MP	45.7 MP
Viewfinder Type	Optical	Electronic
Sensor Size and Type	FX CMOS	FX stacked CMOS
Native ISO Range	100–102,400	64–25,600
Expanded ISO Range	50–3,280,000	32–102,400
Flash Card Memory	256 GB	1.6 TB

Key: MP = megapixels, FX = full frame, CMOS = complementary metal-oxide-semiconductor

The Nikon D5 and Z9 cameras that the crew operated, like most modern digital cameras, use a Bayer color filter in front of the camera's sensor to produce red-green-blue (RGB) color images. In this design, each 2×2 Bayer cell contains one red filter, two green filters, and one blue filter. This filter pattern is designed to reflect the human eye's heightened sensitivity to green light. In the raw image data, each pixel records only a single color (red, green, or blue), corresponding to its placement within the filter pattern. The final RGB color image is produced by de-mosaicking and interpolation. Because cameras with Bayer filters detect color through this indirect reconstruction, they have a limited direct sensitivity to complex, low-luminance colors like brown, which arises from moderate-to-low levels of red and green light, and minimal blue. In contrast, the Apollo crews used film cameras with high-contrast films that tended to brighten and accentuate blues and whites. The digital cameras used during Artemis II therefore produced images with more natural references to greens and browns, offering a different visual characterization of the lunar surface than was possible during Apollo.

The Artemis II crew cameras were not calibrated for science requirements. Prior to flight, the only characterization performed was a geometric lens distortion calibration of the Nikon D5 cameras fitted with first the 80–400mm lens and then the 14–24mm lens, with each lens set at various focal lengths that had been marked on the lenses by Nikon (80mm, 135mm, 200mm, 400mm). The geometric lens distortion calibration was completed on only the Nikon D5s because of the late addition of the Nikon Z9 camera to the flight manifest. No color- or radiometric-calibration imaging was completed, either to characterize the camera sensors themselves or through the Orion windows to characterize the entire imaging stack. Neither the LST nor ISAG was granted access to Orion pre-mission to characterize imaging through the window stack. As a result, the archive of Artemis II science data available in the PDS only includes raw image files, with no calibrated or derived products.

3.2.3 Window Quality Observations

The Orion forward windows are made of a three-layer stack of 0.5-inch-thick panes: an outer thermal pane of fused silica, a middle thermal pane of cast acrylic, and an inner pressure pane of stretched acrylic. These layers, especially the cast acrylic thermal pane, can introduce optical distortions in images taken through them. The docking-hatch window was also made of a three-layer stack of panes: an outer thermal pane of fused silica (0.5 inch thick), a middle thermal pane of fused silica (1.0 inch thick), and an inner pressure pane of stretched acrylic (0.5 inch thick). Because time constraints prevented pre-mission characterization of how the Orion windows affect Nikon camera images, an in-flight assessment was required to confirm whether the planned science-imaging configuration for the lunar flyby needed adjustment (e.g., changes in window selection or camera lens recommendations). **Figure 3.4** shows a diagram of the Orion windows, which are also discussed in detail in the *Artemis II Lunar Science Data User Guide*.



Figure 3.4: Orion Windows. Illustrative schematic of Orion showing the locations of Forward Windows 1–4, the docking-hatch window, and the side-hatch window.

To assess window quality for science observations, V. Glover conducted a developmental flight test objective (DFTO) activity on Flight Day 03. During this activity, V. Glover configured the Nikon D5 to image through the forward windows and the docking-hatch window. Earth was the imaging target, as its clouds could be used to assess the capture of textures and hard contrast shifts. Structures in the clouds were used as points of comparison between images collected from different windows, at different positions within the forward windows (left of center, center, and right of center), and with different focal lengths. The LST and ISAG made qualitative assessments via overlapping and side-by-side comparisons of these images.

The window quality DFTO analysis revealed that Window 2 was the best window for imaging, and that high-quality image data could be acquired at all available zoom levels, up to the planned 400mm focal length. However, when imaging obliquely rather than flush to the windowpane surface (requiring the camera to image through a greater thickness of window material), the LST recommended limiting the focal length to 200mm or to acquire images at multiple focal lengths/zoom levels to mitigate distortion.

The analysis also revealed that the docking-hatch window was optically superior to the forward windows, but relying on it for flyby science observations would restrict observations to a single crew member, a significant departure from the plan for the crew to work in pairs. Therefore, the LST preserved the forward-window configuration for flyby observations, while recommending use of the docking-hatch window for opportunistic and serendipitous science imaging during lunar approach.

Additional details about the window quality DFTO and its results are provided in the *Artemis II Lunar Science Data User Guide* and *Artemis II Lunar Science Operations Report.*

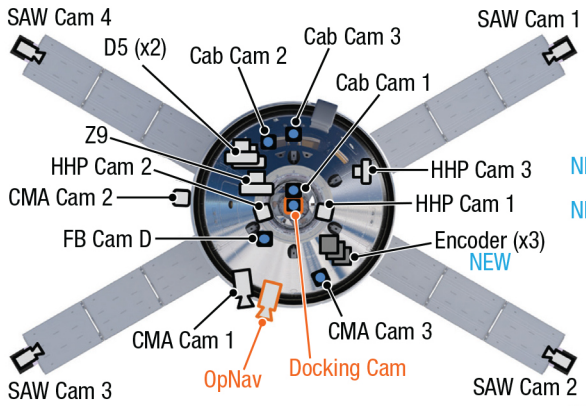
3.3 Vehicle Science Data Collection Plan

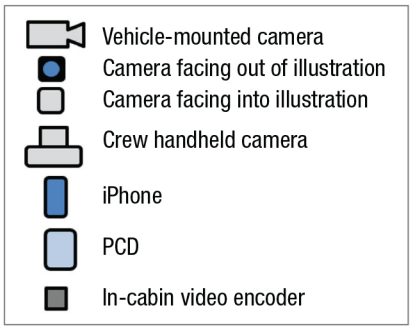
The LST planned imaging from the Orion vehicle-mounted cameras to directly support Artemis II science objectives during the lunar flyby. Although these cameras were primarily intended for spacecraft and engineering assessments, their use during the flyby provided valuable context that complemented the crew's handheld camera data and verbal observations. Two vehicle cameras, both modified GoPro

HERO4 Black cameras, were available for science observations during the flyby based on spacecraft orientation: Cabin Camera 2 (Cab Cam 2), and Solar Array Wing (SAW) Camera 3 (SAW Cam 3). Cab Cam 2 was mounted inside Orion and captured the crew's view through Orion's forward-facing Window 3 (**Figure 3.5**). SAW Cam 3 was mounted externally at the end of SAW 3 and captured views of the lunar surface from outside the influence of cabin windows. Together, these cameras supplied interior and exterior perspectives that enriched the documentation of color, brightness, and the lunar environment.

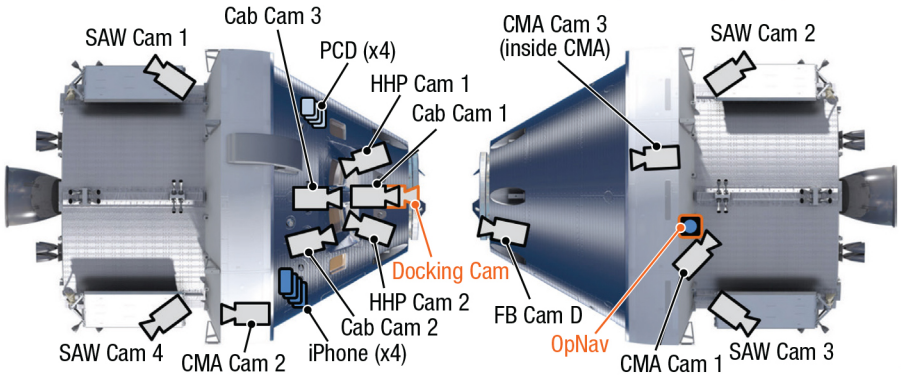
During the uncrewed Artemis I mission, vehicle cameras were the primary imaging instruments, with four modified GoPro cameras mounted externally on Orion, one on the end of each SAW.

Orion Imagery System for Artemis II





	Camera	Batt	GNC	Use	Streaming Formats
	Cab Cam 1,2			Engineering, Jettison Events, Parachutes	Custom, HD
	Cab Cam 3			Crew Monitoring	
NEW	HHP Cam 1,2			Dynamic Flight Crew Monitoring	
NEW	HHP Cam 3	B		Crew Choice Live Video	
	SAW Cam 1,2,3,4	B		Engineering, Vehicle Inspections	
	CMA Cam 1			Engineering, Jettison Events	Custom, SD
	CMA Cam 2			Engineering, Vehicle Monitoring	
	CMA Cam 3			Engineering, Spacecraft Separation	
NEW	Docking Cam		G	Proximity Operations	Custom
NEW	PCD	B		MCC to Crew Conferences (private)	SD
NEW	Nikon D5 (x2)	B		Crew Choice Stills & Video, Live Media Events, Science	HD, UHD
NEW	Nikon Z9	B		Crew Choice Stills & Video, Science	N/A
NEW	iPhone (x4)	B		Crew Choice Stills & Video	
	FB Cam D			High Speed FBC Jettison/ Parachute Ops	
	OpNav		G	Navigation	
NEW	Nat Geo Payload	B		Media Recording	



New for Artemis II
G Owned and operated by GN&C
B Battery-powered device

Nat Geo Payload

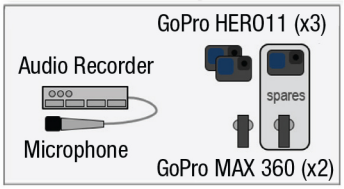


Figure 3.5: Orion Imagery System. The Orion imagery system configuration for Artemis II includes vehicle-mounted cameras used for monitoring spacecraft performance (exterior and interior to the crew cabin), crew handheld devices, navigation sensors, biomedical cameras, and the National Geographic public outreach payload. SAW Cam 3 and Cab Cam 2 had views of the Moon during the lunar flyby. Acronyms: HHP = Human Health and Performance; GN&C = Guidance Navigation and Control; CMA = Crew Module Adaptor; FB = Forward Bay.

During Artemis I, lunar views were recorded on these SAW cameras and streamed to the ground. Individual frames were extracted from those videos as image stills. However, individual video frames have inherently lower spatial resolutions, lower aspect ratios (i.e., the top and bottom of the images are cropped), and reduced image quality relative to the source video and relative to still images taken with the same camera and comparable still-image settings.

For Artemis II, the LST coordinated an improved imaging strategy to maximize image quality for science observations: the vehicle cameras collected high-resolution still images in addition to streamed video. Furthermore, the coordination enabled multi-shot sequences with exposure adjustments, including sets of four images with a range of exposure times (2, 5, 10, and 15 seconds) spaced 15 minutes apart during the solar eclipse to document dynamic visual phenomena.

The *Artemis II Lunar Science Data User Guide* provides additional details about the other imaging systems.

The LST worked closely with NASA's Johnson Space Center personnel from multiple FOD teams led by ISAG to plan vehicle camera science observations during the lunar flyby (**Figure 3.6**). SAW Cam 3 streamed video in real time during the flyby, as well as during other portions of the mission. SAW Cam 3 and Cab Cam 2 also acquired high-resolution still images at a cadence of one image every eight minutes through most of the flyby period to match the cadence of crew imaging and description of

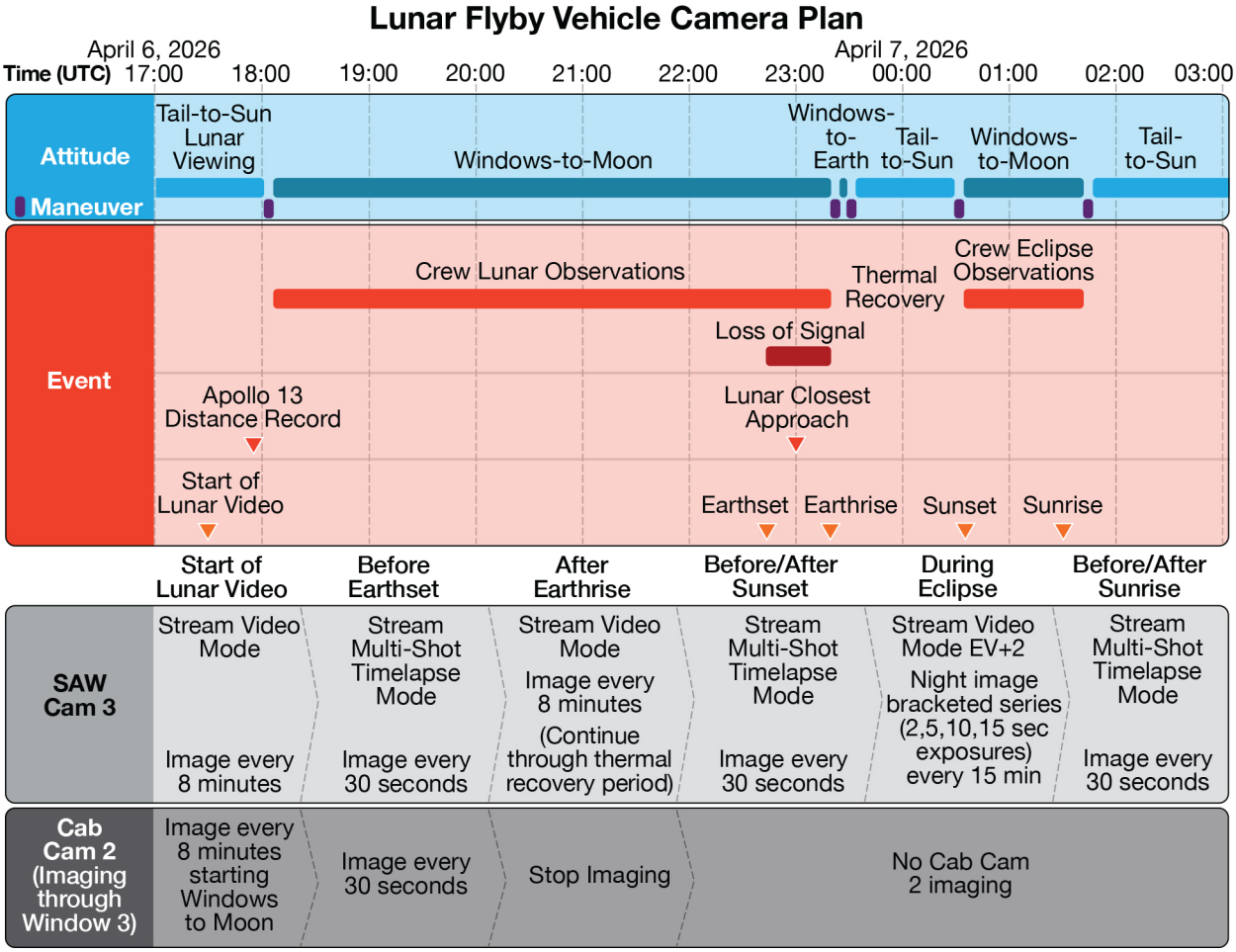


Figure 3.6: Vehicle Imaging Plan. A visual representation of the vehicle camera (SAW Cam 3 and Cab Cam 2) science observations during the lunar flyby. Tail-to-Sun is the Orion attitude orienting the X-axis to the Sun, which allows solar charging. Maneuvers (purple boxes) indicate attitude changes. The *Artemis II Lunar Science Data User Guide* includes a figure with additional details.

targets through the Orion windows. The cameras were switched to a multi-shot timelapse mode at a higher imaging cadence of every 30 seconds to capture the full duration of earthset, the lunar surface through the entirety of the 40-minute period of loss of signal (LOS) with Orion, and through the full duration of earthrise. To capture the dynamic setting and rising of the Sun behind the Moon during the eclipse, SAW Cam 3 was again transitioned to a multi-shot, timelapse mode with a 30-second imaging cadence. During totality, SAW Cam 3 was utilized in night imaging settings, with the illuminator off; still images were captured in a night photo mode in a bracketed series of 2-, 5-, 10-, and 15-second exposures every 15 minutes. The *Artemis II Lunar Science Data User Guide* provides complete details about imaging, video, and cadence/mode shifts and timing.

During the mission, the streamed video from the exterior SAW Cams provided real-time situational awareness and enriched NASA's 24-hour-per-day, live broadcast. The streamed views enabled the LST to be responsive to crew questions during the flyby, such as identifying which planets were visible during the solar eclipse. The videos and images acquired by the SAW Cams include portions of the Orion spacecraft in each frame, providing a visual anchor that is consistent in scale and color between images.

3.4 Crew Training in Support of Lunar Science

From the time they were assigned to the mission, the Artemis II crew were considered members of the mission's Lunar Science Team. Artemis crew members are provided lunar science training based on the fundamental understanding that valuable science contributions can be made through the direct observation of the lunar surface. To that end, the NASA lunar science and geology training team provided foundational geology training to all crew members throughout their NASA careers, followed by fundamental lunar science upon their Artemis mission assignment. This training team, in collaboration with the LST, developed and provided an immersive lunar science and science operations training program to train the crew as mission scientists and to conduct science observations from orbit. This progressive training program built foundational knowledge, strengthened observational skills, and ensured proficiency with the tools and processes required for successful lunar science collection during the mission.

Training covered several core topics, including:

- Lunar geology, lunar exploration history, and fundamental planetary processes that shape terrestrial surfaces;
- Lunar geography, for proficiency in recognizing and navigating lunar features that enabled the crew to orient themselves during the lunar flyby;
- Observational and imaging skills under various viewing and illumination geometries, practiced through classroom exercises, field training, and mission simulations;
- Lunar science objectives guiding the lunar targeting and data collection plans; and
- IVA science operations (developed iteratively throughout the pre-mission timeframe) integrating hardware, software, science training, and crew interactions inside Orion.

The crew were trained across a range of learning environments: from the classroom, to inside the Orion vehicle mockup, and at terrestrial field sites. Early training focused on fundamental science of the Moon and how to perform geologic observations in field settings. Crew members spent one to three weeks in remote field locations to practice observation and interpretation skills of impact craters, volcanic structures and deposits, and lunar analog geologic materials. This training set the stage for later training that increased in operational fidelity and narrowed in focus as launch approached.

The multi-faceted science operations training, led by members of the lunar science and geology training team and the LST, enabled the crew to practice identifying, describing, and imaging features using mission tools (camera systems, headsets, PCDs), mission procedures, and the LTP. With increased exposure to the LTP, the crew provided critical feedback that helped the LST develop best practices, including the establishment of science impact statements, discussion periods, Crew Choice targets, and target bundles that supported comparative observations.

Later in the training flow, biweekly homework, individualized crew feedback, and one-on-one observation tutorials and coaching further increased crew proficiency in lunar science and mission tools and strengthened crew confidence in their scientific observations and descriptions. As launch dates shifted, crew training was responsive to the evolving illumination conditions of the flyby and predicted changes in the LTP, including just-in-time training on eclipse observations. Collaborations between the lunar science and geology training team, the LST, and flight operations teams, alongside support provided by the Chief Training Officer to integrate science into the training flow and simulations, contributed significantly to the success of the mission.

A close partnership developed between the crew and the LST as the crew learned about the Moon and the mission's science objectives. This partnership directly enhanced the scientific return of the mission. C. Koch acknowledged the benefits of this partnership at multiple points during the flyby:

> We are looking forward to working with and for the Science Team. And we are just excited to be so close to finally accomplishing what we've been training for so many years. (C. Koch, O/E-1 voice loops, 16:52:24 UTC)

> I just want to channel everything that you guys [on Earth] are probably feeling right through my eyes and heart. It is awesome to see the side of the Moon. You guys made us excited for this day, and we couldn't appreciate it any more. And we are ready to hopefully deliver on all the awesome training you guys have provided. (C. Koch, O/E-1 voice loop, 17:45:06 UTC)

Beginning with their pre-mission science training, extending through the mission during data collection, and continuing post-mission with data analysis and interpretation, the crew worked collaboratively to execute the LTP in support of the mission's science objectives. The Artemis II crew helped each other to locate lunar features and targets, and engaged in active science dialog during discussion targets, making comparative observations of, for example, color details and superpositional relationships between lunar features. These interactions gave the crew a sense of ownership and agency in their science observations, enhancing the science return as they built on one another's insights to create richer, more complete descriptions (**Section 8.2**).

Additional details related to crew training are provided in the *Artemis II Lunar Science Operations Report*.

3.5 LST-Developed Crew Flight Products

Each crew PCD aboard Orion hosted a pre-loaded, custom-made tool/web-based interface built by the LST to support the crew in lunar observations. The interface hosted the lunar geography review (LGR) and the pre-flight LTP. The LGR provided training reminders, an interactive view of the Moon with notable lunar features labeled, and Artemis II lunar science objectives. The initial LTP provided the crew with a realistic targeting plan based on an assumed April 9, 2026, flyby trajectory. This flyby date was chosen to reflect a launch date in the middle of the early April launch window.

The LTP interface (**Figure 3.7**) was designed to keep the crew on the timelined schedule for each target and quickly provide the crew with information to locate and understand each target, capture images, verbal observations, and annotations (including the ability to easily open OneNote for annotations). It also displayed a collapsible cue card that was developed to remind crew of essential description techniques of remote sensing (e.g., target shape, color, structure). Simulated visualizations of the lunar surface at varying camera focal lengths provided to-scale renderings under realistic illumination conditions, based on the exact time and location of Orion.

The design and development of the LTP is provided in more detail in the *Artemis II Lunar Science Operations Report*. Details on the contents of the LTP are found in **Appendix 1** and the *Artemis II Lunar Science Data User Guide*. A static flight-packaged LTP and the outgoing target request (OTR) database are archived in the PDS (**Appendix 2**).

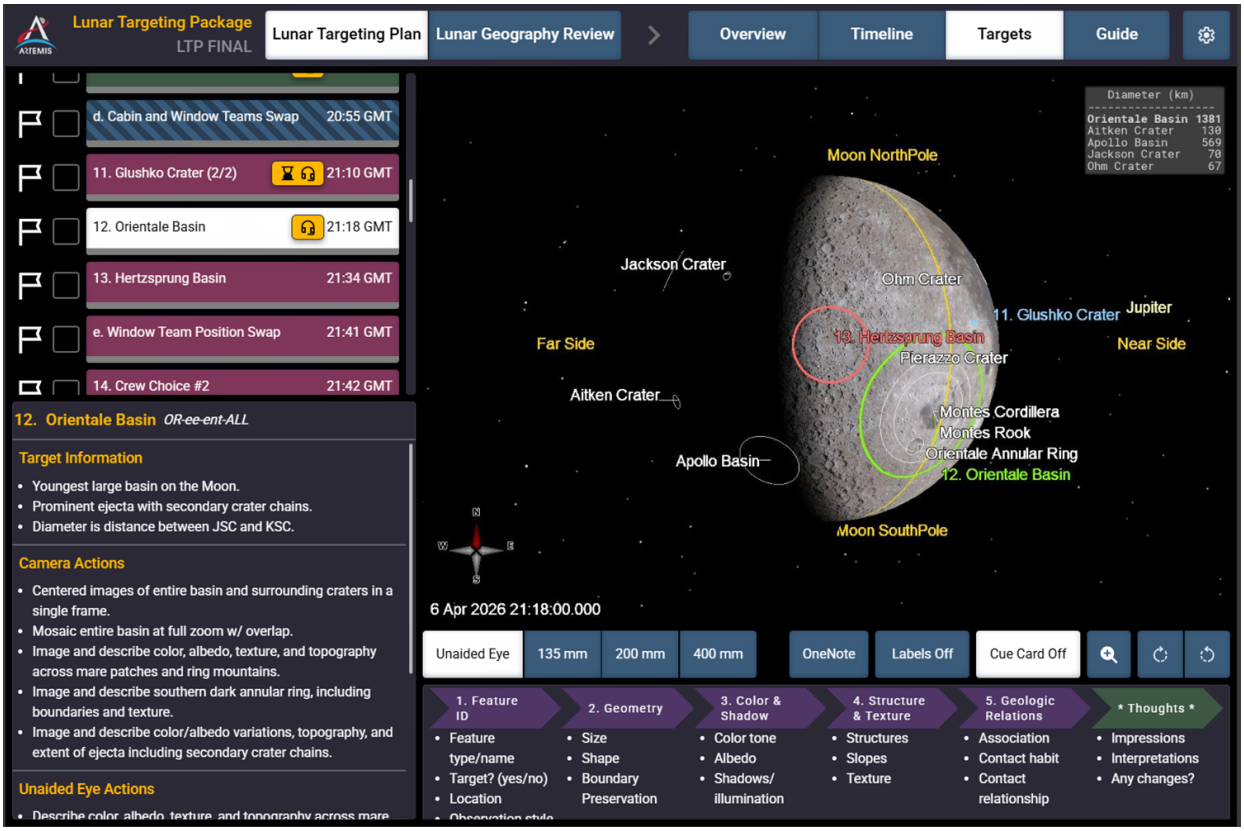


Figure 3.7: The Lunar Targeting Plan. A target page view of the LTP. In this view, the timelined targets are enumerated on the left. Each target included information related to the target, requested actions for the observing crew members with and without the camera, as well as science impact (not visible in this view). Adjacent are various orienteering guides, including labeled features, previous and upcoming targets, and to-scale renderings of the target, illuminated under realistic and time-specific conditions. Beneath the rendering is a cue card designed to facilitate geologic descriptions.

3.6 Pre-Launch Science Planning

During pre-launch science planning, the LST developed a targeting schedule (i.e., the LTP) to maximize science return by the crew and vehicle. Multiple pre-launch LTPs were assembled to support the mission. These LTPs were used to enable crew use during integrated mission simulations and prepare the crew for likely lunar illumination scenarios, while also preparing the LST for the in-flight assembly process. A pre-launch LTP was also developed specifically for each launch window and uploaded to the PCDs to enable in-flight, pre-flyby study of potential targets by the crew. In all instances, the LTP was formulated following the same process:

Step 1. Ingesting a realistic trajectory, realistic timing assumptions, and a feature almanac (described in the following paragraph), into an interactive live encounters guide (LEG).

Step 2. Downselecting almanac features into targets through a collaborative target prioritization evaluation process, taking into account the STM science objectives and viewing conditions resulting from the provided trajectory of interest.

Step 3. Ordering and scheduling observations into a timeline, specific to the minute.

Step 4. Revising science observation actions to be specific to the science decisions involved during downselect (Step 2) and to the viewing conditions afforded by the trajectory of interest.

Step 5. Exporting an OTR database of results from Steps 2–4.

Step 6. Creating and delivering the LTP using the OTR database.

Pre-launch, the LST assembled a list of more than 150 lunar, Earth, and deep-space features of scientific interest and several non-target activities (e.g., suggested discussions based on broad lunar or deep space observations). These features and activities were assembled into an almanac, which captured the following types of data for each entry for incorporation into an OTR database/LTP:

- Geographic metadata for target location;
- Phonetic guide for target pronunciation;
- Plain-language target descriptions for crew background;
- Actions for the crew member making observations with a camera;
- Actions for the crew member making observations with the unaided eye;
- Plain-language summary of the science intent guiding the crew actions; and
- Tracing of potential observations to STM science objectives.

Each LTP was developed to support the lunar science objectives defined by the STM (**Table 1.1**) and was tailored to the viewing conditions afforded by a given trajectory. The spirit of the LTP emphasized not only maximizing science return but also fostering crew exploration and discovery. To support this philosophy, several Crew Choice observation blocks were incorporated, giving the crew opportunities to image and describe features, patterns, or regions of personal intrigue. Additionally, crew discussion periods were strategically included to encourage comparative observations and interpretations and collaborative hypothesis-building (**Section 8.2**).

3.7 In-Flight Science Planning

The LST created an in-flight science planning schedule that enabled the LST and science-supporting flight team, including the crew, to adapt to elements of the mission that were likely to change after launch. This in-flight planning schedule spanned all ten flight days, beginning at launch and ending at splashdown.

After launch, the LST coordinated forthcoming mission staffing schedules based on pre-mission planning, now taking into account the specific launch time. The LST set up the SER and SMOR, established reliable communication across the team and these two facilities, and conducted final checks of workstations and tools. Flight Day 01 included a review of the almanac to ensure accuracy and clarity of descriptions of potential targets based on the launch timing and their potential to address the STM. The trans-lunar injection (TLI) maneuver occurred on Flight Day 02, which established the trajectory of the flyby and determined the visibility of targets in the almanac by the crew. Establishing a trajectory and target visibility kicked off the sequence of science-planning steps described in **Section 3.6**: LEG generation on Flight Day 02 was followed by downselecting targets, scheduling target observations, and creating the OTR database on Flight Day 03. As practiced pre-flight with multiple pre-launch LTPs, targets were downselected based on highest science value, evaluated using multiple variables including suitability to address STM objectives, the priority rankings of each STM theme, and trajectory-specific target viewing and illumination conditions. The high-value targets were assessed holistically to build an LTP that achieved a balance of STM broad coverage and depth. A table of these activities, along with a complete discussion of the LTP generation, is provided in the *Artemis II Lunar Science Operations Report*.

The LTP (**Appendix 1**) ultimately included 28 targets and activities (**Figure 3.8**). The plan was assembled based on the in-mission OTR database and an LST-wide review of the LTP that was conducted on Flight Day 04 prior to final uplink to the crew. The targets selected for the LTP were reviewed against the STM and covered all ten science themes in the STM. The LTP included observations blocks for the crew to conduct structured science discussions of different topics (Whole Moon, Nearside/Farside Transition, Farside Color/Albedo, Terminator, Limb, and Forward Look) and multiple Crew Choice blocks, in addition to the specific targets selected by the LST. These designations in the schedule encouraged crew to leverage their science training, gave them time to explore the surface, and discuss and debate hypotheses based on their real-time observations. Time allocated per target was iteratively

developed based on crew feedback and repetitions making observations in classroom and simulation activities. Variables included wanting to maximize total number of targets while not overburdening the crew in terms of mental fatigue and management of hardware, as well as the number and detail of crew actions requested for each target.

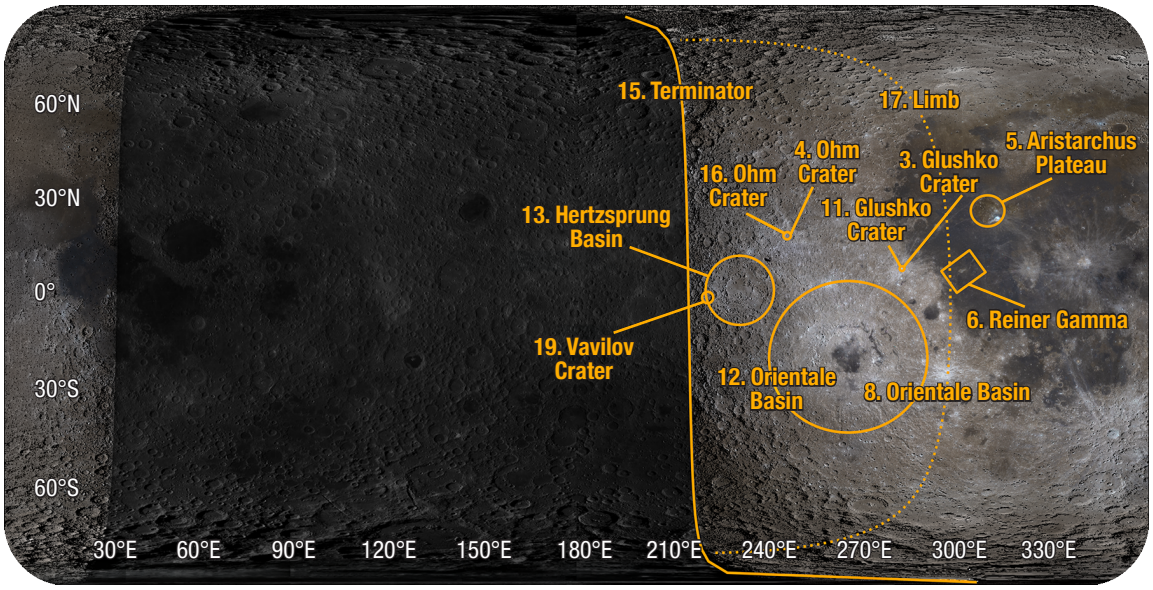


Figure 3.8: LTP Targets. Targets from the LTP (**Appendix A**) are visualized on an illumination-specific basemap (hill-shade-style shadows and nightshade, darkening the non-sunlit areas, calculated at center of flyby time). Targets are numbered sequentially in time. Numbers associated with targets without a bounded spatial representation (i.e., Whole Moon, Crew Choice) are omitted. Dashed line indicates limb points from the crew's perspective at the time of that target (April 6, 2026, 22:28 UTC).

The in-flight science planning also involved coordination between the LST, vehicle image science lead, and ISAG to adjust and modify imaging plans for the vehicle cameras (**Section 3.3**). This work included implementing and evaluating capture of high-resolution still images and video for science. This coordination occurred after launch, TLI, and after the final course correction burn, but before the lunar flyby to adjust fine details regarding pointing and timing of observations.

Flight Days 05–07 focused on evaluating downlinked data to prepare for the post-flyby crew conference that occurred on Flight Day 07. Data evaluated during this time led to questions for the crew that facilitated discussion between crew and the LST, with the intent of focusing these clarifying field-debrief questions on priority science targets to leverage fresh memories of crew within hours after the lunar flyby concluded. The LST used the days following the flyby through splashdown to focus on prioritization and analysis of downlinked data, to develop science highlights for communication to the public, and to create an internal in-mission lunar science report for mission management. This evaluation included determining final STM coverage based on what planned and additional data were collected in mission. An STM objective was considered covered when the crew intentionally targeted a known feature that corresponded to that objective. By deliberately targeting a feature, the crew collected images, audio descriptions, and sometimes annotations, data types that the LST considered sufficient for addressing an STM objective. While in flight, the LST did not assess whether an STM objective was scientifically fulfilled (which would rely on the final returned catalog of scientific data); instead, it focused solely on determining operational completion.

4.0 LUNAR SCIENCE DATA SUMMARY

This section provides an overview of the lunar science data collected during the Artemis II mission, summarizing execution of crew observations guided by the LTP (**Section 4.1**) and the data products returned to and archived by the LST (**Section 4.2**).

4.1 As-Executed LTP Observations

The timeline of LTP observations as executed by the crew is displayed in **Figure 4.1**. The timeline was constructed from PCD audio recordings during the lunar flyby and identifies which crew member is making observations, and with which tool (by unaided eye or aided by the camera). All observation blocks map to targets defined in the LTP, excluding one annotated Impact Flash block that was completed by the crew (as confirmed in audio recordings), but could not be correlated to a specific time or duration.

The spatial distribution of crew images taken in support of the LTP is shown in **Figure 4.2**, which illustrates the footprints of the subset of images that could be georeferenced. Although only ~30% all crew images were able to be georeferenced (due to limitations in the algorithm from (1) affine transformation assumptions; (2) harsh illumination impacting feature correspondence matching; and (3) relative size-in-image of the lunar disk in low focal length, high-altitude images), this subset provides a useful depiction of the regions where handheld imaging was concentrated across the lunar surface during the flyby. The resulting pattern highlights the intentional use of varied focal lengths to support the mission's lunar science objectives. The mapped footprints demonstrate how crew image-acquisition strategies, combined with vehicle orientation and timeline planning, enabled targeted coverage of science targets and produced a dataset that directly supports post-mission analysis of Artemis II science objectives by the broader planetary community.

4.2 Types and Volumes of Data Collected

Science data from crew and vehicle observations collected during scheduled and serendipitous science events (**Section 1.2**) were received by the LST during the mission via downlink and post-mission via direct retrieval of returned data storage cards. **Table 4.1** shows a summary of the total number and volume of source data files curated by the LST. Science data were managed and processed according to the *Artemis II OSDMP,* and archived in the PDS, accompanied by the *Artemis II Lunar Science Data User Guide* prepared by the LST to describe the data products and archive structure in detail. A guide to these documents and their locations is provided in **Appendix 2**.

Crew images total more than 10,000 files, including those taken with the two handheld Nikon D5 cameras (Nikon RAW (NEF) file format), one Nikon Z9 camera (Nikon RAW (NEF) file format), and four iPhone 17 Pro Max cameras (DNG and JPEG file formats). Orion vehicle cameras acquired more than 1,000 still images, including from SAW Cam 2, 3, and 4 (JPEG format), Cab Cam 2 (JPEG format), OpNav (optical navigation) camera (TIFF format), and Docking Cam (PNG format). Operations of the OpNav camera and Docking Cam were not within the LST science plan, but are included in the data archive where relevant to the lunar science objectives (**Section 3.3**). SAW Cam 3 also acquired video (MP4 and MXF formats). Curated science mission audio includes audio recorded on crew PCDs during flyby observations (M4A format), on Orion-to-Earth (O/E) voice loops (MP3 format), and Nikon voice notes embedded on images (WAV format). Finally, crew annotations are available in PDF format from their source OneNote files.

In support of future Artemis lunar surface missions, temperature and humidity data obtained from data loggers within Orion sample storage lockers were provided to the LST and include measurements on the environmental conditions that may be expected for the storage of Artemis collected lunar samples. Measurements were acquired over the course of the mission and are available in CSV table format.

Source data listed in **Table 4.1** are included with detached metadata label files in the science data archive within the NASA PDS and, where necessary, were reformatted to comply with the required

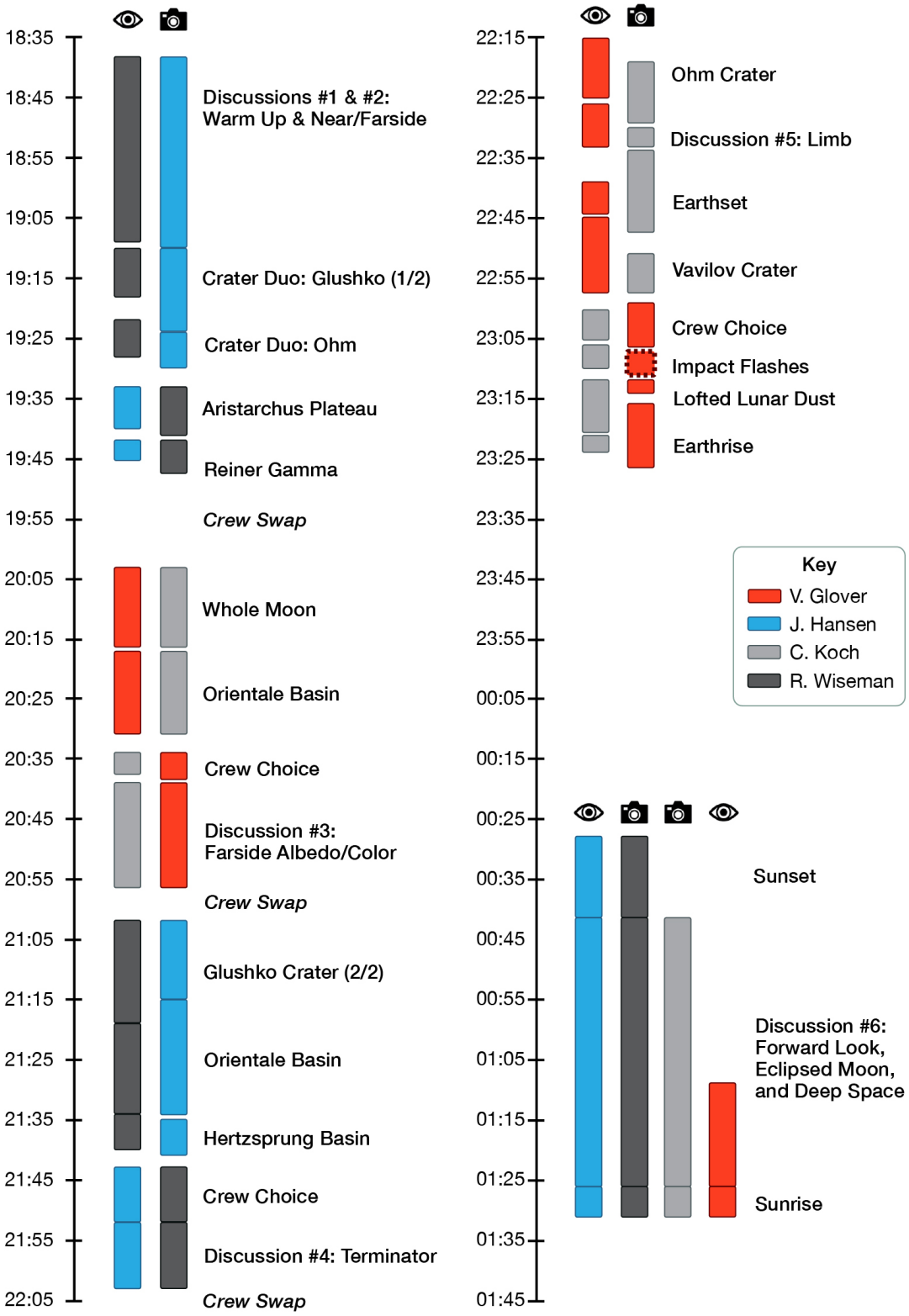


Figure 4.1: As-Executed Timeline. Graphical representation of the lunar flyby timeline, including LTP observation targets as executed by each crew member. The eye icon indicates the crew member making observations with the unaided eye; the camera icon indicates the crew member making observations with a camera. Times are in UTC and span Flight Day 06. Note: There was an observation break spanning 23:25:00–00:25:00 UTC.

Table 4.1: Science Data Summary. Science data received and archived by the LST, including the number, volume, and formats of files.

Total Mission Science Data	File Count	Volume (GB)	Source Format	Additional Archive Format
	11591	814.51		
Crew Camera (Serial Number)				
Nikon D5 (3500015)	7011	118.05	NEF	TIFF
Nikon D5 (3500017)	553	10.23	NEF	TIFF
Nikon Z9 (3920019)	2775	79.71	NEF	TIFF
iPhone 17 Pro	68	2.30	DNG, JPEG	TIFF
Total Crew Camera	10407	210.29		
Orion Camera (Still)				
SAW Cam 2	10	0.02	JPEG	TIFF
SAW Cam 3	189	0.50	JPEG	TIFF
SAW Cam 4	12	0.03	JPEG	TIFF
CAB Cam 2	176	0.39	JPEG	TIFF
OpNav	404	2.00	TIFF	TIFF
Docking Cam	249	0.20	PNG	TIFF
Total Orion Camera (Still)	1040	3.14		
Orion Camera (Video)				
SAW Cam 3 (Video)	22	598.20	MXF	MP4
Total Orion Camera (Video)	22	598.20		
Mission Audio				
PCD Audio	53	0.70	M4A	M4A
Orion/Earth 1, 2 Voice Loops	20	2.10	MP3	MP4
Nikon Audio	42	0.06	WAV	*see Notes
Total Mission Audio	115	2.86		
Mission (Other)				
Crew Annotations	5	0.02	OneNote, JPEG	PDF
Temperature/Humidity	2	0.00	CSV	CSV
Total Mission (Other)	7	0.02		

*Notes: For the data archive, the brief transcriptions of Nikon audio WAV files were added to the metadata of associated Nikon images. Separate transcripts in CSV and SRT format were also prepared for PCD and voice loop audio files.

formatting standards of the PDS. These additional archived data products are described in detail in the *Artemis II Lunar Science Data User Guide*. For each crew camera source image, the archive also includes a Nikon RAW (TIFF) image that preserves the original Bayer pattern and a de-mosaiced, processed TIFF image generated using Nikon NX Studio software. Orion camera source images with

compression (JPEGs and PNGs) were also processed into separate PDS-compliant TIFF files. Further, the LST received and prepared with the PDS, preliminary Orion spacecraft ephemeris, orientation, clock and camera and spacecraft geometry information in the form of archived PDS Spacecraft, Planet, Instrument, C-matrix, Events (SPICE) kernels. The LST anticipates subsequent PDS releases of the SPICE kernel will include refined Orion ancillary information as they are made available by mission teams. Complete science data archive and data product details are provided in the *Artemis II Lunar Science Data User Guide*.

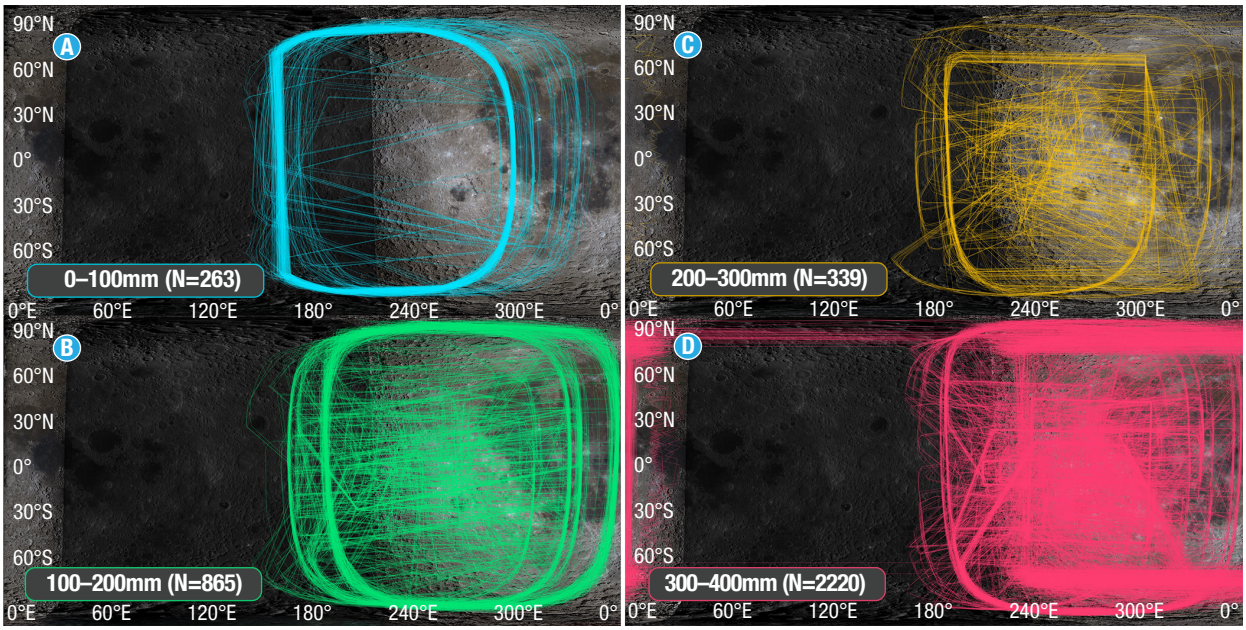


Figure 4.2: Distribution of Image Footprints by Focal Length. These maps display the spatial distribution of crew-image footprints *(extent of lunar surface visible in the image)* as a function of focal length bins, as well as the number *(N)* of images within each bin. The panels display images acquired at focal lengths between (**A**) *0 and 100mm (N=263)*, (**B**) *100 and 200mm (N=865)*, (**C**) *200mm and 300mm (N=339)*, and (**D**) *300mm and 400mm (N=2,220)*. This figure only includes images that the LST could georeference *(3,687 of 10,339 images or ~35% of all Nikon images)*.

5.0 SCIENCE DISCUSSION

This section highlights science data and preliminary discussions related to each of the ten science themes in the STM (**Table 1.1**). As noted in the **Foreword**, the level of detail of these discussions varies across themes, reflecting the data collected within the constraints of the Artemis II mission profile. These discussions showcase the richness of observations enabled by the Artemis II mission and highlight data relevant to each science theme, establishing a foundation for deeper community-led analyses. The full release of lunar science data to the PDS will support continued analysis by the public and external stakeholder communities, and the LST looks forward to future science discoveries enabled by the Artemis II data.

Scientific analysis of the Artemis II lunar science data relied heavily on crew observations, especially the voice recordings and their transcriptions (produced during the LST's first data-downlink shift). These verbal descriptions served as the primary scientific record for color, tone, brightness, and temporal changes in surface appearance, capturing nuances not recoverable from uncalibrated still images. Crew annotations were essential for capturing observational intent and correlating verbal descriptions and handheld images to specific lunar features. The accompanying Nikon camera images provided critical contextual support. They delivered a unique vantage point enabled only by human observers interpreting the lunar surface from Orion's position. The vehicle camera images and video added complementary

perspectives, both interior and exterior to the cabin, and offered an independent dataset with different sampling rates. Together, these data sources form a multi-layered observational record that strengthen scientific interpretation, as discussed in **Section 8.1**.

Crew Quotes and Mission Images: All crew quotations included in this section, unless otherwise noted, are from Flight Day 06, which spanned April 6, 2026, 14:50:12 to April 7, 2026, 15:35:12. Blue outlines around figures indicate images taken by the Artemis II crew or the Orion vehicle cameras. On occasion, the crew used clock-direction vernacular to describe positions of features. Orion pointing was nose-to-lunar-north (i.e., the docking-hatch window faced the approximate same direction as the lunar north pole). Crew orientation within the window, however, varied over time and between crew members, ranging from aligned with Orion (i.e., viewing the Moon as north-up) to anti-aligned (viewing the Moon as south-up). Therefore, it is important to interpret crew descriptions using the contemporaneous crew images.

5.1 Impact Flash Observations

The present-day cis-lunar environment is dynamic, with impacts from micrometeoroids, which are naturally occurring fragments of comets, asteroids, and planetary impact debris that travel through space. When these meteoroids strike the lunar surface, the kinetic energy of the impact creates seismic waves (Moser et al., 2015; Madiedo et al., 2019).

These impact events can be visible as a bright flash on the lunar surface and hence are observable from Earth and in cislunar space (Ortiz et al., 2000; Liakos et al., 2020). In at least three instances, Apollo astronauts recorded observing impact flashes from orbit: one impact flash during Apollo 16 and two flashes during Apollo 17. According to NASA's Meteoroid Environment Office (MEO), at the time of this writing 443 impact flashes have been observed by Earth-based telescopes through a variety of observing campaigns, and NASA's Lunar Reconnaissance Orbiter (LRO) spacecraft has documented multiple new impact craters that have formed since its launch in 2009 (Moser et al., 2015; Sheward et al., 2022, 2025; Rizos et al., 2026).

Given previous observations of impact flashes during Apollo (NASA, 1972a, 1972b), plus ground-based observations and LRO datasets (e.g., Suggs et al., 2014; Moser et al., 2015; Sheward et al., 2022, 2025; Rizos et al., 2026), the LST strategically planned observation time for impact flash surveys, both by crew (**Appendix 1**) and by the Orion vehicle exterior cameras. More specifically, the crew had dedicated time scheduled to observe impact flashes as a specific LTP target and during the eclipse period of the flyby. The eclipse period enabled observations at a time when the Sun was eclipsed behind the Moon. This provided dark viewing conditions with the Moon not directly illuminated by sunlight (only partially lit by earthshine) and removed any direct sunlight within the crew's field of view (FOV), which aided with dark adaption for the crew's eyes to adjust and be able to see fainter phenomena. Furthermore, the crew were trained to report any impact flashes observed at any point during the mission, even outside of scheduled surveys.

Additionally, a coordinated Earth-based observation campaign was also undertaken, including the MEO at NASA's Marshall Space Flight Center through the Lunar Impact Flash Monitoring Program and complemented by an SMD citizen science campaign to increase public engagement and observing opportunities (**Section 6.2**). Earth-based observations were optimized to collect data near the times of the Artemis II crew observations, though this was not always possible given that ground-based observations require views of shadowed (non-illuminated) lunar terrain, which were not always present from the vantage point of Earth during the crew's lunar flyby.

5.1.1 Characterizing Impact Events

Observations of impact flashes (or a lack thereof) during dedicated observation periods help characterize the modern impact environment and the scale of what may be observable from cis-lunar space. Of particular interest are constraining the meteoroid size and frequency distributions, as well as

the timing, location, and brightness of individual flashes. The frequency distribution of impact flashes across the lunar surface can help constrain the impactor flux as a function of geographic location on the Moon (Ortiz et al., 2006). The frequency of flash observations, correlated with the presence (or absence) of known meteor showers during the observing periods, can provide insight into the sources and rates of the flashes (Madiedo et al., 2015; Ortiz et al., 2002; Liakos et al., 2024). The timing and location of flashes also enable follow-up studies to possibly image and characterize resulting craters and to investigate impact-crater processes. In addition, analysis of the observational data can reveal whether and how future measurements might constrain the seismic source and timing of impacts, especially once ground-based geophysical instrumentation is on the lunar surface. The brightness (or intensity) of the flash itself can be correlated with the size of the impactor and resultant energy of the impact event (Bellot Rubio et al., 1998). For Artemis II, the strongest impact-flash-related dataset is the number of observed impact flashes (i.e., their frequency distribution).

The Artemis II impact-flash observation campaign was designed to inform techniques for future observations and guide subsequent science investigations. For example, the statistics of impact-flash detections made by the crew, correlated with corresponding observing time, provide data on the detection frequency and probability for varying observing durations on future missions. These results can support the planning of observing surveys on crewed missions, as well as the selection of optimal detector systems for future flight missions. Additionally, the observing assets on Artemis II may constrain the expected frequency and magnitude of future impact flashes, thereby informing detection limits for future observations and highlighting the potential value of additional observing techniques, such as a dedicated automated flash-detection camera with increased sensitivity and/or resolution (**Section 9.7**). Overall, impact flash observations will contribute to future Artemis mission planning by improving understanding of the cis-lunar space environment and present-day meteoroid activity.

5.1.2 Impact Flash Observations

Five distinct impact flashes were reported by the crew during the period of the solar eclipse as seen from the vantage point of the Orion spacecraft. The crew possibly observed several additional impact flashes but did not formally report them. Crew members reported flashes in the crew PCD audio files, through O/E audio communication live during the flyby, and via an annotated image that was prepared by the crew and downlinked to the LST after the flyby on which the crew marked their approximation of where the five confirmed flashes were located on the lunar surface (**Figure 5.1**). Several of the flashes were observed simultaneously by multiple crew members, cross validating the observations as true impact-flash detections.

All definitive flashes observed by the crew were seen during the lunar eclipse period of the lunar flyby, and no flashes were associated with any color. All the impact flashes were observed on the non-illuminated portion of the Moon, and no flashes were reported in earthshine during the eclipse. No flashes were observed when any portion of the Moon was illuminated by the Sun; therefore, these flashes are likely the faintest ever observed by human eyes, suggesting small impactors on the order of several cm in diameter. Artemis II flew during a low meteoroid flux time of year outside of any major annual meteoroid streams, and thus these observations place a lower bound on the impact flux at the lunar surface.

The first impact flash was reported by R. Wiseman:

> I just saw a flash! 100% I just saw flash! 100% it was on the like if you go right to the center point, it was at the 7 or 8 o'clock. (R. Wiseman, camera, PCD crew audio, art002a000052, 00:41:01 UTC)

Shortly after, R. Wiseman and J. Hansen reported observing the same impact flash:

R. Wiseman	Oh, I just saw another meteorite. 100%. Just saw a meteorite.
J. Hansen	Did you see it in the, was it lower?
R. Wiseman	Yeah. Yup.
J. Hansen	Like a third from the bottom, up from the bottom?
R. Wiseman	Yeah.
J. Hansen	Yup.
J. Hansen	But it's a pinpoint of light.
R. Wiseman	Yup.
J. Hansen	It's not like a meteor, you didn't see anything else, it's just like a bloop.
R. Wiseman	Yeah.
J. Hansen	So, Reid and I both saw the same thing there. We saw an impact flash. It wasn't very big. For me it was a pinprick. It was about a third of the way up from the bottom of the Moon for us.

R. Wiseman, camera, and J. Hansen, unaided eye, PCD crew audio, art002a000052, 00:51:15 UTC)

During the post-flyby crew conference between the crew and the Science Officer on Flight Day 07, the crew described that these observations were reported as impact flashes because they were distinct from other transient phenomena, such as cosmic ray hits to the eye or spacecraft glint. During the conference, the crew also reported that more flashes may have been observed than were recorded. The crew intentionally did not include any ambiguous flashes in their annotation (**Figure 5.1**), thus lending more credence to the validity of the reported detections.

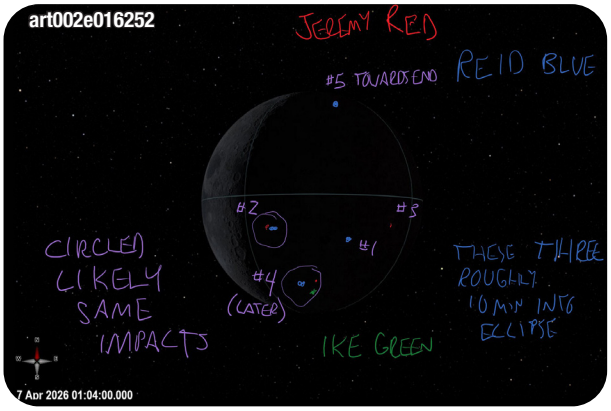


Figure 5.1: Impact Flash Annotation. Annotation art002e016252 made in-flight by the Artemis II crew showing general locations of reported impact flashes observed by R. Wiseman (blue), J. Hansen (red), and V. Glover (green). Purple was used for annotation and not representative of a specific crew member.

The MEO at Marshall assessed a SAW Cam 3 video that recorded for ~2 minutes during the lunar eclipse at its highest frame-rate setting (30 frames/second). No impact flashes were detected in this dataset, though the video covered a limited time period. Additional details on this SAW Cam 3 video are available in the *Artemis II Lunar Science Data User Guide*.

The LST also collaborated with the LRO team and determined that potential follow-up observations of new craters formed from the crew-observed impact-flash events are probably infeasible since the impact crater size is likely too small to be resolvable by the LRO Camera (LROC). Additionally, information related to impact flash locations from visual crew observations is insufficient for LRO targeting purposes.

5.2 Color Provinces and Albedo Variations

Crew data related to color provinces and albedo variations help address what humans can uniquely perceive at the Moon and provide information on lunar geologic features. Because none of the handheld or vehicle camera images were calibrated for this mission, analysis of color and photometric characteristics are necessarily qualitative. The crew's verbal descriptions of color serve as the primary science data for this theme. The accompanying crew images acquired during their verbal descriptions provide critical geologic context, including relative color and albedo properties (**Figure 5.2**), morphological



Figure 5.2: Lunar Color and Albedo Variations. Color-stretched image (modified crew image art002e010014) showing the nearside-to-farside transition. The color-stretch enhancement emphasizes the browns and greens across the Aristarchus Plateau described by the crew.

context, and spatial reference, but cannot independently be used to quantify color or albedo across the mission dataset.

The LTP included a variety of dedicated targets to explore the color and albedo diversity of the Moon, including swirls (Reiner Gamma), geologically young highlands regolith (Glushko and Ohm crater ejecta), geologically older highlands materials (Hertzsprung basin, Vavilov crater, Orientale basin), and volcanic materials (Aristarchus Plateau, host terrain of Reiner Gamma, maria in Orientale basin) (**Appendix 1**). The LTP also included several discussion periods with themes centered on color and albedo, including comparisons between nearside and farside maria, as well as observable patterns and variations in farside highlands, along the terminator, and along the limb (**Appendix 1**). Additionally, the crew collected a unique set of color data observing, describing, and imaging the Moon during the eclipse (**Section 5.2.3**). During the eclipse, the Sun was located behind the lunar disk and the only illumination on the Moon was earthshine, which has a unique color spectrum in comparison to solar illumination. Finally, the color and albedo of non-lunar-surface features were investigated with LTP targets of impact flashes (**Section 5.1**), lofted lunar dust (**Section 5.5.1**), Earth (**Section 5.10**), Mars and other planets (**Section 5.5.2**), zodiacal light (**Section 5.5.2**), and the solar corona (**Section 5.5.3**) (**Appendix 1**).

Additional data related to color and albedo were collected during the post-flyby crew conference, as discussions between the crew and Science Officer included how the presence of Earth affected the crew's perception of lunar color and brightness (**Section 5.2.4**). Discussions of how the crew's perception of color and brightness changed over the course of the flyby in response to their viewing geometry are included in **Section 5.3**, and discussions of how non-lunar brightness and color (e.g., from the, Sun, cabin lights, and cabin equipment) impacted the crew's observations are in **Section 7.2**.

5.2.1 Color/Albedo Associated with Different Physical and Compositional Properties

Multiple factors affect the color/albedo of the lunar surface, including physical properties (e.g., terrain roughness, regolith texture, rock abundance, surface temperature) and compositional properties (e.g., mineralogy). The descriptions made and images taken by the crew provide valuable qualitative data that can be used to correlate observed color/albedo variations with existing physical and compositional datasets of the lunar surface. The crew's observations and images span a deliberately diverse set of targets that represent a range of physical characteristics (e.g., from smoother maria to rougher highlands; from older, more degraded crater materials to younger, rougher crater materials) and a range of compositional provinces (e.g., from felsic highlands to mafic mare basalts to non-mare volcanic terrains).

Initial discussions correlating crew color/albedo observations with physical and compositional properties appear in **Section 5.4.3** (high-albedo associated with fresh materials), **Section 5.4.4** (color/albedo variations associated with crater and ejecta properties), **Sections 5.4.4**, **5.9** (color variations related to impact melt and mare compositional differences), and **Section 5.9.2** (color variations associated with non-mare, volcanic diversity), and in the remainder of this section, via a discussion of Orientale. Overall, the diversity of Artemis II data collected in support of the LTP enables future studies to examine in detail how surface properties manifest in color and brightness when viewed by humans from orbit.

Correlation of remotely sensed data with Artemis II data can also help place the crew observations of color/albedo into broader geologic context. As an example, the LST synthesized Artemis II data of Orientale basin with independent orbital datasets acquired by the LRO and Clementine spacecraft to provide the foundation for an integrated physical and compositional interpretation of the basin (**Figure 5.3**). Orientale (also discussed in **Section 5.4.4.1**) is a ~950-km-diameter multi-ring basin

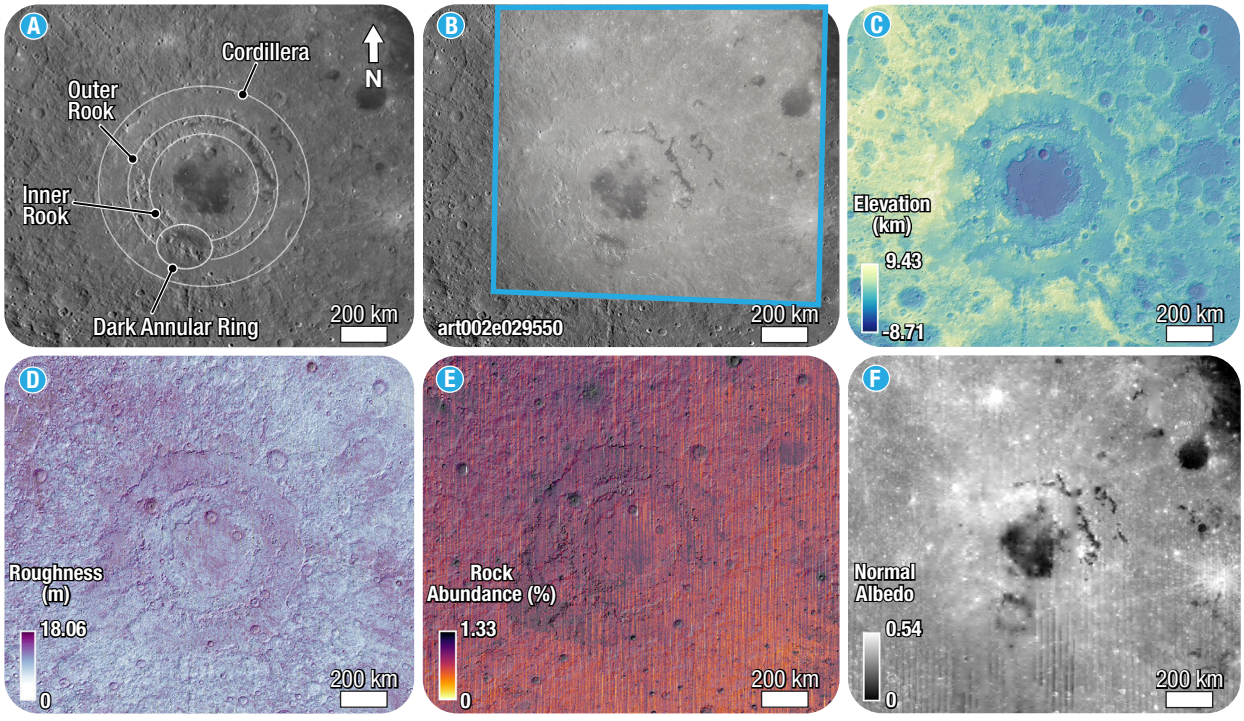


Figure 5.3: Orientale Basin Seen By Multiple Instruments. This compilation shows a variety of remotely sensed data for Orientale basin. (**A**) Annotated LROC WAC Global Morphologic Mosaic (Speyerer et al., 2014) annotating the boundaries of Orientale basin's Inner Rook, Outer Rook, and Cordillera rings, as well as Orientale's dark annular ring. (**B**) Crew image art002e029550 overlaid on the LROC WAC Global Morphologic Mosaic. (**C**) LOLA-derived topography (Barker et al., 2016) overlaid on LOLA DEM-derived (digital eleveation model) shaded relief. (**D**) LOLA-derived surface roughness (Smith et al., 2010) overlaid on LOLA DEM-derived shaded relief. (**E**) LRO Diviner Radiometer-derived rock abundance (Bandfield et al., 2015). (**F**) LOLA-derived albedo map (Lemelin et al., 2016).

centered on the western edge of the lunar nearside. It is one of the youngest and best-preserved basins on the Moon and exhibits large-scale morphological and compositional diversity. The crew provided verbal descriptions, images, and annotations of Orientale that captured nuances in basin structure, texture, and color.

Related to structure, J. Hansen described how "looking back at the eastern wall of Orientale, [...] there are like cliffs, absolute cliffs. It's like it just dropped, the whole basin just dropped straight down there. That shelf is amazing" (J. Hansen, camera, PCD crew audio, art002a000039, 21:19:11 UTC, 21:20:40 UTC).

J. Hansen also described variations in the degree of ring preservation:

> And then you go out and you can see collapsed wall on the western edge. It's collapsed and it's gone halfway to that inner ring. And so, you just don't see the elevation there. It's all collapsed. Same in the south and the southeast. But when you get to the eastern wall, from 3 o'clock to 11 o'clock really, it hasn't collapsed. It's just still -- the walls are still intact. And they haven't filled in that floor nearly as much. There's some collapse there. It's just so neat. (J. Hansen, camera, PCD crew audio, art002a000039, 21:21:20 UTC)

The drastic relief and cliffs, as well as differences in ring degradation between the eastern and western halves of Orientale that J. Hansen described are evident in LRO Lunar Orbiter Laser Altimeter (LOLA)-derived topographic data (**Figure 5.3C**).

Related to texture, the crew defined several regions within Orientale with distinct textural properties. Starting central to the basin, the crew noted:

> The texture in the inner basalt filled center is very smooth, and it only gets rougher from there. After the basalt area [of Mare Orientale], there is a rim that has a little bit of a rougher texture. There's some more little [basalt] infills there, here and there. (C. Koch, camera, PCD crew audio, art002a000006, 20:22:37 UTC)

This textural change is apparent in the LOLA-derived roughness map (**Figure 5.3D**), but not in the LRO Diviner-derived rock abundance map (**Figure 5.3E**), suggesting that the scale of texture differences observed by the crew is related to hectometer-scale terrain properties to which LOLA is sensitive, rather than the distribution of 1–2 m-scale rocks to which Diviner is sensitive.

Continuing outward from the basin center, the crew reported "the texture changes from a very smooth texture inside [the Cordillera ring] to a rough, almost mossy-looking texture that has some very much green tones to it" (C. Koch, camera, PCD crew audio, art002a000006, 20:21:42 UTC). The rings themselves were described as "almost hummocky" (C. Koch, camera, PCD crew audio, art002a000006, 20:25:41 UTC), with the Cordillera ring being "much more pillowy" than either Rook ring (R. Wiseman, unaided eye, PCD crew audio, art002a000024, 21:38:02 UTC). Beyond the rings, the crew noted "there's a lot of texture in the rays that are south of Orientale" (C. Koch, camera, PCD crew audio, art002a000005, 20:05:24 UTC) and "the pillowing, the blanketing of ejecta [...] almost looks like a windswept desert, but nothing like a dune" (R. Wiseman, unaided eye, PCD crew audio, art002a000024, 21:27:46 UTC). These crew-reported morphologic characteristics related to texture, in conjunction with remotely sensed data, could be used to define map units, and to investigate geologic processes responsible for creating and altering these textures and morphologies.

Related to color of the basin, the crew noted regional "shades of gray" (R. Wiseman, unaided eye, PCD crew audio, art002a000024, 21:21:42 UTC), "brownish hues" (J. Hansen, camera, PCD crew audio, art002a000039, 21:29:40 UTC), and a "kind of a tannish" that appeared "more tan" toward the central maria (C. Koch, camera, PCD crew audio, art002a000005, 20:05:33 UTC). As noted previously, the Cordillera ring was reported to have green tones "almost like swamp-like colors, there's almost even some green in there" (C. Koch, camera, PCD crew audio, art002a000005, 20:11:16 UTC), and

that these colors were "most apparent in -- the valleys of all of the rings" (C. Koch, camera, PCD crew audio, art002a000006, 20:25:14 UTC). Compositional data of the basin could provide insight into whether these green tones correspond to compositionally distinct units. Additionally, V. Glover reported "dusted peaks" and "white on the very edges of [the mountains], the spines, the ridgebacks" (V. Glover, unaided eye, PCD crew audio, art002a000035, 20:17:03 UTC, 20:18:23 UTC) that could be related to reflective regolith properties or sunlight reflecting off topographic highs.

Related to color and albedo of the maria within Orientale, the crew reported "the inner darker Mare [Orientale] has some, some complexity to it," with variations in gray, where "the darkest part looks like an M or maybe a W" (V. Glover, unaided eye, PCD crew audio, art002a000035, 20:17:18 UTC, 20:17:44 UTC). The crew described maria associated with the Outer Rook and Cordillera rings as being "the darkest mare [deposits]" (C. Koch, camera, PCD crew audio, art002a000006, 20:22:14 UTC) in their view, and that the southern portion of Mare Orientale as almost as dark. Crew-reported albedo characteristics such as these, compared to what is recorded in their Nikon images and in remotely sensed data, may provide insights into how to interpret and correlate qualitative perception of color to more quantitative measurements, such as measurements of surface reflectance made by the LOLA at 1064 nm (**Figure 5.3E**).

Overall, the qualitative integration of Artemis II data with orbital datasets for Orientale demonstrates that the crew's observations are consistent with and provide human-eyewitness context for existing interpretations derived from orbital datasets. Future studies and geologic analyses can build on these comparisons to explore how human observations enrich, and are enriched by, remotely sensed datasets through the detection, interpretation, and contextualization of surface variations from orbit.

5.2.2 Albedo Anchors Used for Orienteering and Comparisons

The crew frequently used relative-albedo reference points (such as the darkest or brightest features in view) to anchor their descriptions of surrounding features. They implemented a simple quantitative scale, where one indicated the darkest feature and ten indicated the brightest. This approach proved effective, as it established a shared vocabulary between crew members throughout the flyby, supported inter-crew consistency checks, and enabled comparisons between known reference points as the crew used these anchors to contextualize nearby features. On the darkest end of the spectrum, the crew consistently used Grimaldi as an anchor, and on the brightest end of the spectrum, the crew typically established Byrgius A, Glushko, and Aristarchus as anchor points.

Human perception of albedo is dependent on FOV, viewing geometry, and visual adaptation, all of which were evident in the observational data. The crew member using a camera had a narrower FOV and therefore fewer reference points than the crew member viewing the surface with the unaided eye, explaining why crew using different tools sometimes perceived relative darkness in different ways. Viewing geometry (i.e., changes in the observer's position and illumination angles, which affect the degree of shadowing and contrast), also influenced the apparent brightness and contrast of features, which is discussed in detail in **Section 5.3**.

Throughout the flyby, the crew identified and described several locations on the lunar surface using brightness characteristics. Their observations highlight that brightness variations served as a primary visual cue for feature recognition during surface observations, suggesting that high-albedo features may be effective navigation references for future orbital observational campaigns. Additionally, the crew's observations illustrated that feature detectability was influenced by brightness characteristics, rather than physical size alone. The smallest features observed by the crew (>~6 km in diameter; discussed in detail in **Section 7.3**) were typically identified due to their high-albedo properties:

> And then there are two new craters on the farside regolith and right in the center is Glushko. Uhm, anyway, you'll never find that on a map. Out near where we named Integrity off the 12 o'clock of Orientale, there's just a spot of white. It's probably a new crater, but I can't see

a crater here. To me, it just looks like a spot of white. And that albedo is very similar to [the albedo of] Glushko, but that albedo is whiter than [the albedo of] Glushko. (R. Wiseman, unaided eye, PCD crew audio, art002a000019, 19:15:22 UTC)

And then between Orientale and that very defined crater in the ray system, there is a white spot that's a one [on the] albedo [scale]. It's a little more north of the center line between these two features, but it is a very high albedo, but no ray system, no rays at all. (V. Glover, unaided eye, PCD crew audio, art002a000035, 20:23:55 UTC)

5.2.3 Color/Albedo Under Earthshine

Earthshine is the combined irradiance from reflected sunlight and thermal emission from Earth and can provide an illumination source for the Moon and other objects in space (e.g., Goode et al., 2003; Glenar et al., 2019). On the Moon, earthshine is typically dwarfed by the irradiance from sunlight, but Orion's configuration during the Artemis II eclipse viewing provided the crew with a unique opportunity to observe earthshine on the Moon (**Figure 5.4**), as the Sun was hidden directly behind the Moon and the only direct illumination on the visible lunar surface was earthshine.

Earthshine has a unique spectral radiance that can affect human perception of color and albedo. For example, Earth reflects a bluer light than the Sun primarily due to Rayleigh scattering in its atmosphere (Woolf et al., 2002; Goode et al., 2003), which could bias color perception toward cooler, blue-shifted tones. At the same time, earthshine has a substantially lower illuminance than sunshine, which could reduce the crew's ability to resolve color variations or albedo contrasts that are perceptible under sunlight. The lack of direct sunlight could also flatten the apparent albedo of the landscape, making it appear dimmer and more uniform (Hurlbert & Yu, 2025), as no shadows are present to reveal topography and help calibrate the eye to surface brightness.

Comparing images of the Moon acquired under solar illumination to those taken during the eclipse shows the influence of earthshine on the tonality of the lunar surface. **Figure 5.5** shows the difference in the distribution of RGB pixel values (in digital number; DN) for a Nikon Z9 image acquired outside of the eclipse and a Nikon Z9 image acquired during the eclipse. When sunlit, the Moon reflects all three colors measurable by the Z9 camera sensor in nearly equal amounts; the histograms of each RGB channel in **Figure 5.5B** are nearly completely overlapping and have median pixel values of 114, 113, and 114 DN, respectively. The Sun emits light in near-equal quantities across the visible spectrum, so this RGB histogram matches the expectation of reflected sunlight. In the eclipse period however, there was no direct sunlight illuminating the lunar surface from the vantage point of the crew, only

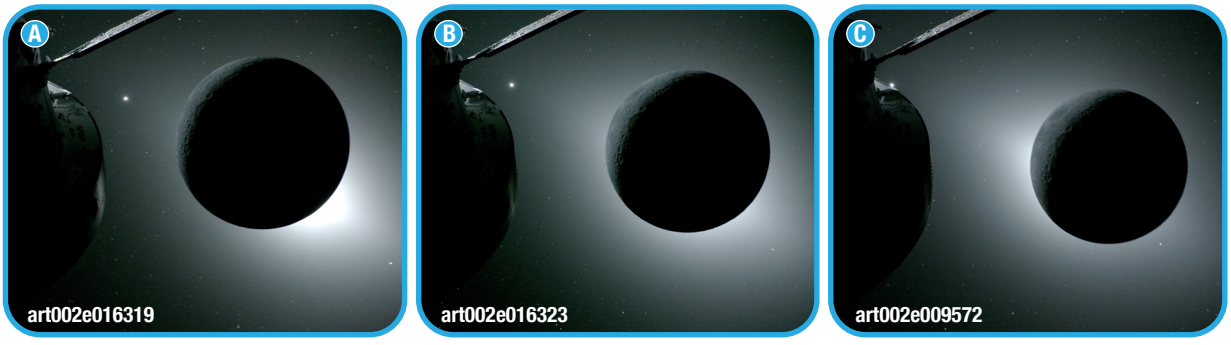


Figure 5.4: Earthshine on the Moon. Vehicle camera images (**A**) art002e016319 acquired on April 7, 2026, 00:41:24 UTC, (**B**) art002e016323 acquired on April 7, 2026, 00:56:19 UTC, and (**C**) art002e009572 acquired on April 7, 2026, 01:11:14 UTC, provide views of changes in earthshine across the eclipse, from outside the influence of the Orion cabin. These images were acquired utilizing night imaging settings with the illuminator off and a night photo mode with exposures of 10 seconds.

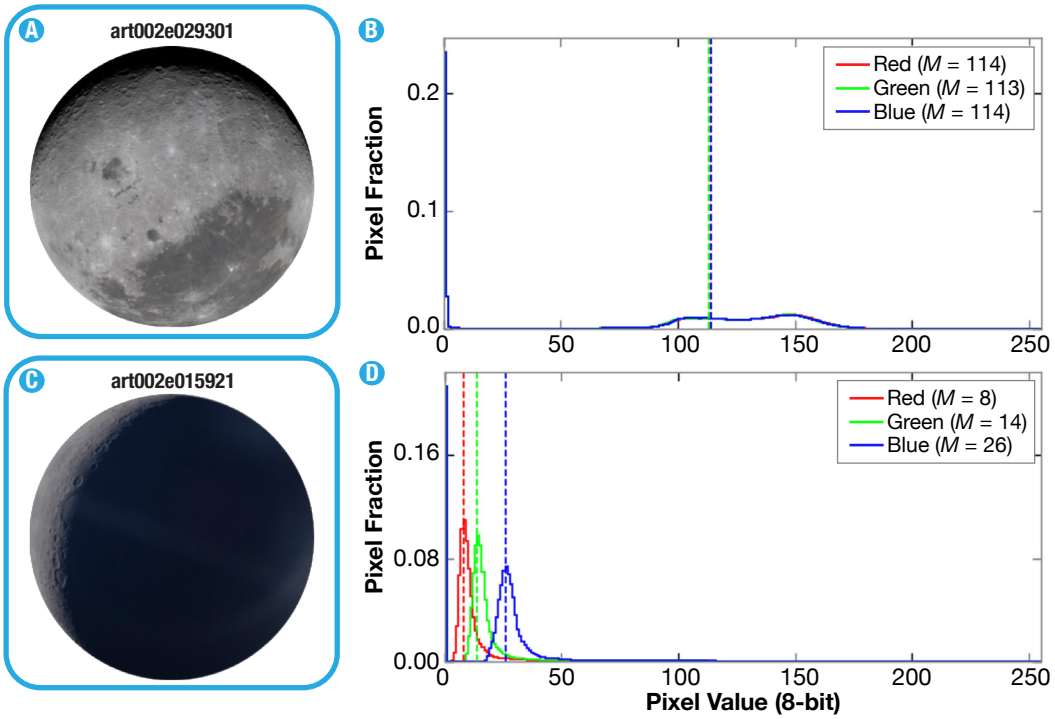


Figure 5.5: Tonality of the Moon. These plots show the distribution of pixel values (DN) for RGB channels (**B**,**D**) for sample images of the lunar surface acquired when the Moon was (**A**) illuminated by the Sun (crew image art002e29301) and (**C**) illuminated only by earthshine (crew image art002e15921). Median values (DN) of red, green, and blue bands are shown in each histogram legend. Histograms are created by cropping the lunar surface from each crew photo, splitting the image into red, green, and blue bands, then binning the intensities of all pixels in each band.

earthshine, and a different RGB histogram is captured in the crew images. In the histogram for this Moon image (**Figure 5.5D**), blue tones register higher pixel values (a measure of intensity), indicating that the earthshine has predominantly bluer tones.

Throughout the eclipse, the crew made several independent descriptions of earthshine on the lunar surface, describing it to be "very distinct" (V. Glover, unaided eye, PCD crew audio, art002a000045, 22:39:56 UTC) and "really clear" (J. Hansen, unaided eye, PCD crew audio, art002a000052, 00:38:56 UTC). The fraction of the Moon illuminated by earthshine appeared to increase from "an eighth of the Moon" (J. Hansen, unaided eye, PCD crew audio, art002a000052, 00:38:57 UTC) at the start of the eclipse to "probably 20%" (R. Wiseman, camera, PCD crew audio, art002a000053, 01:10:50 UTC) or "a quarter Moon" (J. Hansen, unaided eye, PCD crew audio, art002a000052, 01:03:27 UTC) thirty minutes later. The crew's fractional estimates are very well-aligned with the true fraction of the visible disk that was illuminated by earthshine at this time (**Table 5.1**), suggesting that the increase in earthshine reported by the crew was not an artifact of their eyes adjusting to the illuminated fraction over time.

The crew were not able to able confidently discern any lunar features illuminated by earthshine, noting difficulties in their eyes adjusting. Only at the very end of the eclipse did the crew begin to recognize large-scale features, as V. Glover reported that they "aren't able to distinguish which [maria are visible]," but they "can clearly see mare [deposits] in the earthshine" (V. Glover, O/E-1 voice loop, 01:17:18 UTC). R. Wiseman concurred: "Yeah, I cannot tell you which ones we're seeing, but I can definitely see [maria] over there [on the face of the Moon illuminated by earthshine] now" (R. Wiseman, camera, PCD crew audio, art002a000053, 01:17:09 UTC).

V. Glover reported that "the camera settings for earthshine are challenging. This [view is] challenging to capture. What we're seeing, we're just not picking up on the cameras" (V. Glover, O/E-1 voice

loop, 00:50:18 UTC). These images, though challenging to capture, hold important scientific value in characterizing the properties of earthshine (**Figure 5.6**). Earthshine provides a measure of Earth's albedo, a major factor in the energy budget driving Earth's climate (Goode et al., 2021). The images can be used to constrain earthshine brightness and how it varied over time, potentially contributing to calibration of terrestrial and remote sensing measurements, which contend with artifacts including atmospheric extinction and sensor drift.

Table 5.1: Evolution of Earthshine's Extent. This table compares the modeled fraction of the visible disk illuminated by earthshine compared to that reported by the crew during their eclipse observations, as a function of time. Crew observations are rounded to the nearest 5-minute increment.

Time (UTC)	Modeled	Reported by Crew
00:35:00	0.1460	-
00:40:00	0.1580	There's an eighth [0.125] Moon on the earthshine. (J. Hansen, unaided eye, PCD crew audio, art002a000052, 00:38:57 UTC)
00:45:00	0.1699	-
00:50:00	0.1816	As far as earthglow goes, it's now up to about an eighth [0.125] of the Moon, I guess. (J. Hansen, unaided eye, PCD crew audio, art002a000052, 00:48:45 UTC)
00:55:00	0.1931	-
01:00:00	0.2043	-
01:05:00	0.2153	We're about a quarter [0.250] Moon. (J. Hansen, unaided eye, PCD crew audio, art002a000052, 01:03:27 UTC)
01:10:00	0.2261	I'd say probably 20% of the left side of the Moon is lit up in earthshine. (R. Wiseman, camera, PCD crew audio, art002a000053, 01:10:50 UTC)
01:15:00	0.2366	-
01:20:00	0.2468	-
01:25:00	0.2568	-



Figure 5.6: Earthshine Views. This comparison shows views of earthshine during the eclipse, including from (**A**) crew image art002e015921, (**B**) vehicle image art002e16321, and (**C**) a scientific visualization created by the LST. Crew and vehicle images were acquired within a three-minute interval of one another, and the visualization was modeled to for a time in between.

Finally, it is also possible that earthshine affected crew observations outside of the eclipse. At the start of the flyby, R. Wiseman reported:

> Something is causing the right half of the Moon to do something different than the left half of the Moon. And if I look hard out the right window, it's Earth. And we can see Earth, and we can see one planet, and Earth is a little crescent. Earth is so bright, the clouds and the Sun glint off the ocean of Earth. I cannot see any color on Earth right now. I just, Earth is almost like blindingly bright. And now I'm looking back to the Moon, and the Moon is not as bright as Earth. Significantly not as bright as Earth out these two windows. So, that is really cool to be able to just look out and compare and contrast. (R. Wiseman, unaided eye, PCD crew audio, art002a000017, 18:47:53 UTC)

5.2.4 Comparisons of Color/Albedo Between the Earth and the Moon

The conjunction of the Earth and Moon during the lunar flyby enabled direct comparisons between the two bodies. As soon as the start of lunar flyby activities, the Earth was visible to the crew out of at least one window. C. Koch reported on the comparative brightness of the Earth's and Moon's surfaces in an early SitRep:

> It's interesting because the Earth looks way brighter, so the Earth itself seems to have a much higher albedo than the Moon. We think this is independent of our eyes focusing because, of course, the Earth is much smaller than the Moon in our view. (C. Koch, O/E-1 voice loop, 18:48:44 UTC)

Later on in the flyby, Earth and the Moon were observable in a single view through the observing windows. Before earthset and after earthrise, Earth was notably covered by distinctively bright clouds, which increased Earth's albedo and reflectiveness (**Figure 5.7**). At the beginning of earthset, V. Glover commented on the color differences between the Moon and Earth. With both planetary bodies in the same view, he described how having the bright Earth in his view drowned out any color subtleties that his eye could otherwise have perceived on the lunar surface:

> And you're not able to pick up colors on the Moon, but now with the brightness of the Earth in the background and the swirls and the colors all in the Earth, even the few that we can see from here, it definitely drowns out anything that I can pick up in the Moon. (V. Glover, unaided eye, PCD crew audio, art002a000045, 22:40:25 UTC)

C. Koch further described how the brightness of the Earth impacted observations of the Moon:

> The Earth being so bright it -- it does really make the Moon look dark, but it doesn't look blue. It just looks -- it actually kind of looks grayish blue, almost more almost like black and white. […] I think it's just because it's so bright, but we are seeing an absolutely gorgeous landform. […] Here [the Earth] comes. The first bit is going to touch the Moon. It's behind. The first lit part [of Earth] is behind [the Moon]. It actually looks like it's going over the edge because it's so bright. It looks like it's punching into the wind. There it is. Now it finally looks like it's behind. It's so beautiful. So beautiful. (C. Koch, camera, PCD crew audio, art002a000011, 22:39:40 UTC)

When describing earthset in the post-flyby crew conference, C. Koch described the Earth as "a sponge of light" (C. Koch, O/E-1 voice loop, 19:16:21 UTC, Flight Day 07). The crew reported that the presence of Earth in the same FOV as the Moon made the lunar surface appear duller after earthrise, though some colors were still visible:

> [The Moon] got like a browner […] taupe color, like almost an olivey brown, kind of like the boys' pants. Not like my pants, but like these pants [*pointing to crew members' pants*]. And whereas before, I would have said it was more like electric gray in its grayer areas. So, for me, it turned more brown, but a very matte brown. (C. Koch, O/E-1 voice loop, 19:16:47 UTC, Flight Day 07)

Nuanced brightness and color observations such as these highlight the value of having humans make visual assessments alongside image acquisition. The unique capabilities of the human eye and the perspective of the Artemis II crew allowed the collection of verbal science data that images alone could not fully capture.

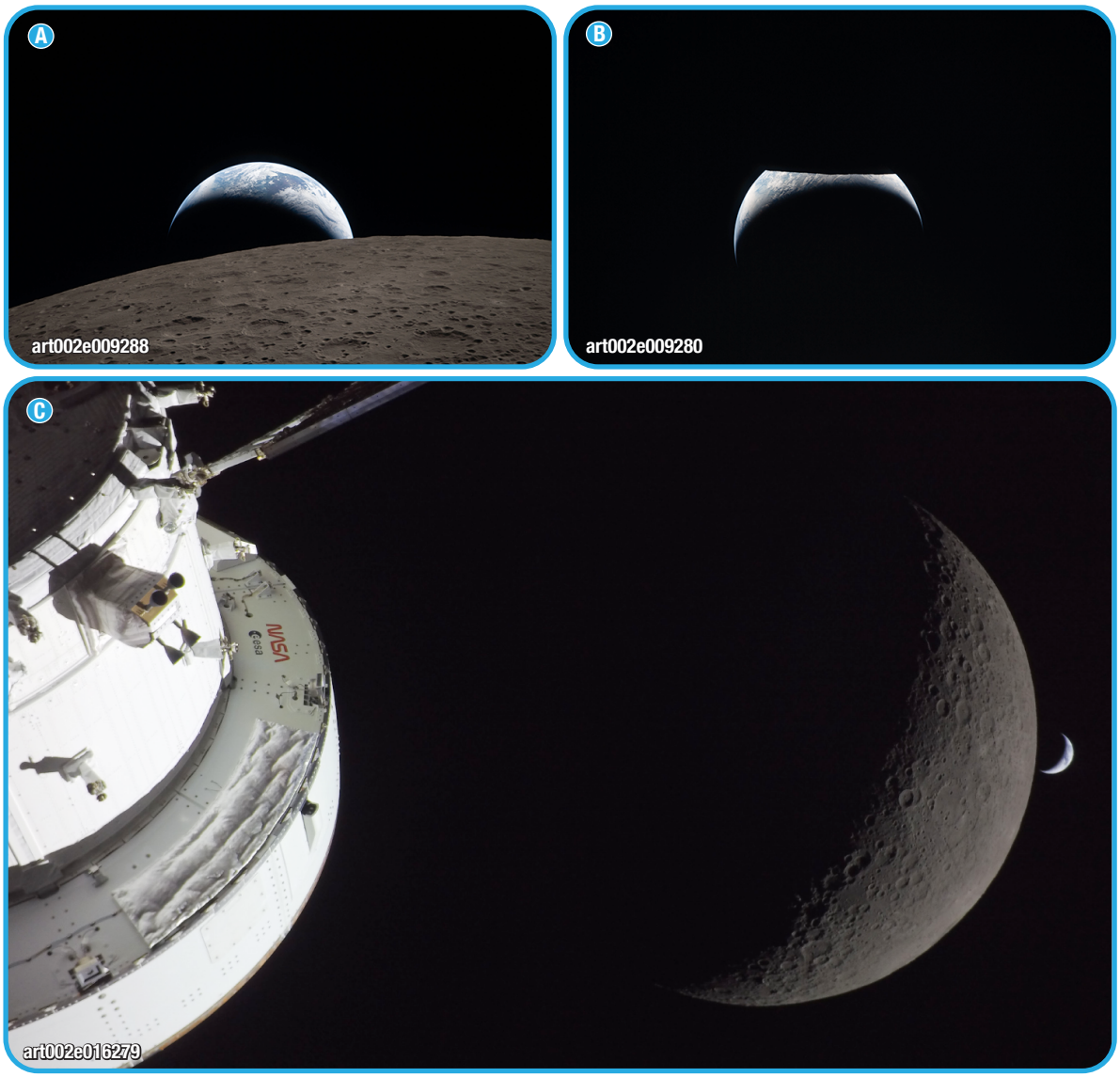


Figure 5.7: Earthset and Earthrise. Crew-captured images show (**A**) earthset (crew image art002e009288) taken on April 6, 2026, and (**B**) earthrise (crew image art002e009280) captured 40 minutes later. (**C**) The vehicle camera image art002e016279 provides an exterior context view of earthset, outside the influence of Orion's windows.

5.3 Photometric Observations

Over the course of the lunar flyby, the crew's view of the Moon was naturally affected by varying illumination conditions and viewing geometries (including phase and emission angles). As part of the LTP, the crew conducted repeat, phase-dependent observations of key features, generating perceptual data capturing how color, tone, brightness, contrast, and apparent texture vary to the human eye with changing viewing geometry (**Appendix 1**). These perceptual observations can be linked to specific surface materials (e.g., their composition and surface roughness; **Section 5.2.1**) to understand various qualities of the Moon as a non-Lambertian surface.

Quantitative image-based photometric analysis requires radiometrically calibrated images, which are not available from this mission (**Section 3.2.2**). However, a unique human data product not obtainable by any robotic mission is the crew's real-time visual perception of the changing appearance of the surface as viewing geometry evolved during the flyby. As an example, V. Glover reported:

> It is interesting just looking at Orientale that my first impression of it is all of the dark areas appear lighter [than before], which I think makes sense because it is now facing, well, it's still relatively the same to the Sun, but my angle to it is different. So, I'm looking at it from a little more, even further to the side as we pass it. But all the darker features appear to be just a little bit lighter from this vantage point. The darker ring structure in the outer and inner ring and the interior as well as the annular ring portion, everything seems to be just a smidge lighter at this point. (V. Glover, O/E-1 voice loop, 21:27:42 UTC)

5.3.1 Changes in Color/Albedo Variation

One dedicated photometric investigation in the LTP (**Appendix 1**) targeted Glushko crater, a 43-km-diameter Copernican crater with high-albedo materials and a prominent ray system. In this investigation, two crew members conducted repeat observations of Glushko, separated by a ~33° phase-angle change while maintaining a nearly constant incidence angle (~25°). When viewing Glushko from a smaller phase angle, the crew reported the crater appeared to be relatively bright, with a "gray brownish color" (R. Wiseman, unaided eye, PCD crew audio, art002a000019, 19:15:50 UTC) and prominent ray system. In contrast, during their higher-phase-angle observations, the crew reported that colors were "so much more muted than [they] were a while ago" and rays were "less pronounced now" (R. Wiseman, unaided eye, PCD crew audio, art002a000023, 21:05:29 UTC, 21:11:47 UTC). While colors were reported to be muted, the crew reported there were "no primary color changes" between observations (R. Wiseman, unaided eye, PCD crew audio, art002a000023, 21:11:17 UTC). Overall, these dual observations of Glushko can be used to link real-time human perception to surface materials and roughness characteristics in future analyses, offering insight into the non-Lambertian behavior of lunar terrains.

Because of their training, the crew were keenly aware of how viewing geometry could influence their perceptions of color, brightness, and surface morphology. As a result, they reported several times when viewing geometry could have affected their perceptions and interpretations, with caveats such as "that could just be Sun angle changing the albedo of the regolith" (R. Wiseman, unaided eye, PCD crew audio, art002a000018, 19:08:35 UTC); "I think the darkness in the ejecta region itself are maybe just caused by shadows" (J. Hansen, camera, PCD crew audio, art002a000039, 21:28:43 UTC); "it's hard to tell if that's color or just lighting" (V. Glover, unaided eye, PCD crew audio, art002a000043, 22:24:57 UTC); and "I think all of the differences in albedo and color that I'm seeing are due to lighting" (C. Koch, unaided eye, PCD crew audio, art002a000012, 22:57:04 UTC). This discipline in separating potential lighting artifacts from real surface properties is especially vital as upcoming Artemis landed missions venture into the polar regions, where extreme, low-angle illumination conditions will challenge human perception. Disentangling lighting artifacts from true geologic signals is key for safe navigation, accurate documentation, and confident scientific interpretation.

Additionally, the crew reported several instances later in the flyby when the color of the lunar surface appeared muted relative to how it appeared earlier in the flyby. For example, R. Wiseman reported that Orientale displayed an "absence of color" (R. Wiseman, unaided eye, PCD crew audio, art002a000024, 21:23:55 UTC), though earlier, several colors were reportedly observed in the basin, including "gray bordering on blue tint" in the maria and "swamp-like colors" outside the second ring (C. Koch, camera, PCD crew audio, art002a000005, 20:09:08 UTC, 20:11:16 UTC). As another example, V. Glover reported:

> The Moon from this perspective, 3,820 nautical miles away -- it's maybe the incidence angle that we are, the Moon's roughly being lit the same by the Sun, but our angle from it makes color less [intense]. I don't see as many colors as I did before. (V. Glover, unaided eye, PCD crew audio, art002a000043, 22:16:55 UTC)

5.3.2 The Opposition Effect

The opposition effect (also called the opposition surge) is a sharp increase in the brightness of a surface when the Sun is directly behind the observer, meaning the phase angle approaches 0°. Most planetary bodies whose surfaces include fine particulates (e.g., regolith) show some level of opposition effect, but it is especially notable on the Moon (e.g., Cudnik, 2023).

The two main mechanisms that contribute to the opposition effect include shadow hiding opposition effect (SHOE) and coherent backscatter opposition effect (CBOE). At nonzero phase angles, particles on the lunar surface cast shadows on each other. SHOE occurs as the phase angle approaches zero, and each particle hides its own shadow, causing a sudden increase in brightness. CBOE is a quantum mechanical effect where light waves traveling along multiply scattered paths within the regolith interfere constructively when the phase angle is near zero, further enhancing brightness.

Observations (e.g., by LRO) and laboratory studies indicate that both SHOE and CBOE contribute to the opposition effect on the Moon (e.g., Cudnik, 2023). For typical highlands terrain, coherent backscatter accounts for nearly 40% of the effect in the ultraviolet, increasing to over 60% in the visible red. The brightness surge is about 40% between phase angles of 4° and 0° and is stronger in the lunar highlands due to textural differences. Other phase-angle effects include phase reddening where, as the wavelength and albedo increase, multiple scattering between regolith particles becomes more significant, causing the Moon's surface to appear redder at larger phase angles. One important implication of the opposition effect is that it can wash out surface features, diminishing contrast and making it difficult to see details when the Sun is nearly behind the observer. This is a challenge for both human and robotic exploration, as it affects hazard assessment and navigation.

Understanding the opposition effect is crucial for an accurate interpretation of lunar reflectance data, which informs studies of surface composition, texture, and regolith properties. While the Artemis II cameras were not radiometrically calibrated (**Section 3.2.2**), future qualitative analyses of image color and brightness properties may still be possible. Such analyses could explore photometric behavior across the lunar surface by, for example, comparing relative brightness properties under different viewing geometries, or assessing contrast changes as features move toward the limb. Thus, the Artemis II images and data related to how illumination conditions affect human perception of regolith properties from orbit (e.g., **Section 5.3.1**) together provide a foundation for future investigations into how photometric and perceptual effects shape the appearance of lunar features as observed by human eyes and captured by handheld cameras.

5.3.3 The Evolution of the Crew's Perception of Grimaldi

Throughout the flyby, the crew used the mare-covered floor of Grimaldi basin as a brightness anchor, to make comparative descriptions of color between the maria within Grimaldi and other lunar features. The crew characterized the darkness of Mare Grimaldi as a one on their albedo scale, where one indicates

the lowest albedo and ten indicates the highest (**Section 5.2.2**). Mare Grimaldi (referred to by the crew as simply "Grimaldi") was consistently identified as one of the darkest viewable features, and sometimes the singular darkest feature. Other similarly dark features included "patches of very dark mare" that were "equally as dark as [Mare] Grimaldi" (R. Wiseman, unaided eye, PCD crew audio, art002a000019, 19:11:43 UTC, 19:11:52 UTC) and portions of Orientale and its rings.

The crew's perception of Mare Grimaldi's darkness varied over time, as the apparent size of the Moon increased on approach. For example, R. Wiseman reported: "I know I reported that [Mare] Grimaldi was the darkest thing that we saw when we were far from the Moon, and I would still stand by that, although it is fairly similar to the [maria] now" (R. Wiseman, unaided eye, PCD crew audio, art002a000017, 18:41:33 UTC). Additionally, the crew began to recognize darkness variations within Mare Grimaldi as they approached closer to the Moon. V. Glover reported that the crew were seeing "albedo variation inside of Grimaldi. […] It is just not as uniform as it looked when we were farther away. We're starting to differentiate the striations of albedo inside of Grimaldi" (V. Glover, O/E-1 voice loop, 18:57:32 UTC). These variations enabled the crew to make direct comparisons between specific regions within Mare Grimaldi and other low-albedo features, including lunar maria, such as when R. Wiseman reported "a little bit of mare" that had "the same [albedo] as the lower left-hand part of Grimaldi" (R. Wiseman, unaided eye, PCD crew audio, art002a000017, 18:58:37 UTC).

Images of the lunar surface taken by the crew at the same time as their reported descriptions can be used to analyze relative brightness properties. For example, **Figure 5.8** shows an image acquired during V. Glover's comparative descriptions of Grimaldi and Orientale. V. Glover reported that "to the north, Grimaldi does get lighter" (V. Glover, unaided eye, PCD crew audio, art002a000035, 20:24:55 UTC), which is confirmed with the relatively lower pixel values within southern Mare Grimaldi in comparison to northern Mare Grimaldi (**Figure 5.8**).

V. Glover reported that "the southern part of Grimaldi is pretty uniformly dark. (V. Glover, unaided eye, PCD crew audio, art002a000035, 20:24:55 UTC, 20:25:19 UTC), which is also supported by the image data: southern Grimaldi mare has a standard deviation of 7.55 DN, while northern Grimaldi mare has a standard deviation of 12.61 DN, indicating that southern Grimaldi mare indeed has less contrast and tonal variation relative to northern Grimaldi mare.

Furthermore, the crew-captured images relative to the crew-reported descriptions also provide insight into the crew's comparative perspectives of different features. For example, V. Glover reported that "the darkest parts of the basin in Orientale are the same as almost the average darkness of Grimaldi" (V. Glover, unaided eye, PCD crew audio, art002a000035, 20:24:47 UTC), which is consistent with the distributions plotted in **Figure 5.8**, where pixel values within Orientale's floor fall between those in south and north Grimaldi. Future analyses of calibrated photometric observations from other orbital missions would provide an important point of comparison.

5.4 Impact History

Impact structures of a range of sizes were visible to the Artemis crew, from basins extending several hundreds of kilometers across, to smaller craters possibly as small as the kilometer scale (see discussion of smallest resolvable features in **Section 7.3**). Crew observations describing impact feature morphology, structure, and color and albedo variations, along with crew comparisons of various impact features visible at the same time, provided observational data of multiple impact structures related to differences in age, geologic history, and mode of formation.

The LTP included several targets that were selected to enable investigations of lunar impact structures: Glushko crater, Ohm crater, Orientale basin, Hertzsprung basin, and Vavilov crater as stand-alone targets, and Pierazzo crater and Byrgius A crater within the Farside Albedo/Color discussion (**Appendix 1**). The key observation actions specified in the LTP for geologically young craters (Glushko, Ohm, Pierazzo, and Byrgius A) included providing descriptions of color, albedo, and texture variations along and between crater ray systems, characterizing the extent of ray systems, and comparing crater characteristics.

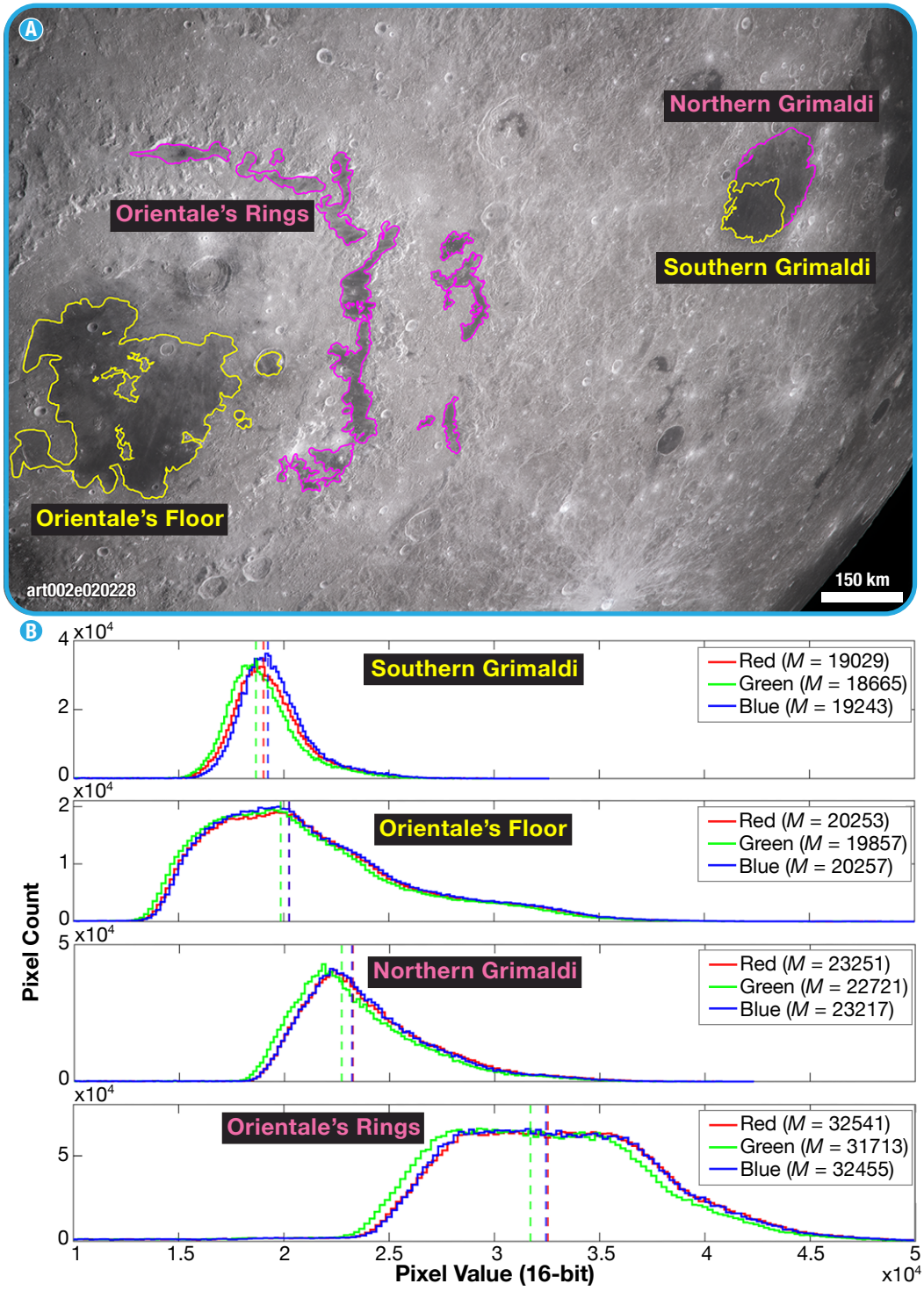


Figure 5.8: Grimaldi and Orientale Maria. (A) Crew image art002e020228 captures Orientale and Grimaldi, where regions of low-albedo are grouped into four maria surfaces described by the crew: central to Orientale's floor, between Orientale's rings, in southern Grimaldi, and in northern Grimaldi. (B) The histograms display the distribution of pixel values (DN) in the 16-bit crew image (not geometrically rectified), for each of the four outlined mare surfaces. The histograms display pixel counts for the red, green, and blue channels separately, and the median (M) pixel value (DN) for each channel is reported in the legend of each plot.

The key observation actions for basins (Orientale, Hertzsprung) included describing color, albedo, texture, and topography across basin rings, floors, and ejecta deposits, and making geologic comparisons between the relatively older Hertzsprung and younger Orientale basins. Finally, key observation actions for Vavilov, which has an intermediate formation age relative to the targeted young craters and older basins, included describing Vavilov's central peak, terraced walls, and any visible ejecta, as well as describing color, albedo, and texture variations across the crater's floor. The crew described and imaged all of these planned impact targets during the flyby. Furthermore, the crew described and imaged impact structures beyond those included in the LTP during SitReps, Crew Choice blocks, and discussion periods. These additional impact structures included, but were not limited to, Sundman J, Zeeman, and Pythagoras craters, along with Carroll and Integrity (18.9°N, 273.5°E; 2.7°N, 255.1°E), the two craters that the crew proposed to name at the start of their lunar flyby.

This section highlights the diversity of impact structure features (**Section 5.4.1**), geologic relationships (**Section 5.4.2**), and young craters (**Section 5.4.3**) observed by the crew, and provides a synthesis discussion related to observations of particular structures (**Section 5.4.4**) including Orientale basin, Vavilov crater, Glushko crater, Pierazzo and Byrgius A craters, Sundman J and its low-albedo halo, Ohm crater, and the proposed Carroll and Integrity craters.

5.4.1 Features of Impact Structures

The crew observed a wide range of impact-related geologic structures across the near and far sides of the Moon, including central peaks, peak rings, wall terraces, and ejecta. The crew also observed a diversity of crater characteristics including morphology, texture, color and albedo, preservation state, and spatial relationships to other geologic features.

Across the lunar surface, the crew described distinct morphological differences between simple and complex craters, as well as between younger and older craters. For example, the crew reported clean, crescent-shaped shadow geometries along the inner walls of fresh simple craters, whereas they reported slumped and collapsed rims, irregular shadow patterns, and softened textural signatures for older simple craters. As C. Koch described: "the newer, simpler craters have that crescent shape of shadow. Some of the older ones have more shapes to that, as their crater walls have fallen and shade differently" (camera, PCD crew audio, art002a000005, 20:07:21 UTC). Observations along the terminator further enabled vivid descriptions of impact structures, as shadows accentuated steep crater walls, central peaks, and degraded crater populations that are less apparent under higher solar elevation angles (**Section 5.8.2**).

The crew also made comparative observations of the large multi-ring basins Orientale and Hertzsprung, distinguishing their floors, rings, and adjacent terrains by differences in texture, color, and crater density, and noting superpositional relationships between the basins' ejecta systems. The crew described Orientale's ejecta as deep scours extending southward and as having "pillowing" textures interacting with Hertzsprung to the northwest (R. Wiseman, unaided eye, PCD crew audio, art002a000024, 21:27:46 UTC). Hertzsprung's interior appeared notably smooth relative to the pillowed textures on its outer ring, suggesting differential resurfacing or ejecta infill, most likely sourced from Orientale (Stockhill & Spudis, 1998; Meyer et al., 2016).

Additionally, the crew made several observations of secondary impact craters (i.e., those formed by the fallback of ejecta from a primary impact), often seen as clusters or chains emanating from their source crater. The crew vividly described these secondary features in Orientale as grooves resembling long gorges and canyons (also discussed in **Section 5.4.4.1**).

5.4.2 Geologic Relationships

The crew were able to infer relative ages by observing superpositional relationships between craters and by examining how impact ejecta interacted with the surrounding terrain. For example, the crew reported several descriptions relating Vavilov to other impact structures: "Vavilov is a newer crater on top of an older crater" (R. Wiseman, unaided eye, PCD crew audio, art002a000017, 18:43:04 UTC); "It's just so

cool how Vavilov came and slapped itself down right on top of that other crater" (R. Wiseman, camera, PCD crew audio, art002a000042, 21:54:38 UTC); "I can see a trace of that, the rim from the previous crater that the newer one in Vavilov impacted" (V. Glover, camera, PCD crew audio, art002a000046, 22:54:24 UTC). The crew also emphasized the lack of superposed craters on top of Vavilov itself: "There are no craters superimposed on anywhere in Vavilov, not its rim, not its center, that are big enough to discern" (C. Koch, unaided eye, PCD crew audio, art002a000012, 22:53:10 UTC).

The relative ages of Orientale and Hertzsprung basins was also a topic of discussion amongst the crew. By observing how ejecta and secondary craters from Orientale basin overlayed surrounding terrains, the crew reasoned that Orientale was younger than Hertzsprung and older than nearside maria. As R. Wiseman described:

> I think Hertzsprung is in the primary bouldering ejecta from Orientale. And to the left of Hertzsprung, you can just see the streaks of gouging in the regolith that leave Hertzsprung. But I don't think they're from Hertzsprung. I think they're from Orientale […] because those scarrings cross into Hertzsprung. And you can see the Orientale boulder marks that go across Hertzsprung. (R. Wiseman, unaided eye, PCD crew audio, art002a000023, 21:09:57 UTC)

In subsequent debrief meetings between R. Wiseman and the LST, it was affirmed that boulder marks and other references to Orientale boulders in audio recordings refer to catenae and discontinuous hummocky ejecta from the Orientale impact.

Another observation underscored the stratigraphic relationships between Orientale and the nearside maria:

> Why don't the [ejecta patterns] from Orientale go out the nearside as far as they go out the farside? That tells me Orientale is older than the [maria] on the nearside. The [maria] must have come after Orientale. Otherwise, those [ejecta patterns] would be there because they're everywhere else. (R. Wiseman, unaided eye, PCD crew audio, art002a000019, 19:17:49 UTC).

Furthermore, C. Koch described the effect of Orientale on the region:

> In the really, really outer […] ring of Orientale, it's almost like Orientale is like a smoothing function and just kind of washes out some of those -- some of that cratering because there's a whole size range of craters that just doesn't seem to be apparent in the area around Orientale. (C. Koch, camera, PCD crew audio, art002a000005, 20:08:18 UTC)

Collectively, these observations establish a stratigraphic sequence in which Orientale's primary boulder-rich ejecta postdates and overprints Hertzsprung basin, and its ejecta emplacement predates nearside mare volcanism. This sequence of events reported from human observations supports the geologic chronology that has been tested with quantitative mapping and crater-density statistics (e.g., Head et al., 1993; Guo et al., 2018). In addition, these observations and descriptions highlight the value of geology training (**Section 3.4**) in enabling crew members to make informed, high-quality orbital observations and geologic interpretations.

5.4.3 Features of Young Crater Systems

The crew repeatedly identified relatively young geologic materials by their high-albedo appearance, using surface brightness as a first-order indicator of freshness. They were struck by the abundance of small, fresh craters, and by how intensely these features stood out against the surrounding terrain. C. Koch described these craters as "little pinpricks of super white light" that made the lunar surface look

"like a lampshade with a tiny pinprick hole and a light shining through" (C. Koch, camera, PCD crew audio, art002a000005, 20:06:15 UTC; C. Koch, unaided eye, PCD crew audio, art002a000030, 19:29:53 UTC). These high-albedo characteristics are indicative of the very fresh material excavated during geologically recent impact events. These observations can be used to identify surface areas containing fresh craters for further analysis with complementary orbital datasets, such as albedo measurements, surface temperatures, or high-resolution images acquired by LRO.

The crew also compared the prominent high-albedo ray systems of Glushko, Ohm, Kepler, Integrity, and Carroll craters. As R. Wiseman noted, "Kepler to me, very similar to Glushko in the ray colors, ray albedo. So, Kepler's a good analog, I would say, for Glushko" (R. Wiseman, unaided eye, PCD crew audio, art002a000028, 19:06:38 UTC). The crew further noted that the perceived prominence of ray systems varied with viewing geometry and solar elevation angle, while the rays' color remained relatively consistent (**Section 5.3.1**). For example, R. Wiseman emphasized that while "Glushko is still fairly bright. It is, right now I would say it's up there as the brightest thing that I see on this particular look at the Moon," the changes in viewing geometry muted the appearance of its ray system: "I noticed that the rays are a touch less prominent now, no primary color changes there" (R. Wiseman, unaided eye, PCD crew audio, art002a000023, 21:11:06 UTC, 21:11:17 UTC).

5.4.4 Discussion of Specific Impact Features

5.4.4.1 Orientale Basin

Orientale basin (**Figure 5.9**; also discussed in **Section 5.2.1**) is the most well-preserved multi-ring impact basin on the Moon and was repeatedly observed and described by the crew during the flyby as the dominant structural and geomorphic feature on the observable lunar farside (**Figure 5.10**). The crew's

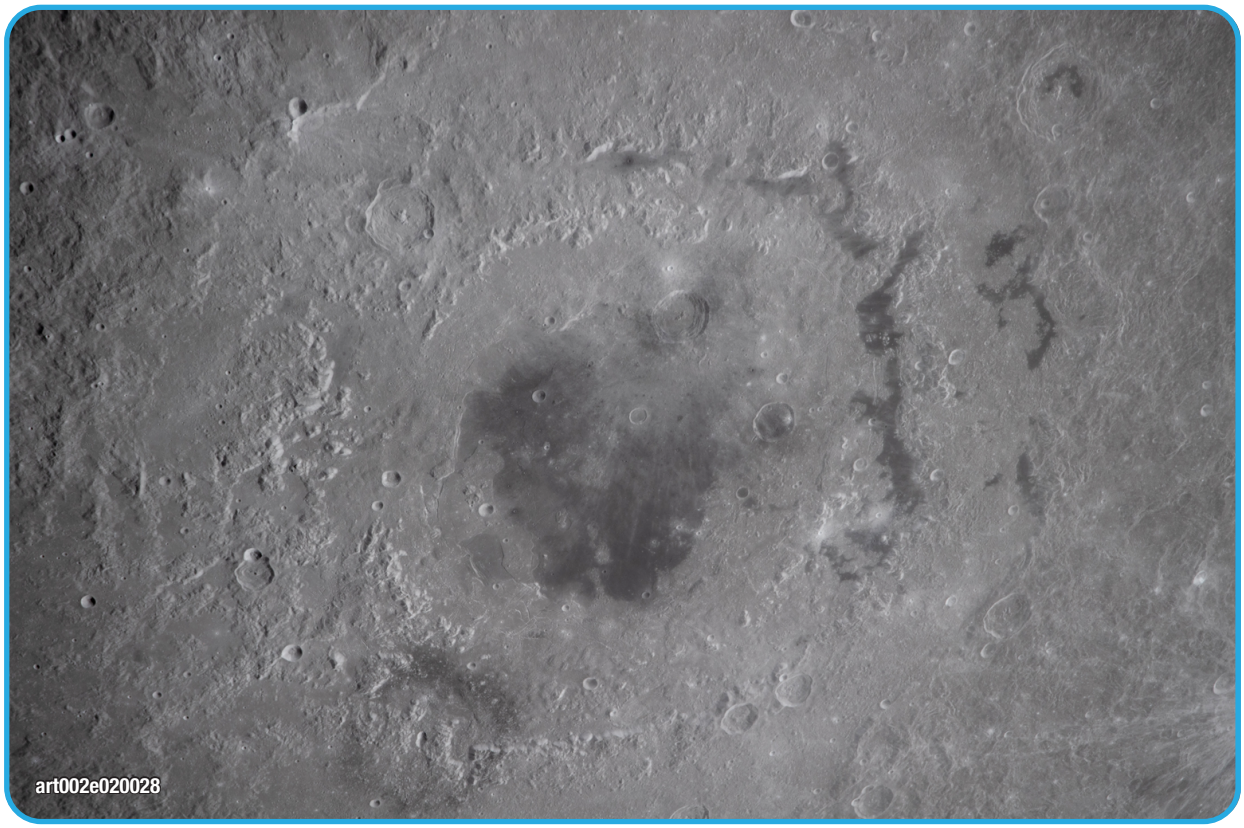


Figure 5.9: Orientale Basin. Crew image art002e020028.

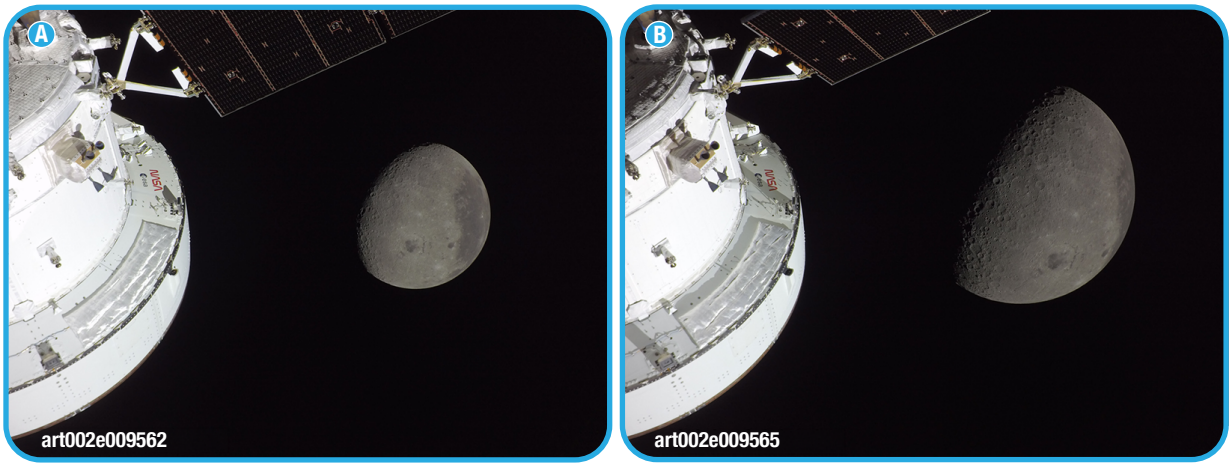


Figure 5.10: Orientale Views from Orion. Vehicle camera images show views of Orientale at different times in the flyby. (**A**) Vehicle camera image art002e009562, acquired April 6, 2026, 19:18:24 UTC, is from early in the flyby and (**B**) vehicle camera image art002e009565, acquired April 6, 2026, 21:10:24 UTC, is from later in the flyby, shortly before earthset.

observations provided a rare human-eyewitness dataset of basin-scale morphology and ejecta interactions under changing illumination conditions, enriching interpretations derived from orbital remote sensing.

In flight, C. Koch annotated on her kneeboard several textural differences within and around Orientale, noting smoother material interior to the outer ring and hummocky-smooth areas exterior to it. Her sketches highlight boundaries and apparent stratigraphic layering between these terrains (**Figure 5.11**). Such textural contacts may reflect variations in ejecta composition, thickness, excavation depth, degree of melting, or emplacement process across different regions of the basin (e.g., Zhu et al., 2015; Morse et al., 2018).

As discussed in **Section 5.2.1**, color and brightness differences across Orientale were consistently noted by the crew. For example, R. Wiseman reported that "the color of the annular ring is distinctly different than the color of the [maria] in Orientale," specifying that "this annular ring is -- this is a different shade of gray. I'd almost say [the annular ring] has more brown tones and [the maria] has more gray tones" (R. Wiseman, unaided eye, PCD crew audio, art002a000024, 21:20:10 UTC). Such differences in color likely correspond to variations in lithology and composition between the annular ring **Section 5.9.2**) and the basaltic materials of the maria.

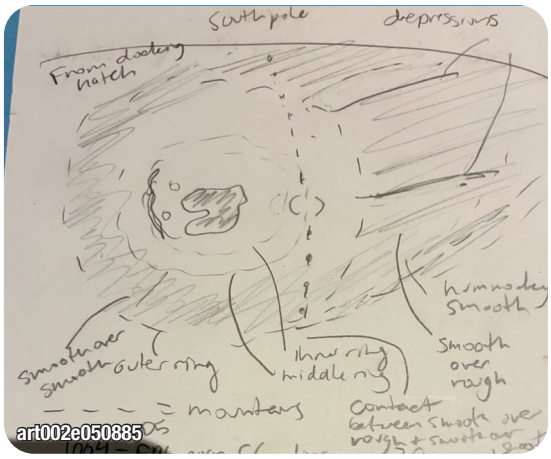


Figure 5.11: Orientale Sketch. This C. Koch annotation (art002e050885) is of Orientale Basin as she observed it through the docking-hatch window. Note that orientation is unconventional, with the south pole positioned at the top of the figure.

The crew additionally described high-albedo patches observed along portions of the basin walls, notably on the eastern sides. R. Wiseman reported: "Where I would expect to see shadowing on the east side of Orientale, I see a very high albedo. I would actually say right now, it's a ten [on the albedo scale]. On the farside, it's the brightest albedo I see" (R. Wiseman, unaided eye, PCD crew audio, art002a000024, 21:24:27 UTC). V. Glover also noted high-albedo highlights along the peaks and edges of the ring structures, likening them to dusting or snow cover:

> From this lighting, you can really see highlighting high-albedo features around the inner edges of the rings. On the outer ring, it's almost as if there was a snowfall that created, you know, dusted the peaks there. It's just like -- it's just on the edges. (V. Glover, unaided eye, PCD crew audio, art002a000034, 20:05:15 UTC)

These high-albedo patches may represent fresh exposures of crustal material or reflective lithologies accentuated by low-Sun illumination.

Crew observations also illustrate how human depth perception aids recognition and interpretation of large-scale topography. Comparisons to neighboring basins emphasized differences in basin depth, rim height, and mare infill. J. Hansen observed that "Orientale looks way deeper to me [than Hertzsprung]. And it has [maria] in the bottom, which makes sense if it's deeper" (J. Hansen, camera, PCD crew audio, art002a000028, 18:48:50 UTC). He later commented on the significant elevation of Orientale's ring structures, remarking, "Oh my gosh, the elevation in Orientale is just insane" (J. Hansen, camera, PCD crew audio, art002a000039, 21:19:11 UTC).

V. Glover further described the dramatic elevation changes across the ring systems as Orientale rotated over the limb, offering a striking cross-sectional perspective:

> And so, I'm just kind of watching the structures interior to Orientale pop out to the horizon and you can see the inner mare, the edges of it are raised. And in fact, in the north, I see one distinct peak and then it goes down and then there's a raise in the middle. I took a picture of this a second ago. There's one kind of smooth-plateau raise and then there's jagged raises to the south. And there's like one, two, three, three raises, so like three ridges right in a row that radiate outward toward the edge of the [maria]. And so, it's like looking at a cross section. Actually, it's what it is, looking at a cross section of the terrain interior to Orientale Basin. Pretty cool. (V. Glover, unaided eye, PCD crew audio, art002a000044, 22:28:55 UTC)

Crew descriptions and images underscoring Orientale's pronounced topographic relief and its clear expression as a well-preserved, multi-ring basin are further discussed in **Section 5.8.1**.

A recurring theme across all crew observations was the dominance of Orientale ejecta across the observable farside terrain (**Figure 5.12**):

> I do want to say, it's also just very apparent right now that Orientale is the primary feature on the farside of the Moon. I mean it, it has just created chaos across that entire area. (R. Wiseman, unaided eye, PCD crew audio, art002a000019, 19:17:26 UTC)

The crew likened the secondary crater chains emanating from Orientale to scours, ravines, and riverbeds. C. Koch reported the catenae "just look like bubbles rising from a team of scuba divers below. And of course, a lot of [the secondary craters] are in very straight lines, very close together, but some of them are just all over" (camera, PCD crew audio, art002a000005, 20:11:52 UTC).

Even during their Nearside/Farside Transition Discussion, the crew observed the influence of Orientale ejecta, identifying a feature they deemed a canyon west of Glushko:

> Oh gosh, look at that. Alright, I'm just going to change subject for a second. If you go directly west from Glushko, there is a canyon on the Moon. It is almost directly south of Carroll crater. Slightly further west. It starts -- its southern boundary is almost the east-west line coming out of Glushko, um, and then it goes almost straight north, and its northern boundary is halfway to Carroll crater, and it just looks so deep to me. (J. Hansen, camera, PCD crew audio, art002a000029, 19:14:58 UTC)

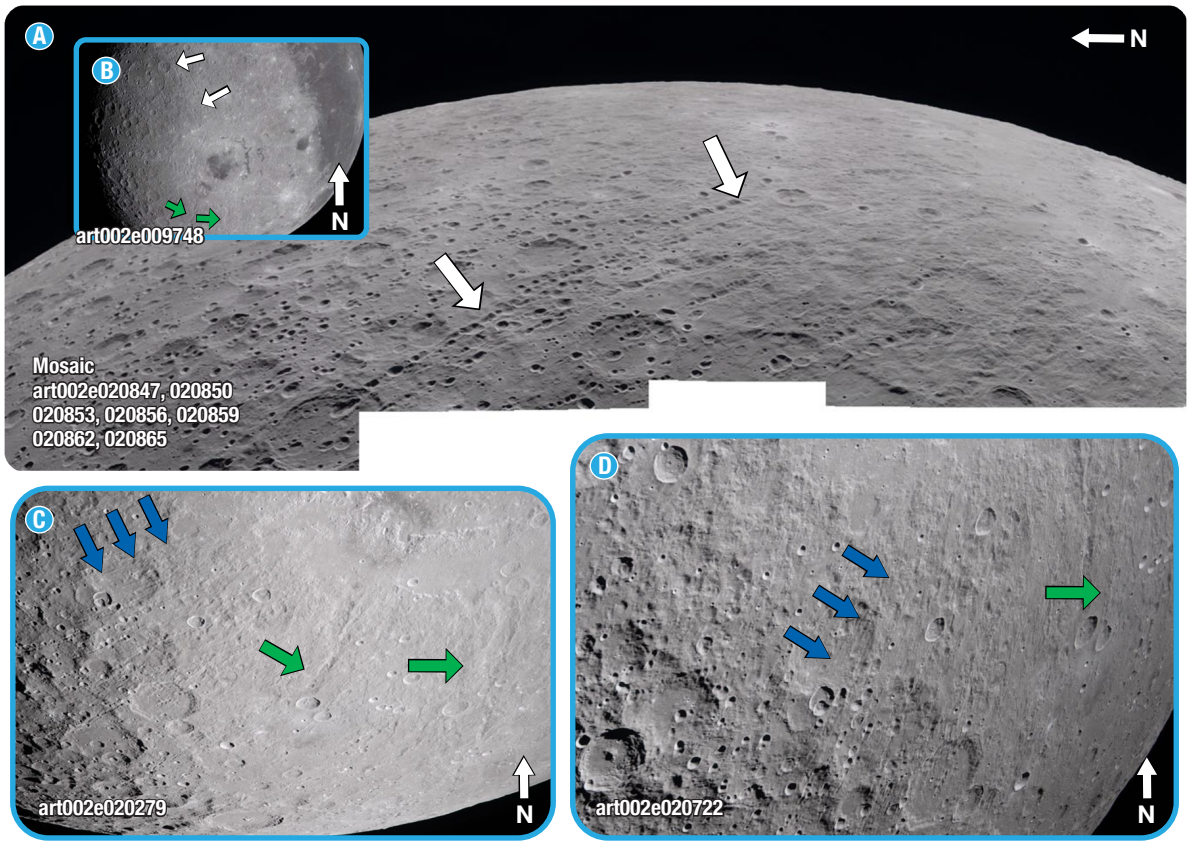


Figure 5.12: Orientale Ejecta. This compilation shows multiple perspectives of Orientale textured ejecta described by the crew and imaged at different times during the lunar flyby. (**A**) A mosaic of the limb to the east shows the northern portion of Orientale ejecta, with white arrows identifying examples of prominent secondary crater chains (mosaic from crew images art002e020847, art002e020850, art002e020853, art002e020856, art002e020859, art002e020862, and art002e020865). (**B**) Arrows on top of crew image art002e009748 indicate secondary crater chains and scours. (**C**) Crew image art002e020279 shows the southern portion of Orientale ejecta. Green arrows point to prominent scours and blue arrows indicate an example of scratch-like texture described by the crew. (**D**) Crew image art002e020722 shows the scratch-like textures of the southern ejecta, accentuated due to change in viewing geometry.

The LST identified the canyon as Vallis Bohr, which is a feature formed from impact-derived scouring associated with Orientale ejecta (e.g., Byrne, 2005).

The crew also reported distinct regional difference in ejecta morphology (e.g., **Figure 5.12**): ravines and scratches dominated in the south, whereas boulders were more prominent to the north and northwest, which support observations made telescopically (e.g., Wilhelms, 1970), maps derived from Lunar Orbiter images (e.g., Scott et al., 1977), and other interpretations from remotely sensed datasets (e.g., Spudis, 1993; Morse et al., 2018). The crew's vantage adds new details to existing orbital datasets by allowing comparisons across varying observing angles and different zoom levels.

South of Orientale, the crew reported canyon-like lineations extending radially from the outer ring, showing higher-albedo centers and darker flanks: "the textures and the canyons, or mountains, or whatever is going on there, is nuts. And it goes straight south. It just looks like a whole canyon system" (J. Hansen, camera, PCD crew audio, art002a000030, 19:29:18 UTC). C. Koch reported that catenae "are less pronounced on the south, but there are other types of rays that look more like sinuous ridges or valleys. […] It doesn't look like water flowing valleys, but more like glacier-cut valleys" (C. Koch, camera, PCD crew audio, art002a000005, 20:18:03 UTC). The north-south differences in ejecta style

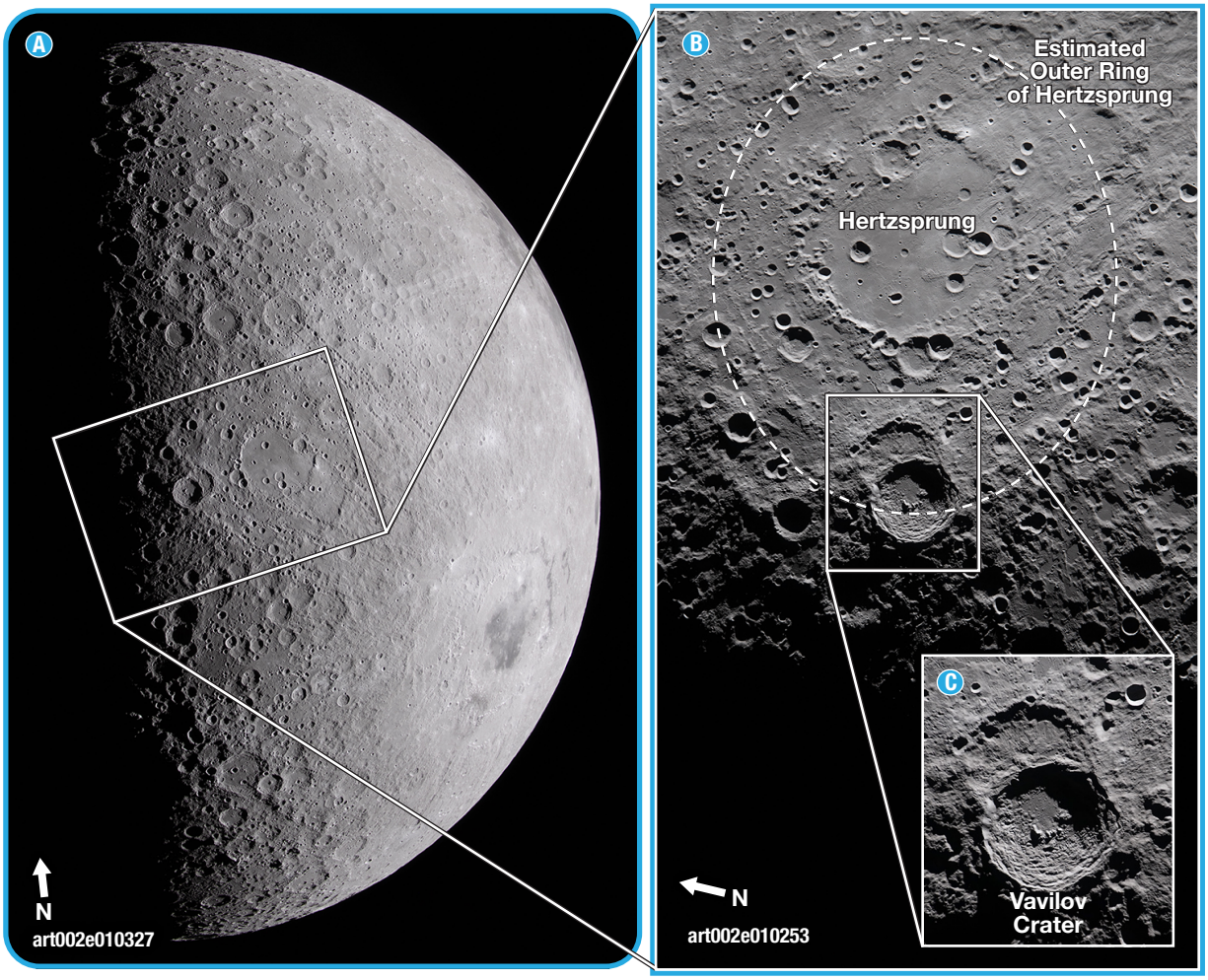


Figure 5.13: Vavilov Crater. Artemis II crew images of Vavilov crater (diameter of ~98 km), including (**A**) a full-disk view in crew image art002e10327, and higher-resolution views captured at longer focal lengths: (**B**) crew image art002e010253 shows Vavilov, superposed on the rim of Hertzsprung basin; (**C**) crew image art002e10256 highlights textural variations across the crater and surrounding terrain.

observed by the crew could be related to asymmetries in ejecta emplacement related to variations in ejecta size, material, or impact velocity (e.g., Morse et al., 2018).

Overall, Orientale basin, which had never before been observed directly by humans, made a lasting impression on the crew, encapsulated by a single remark made by the Artemis II Commander when observing Orientale ejecta: "I think if I was going to do a Ph.D., that is what I would do my Ph.D. in" (R. Wiseman, unaided eye, PCD crew audio, art002a000024, 21:28:11 UTC).

5.4.4.2 Vavilov Crater

Vavilov crater is a ~98-km-diameter complex crater located on the western outer rim of Hertzsprung basin on the lunar farside. First imaged by the USSR's Zond 6 spacecraft in 1968 (Kopal, 1974a), Vavilov has drawn renewed scientific interest following interpretations that samples returned from the Chang'e 6 originated from this crater (Xu et al., 2024). During the crew's scheduled observations of Vavilov during the Artemis II flyby, the crater was positioned ~200 km from the terminator in a viewing geometry that produced pronounced shadowing, enhancing the visibility of its textural and morphological characteristics (**Figure 5.13**).

As the crew examined the surrounding terrain, including the underlying Vavilov D crater and Hertzsprung basin, they noted substantial erosion and overprinting by subsequent impacts. In contrast, Vavilov itself showed few superposed craters. As C. Koch reported, "there are no craters superimposed on anywhere in Vavilov, not its rim, not its center, that are big enough to discern" (C. Koch, unaided eye, PCD crew audio, art002a000012, 22:53:18 UTC). This relative paucity of superposed craters indicates that surface age of Vavilov is younger than adjacent surfaces, consistent with previous interpretations of stratigraphy and chronology of this region of the Moon (Kopal, 1974b). This recognition guided the crew's comparisons across nearby terrains.

Transitioning into the crater's interior, the crew described notable texture variations, ranging from smooth to hummocky (**Figure 5.13C**). As described by C. Koch, "you get down to floor of the crater, to like a hummocky floor. It doesn't seem like a fractured floor. There aren't cracks in the floor. It just seems more hummocky" (C. Koch, unaided eye, PCD crew audio, art002a000012, 22:55:29 UTC).

The crew also remarked on Vavilov's central peak morphology. V. Glover noted that the older outer ring of the Hertzsprung basin appeared to influence the shape and curvature of the younger Vavilov peaks. As described by V. Glover:

> The [Hertzsprung] crater ring is creating some central structure in the newer crater [Vavilov], the one that's further to the west. So, maybe a combination of any uplift in the center that happened due to the force of impact, but also the structure remaining of the crater wall, of the previous crater that it impacted, are creating this arc of uplift in the center. (V. Glover, camera, PCD crew audio, art002a000046, 22:46:00 UTC)

Future analyses integrating remote-sensing datasets and dynamical simulations could provide insight into the conditions that resulted in Vavilov's central peak structures, to contextualize these crew descriptions.

Illumination during the flyby also allowed the crew to characterize variations in crater wall morphology. C. Koch described the crater walls as textured, variably slumped, and flour-like in appearance. The eastern wall appeared steeper and less terraced in comparison to the western wall, which exhibited extensive terracing with "too many [terraces] to count" (C. Koch, unaided eye, PCD crew audio, art002a000012, 22:56:48 UTC). These variations may be consistent with differential wall collapse or uneven erosion. As described by C. Koch:

> The western inner wall of the crater is very terraced and very scree-like. It looks like […] there's some ability of the regolith to stay composed and to adhere to itself that makes it […] not completely fall away evenly, but it's more dominated by its ability to separate. So, in other words, it's not like distinct cliffs, which would be more composed and held together, but it's also not like fully just sandy, kind of fell down. That kind of scree slope, the […] circumferential terraces, kind of gives way once you get down to the floor of the crater to like a hummocky floor. (C. Koch, unaided eye, PCD crew audio, art002a000012, 22:54:31 UTC, 22:56:33 UTC)

C. Koch also described localized erosion:

> The only apparent weathering or erosion in the crater wall of Vavilov is at the 5:30 p.m. position, where it appears that part of the peaky crater rim has kind of caved in a little bit, almost like it kind of preserved its shape, but sort of fell in. Like maybe there was some raised regolith beneath it that weakened, and it fell. (C. Koch, unaided eye, PCD crew audio, art002a000012, 22:53:28 UTC)

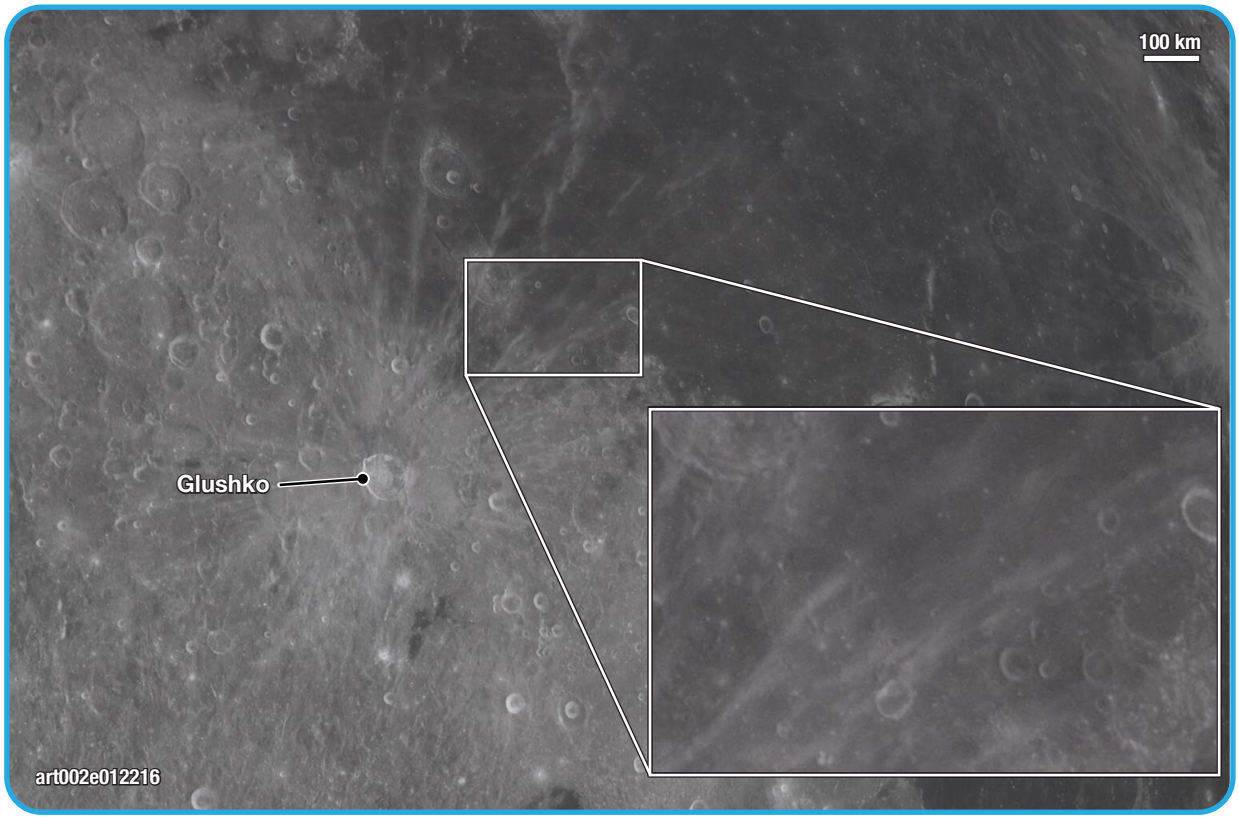


Figure 5.14: Glushko Crater. Crew image art002e012216 shows Glushko crater (diameter of 43 km). The inset shows high-albedo rays of Glushko that cross over the highlands into the nearside maria.

These details demonstrate the crew's ability to parse subtle structural and textural variations, especially in low-Sun lighting conditions.

5.4.4.3 Glushko Crater

Glushko is a 43-km-diameter impact crater estimated to be between 100 and 800 Myr (Neish et al., 2013), located on the nearside-farside transition, west of Oceanus Procellarum. This crater exhibits a prominent ray system that covers highlands to the west and maria to the east (**Figure 5.14**). As discussed in **Section 5.3.1**, Glushko was the target of an Artemis II photometric investigation.

The crew described pronounced albedo variations within Glushko, noting that the west-to-south crater walls exhibit distinctly higher albedo, while the eastern wall appears significantly darker. J. Hansen reported:

> I see a very bright-albedo crater rim from its one o'clock position counterclockwise to the 6:30 position. And when I look at the three o'clock wall of the crater, it is dark. It's a dark albedo and it's like I'm looking at it from the side. (J. Hansen, camera, PCD crew audio, art002a000029, 19:13:03 UTC)

Glushko lies within the transition between thinner, mare-rich nearside crust and thicker, feldspathic farside highlands. Impacts into such mixed crustal environments can excavate materials with markedly different lithologies, which could explain some of the asymmetric albedo exposures across the crater. The lower-albedo ejecta and eastern wall exposures described by the crew may represent excavation through underlying basalt, whereas the higher-albedo materials on the west-to-south walls may represent exposed highland lithologies.

However, during impact events, impact melt can be emplaced outside the crater, often in an asymmetric pattern due to the rim topography and impactor angle (Hawke & Head, 1977; Campbell, 2016). Such emplacement of impact melt has been observed for Glushko (Carter et al., 2012; Campbell, 2016) in an area that is consistent with J. Hansen's observation of low-albedo material north of the crater (**Figure 5.14**): "Interesting, just going out from the 11:30 to the two o'clock position is sort of a darker [maria] just outside the rim of the crater" (J. Hanson, camera, PCD crew audio, art002a000029, 19:13:33 UTC). Such impact melt emplacement could also be consistent with the crew's description of albedo variations along Glushko's walls and the low-albedo deposit north of the crater rim: "I'd say that's an albedo of, uh, three, two or three on my scale. And similar in albedo to that [dark material on the] eastern wall that I talked about" (J. Hansen, camera, PCD crew audio, art002a000029, 19:13:45 UTC).

Glushko's extensive ejecta ray system (**Figure 5.14**) varied in appearance over the farside highlands to the west and the nearside maria to the east. The crew noted that the extent of Glushko's rays appeared to differ drastically depending on the terrain they crossed, with some rays traveling far across the highlands, while others attenuated quickly over maria. These observations, like those of Ohm's rays (**Section 5.4.4.6**), may provide data on how crater rays respond to surface roughness and topographic gradients across the nearside-farside transition. The also crew observed notable changes in color where rays crossed darker mare surfaces. J. Hansen reported:

> When Glushko's rays fall into the dark maria -- they create that brownish color. They're bright, um, they're higher albedo along their line, but around them they sort of look like they've smeared out to create that brownish color that we're talking about. So, whatever was excavated out of Glushko, when it lays on top of the dark maria, it creates sort of that brown that I see. (J. Hansen, camera, PCD crew audio, art002a000029, 19:17:43 UTC)

Building on this, the crew discussed possible explanations for their observations, hypothesizing that the brown-colored ray features could represent a thin layer of fine ejecta:

> I mean, sort of what I'm thinking is when these rays land, they're sort of the finer, when it's not thick enough to see it as a ray, it's a ray to the ground. (J. Hansen, camera, PCD crew audio, art002a000029, 19:21:44 UTC)

R. Wiseman concurred: "On the nearside [maria] of Glushko, I see some of those browns, and it could be a blanket of fine ejecta" (R. Wiseman, unaided eye, PCD crew audio, art002a000020, 19:22:11 UTC). High-resolution LRO Mini-RF same-sense circular polarization radar images of Glushko's rays have shown that the rays are clusters of secondary craters with radar-bright ejecta blankets and debris flows (Neish et al., 2013). Future investigations involving additional remote sensing data could reveal links to compositional properties, topographic features, and source depths of excavated materials.

In addition to these color and albedo observations, the crew noted that Glushko's rays appeared jagged, winding, and uneven, and attributed these characteristics to rays crossing terrain with variable elevation. As J. Hansen hypothesized: "I guess what it must be is changes in elevation showing up, so they probably are rays out of Glushko and they just hit the different elevations" (J. Hansen, camera, PCD crew audio, art002a000038, 21:09:40 UTC).

5.4.4.4 Sundman J Crater

J. Hansen (camera) and R. Wiseman (unaided eye) independently described a small crater near Glushko that was surrounded by dark material interpreted by the crew to be maria (**Figure 5.15**). J. Hansen reported:

> It's a very prominent crater. It's about a tenth the size of Glushko. But it's prominent because it is surrounded by mare [that is a] […] one [out of ten] on the [albedo] scale. It is

> dark, dark mare. […] And it's just so cool looking. (J. Hansen, camera, PCD crew audio, art002a000029, 19:15:50 UTC)

Similarly, R. Wiseman also described the albedo of the material surrounding the crater: "There's one blacker mare patch. I don't know that you'll ever see it" (R. Wiseman, unaided eye, PCD crew audio, art002a000019, 19:16:57 UTC).

The crew descriptions correlate with Sundman J, which is a ~10-km-diameter Copernican crater surrounded by low-albedo material (**Figure 5.15**). The observed low-albedo material may be due to a volcanically sourced exposure of cryptomaria (**Section 5.9.3.3**), as hypothesized by the crew, or, alternatively, it could be an exposure of iron-rich impact melt (Hu et al., 2025). The juxtaposition of dark halo craters in the region, such as near Sundman J (**Figure 5.15B**), to neutral-albedo craters (**Figure 5.15C**) and high-albedo craters in the region (e.g., **Figure 5.16**) raises further questions about the origin of dark halo craters in this region as potentially volcanic vents or exposed Orientale impact melts. Future detailed analyses of the region and the distribution of craters with ejecta of varied albedo could help shed light to the origin(s) of these features that stood out to the Artemis II crew.

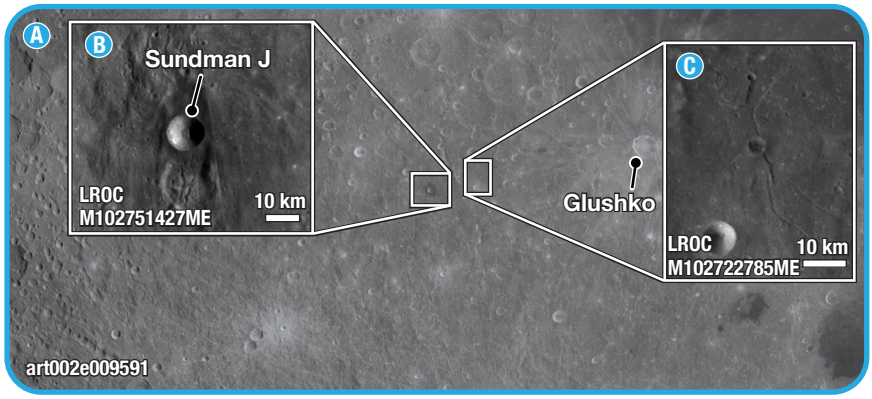


Figure 5.15: Sundman J and Glushko Craters. (**A**) Crew image art002e009591 of Glushko and Sundman J craters. Insets are close-up LROC images of (**B**) the dark-halo surrounding Sundman J and (**C**) a neutral-albedo crater (Credit: NASA/GSFC/Intuitive Machines).

5.4.4.5 Pierazzo and Byrgius A Craters

Pierazzo and Byrgius A are relatively young craters, with diameters of ~9 and ~19 km, respectively. Neither crater was listed as a specific target in the LTP, but both were noted as potential features of interest during the discussion block on Farside Albedo/Color (**Appendix 1**).

The crew frequently used Byrgius A (**Figure 5.16C**) as a reference mark for orientation to other features on the lunar surface because it was easily identifiable due to its high-albedo properties (e.g., "just north of Byrgius Alpha," J. Hansen, camera, PCD crew audio, art002a000028, 19:00:05 UTC).

The crew described Byrgius A's ray system as resembling "a dandelion or daffodil," with exceptionally long and wispy rays extending across the highlands (V. Glover, camera, PCD crew audio, art002a000037, 20:49:48 UTC). C. Koch concurred with this analogy, describing that there were some rays that "are so long" and the crater system looked "like a dandelion because it also has like a high-albedo circle around it, like a glow" (C. Koch, unaided eye, PCD crew audio, art002a000008, 20:50:09 UTC).

The crew also described color variations around the crater that may indicate changes in regolith composition: "Around Byrgius Alpha, do you see red? It looks a little greener to me" (R. Wiseman, unaided eye, PCD crew audio, art002a000029, 19:20:48 UTC). Such observations, complemented by the crew's contemporaneous images, can guide future studies investigating the composition of the crust in and around Byrgius A (e.g., Raney et al., 2012).

In comparison, Pierazzo's ray system (**Figure 5.16**) appeared far more diffuse and could not be easily discerned from orbit: "I don't really see too many rays. It's just kind of like ombre. It just goes away" (C. Koch, unaided eye, PCD crew audio, art002a000008, 20:50:09 UTC). This comparatively diffuse ray

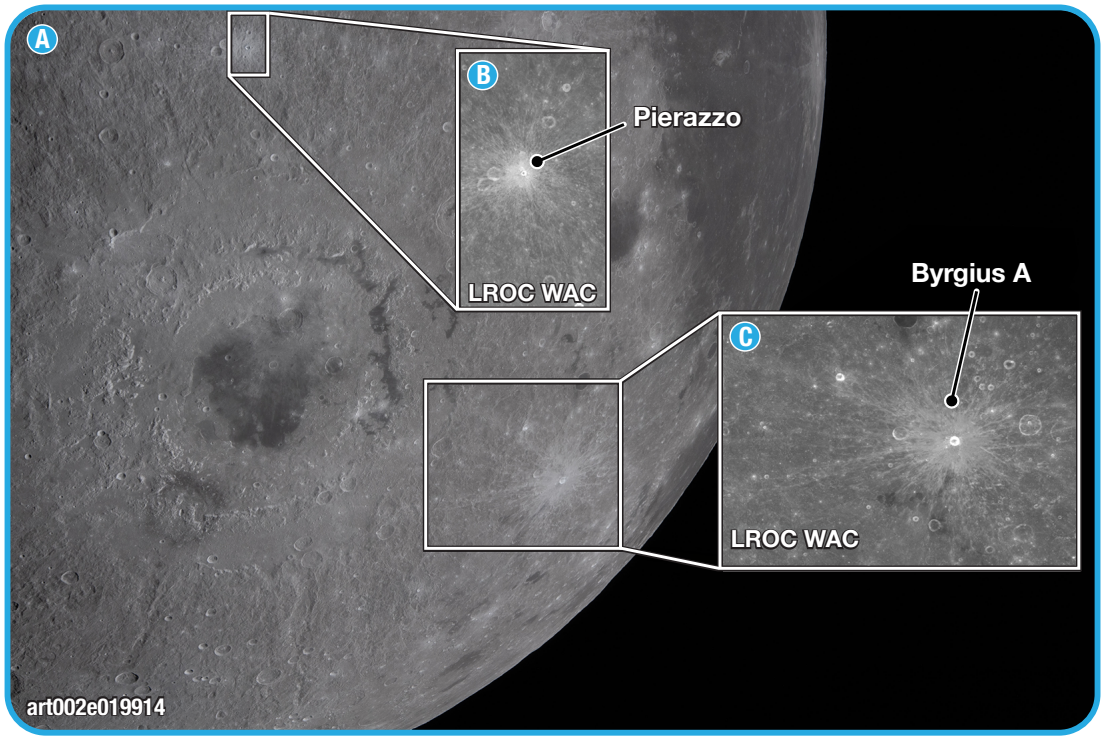


Figure 5.16: Pierazzo and Byrgius A Craters. (**A**) Crew image art002e019914 of the Moon's southwestern limb, capturing Pierazzo crater and Byrgius A crater in the same view. Close-up views from LROC images are shown of (**B**) Pierrazzo and (**C**) Byrgius A (Credit: NASA/GSFC/Intuitive Machines).

expression may indicate weaker compositional contrast between the rays and underlying host terrain or viewing geometry effects influencing the crew's perception of color and albedo.

5.4.4.6 Ohm Crater

Ohm crater is a prominent farside impact crater distinguished by its striking asymmetrical ray system (**Figure 5.17**). The crew described distinct color hues associated with Ohm crater and noted how these hues changed with distance along Ohm's ray system. Variations in ray color may reflect differences in the thickness of ejecta or differences in primary and secondary ejecta excavated from varying depths and geologic units, offering potential insights into the crustal stratigraphy of the farside highlands. As C. Koch observed:

> The color change is more distinct on the northeast ray, and between north of it and south of it, than on the northwest ray, where the color change is less distinct, because the color to the west of Ohm is a little bit darker. So, the wedge is the darkest, but the color to the west of Ohm is mid-range, and then the color to the east and south of Ohm is lightest. (C. Koch, camera, PCD crew audio art002a000009, 22:24:57 UTC)

These crew-reported color differences are consistent with analyses of remote sensing data. For example, Patel et al. (2023) documented compositional variations in mafic minerals within Ohm's ray system, which could account for the color differences reported by the crew.

Ohm's crater rays extend well into the Oceanus Procellarum maria, forming a sharp visual boundary also evident in several remote sensing datasets (e.g., **Figure 5.17C**). As the rays cross terrains of differing composition and roughness, from highlands to maria, their visibility and continuity shifted. J. Hansen described this behavior:

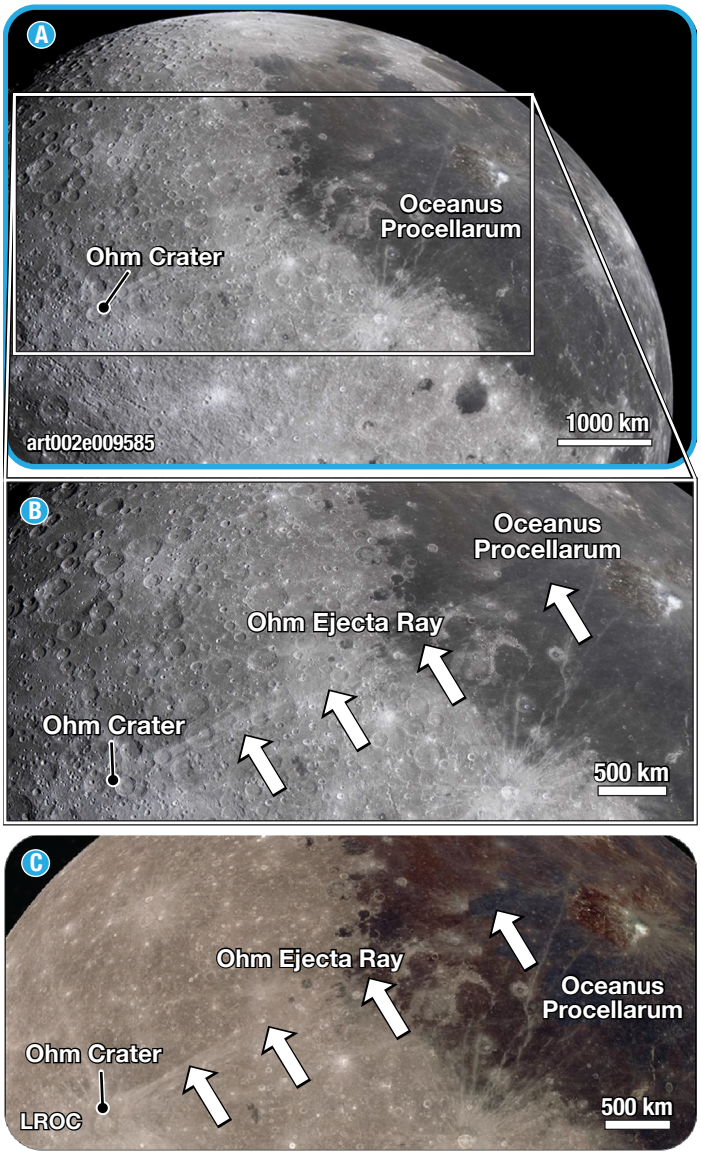


Figure 5.17: Ohm Crater. (A) Crew image art002e009585 capturing Ohm crater and its extended ray system, enlarged in (B) with ejecta rays indicated by arrows. (C) LROC WAC Hapke color mosaic emphasizes contrast and extent of rays (Credit: NASA/GSFC/Intuitive Machines).

> Ohm's rays get halfway to the [maria]. [They are] very prominent. Then it peters out a little bit. I know they extended into the [maria] […] I can see the ray goes all the way to Aristarchus Plateau, the main ray, but it just gets, like, thin there. So, when it's over top of the [maria], it's visible again, but halfway to the [maria], it kind of disappears for me. Then you pick it up again. (J. Hansen, camera, PCD crew audio, art002a000030, 19:27:10 UTC)

This fading and reappearance of rays across changing terrain provides a human-observed example of how ejecta interacts with surfaces of different physical properties and provides insights that help constrain how regolith roughness and surface textures influence ray continuity and preservation.

5.4.4.7 Carroll and Integrity Craters

Just prior to the flyby, the crew contacted the ground to request names for two bright craters in their FOV: one in honor of their spacecraft, *Integrity*, and one in memory of a fallen team member, Carroll (R. Wiseman's late wife) (**Figure 5.18**). The LST is preparing a formal submission to the International Astronomical Union for the names of Integrity crater (2.68°N, 255.08°E) and Carroll crater (18.86°N, 273.47°E).

Both Integrity and Carroll are classified as simple craters. Integrity crater, located on the farside, is ~10.5 km in diameter. Carroll crater is ~5 km across and shone brightly in the crew's view. Carroll lies near the nearside-farside transition, to the northeast of Einstein A crater and can sometimes be observed on the lunar limb from Earth when the libration of the Moon tilts Carroll crater into view from Earth. Carroll crater is geologically young and exhibits a high-albedo ejecta ray system. Its brightness made it a reliable landmark for the crew, who used it to guide them toward additional features of interest on the lunar surface throughout the flyby.

5.5 Lunar Environment and Deep Space

In addition to the several themes focused on lunar surface science, the STM included a theme related to investigating the lunar environment and deep space. Crew observations during the flyby were designed to address key questions about the presence and behavior of lofted lunar dust (**Section 5.5.1**), as dedicated observation periods (including prior to earthrise and during the eclipse) enabled the crew to

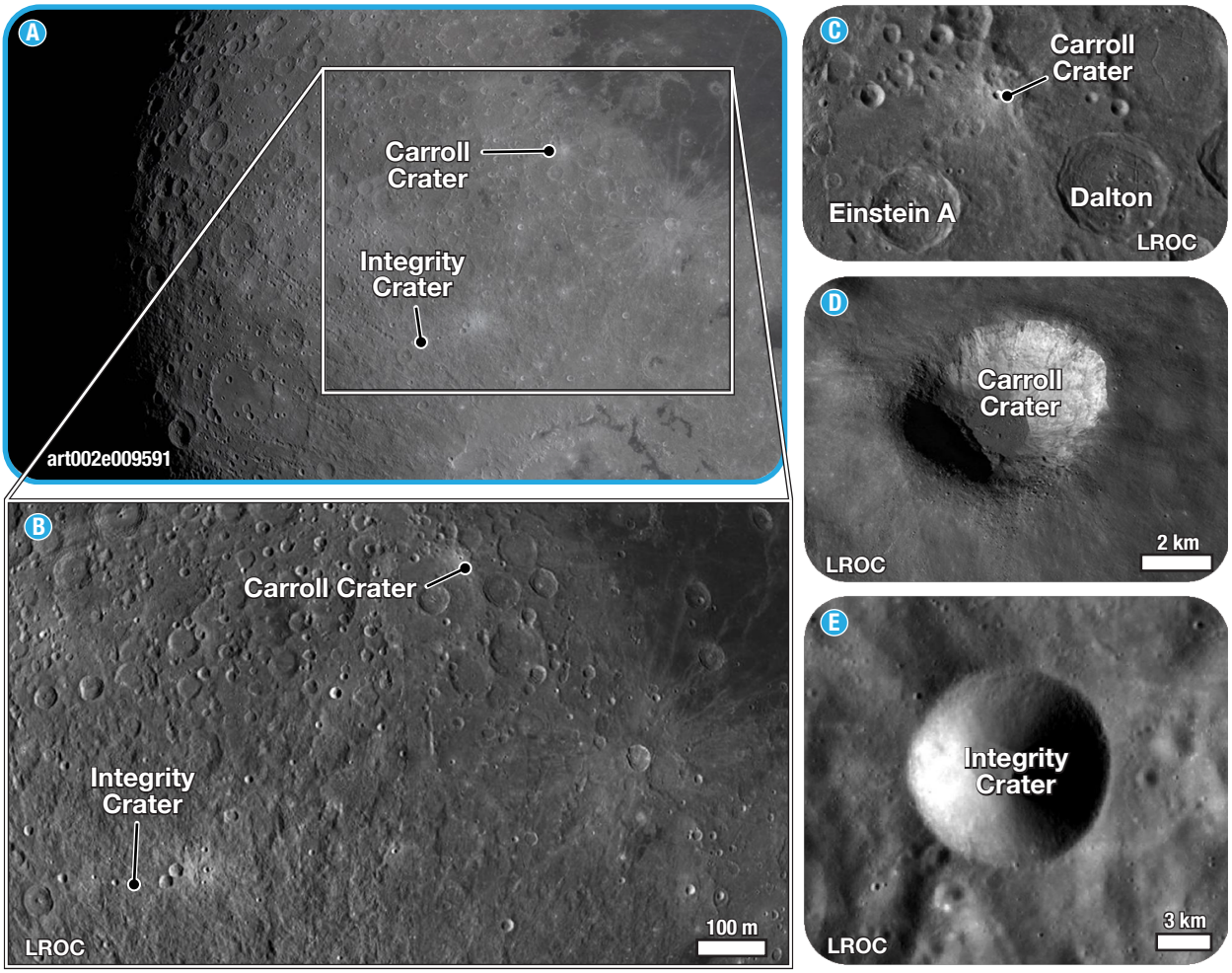


Figure 5.18: Proposed Carroll and Integrity Craters. Views of craters with newly proposed names in (**A**) crew image art002e009591 and (**B**) LROC WAC mosaic (Credit: NASA/GSFC/Intuitive Machines). Enlarged views of (**C**, **D**) Carroll crater and (**E**) Integrity crater from LROC narrow-angle camera (NAC) images (Credit: NASA/GSFC/Intuitive Machines).

search for dust lofting and exospheric glow. Crew observations were also designed to capture phenomena observable in deep space from the lunar sphere, including other planets and stars (**Section 5.5.2**) and solar structures visible during the eclipse (**Section 5.5.3**).

5.5.1 The Lunar Dust Environment

The crew conducted dedicated searches to explore for lofted lunar dust at multiple times throughout the flyby, but no definitive lofted lunar dust was observed. Observing time for lofted lunar dust was scheduled during the eclipse and just prior to earthrise, when the Sun and Earth, respectively, could serve as an illumination source to backlight any lofted dust. During the eclipse, J. Hansen reported: "The other thing to look for is lunar regolith lofting. I haven't seen anything. Yeah, I haven't seen any of that" (J. Hansen, unaided eye, PCD crew audio, art002a000052, 00:43:27 UTC).

Just prior to earthrise, C. Koch reported a potential sighting of dust:

C. Koch	There's some lofted dust. Do you guys think so?
R. Wiseman	No --
C. Koch	Well, but it was like --
R. Wiseman	I think that's mountains.
C. Koch	But no, it was gray where it was popping out. I mean, it could just be an optical [illusion].

(C. Koch, camera, R. Wiseman, unaided eye, PCD crew audio, art002a000015, 23:22:39)

This observation was discussed during the post-flyby crew conference, during which C. Koch noted that her crewmates did not see this gray phenomenon the same as she did. She described seeing the Earth rising as a crescent, and right before the crescent appeared, she saw something that was a slightly different gray color, specifying it was not tall. She hypothesized that it could have been an optical effect rather than lofted dust, or potentially sunlight reflecting off Earth and creating a slight glow right before the brightest part of the crescent Earth came over the horizon.

R. Wiseman reported in the crew conference that he really wanted to see lofted dust but did not see any. R. Wiseman even chose to search for lofted lunar dust as part of his Crew Choice observation block and reported no detections.

With no lofted dust or exospheric glow definitively detected, future Artemis missions could consider carrying a dedicated low-light camera optimized for limb observations (**Section 9.7**) due to unresolved discrepancies in possible lunar dust observations over multiple missions. For example, Apollo crew member observations varied on what they saw in the lunar exosphere. Apollo 17 astronaut Gene Cernan reported rays of light along the lunar limb during sunrise/sunset, attributed by some researchers to forward-scattered light from a high-altitude dust exosphere (McCoy & Criswell, 1974). All three crew members onboard Apollo 17 agreed that dust lofting was observed but did not agree on the time sequence that the dust streamers were visible. According to McCoy & Criswell (1974), Apollo 10 and 17 crews observed dust lofting as "typical sunrise phenomena," which may possibly have been observed by Apollo 8 and 15 crews as well, but the Apollo 16 crew did not observe streamers.

Adding to the mysteries of potential dust lofting above the lunar surface, the Surveyor landers and Clementine spacecraft imaged horizon glow that has been attributed to electrostatically lofted dust near the lunar surface (Criswell, 1972, 1973; Zook et al., 1995). In addition, the Lunar Ejecta and Meteorites (LEAM) experiment deployed during Apollo 17 showed an increase in impact events at sunset and sunrise, corresponding with terminator crossings (Berg et al., 1976). These data may suggest dust lofting and transport associated with terminator-induced dust particle charging (Colwell et al., 2007).

The Lunar Atmosphere and Dust Environment Explorer (LADEE) measured an exospheric dust density of <100 particles/m^3 at 100 km altitude (Sharma et al., 2021), which would likely not be observable by crew. The dust exosphere measured by LADEE is generally persistent, with variations attributed to the presence of meteor showers (Horányi et al., 2015). However, this persistently lofted dust is at too low a concentration to be easily seen by the Artemis II crew. This suggests the Apollo crew observations may be of a more transient or stochastic phenomenon. Future crews should be trained to look for such phenomena during any solar occultation event.

5.5.2 Deep Space

Multiple deep space objects were observed by the crew from the unique vantage point and trajectory of Orion. Deep space astrophotography revealed stunning images of multiple celestial objects including, but not limited to, stars and star clusters in our galaxy, the Large Magellanic Cloud (a satellite galaxy to our Milky Way), and the Carina Nebula (which includes the unstable hypergiant star Eta Carinae) (**Figure 5.19**). During the eclipse, V. Glover reported:

I'm not sure if we talked much about the star field, but we've got lots of stars. You've got the nice glow around the Moon, but, you know, right off the, well, we're upside down now, but from upside down, 4 o'clock, right off the edge of the Moon, looks like a planet, that line of planets. […] There are definitely stars. I think some of those planets that you said we might see, we're seeing. And so, an unreal view. Yeah, the Moon in the foreground is one of the darkest things we see out the window. And now it's deep space behind it. It's kind of dark blue, like it looks from Earth, but we can also still see stars. It's quite a wicked view. (V. Glover, O/E-1 voice loop, 01:14:07 UTC)

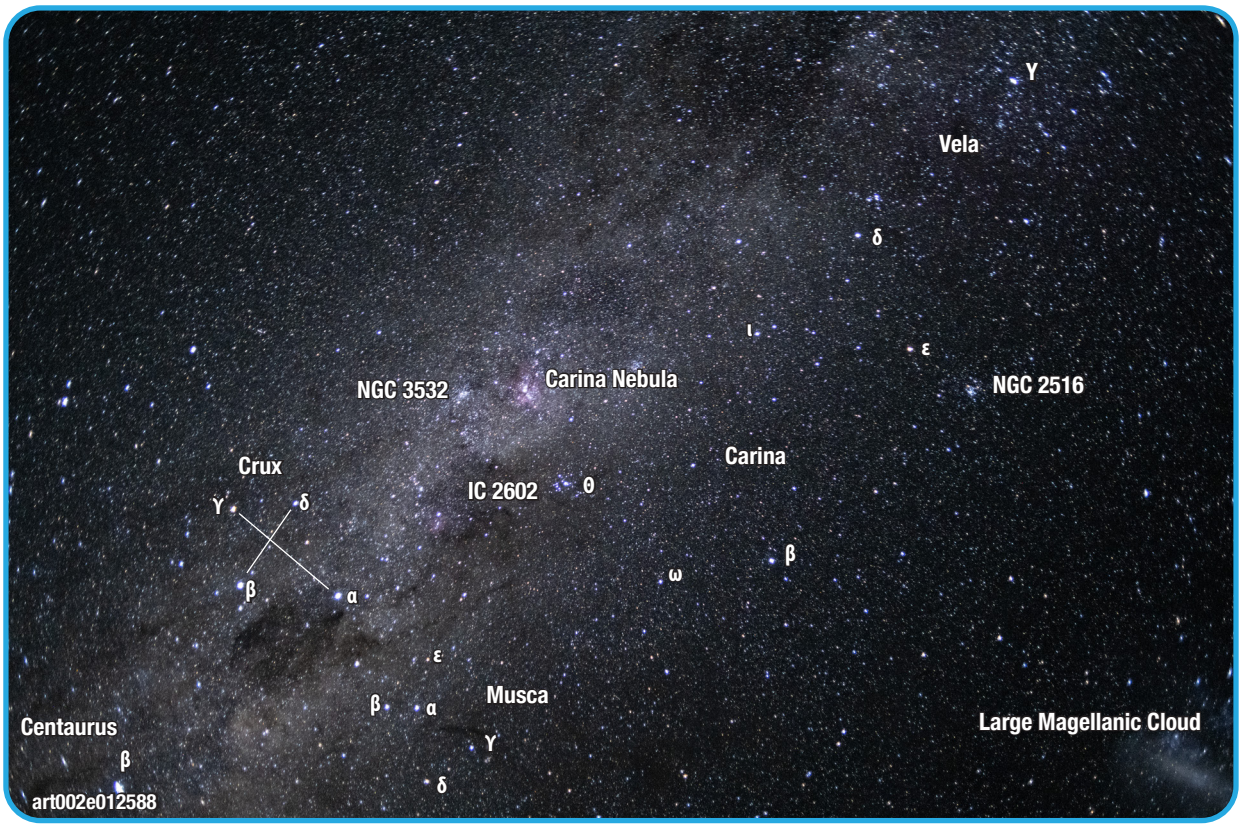


Figure 5.19: Deep Space. Crew image art002e012588 (35mm lens at f/2.8, 10-second exposure, ISO 12800) shows a view of deep space outside of the Orion spacecraft. Greek letters are the Bayer designations identifying bright stars in the southern constellations Vela, Carina, Musca, Crux (the Southern Cross), and Centaurus. NGC and IC numbers identify open star clusters. The Large Magellanic Cloud is a dwarf galaxy, a satellite of the Milky Way. The Carina Nebula is a large diffuse nebula and active star-forming region famously photographed by the Hubble and Webb space telescopes.

Crew images and verbal observations also identified multiple planets in the FOV during the eclipse, including Mercury, Mars, Saturn, and Venus. Mid-way through the eclipse observations, R. Wiseman noted: "Well, now I see two red ones. One -- one is in the -- in the limb. [...] That is -- definitely has a reddish glow to it" (R. Wiseman, camera, PCD crew audio, art002a000053, 1:15:51 UTC). These two bodies were Saturn (closer to the limb) and Mars, both captured in **Figure 5.20**. V. Glover reported over O/E-1 that "Yeah, we can absolutely see the color of Mars. That's awesome" and described the color as "orange" (V. Glover, O/E-1 voice loop, 01:15:52 UTC).

During the lunar eclipse period, the crew also reported visual observations of zodiacal light, and images acquired by both the crew and also the vehicle SAW cameras captured this phenomenon (**Figure 5.20**). Zodiacal light is a diffuse glow caused by sunlight reflecting off interplanetary dust particles in the plane

of the ecliptic within our Solar System. Zodiacal light was also captured during opportunistic Earth imaging, as described in **Section 5.10**.

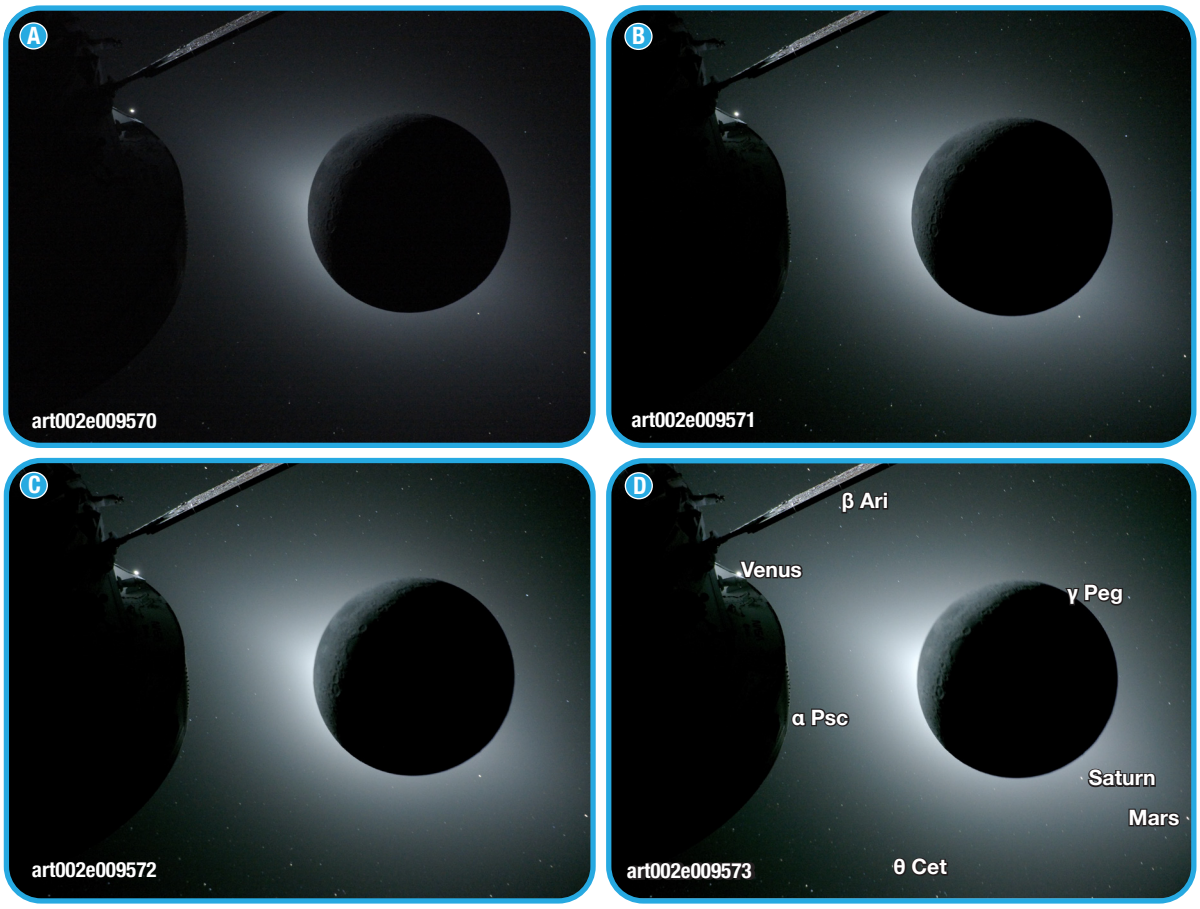


Figure 5.20: Vehicle Views of The Eclipse. Vehicle camera images providing context at multiple exposures during the eclipse. SAW Cam 3 was operated using night-imaging settings with the illuminator off and still images were captured in a night-photo mode in a bracketed series acquired every 15 minutes with four exposures: (**A**) vehicle camera image art002e009570 (exposure of 2 seconds, acquired at 01:10:19 UTC), (**B**) vehicle camera image art002e009571 (exposure of 5 seconds, acquired at 01:10:44 UTC), (**C**) vehicle camera image art002e009572 (exposure of 10 seconds, acquired at 01:11:14 UTC), and (**D**) vehicle camera image art002e009573 (exposure of 15 seconds, acquired at 01:11:49 UTC). This sequence of images reveals multiple stars (Beta Arietis, Alpha Piscium, Gamma Pegasi, and Theta Ceti) and planets in the FOV (Mars, Saturn, Venus).

5.5.3 Solar Structures

The solar corona was observed by the crew during sunset and sunrise of the eclipse period (**Figure 5.21**, **5.22**). Observations were continuous, spanning the duration between sunset and sunrise (**Figure 4.1**), and included crew descriptions and images. During sunset, the crew observed several distinct coronal streamers (also known as helmet streamers, which are elongated structures in the Sun's corona that are formed by closed magnetic loops). These streamers were very dynamic, coming and going, with some being persistent but "pulsating." The crew noted that the sunrise corona was more symmetrical than the sunset corona, consistent with data acquired by the Solar and Heliospheric Observatory (SOHO) during the same period.

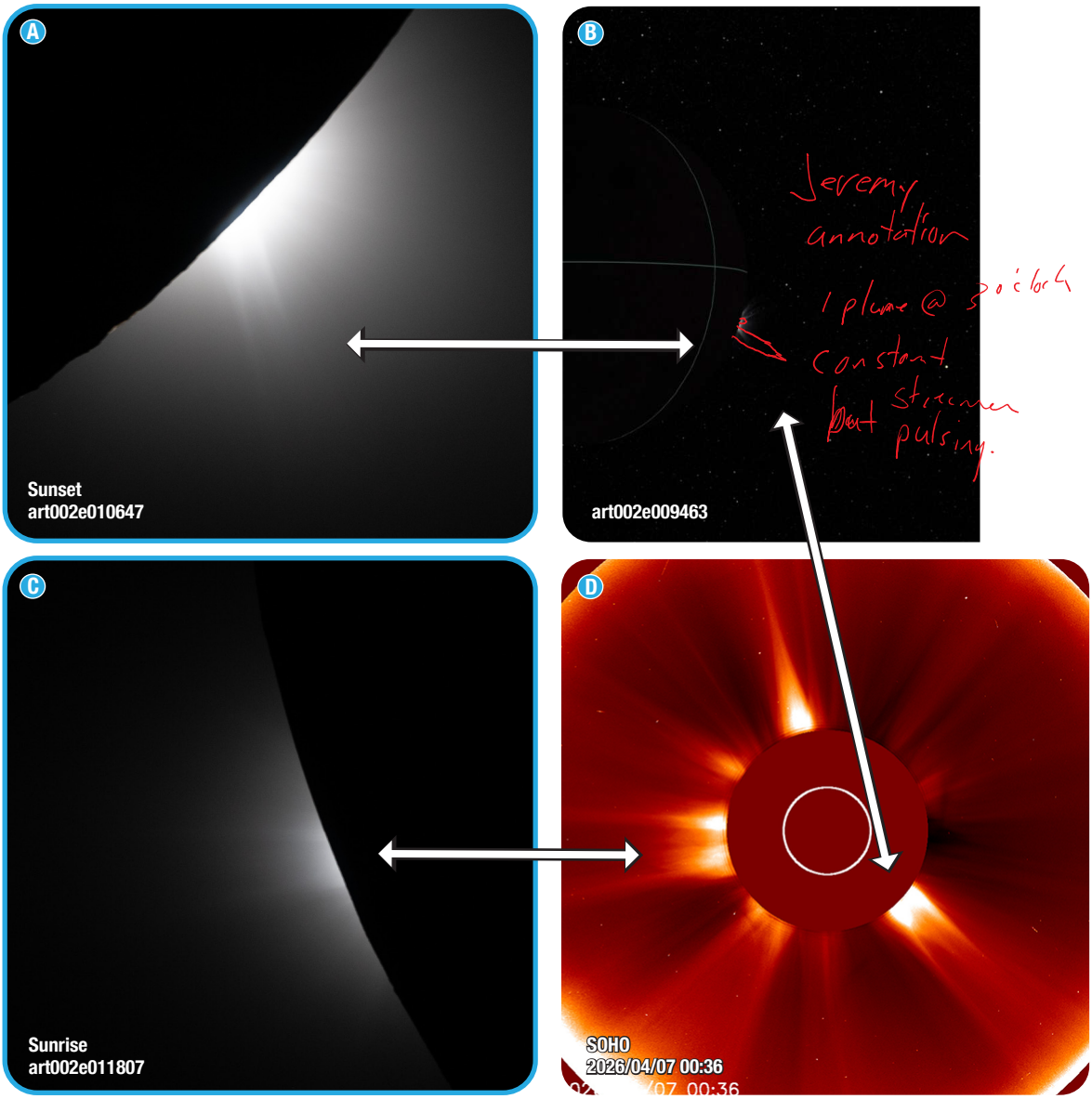


Figure 5.21: The Solar Corona. Crew images (**A**) art002e010647 of sunset and (**C**) art002e011807 of sunrise reveal structures of the solar corona observed during the eclipse. (**B**) Crew annotation from J. Hansen denotes a "pulsating" streamer observed during sunset, also captured in crew images. (**D**) An image of the Sun from the ESA/NASA Solar and Heliospheric Observatory (SOHO) LASCO C2 instrument acquired April 7, 2026, at 00:36, one minute after image (**A**) was taken, capturing corresponding solar activity.

5.6 Tectonic History

Tectonic features are distributed across the lunar surface and are commonly associated with basins, craters, and volcanic features. An understanding of tectonic features informs our understanding of crustal dynamics and the evolution of crustal morphology. The visual detection of tectonic features, including faults, graben, and wrinkle ridges can be challenging in visible-wavelength images and typically requires observation/imaging under moderately low solar elevation angles (between ~20° and 35°). During the lunar flyby, only a fraction of the visible lunar surface was favorably illuminated for visual identification of subtle morphologies and tectonic features, and this fraction varied over time throughout the flyby (**Figure 5.23**). Only between 20:00:00 and 21:00:00 UTC were any visible surfaces

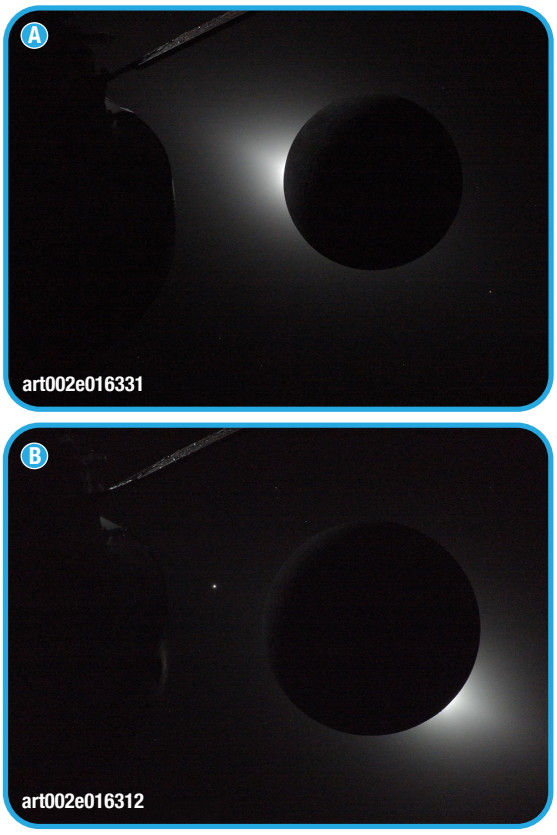


Figure 5.22: Vehicle Views of Sunrise and Sunset. Vehicle camera context views of (**A**) sunrise (vehicle camera image art002e016331, acquired April 7, 2026, 01:25:39 UTC) and (**B**) sunset (vehicle camera image art002e016312, acquired April 7, 2026, 00:37:39 UTC) showing details of the solar corona outside the influence of the Orion cabin windows. They were not acquired at the same time as the crew images in **Figure 5.21**, and thus show different moments during the sunrise and sunset.

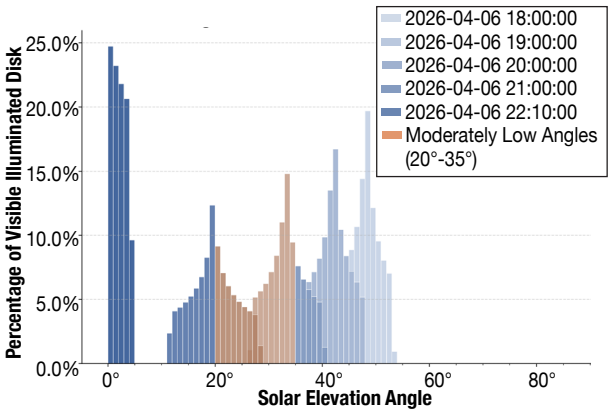


Figure 5.23: Illuminated Lunar Disk. Histograms of the percentage of the visible illuminated disk that was observed from Orion as a function of solar elevation angle. Each histogram represents a specific point in time during the lunar flyby, beginning at 18:00:00 and in time steps of one hour. Moderately low solar elevation angles helpful for resolving subtle morphologies and tectonic features are shaded in orange.

within optimal viewing conditions. Furthermore, the distance between the crew and the lunar surface limited crew observations of features smaller than ~6 km in diameter with the unaided eye (**Section 7.3**), thus limiting observations of small-scale tectonic features during the flyby. Despite these challenges, the crew were able to resolve some features of tectonic origin, and crew-acquired images further revealed tectonic features across the highlands (**Sections 5.6.1–5.6.3**).

5.6.1 Regional-Scale Fault Complexes

A regional-scale fault complex is defined as an interconnected system of related geologic faults formed as the result of a common regional stress field. Although fault complexes are present on the lunar surface (e.g., Guest & Fielder, 1968, Binder & Gunga, 1985), prominent regional fault complexes were not visible to the crew during the flyby. The LTP did include three targets that incorporated specific features relevant to more local-scale tectonic investigations: Aristarchus Plateau, Orientale basin, and Nearside/Farside Transition Discussion (**Appendix A**). For Aristarchus, the LTP included observation actions to describe and image topography and faults or fissures visible across the plateau. For Orientale, observation actions included describing and imaging topography, faults or fissures, and other visible feature characteristics within mare patches and across ring mountains and ejecta. For the Nearside/Farside Transition Discussion, observation actions included describing and imaging topography and faults or fissures visible within the maria and proximal highlands.

During the flyby, the crew noted that the Orion ground track was far from Aristarchus, which made identification of specific small-scale features there difficult. Even so, the crew were able to resolve curvilinear features on the plateau, including the volcanic feature Valles Schroteri (commonly referred

to as the Grand Canyon of the Moon), but they did not specifically resolve features of tectonic origin within the region.

For Orientale, the crew were struck by the steep cliffs associated with the multiple basin rings, and they noted where collapse had occurred along the ring walls. "Wow. Those rings, wow. The crater wall is -- it is like a drop. There's so much variation in that terrain, just in that ring. Like, wow" (V. Glover, camera, PCD crew audio, art002a000037, 20:53:24 UTC). The outermost basin rings of Orientale have been interpreted to be regional-scale normal faults (Nahm et al., 2013), and the observations made by the crew further support a dynamic tectonic history that occurred as a result of the Orientale impact event.

In later discussions, the crew posited about the origin of relatively high-albedo, curvilinear features in western Oceanus Procellarum that struck their interest:

R. Wiseman	Okay, so looking over at Glushko […] The rays almost look like they track in the maria and then curve northward. But I think that's just looking at the whole Moon and the way those rays bend around the Moon. […] Looking out to the east end of the maria of Glushko, it almost looks like some of those rays absolutely loop at 180 back to the north.
J. Hansen	My leading theory on that, probably completely wrong, is that that is because they're hitting elevation. [...]
R. Wiseman	[...] I'm gonna take a note here because I am fairly convinced, looking out the window, that I see looping on Glushko's [rays]. -- I just drew in red on OneNote on [LTP Target] Glushko 2 of 2, and I really want to look more at that when I get home because it really looks to me like there is looping coming out the west side of Mare Humorum looks like one ray. But that looks like it bends around from Glushko. It's probably just an optical illusion. But it bends all the way around and starts coming back on itself over towards Orientale. I would love to just sit there with a picture and try to talk through that when I get home.

(R. Wiseman, unaided eye, PCD audio art002a000023, 21:11:02 UTC; J. Hansen, camera, PCD audio art002a000038 21:14:06 UTC)

Analyses by the LST, in collaboration with the crew during post-flight discussions, indicate that the observed features include a very subtle wrinkle ridge system in Oceanus Procellarum spanning from Glushko's ray system to Reiner Gamma, and onward toward Grimaldi Basin (**Figure 5.24**). Scarps that comprise this arcuate system of wrinkle ridges are fairly uniformly around 100 m in height. Several possibilities could explain how crew members were able to confidently observe this continuous wrinkle ridge system. First, all crew members were able to perceive topography near the horizon, most notably at Orientale. However, the mountain features observed at Orientale are 1–3 km tall, an order of magnitude larger than these scarps. Second, the wrinkle ridge scarps in this system have a 3–5° slope, which, at the time and position of their observations, would have served to decrease phase and emission angles along the wrinkle ridge scarps (measuring 5–10 km wide). This slight change in illumination condition, consistent over a trace of ~600 km, may have provided enough of an apparent albedo change to be similar in appearance to the nearside distal rays of craters, including Glushko.

Lastly, although the crew did not verbally describe regional tectonic features during the Nearside/Farside Transition Discussion, they imaged several regional features. For example, Rimae Repsold, a prominent linear rille system associated with either tectonic or volcanic activity in the floor of Repsold crater (e.g., Atlas, 2005; Byrne, 2008), can be seen cross-cutting the terrain between Repsold and Galvani craters (**Figure 5.25**). Further analyses using complementary datasets could resolve the origin of this and other linear or arcuate rille systems that extend across the nearside/farside transition.

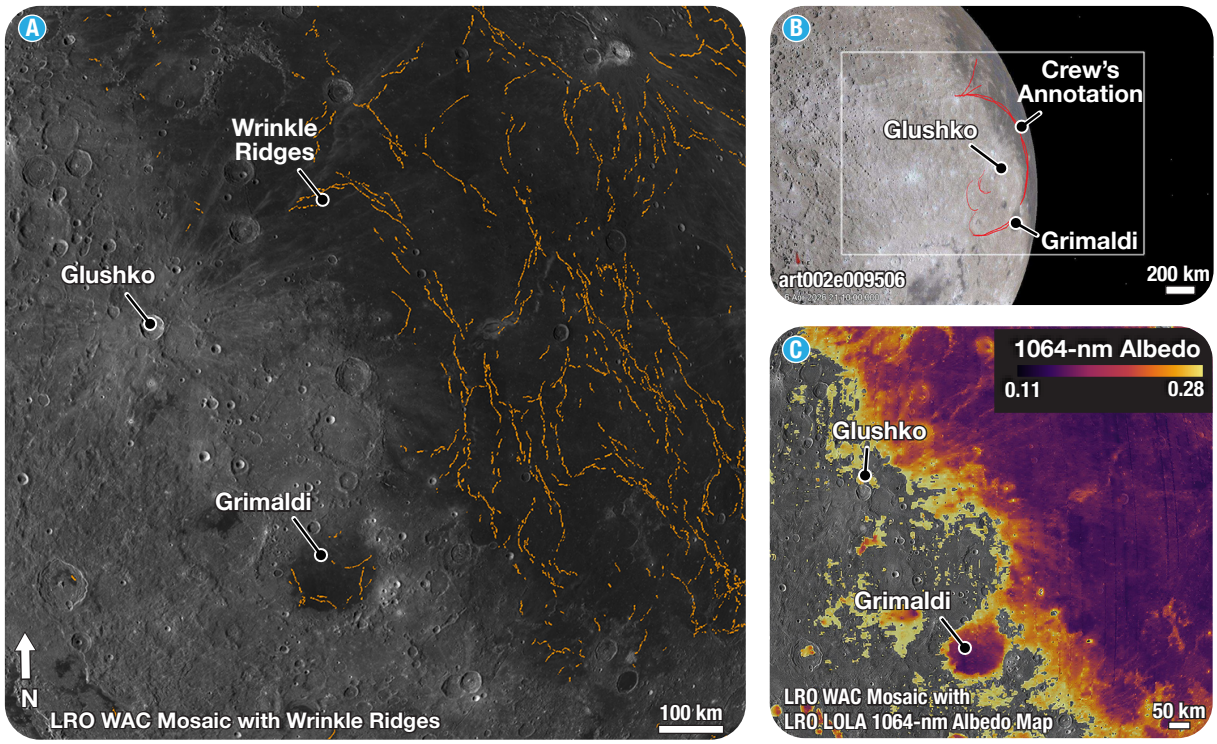


Figure 5.24: Curvilinear Features. (**A**) Wrinkle ridges (orange lines) are traced in the maria on an LRO mosaic (from Thompson et al., 2017). (**B**) An in-flight annotation art002e009506 by R. Wiseman denotes bright curvilinear features observed by the crew, marked in red. (**C**) An LRO LOLA 1064-nm reflectance map shows that the curvilinear features observed by the crew are not associated with any distinct enhancement in surface reflectance (Credit: NASA/GSFC/Intuitive Machines).

5.6.2 Floor-Fractured Craters

The flyby trajectory did not afford favorable viewing opportunities of floor-fractured craters, and thus the LTP did not include these as targets for detailed crew observations. However, the crew did capture floor-fractured craters in several images, including Repsold and Repsold G in **Figure 5.25**. Crew-captured images could serve as a complementary dataset to the existing orbital images used to analyze floor-fractures craters (Jozwiak et al., 2012) by offering perspectives and viewing geometries not attainable from orbital spacecraft.

5.6.3 Massifs of Non-Volcanic Origin

Massifs of non-volcanic origin are evident across the lunar surface, in particular within maria and along transitions between maria and highland terrains. Interpretations of whether such massifs formed as the result of tectonic or impact processes warrant further analysis on a case-by-case basis. As with floor-fractured craters, the flyby trajectory did not afford favorable viewing opportunities of lunar massifs, and thus none was included as an observation target in the LTP. Although the crew did not describe massifs, some of their images revealed impressive views of Mons Pico, Montes Teneriffe, and the rim of Plato crater on the eastern limb on the nearside (**Figure 5.26**). This crew image captures the stark difference between the smooth, low-albedo maria and the prominent, higher-albedo montes that peek out of the maria along the northern Oceanus Procellarum-highland boundary. These limb images capture the types of views enabled by human explorers' flexibility to rapidly pivot to acquire observations and images from multiple perspectives and orientations without having to reorient the spacecraft.

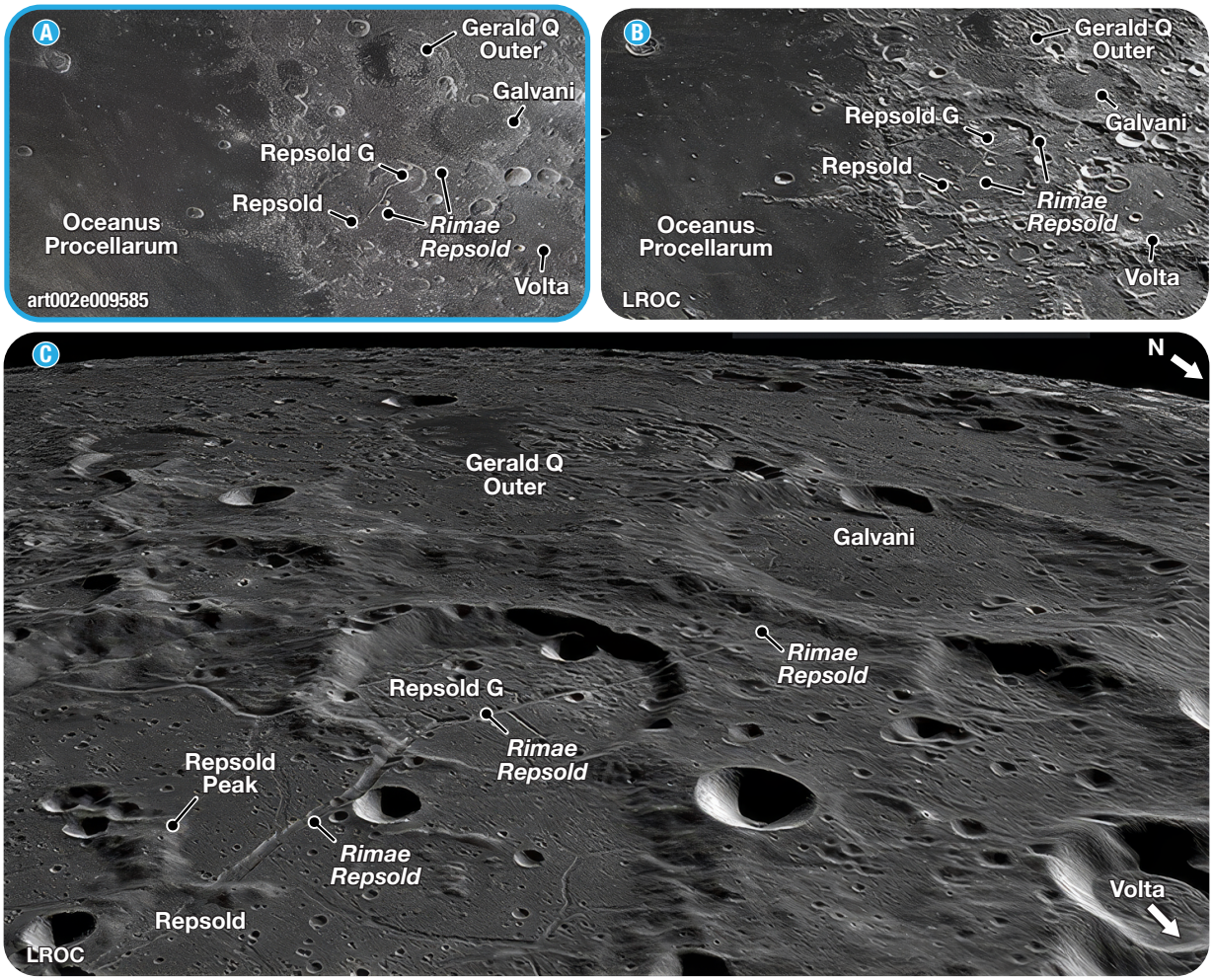


Figure 5.25: Rimae Repsold. Rimae Repsold as seen in Artemis II and LRO observations of the nearside/farside transition. (**A**) Crew image art002e009585 showing Rimae Repsold, the curvilinear feature striking across Repsold, Repsold G, and Galvani craters. (**B**) Annotated LRO mosaic (Credit: NASA/GSFC/Intuitive Machines) showing the same area as the crew image, for comparison. (**C**) Oblique view of Rimae Repsold rendered from LRO data. Note that there is a network of linear rilles in the floors of Repsold and Repsold G. These show the superpositional relationships, where Rimae Repsold cross-cuts Repsold Peak.

5.7 Future Sites and Poles

During the Artemis II flyby, the crew made several observations and acquired multiple images of past landing sites, selected and upcoming landing sites, and potential future landing sites.

5.7.1 Regional Context of Past Landing Sites

The LTP included observation actions related to characterizing the broader geologic context of past landing sites early on in the flyby, when Oceanus Procellarum and Mare Imbrium were visible. Image analyses revealed that the landing sites of the Apollo 12, Apollo 14, Chang'e 3, Chang'e 5, Luna 17, and Surveyor 1 missions were visible at the start of the flyby (**Figure 5.27**), though the specific landing regions were beyond the crew's resolution.

5.7.2 Regional Context of Future Landing Sites

The LTP also included observations of regions that have been selected for exploration (Reiner Gamma) and regions that have been proposed for future robotic and/or human missions to the Moon (e.g.,

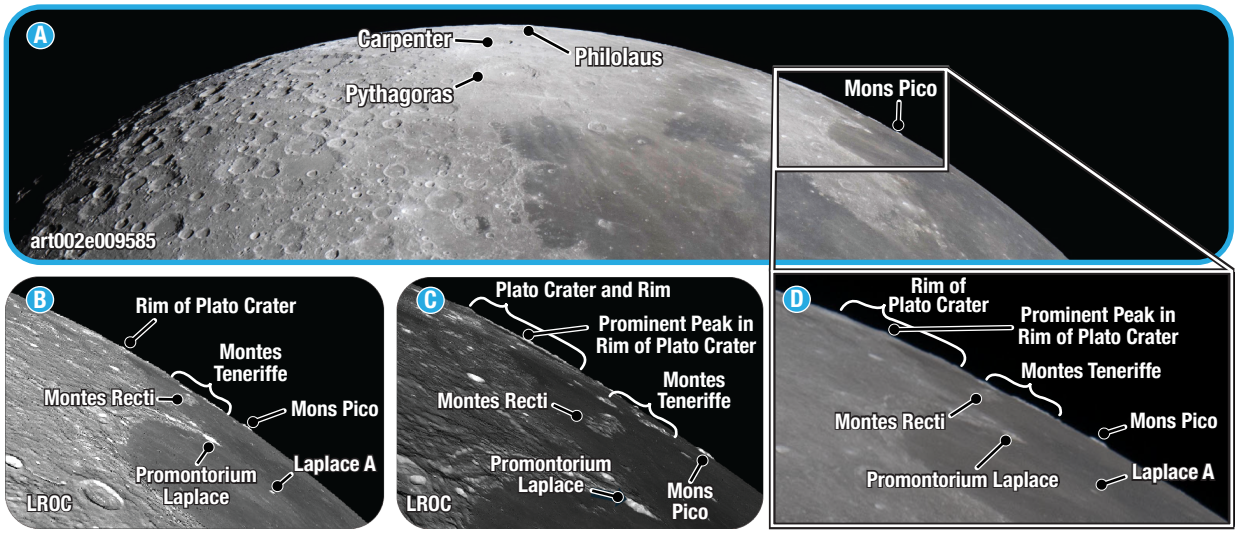


Figure 5.26: Limb Observations. (**A**) Limb observations of Mons Pico, Montes Teneriffe, and the rim of Plato crater, in crew image art002e009585, with an enlarged inset (**D**). (**B**) An LROC mosaic of the area in the enlarged inset (Credit: NASA/GSFC/Intuitive Machines). (**C**) The LROC mosaic rotated to the left to reveal features visible on the limb.

Aristarchus Plateau). The crew's observations provide complementary datasets to the existing wealth of orbital data in characterization of these high-priority science sites.

5.7.2.1 Reiner Gamma

The Reiner Gamma region of the Moon is known for its enigmatic swirl features on the lunar surface (e.g., Hood & Schubert, 1980; Schultz & Srnka, 1980; Hood & Williams, 1989; Blewett et al., 2011). Swirl features are unique to the Moon, and their origin has long been debated. A leading hypothesis is that lunar magnetism in these regions may protect the lunar regolith against space weathering, resulting in the albedo differences between the swirls and the surrounding terrain. To further understand the origin and nature of lunar swirls, NASA's Commercial Lunar Payload Services (CLPS) program will deliver the Lunar Vertex investigation, which includes instruments on a lander and a rover platform, to Reiner Gamma. This investigation is specifically designed to investigate the origin of lunar magnetic anomalies, the origin of lunar swirls, space weathering, and the structure of the mini-magnetosphere that forms over the Reiner Gamma magnetic anomaly (Blewett et al., 2023).

For Artemis II, Orion's trajectory provided an oblique and short-duration view of Reiner Gamma near the start of the flyby (**Figure 5.28**), before the target moved out of view. R. Wiseman described the shape as "an amoeba, the head of it, and then the tail kind of goes off" (R. Wiseman, camera, PCD crew audio, art002a000022, 19:42:50 UTC), while J. Hansen likened the structure of Reiner Gamma to a "sperm" (J. Hansen, unaided eye, PCD crew audio, art002a000033, 19:47:16 UTC). J. Hansen also described uniformly high-albedo properties of the swirl, while noting a lower-albedo feature in its center:

> The albedo of Reiner Gamma is about a 7 compared to Aristarchus, which would be about a 10 [on the albedo scale]. And it's a very uniform albedo. I do see in the middle of the sperm head is, you know, something dark there with my naked eye. And so it looks like there's a bit of [maria] or something in the middle of it. (J. Hansen, unaided eye, PCD crew audio, art002a000033, 19:47:51 UTC)

Additionally, J. Hansen reported brownish hues in the region that "look like deposits from the Glushko rays on top of the highlands. And the boundary is sort of the tail of the sperm of Reiner Gamma" (J. Hansen, unaided eye, PCD crew audio, art002a000033, 19:47:16 UTC). R. Wiseman similarly

reported that Reiner Gamma "is streaked by rays" (R. Wiseman, camera, PCD crew audio, art002a000022, 19:42:50 UTC):

> There's a dusting of rays that come across. Some are from Glushko, but some, the ones that come right across Reiner Gamma, are not from Glushko. (R. Wiseman, unaided eye, PCD crew audio, art002a000022, 19:47:51 UTC)

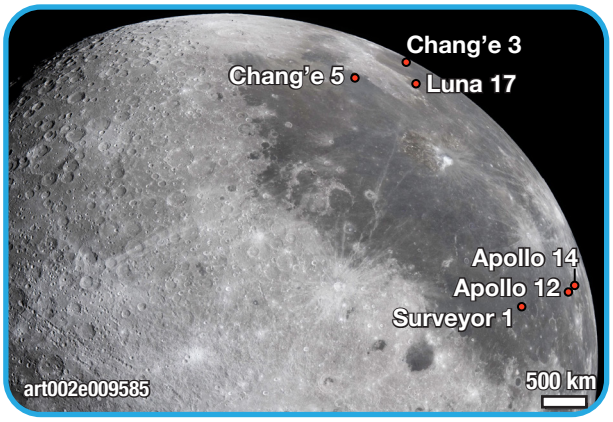


Figure 5.27: Past Landing Sites. Crew image art002e009585 of the nearside-farside transition is marked with locations (red filled circles) of the Chang'e 3, Chang'e 5, Luna 17, Apollo 12, Apollo 14, and Surveyor 1 historic landing sites.

5.7.2.2 Aristarchus Plateau

The Aristarchus Plateau (discussed in detail in **Section 5.9.2**) remains a priority landing region for the planetary science community due to its rich diversity of volcanic features and complex geologic history (e.g., Coombs et al., 2012; Jawin et al., 2019, 2021; Glotch et al., 2021; Morgan et al., 2023). The Aristarchus region contains the largest pyroclastic deposit on the Moon (Gaddis et al., 2003), the widest and deepest sinuous rille on the Moon (Schubert et al., 1970; Hurwitz et al., 2013), and intrusive and extrusive examples of evolved, thorium-rich silicic lithologies (Flahaut et al., 2012). This area was one of the proposed landing sites for the cancelled Apollo 18 mission to sample exposed bedrock in the deepest sinuous rille on the Moon (Wilhelms et al., 1987), and a proposed region of interest within the Constellation Program for investigating its geologic complexity and resource potential (Connolly, 2006).

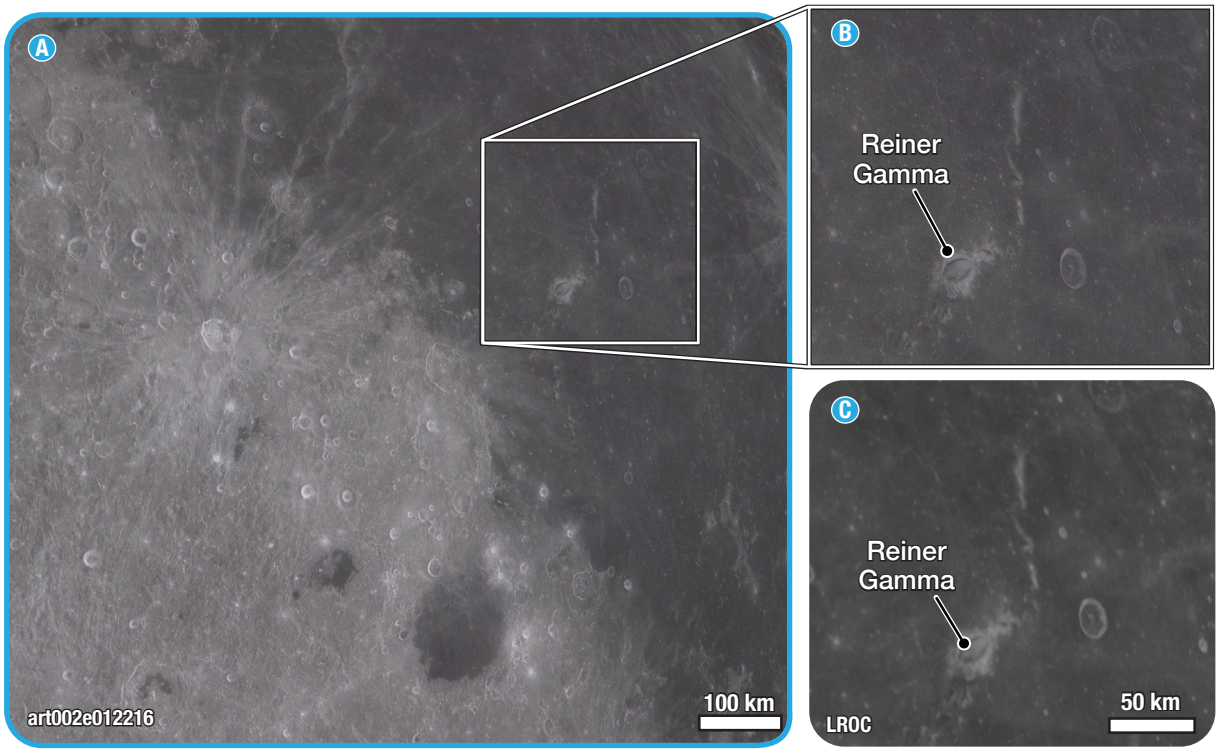


Figure 5.28: Reiner Gamma. (**A**) Crew image art002e012216 shows the nearside-farside transition area with Reiner Gamma outlined in the inset, and enlarged in (**B**). (**C**) A shadow-free LROC WAC mosaic of Reiner Gamma is shown for comparison (Credit: NASA/GSFC/Intuitive Machines).

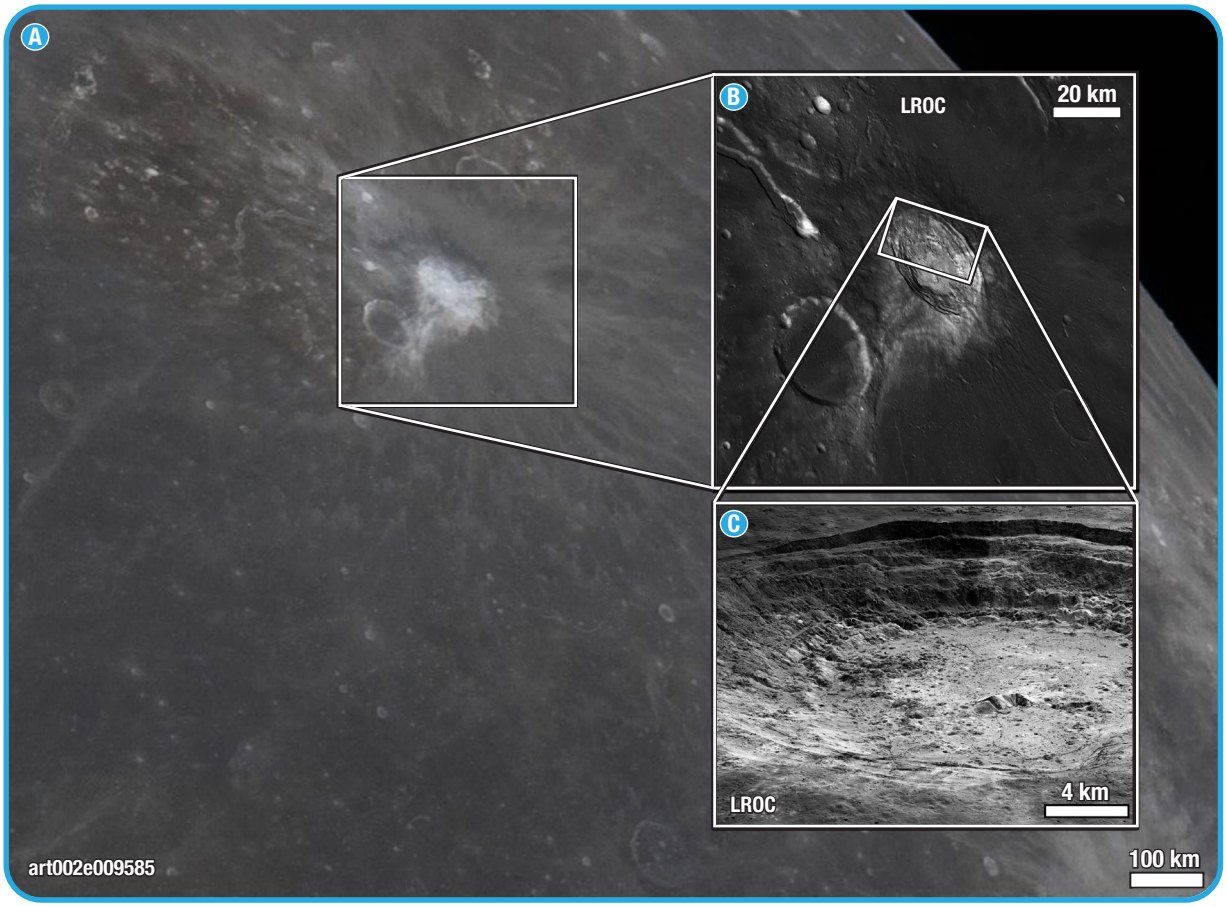


Figure 5.29: Aristarchus Plateau. (**A**) Crew image art002e009585 of Aristarchus Plateau. (**B**) LROC WAC mosaic showing the Aristarchus crater region (Credit: NASA/GSFC/Intuitive Machines). (**C**) LRO NAC image M1259297876LR showing the crater's central peak and high-albedo material.

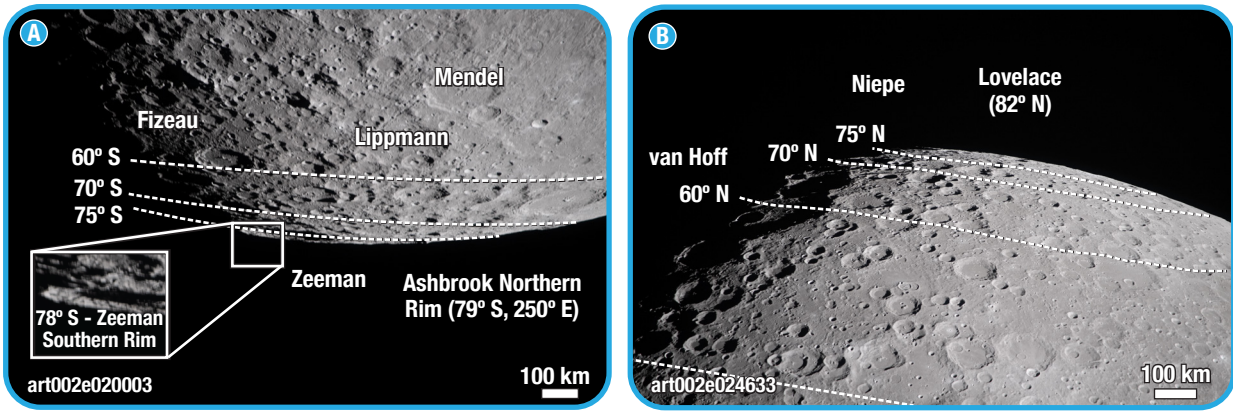


Figure 5.30: Polar Visibility. Artemis II crew images of the (**A**) southernmost (crew image art002e020003) and (**B**) northernmost (crew image art002e024633) regions of the Moon visible during the flyby. Approximate latitude lines are overlain. One of the southernmost discernible features is Zeeman crater (78°S) and the northern most discernible feature is Lovelace (82°N).

During the lunar flyby, the Artemis II crew noted distinct color, albedo, and morphologic attributes of the Aristarchus Plateau. The crew reported the Aristarchus region as having color hue variations ranging from brown to the north and greens to the south and into the east of the plateau, extending toward Rima Prinz. Furthermore, the crew reported Aristarchus crater to be among the highest-albedo features on the Moon (**Figure 5.29**). Such high-albedo properties associated with a complex crater can indicate high-albedo crustal material excavated from depth and thus can provide insights into near-side stratigraphy and composition of the crust, while color hues observed on the surface can provide clues to material properties and compositions, highlighting the region's complex geologic history. Further discussion of Aristarchus Plateau is included in **Section 5.9.2**.

Table 5.2: Polar Visibility. This table shows the latitude limits observable from Orion during the lunar flyby as a function of time, in 30-minute intervals.

Time (UTC)	Northernmost Visible Latitude (°)	Southernmost Visible Latitude (°)
18:00:00	87.56	-83.09
18:30:00	87.01	-82.83
19:00:00	86.36	-82.53
19:30:00	85.57	-82.18
20:00:00	84.60	-81.79
20:30:00	83.42	-81.34
21:00:00	81.98	-80.86
21:30:00	80.27	-80.38
22:00:00	78.36	-80.03
22:30:00	76.54	-80.00
23:00:00	75.31	-80.47
23:30:00	75.02	-81.45
0:00:00	75.59	-82.70
0:30:00	76.62	-83.91
1:00:00	77.77	-84.96

5.7.3 The Polar Regions

No Apollo crew were able to observe the lunar poles due to illumination and viewing geometry constraints. Orion's trajectory provided a lunar flyby nearly centered above the lunar equator, which also precluded direct viewing opportunities of the lunar polar regions; however, latitudes as far north as ~87° and as far south as ~-85° were viewable at the start and end of the Artemis II flyby, respectively (**Table 5.2**), providing a unique opportunity to observe circumpolar features under highly oblique viewing geometry. The LTP included a Terminator Discussion (**Section 5.8.2**), during which crew made observations and acquired images of the most southern to most northern parts of the visible disk (**Figure 5.30**).

During the flyby, the crew often used the terms "north pole" and "south pole" to describe the most northward or southward regions viewable in their specific FOV at a given moment. These regions do not necessarily correspond to the true lunar poles, but rather the northernmost and southernmost portions of the lunar disk visible at the time of observation (which are bounded in **Table 5.2**).

The crew typically described the lunar north polar region as having very high-albedo characteristics. For example, R. Wiseman reported that the north polar region "looks very white up there to me," though "it could just be Sun angle" (R. Wiseman, unaided eye, PCD crew audio, art002a000018, 19:03:27 UTC). He reported:

> The regolith over the north pole looks smooth, with a few very large prominent craters, and it is very white. And then from the northern, up in the north pole, there's a complex crater with rays that come out and dust across the nearside. They dust across that […] greenish-brown [maria] to the northwest of Aristarchus. So that -- man, a polar orbit would be cool to go see it, but the pole is so white, but that could just be grazing angle. I would put the albedo of the north pole at the same level as the [albedo of] ejecta rays that are coming out of Byrgius [Alpha], but it is not as bright as Aristarchus or Byrgius [Alpha]. (R. Wiseman, unaided eye, PCD crew audio, art002a000018, 19:03:27 UTC)

Later on, V. Glover reported: "like five degrees around the north pole, it becomes very high albedo. It becomes much lighter" (V. Glover, unaided eye, PCD crew audio, art002a000037, 20:39:55 UTC). The brightness of the poles as observed by the crew could be attributed to the viewing geometries in which they were observing the Moon, where different phase angles cause surfaces to appear brighter or darker (**Section 5.3**). Similar brightness at the poles can be seen in LROC images acquired at high incidence angles (e.g., Sato et al., 2014). Actual photometric variations on the surface of the Moon can be caused by compositional variations, topography, fine-scale regolith properties, grain size, and maturity, but perceived photometric changes can also be due to viewing geometries.

The lunar polar regions are the intended destination for Artemis landed missions and NASA's Moon Base. To characterize the polar regions prior to these crewed missions, NASA plans to send robotic missions, including the Volatiles Investigating Polar Exploration Rover (VIPER), to provide ground truth data of the polar regions. For example, VIPER will deliver key information on technology performance and real-time operations in the lunar polar environment, helping to optimize the limited surface exploration time available to Artemis crews while simultaneously reducing risk and enhancing crew health and safety on the lunar surface (Heldmann et al., 2026).

5.8 Limb and Terminator Morphology

Observations of the lunar limb and terminator by the Artemis II crew provide insight into the appearance of the Moon from the unique vantage point of the Orion spacecraft. The lunar limb (the visible outer edge of the lunar disk) varies with viewing geometry, and during Artemis II, the crew saw limb perspectives markedly different from those available to Earth-based observers. Their view of the lunar limb also changed throughout the flyby as a function of Orion's trajectory.

The crew's view of the terminator similarly varied during the flyby. The lunar terminator marks the boundary between local day and night on the lunar surface, producing a striking visual contact between illuminated and shadowed terrain. At low solar angles, long shadows accentuate topographic relief, making the terminator region ideal for identifying surface morphologic and structural detail. As the terminator migrates across the lunar surface, different portions of the Moon transition between light and darkness, each becoming briefly optimized for viewing accentuated topography.

The crew's observations of the limb and terminator inform expectations for subsequent Artemis missions. They also provide insight into the scale of features detectable from these unique viewing geometries and may guide imaging needs (e.g., camera selection, required spatial resolution, optimal viewing geometries, etc.) to support future Artemis missions.

5.8.1 The Lunar Limb and Horizon

Views of the lunar limb provided the crew with several opportunities for unique scientific observations. As planned by the LST, the crew monitored visible surface features and topography along the lunar limb, monitored for evidence of lofted dust (**Section 5.5.1**), and characterized how variations in limb topography influenced the timing of visible eclipse structures.

Because the limb they observed was defined by the spacecraft's trajectory rather than Earth's viewing geometry, the crew encountered topography and relief patterns distinct from those familiar in telescopic views. Along the rotating limb, lunar topography appeared especially pronounced, reflecting the Moon's irregular shape and geologic diversity. Crew images and descriptions of the limb included observations of color, albedo, roughness, and topographic structures, including prominent craters and mountain peaks. In particular, the crew described Aristarchus crater, Copernicus crater, Grimaldi crater, Hertzsprung basin, Ohm crater, and Orientale basin, and described impressions of the varying relief.

Observations of limb-based terrain began even before the flyby. Reflecting on the crew's first good sightlines to the Moon, C. Koch described a striking view of Mare Imbrium:

> Houston, Integrity, I wanted to provide an observation, or a little bit of descriptive nature, on something that we saw on the first day we had good Moon views. This was when we saw more of the nearside, and the ground helped me out with identifying Mare Imbrium. Mare Imbrium, when you have the western limb also in view, looks completely different than the normal view we have of the nearside. It is the most striking feature of the western limb view that we had. And the mountain chains that form its eastern side are very prominent, but they actually stand out more than I'm used to seeing, even on the western side.

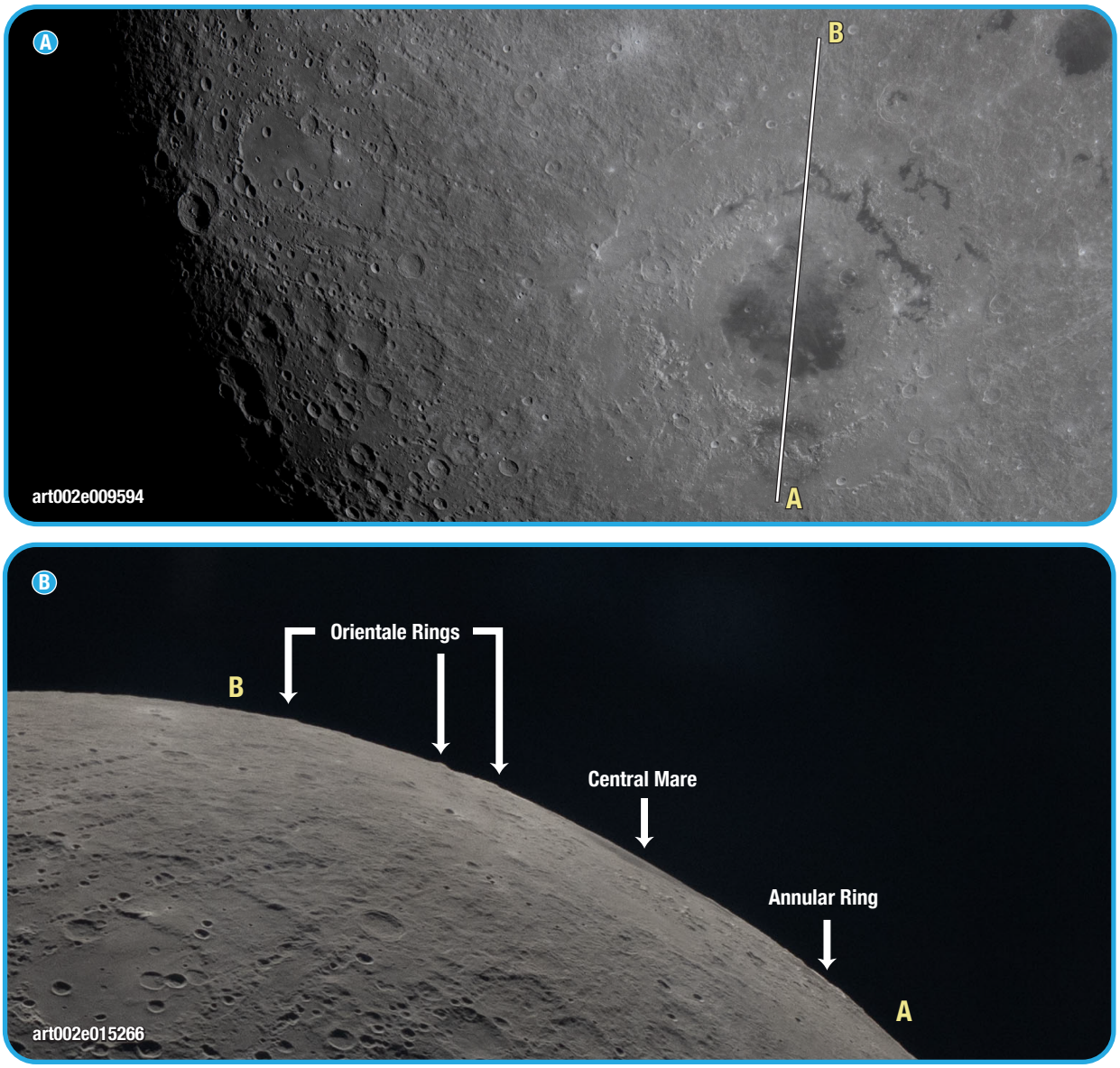


Figure 5.31: Orientale on the Limb. (A) The crew image art002e009594 of Orientale basin is annotated with a white cross-sectional profile, approximately located from the south (Line end A) to the north (Line end B), tracing to the cross-sectional view along the limb, captured in (B) with crew image art002e015266. White arrows show the locations of prominent topography visible in the limb view. Secondary crater chains can be seen on the northwest and west side of Orientale.

> And the whole thing just feels like a big bump. It actually looks like a large healing wound with a high albedo forming the mountain chain around the impact basin. And I just don't think I had had enough chance to describe how striking it was on that western limb view as we were coming in a couple days ago. (C. Koch, O/E-1 voice loop, 19:34:41 UTC)

The crew also had planned time to observe the lunar limb when backlit by the Earth just before earthrise and by the Sun during the eclipse. The topographic relief visible along the lunar limb could also influence the precise timing of the total solar eclipse, as variations in topography modulate how and when the Sun becomes masked from view. As discussed in **Section 5.5.1**, this lighting condition may also illuminate lofted dust in the lunar exosphere.

The crew often remarked on how striking, yet variable, the relief along the lunar limb appeared from orbit. For example, C. Koch remarked: "Relief on the limb -- you've got to be kidding me. This is a picture of relief on the Moon. You can actually see mountains on the limb of the Moon" (C. Koch, camera, PCD crew audio, art002a000005, 20:15:01 UTC). Later, as the limb featured a different region of the Moon, C. Koch noted contrasting impressions: "I notice on this limb, I don't see as many mountains" (C. Koch, camera, PCD crew audio, art002a000011, 22:35:07 UTC).

Some of the most dramatic expressions of limb topography occurred when Orientale was in view. **Figure 5.31** captures the pronounced topography of Orientale basin and its ring structures along the limb, illustrating how the crew's vantage point provided direct insight into how major basins shape lunar topography.

The crew also highlighted how topography was perceived against the darkness of space. V. Glover stated: "I was taking photos of the horizon on the eastern side and looking at the mountains and things that you can see against the blackness of space" (V. Glover, camera, PCD crew audio, art002a000037, 20:55:37 UTC). He later remarked: "I can see mountains with my unaided eye on the limb. That it is not a smooth, perfect circle, that -- it has terrain, and I can tell that there are mountain peaks out there" (V. Glover, unaided eye, PCD crew audio, art002a000044, 22:26:40 UTC). Similarly, C. Koch observed: "I could see terrain against the blackness of space on the limb" (C. Koch, unaided eye, PCD crew audio, art002a000008, 20:54:46 UTC).



Figure 5.32: Sunset Behind the Limb. Crew image art002e010717 taken at sunset during the solar eclipse shows illuminated topography along the lunar limb.

V. Glover also observed how color and texture diminished with increasing distance from the limb: "Color and texture definitely go away as things move toward the limb, or we move away from the limb" (V. Glover, unaided eye, PCD crew audio, art002a000044, 22:28:32).

During the eclipse, J. Hansen made detailed observations of the topography illuminated from behind by the Sun (**Figure 5.32**):

> One of the other things I want to describe, which was surprising to me, but the entire Moon is lit up. It's glowing behind the entire Moon. I thought it would look dark against the black sky or deep space, but the Sun is lighting up the entire limb of the Moon. You can see the entire perimeter of it, and even now with the Sun far behind the Moon, you can see, you can still make little bits of topography around the entire limb, just bumps as you go around it. (J. Hansen, unaided eye, PCD crew audio, art002a000052, 01:02:04 UTC)

Comparisons between the crew's descriptions of the limb and time-correlated crew images with known features on the Moon can contextualize these observations. **Figure 5.33** shows a view of the lunar limb during earthrise, when the Earth was emerging from behind the black silhouette of the Moon. The image reveals that during earthrise, the crew were seeing topographical features from the rims of Al-Biruni and Goddard craters along the lunar limb (**Figure 5.33**).

5.8.2 The Lunar Terminator

Terminator views (**Figure 5.34**) provided the crew with perspectives of the Moon distinct from those captured in high-Sun LRO images. The LTP (**Appendix 1**) included actions for the crew to monitor how features along the terminator appeared under low solar elevation angles, including variations in apparent sharpness, morphology, and color. Crew descriptions captured how

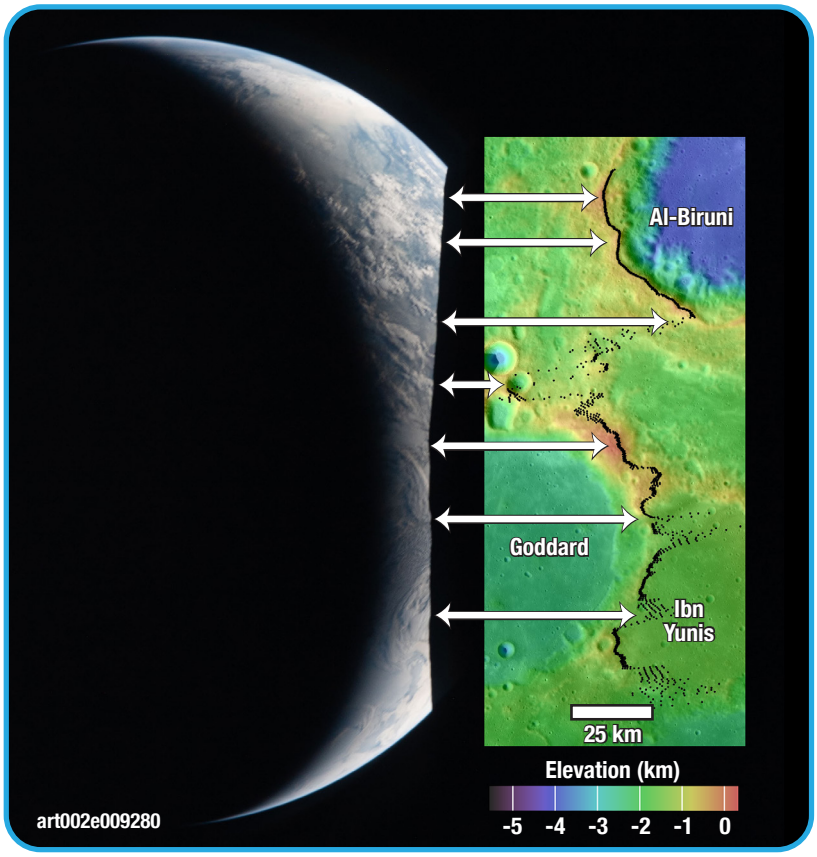


Figure 5.33: Shadows of Lunar Topography. Crew image art002e009280 shows the Earth rising from behind the silhoute of the lunar limb. Features along the lunar irregular limb visible to the crew are the rims of Al-Biruni and Goddard craters. White arrows match limb features to corresponding points on the topographic map, which is based on the NASA/JAXA SLDEM 60-meter global mosaic DEM. Black dots on the map trace the entire limb silhouette. Horizontal spreading of the dots is aliasing that occurs in places where the terrain is too flat to pinpoint the limb contribution.

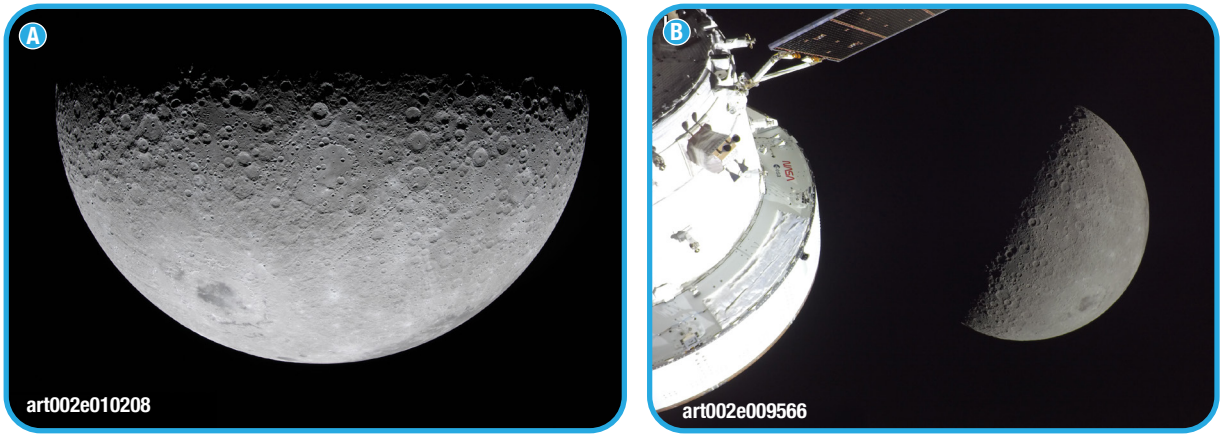


Figure 5.34: The Terminator. Images of the lunar termiantor are provided from (**A**) crew image art002e010032 and (**B**) vehicle camera image art002e009566.

the appearance of the terminator evolved throughout the flyby, noting differences between approach and recession.

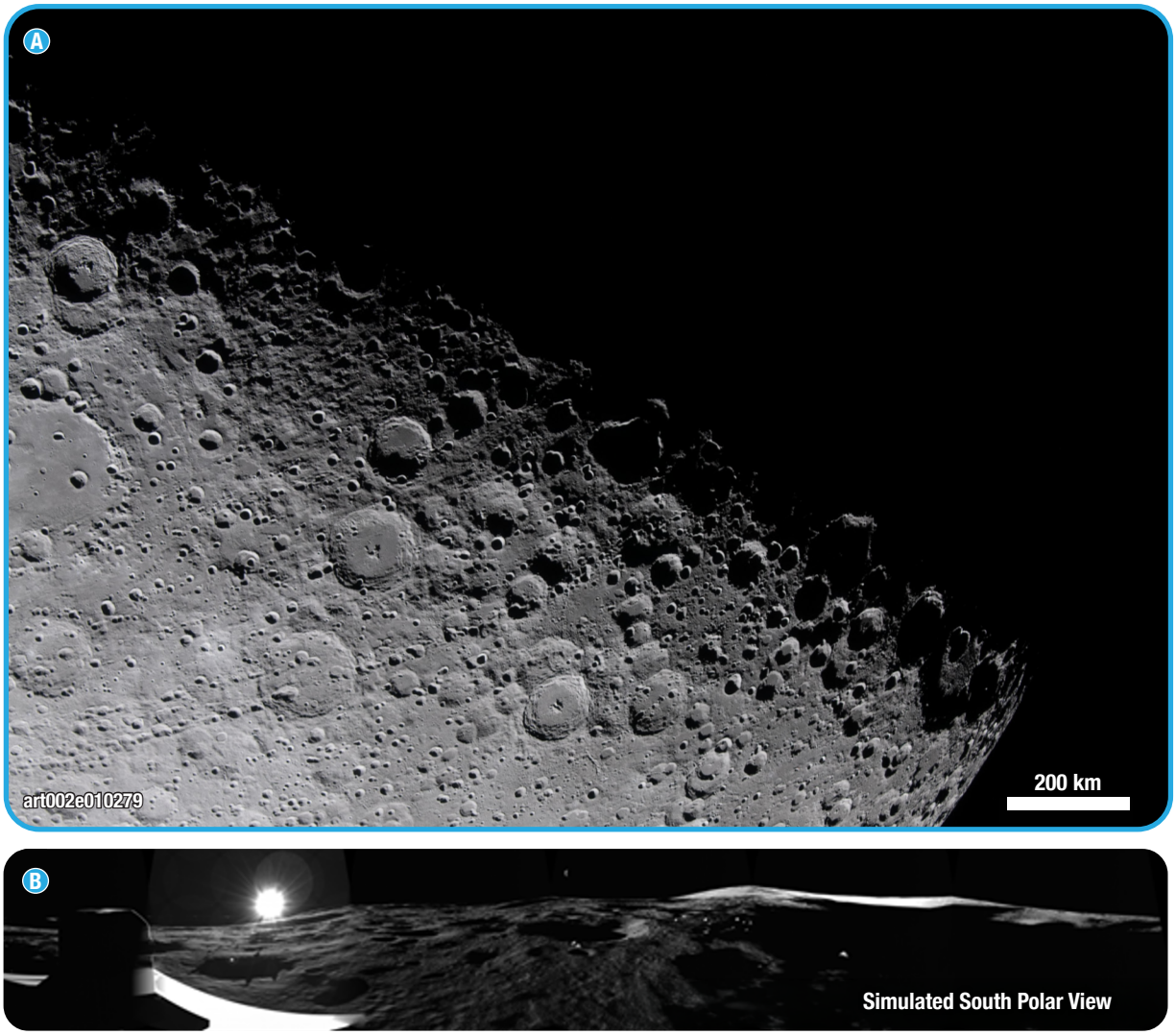


Figure 5.35: South Polar Terminator. (A) Crew image art002e10279 of the terminator can be compared with (B) a simulated surface view in the south polar VIPER landing region (Mons Mouton; Coyan et al., 2025).

The low solar elevation angle at the terminator dramatically highlights the rugged character of lunar topography. This lighting environment serves as a natural analog for illumination at the lunar poles, where the Sun never rises higher than ~1.5° above the horizon and presents a constant, rotating terminator (rather than the temporary day-night terminator observed by the crew from orbit) (**Figure 5.35**). Grazing illumination creates conditions in which shadowing dominates and relief is emphasized. Thus, the terminator observations made by the crew offer valuable context for anticipating lighting and shadow conditions that future crewed and robotic missions will encounter in the south polar region.

The LST tracked the location of the terminator along the full-disk view of the Moon throughout the flyby. The longitude of the morning terminator (the solar co-longitude) varied by ~2° during the flyby. On Flight Day 06 (the lunar flyby), the solar co-longitude was at 217.0°E at 18:45 UTC (start of flyby observations), 215.4°E at 21:56 UTC (when Orion was directly above the terminator), and was at 214.8°E at 23:01 UTC (Orion's closest approach to the lunar surface). The Moon, as viewed by

the crew, was exactly half-illuminated when the spacecraft was directly above the terminator.

The dramatic lighting made by the terminator proved to be one of the most compelling features described by the crew. Several crew members emphasized how strongly topography stood out under these conditions (**Figure 5.36, 5.37**). V. Glover reflected on the visual richness of the scene:

> There's just so much magic in the terminator, the islands of light, the valleys that would look like black holes. You'd fall straight to the center of the Moon if you stepped in some of those. It's just so visually captivating that the terminator is the most striking thing that I've seen so far. (V. Glover, O/E-1 voice loop, 21:53:03 UTC)

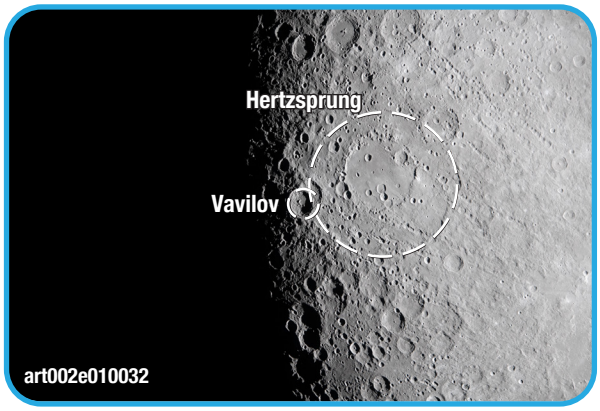


Figure 5.36: Hertzsprung and Vavilov along the Terminator. Crew image art002e010032 of the terminator highlights the topography of Vavilov crater (~98 km diameter), the western edge of Hertzsprung basin, and nearby terrain.

He later reported how the terminator accentuated topography, even for unaided eye observations:

> Houston, Integrity, just one other observation. Looking at the terminator, it's almost a full Moon from this perspective, but we've got the terminator on the western edge of the Moon. About one Orientale diameter from Orientale, and just with our plain eyes, you can really start to see topography. There is elevation on the Moon, not just variation in color. And that already makes the Moon look wildly different. (V. Glover, O/E-1 voice loop, 01:40:08 UTC)

Crew descriptions also highlighted how features entering darkness remained partially illuminated due to their elevation relative to the terminator. As V. Glover reported:

> Wow, yeah, I wish I had some more time to just sit here and describe what I'm seeing, but the terminator right now is just fantastic. It is the most rugged that I've seen it from a lighting perspective. There are little islands -- there are islands of terrain out there that are completely surrounded by darkness, which indicates some real variation and in terrain -- the terminator is not a nice smooth arc. It's just jagged. Like I said, there look to be islands out beyond the terminator because some of the things, gosh, maybe even a Vavilov diameter into the terminator, are catching sunlight on the peaks up to the north and to the south. It's very, very interesting to see. (V. Glover, O/E-1 voice loop, 19:46:02 UTC)

R. Wiseman similarly emphasized how revealing the terminator was, even compared to views of rugged farside terrain under higher solar elevation angles:

> Not really science-related, and we definitely learned this at Apollo, but the thing that is just most fascinating I think, to me and Victor right now is even as rugged as the farside looks, when you look at Orientale and Ohm, it's rugged. But, man, when you look at the terminator, it is just, like, impossibly rugged. And it reminds you that the whole farside is that way. It's just the terminator is really bringing out the shadows and the hills and the valleys. And it is just -- it's unbelievable. It's like no surface of the terminator is not marked by meteor impact. And it's just -- it is very impressive to look at that. And you realize that that is true across the whole farside. You just can't see it due to the Sun illumination right now. (R. Wiseman, O/E-1 voice loop, 20:42:43 UTC)

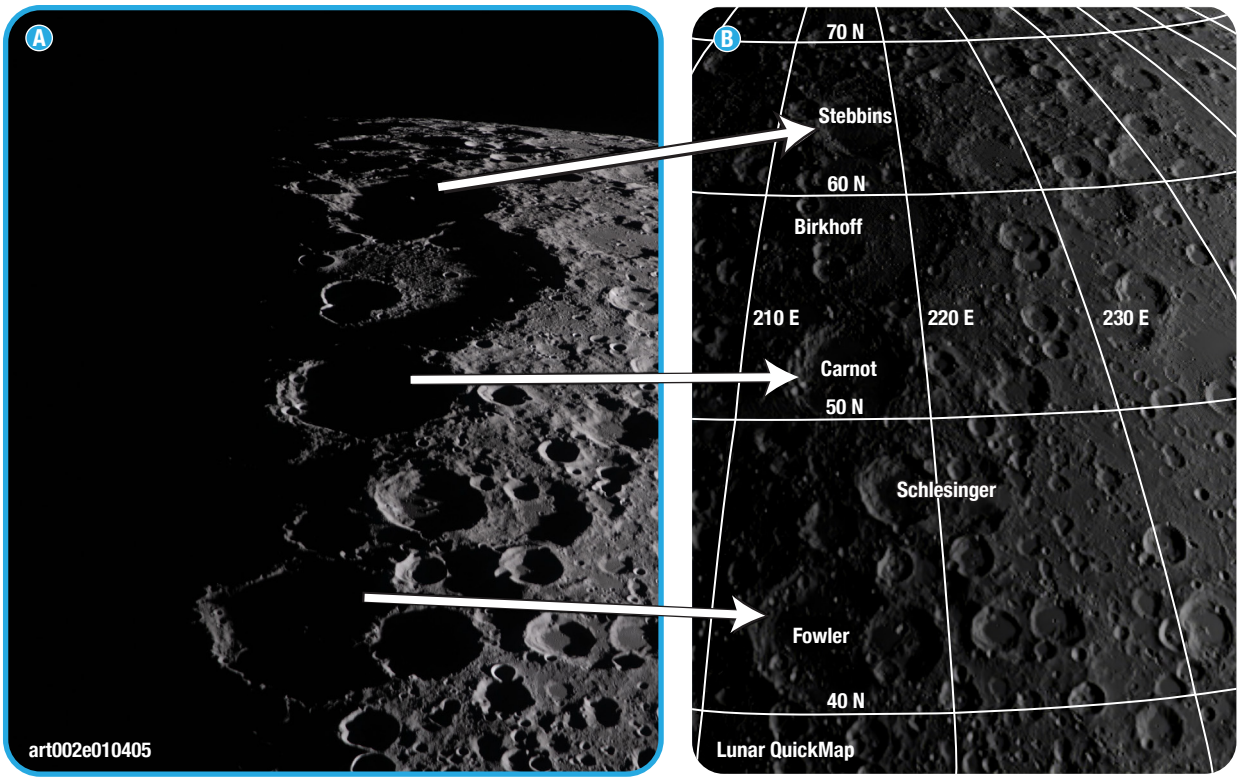


Figure 5.37: Terminator Islands of Light. (**A**) The "islands of light" described by V. Glover captured in crew image art002e010405. These are locations where the topography rises above the shadows along the terminator. (**B**) View of the same features (Stebbins, Carnot, and Fowler craters) rendered in Lunar QuickMap (Credit: NASA/GSFC/Intuitive Machines).

5.9 Volcanic History

Multiple volcanic surfaces representative of differences in emplacement style and timing were visible to the crew during their flyby (**Figure 5.38**), enabling studies of lunar volcanic history. Key science objectives relevant to volcanism were characterizing the variety of mare volcanism, non-mare volcanism, and cryptomare deposits visible within the flight path. Visible features included nearside maria on transit to the Moon and farside volcanic deposits across the nearside/farside transition and into Orientale basin. Identification of color and albedo differences within and across mare basalts in particular may inform composition and/or age relationships between volcanic units. Crew observations of real-time color

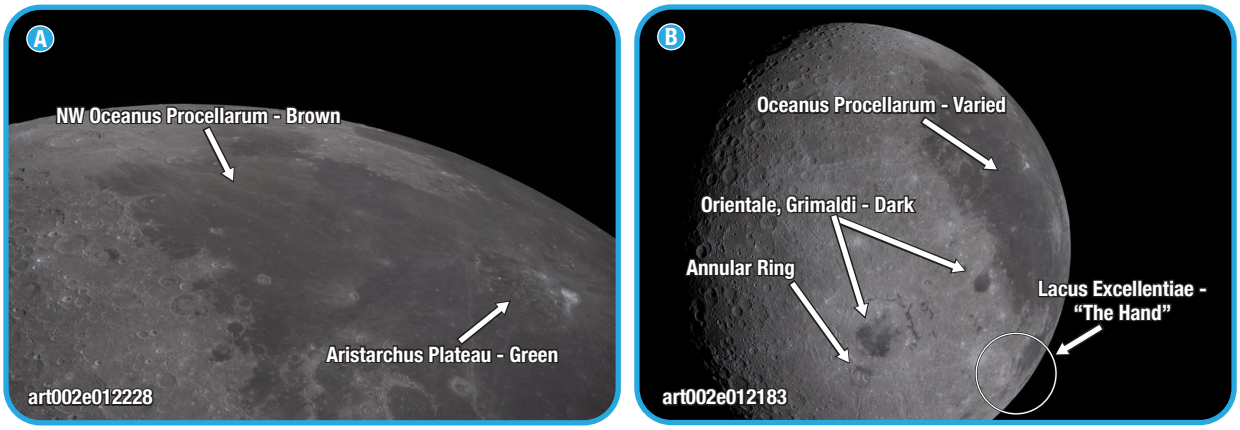


Figure 5.38: Volcanic Targets. Crew images (**A**) art002e012228 and (**B**) art002e012183 show key volcanic targets described during observations of volcanic terrain across the nearside-farside transition.

variations within and across volcanic units provided a new human-eye perspective that can be compared to orbital datasets to refine our understanding of how lunar color is perceived.

The LTP included three primary targets relevant to volcanic investigations: Aristarchus Plateau, the Nearside/Farside Transition Discussion, and Orientale basin (**Appendix 1**). For Aristarchus Plateau, key observation actions in the LTP relevant to the volcanic theme included describing color and albedo variations across the plateau and as compared to proximal maria, as well as describing any visible structures with elevated topography (e.g., mounds, domes) or lava channels cross-cutting the plateau. For the Nearside/Farside Transition Discussion, key observation actions for volcanism included comparing the color, albedo, topography, and texture of nearside and farside maria. For Orientale, observation actions for the volcanic theme included describing color, albedo, texture, and topography across mare patches, as well as describing the boundaries and textures associated with the southern dark annular ring, which has been hypothesized to contain glass-rich pyroclastic materials and likely sourced from a central vent (Weitz et al., 1998; Head et al., 2002; Gaddis et al., 2003; Henderson & Petro, 2023). These observations, in conjunction with other orbital datasets, can be used to inform how lunar volcanism dynamics and compositions change within regions of heightened volcanic activity, as well as across the crustal-thickness boundary along the western limb.

5.9.1 The Variety of Mare Volcanism

During their observations of the Aristarchus Plateau and the Nearside/Farside Transition Discussion, the crew described distinct color variations within Oceanus Procellarum. The crew reported hues of gray overprinted by hues of green, greenish-brown, and brown, with a specific patch of muted brown mare in northern Oceanus Procellarum, northwest of the greenish hue observed around Aristarchus Plateau (**Figure 5.38A**, **5.39**).

R. Wiseman	Jeremy, let's talk color real quick, especially let's go up to Aristarchus and the northern [maria] and then see if we can carry that into the farside at all. My overall impression is, if I was going to label any color, I would give Aristarchus some. To me, it's primarily like a brownish green glass. And then if I went up into the [maria] to the north of Aristarchus, I would give that a very muted brown. So, Aristarchus --
J. Hansen	Yeah.
R. Wiseman	I see like a brownish green glassy color.
J. Hansen	Yeah.
R. Wiseman	Very muted. If I go up and left from Aristarchus, I see kind of that greenish hint, maybe you could call it brown.
J. Hansen	Yeah.
R. Wiseman	And it's different than the rest of the [maria], right?
J. Hansen	To the northwest, right?
R. Wiseman	Like there's clearly a region to the northwest that is different than the rest of the [maria].
J. Hansen	Yeah, [the region to the northwest] really stands out because there's rays coming down into it from the northwest and in between the rays, you see the green.
R. Wiseman	Yes, the greenish-brown. 100% couldn't agree more.

(R. Wiseman, unaided eye, PCD crew audio art002a000017, 18:50:06 UTC; J. Hansen, camera, PCD crew audio art002a000028, 18:51:05 UTC)

The crew observed similar greenish color attributes in the "palm" (Lacus Excellentiae) of the "handprint" shape of Mare Humorum located south of Aristarchus (**Figure 5.38B**), but they noted that the color is distinct from other maria on the nearside and from other maria observed within Orientale.

J. Hansen	If we go to the southeast corner of the Moon, so south of Aristarchus, I see some color hue there too. […] [orients R. Wiseman to "the handprint"]
R. Wiseman	You see color in that?
J. Hansen	Well, I just want to stare at it a little bit and see. [...] The palm of the handprint has got some sort of greenish hue to me. And then that hue continues south of the handprint.
R. Wiseman	Yep. I was going to say, I would agree. And then that handprint that Jeremy and I kind of commented on is dark with a greenish hue. That is not the same color as the [maria] on the nearside. It's not the same color as Orientale. It is different.

(J. Hansen, camera, PCD crew audio art002a000028, 18:55:14 UTC; R. Wiseman, unaided eye, PCD crew audio art002a000017, 18:56:13 UTC)

During their observations, the crew began to interpret the spatial relationships of the color units they identified, noting how the brownish hues appeared to superpose the grayer hues of more typical maria, and may have even extended into the highlands. J. Hansen reported:

> As I stare at this region longer, I see the kind of brownish, greenish brown that Reid and I were talking about earlier and -- when Glushko's rays fall into the dark [maria], the whole Aristarchus Plateau south of that, southwest of that, the highlands I guess we're calling it, they create that brownish color. They're bright, they're higher albedo along their line, but around them they sort of look like they've smeared out to create that brownish color that we're talking about. It looks to me like it's something deposited on top of the darker [maria] that we so typically see. So, whatever was excavated out of Glushko, when it lays on top of the dark [maria], it creates sort of that brown that I see. And when I look to the southwest of Glushko, and I go out the 7 o'clock position of Glushko, I see some of that brownish, let's just call it brown, not green, some of that brownish down there, too. (J. Hansen, camera, PCD crew audio, art002a000029, 19:20:04 UTC)

These observations can be compared with observations of mare composition (e.g., Pieters, 1978), stratigraphic relationships (Whitford-Stark & Head, 1980), and age (e.g., Hiesinger et al., 2003, 2011) to compare how observations with the human eye correlate with and expand upon interpretations made from analyzing other datasets. For example, comparing the extent of the brownish hues observed by crew with the distribution of 2-μm absorption signatures (sensitive to pyroxene composition) measured by the Moon Mineralogy Mapper (M^3) within northwestern Oceanus Procellarum and the "handprint" of Mare Humorum (e.g., **Figure 5.39**) can help refine interpretations of mare basalt composition and emplacement styles, and its variability across the lunar surface.

During their Orientale observations, the crew described darker maria in the northeastern rings of the basin, compared to the center of the basin. They also made several comparisons between the albedo of Orientale maria and the albedo of Mare Grimaldi, as discussed in **Section 5.3.3**. (For additional details about color observations of Orientale maria, see **Section 5.2.1**). During the flyby, the crew asked the LST for the age of the maria within Orientale and how it compares to the ages of maria in Oceanus Procellarum. Through the Science Officer, the LST responded to the crew in real time, informing them that Orientale tended to have younger volcanic rocks than the majority of Procellarum, though there

is a range of age of volcanic deposits in Orientale (e.g., Whitten et al., 2011). The crew described the darker mare patches in Orientale as associated with the smaller patches in the outer mare ponds, which the LST correlated with the youngest lavas in Orientale mapped by Whitten et al. (2011). The crew used their real-time geologic discussion with the Science Officer to contextualize their observations and interpretations of superposing relationships of lunar surface features, underscoring the value and criticality of strategic, real-time connectivity between the LST, through the Science Officer, and the crew to enhance science return from the mission.

5.9.2 The Variety of Non-Mare Volcanism

The Aristarchus Plateau has one of the highest concentrations of volcanic features on the Moon and is the Moon's most diverse volcanic region (Zisk et al., 1977; Whitford-Stark & Head, 1977; Weitz et al., 1998; Mustard et al., 2011). Located on and adjacent to the Aristarchus Plateau are endmembers on the spectrum of volcanic eruption styles (e.g., pyroclastic deposits, sinuous rilles, potential silicic volcanism, irregular mare patches), ages, and compositions (basalts and silicic deposits). Due to its complex geologic and volcanic history, Aristarchus Plateau is of high science priority for future exploration (**Section 5.7.2**). During the flyby, all crew members described yellow and/or greenish hues atop and extending just east of Aristarchus Plateau.

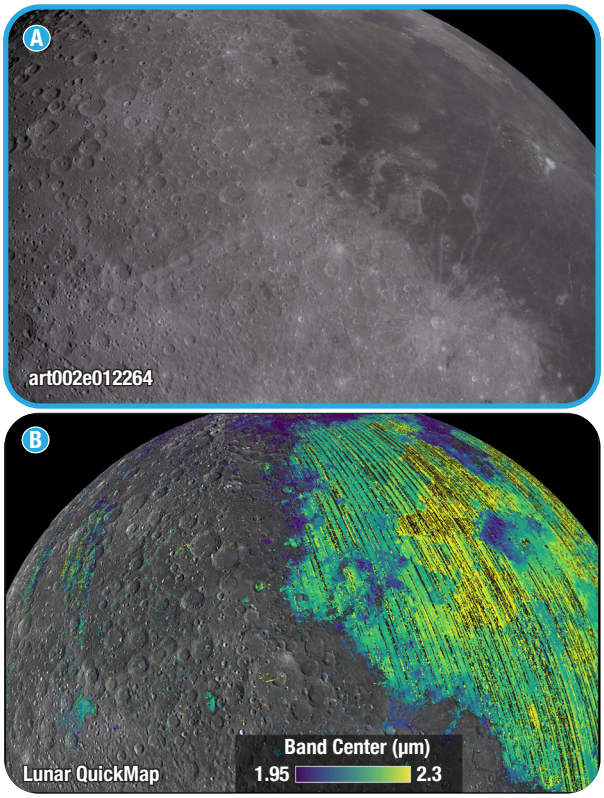


Figure 5.39: Nearside/Farside Transition. (A) Crew image art002e012264 shows the nearside-farside transition and Aristarchus Plateau. (B) Overlain on an LROC mosaic is a colored map showing the central position of the 2-µm spectral absorption band, sensitive to pyroxene composition (Boardman et al., 2011; Moriarty & Pieters, 2016). Shorter- (purples) and longer- (yellows) wavelength band centers are associated with higher abundances of Mg-bearing orthopyroxenes, and Ca-,Fe-bearing clinopyroxenes, respectively (Credit: NASA/GSFC/Intuitive Machines).

> So, Aristarchus Plateau, I could never see the color before that they were talking about, but I completely see it now. It is like a yellow snow-capped mountain, where the snow is the Aristarchus, I guess, craters that are on its eastern side, very high albedo, and then a more textured area that's just kind of hummocky and bumpy that is distinctly yellow. Like I said before, it's like a jaundiced cheek of the Moon. (C. Koch, camera, PCD crew audio, art002a000005, 20:15:33 UTC)

> My overall impression is, if I was going to label any color, I would give Aristarchus, to me it's primarily like a brownish green glass. (R. Wiseman, unaided eye, PCD crew audio, art002a000017, 18:50:16 UTC)

> We're seeing the greens on top of the dark [maria] of Aristarchus. (J. Hansen, camera, PCD crew audio, art002a000017, 18:52:48 UTC)

> But there are so many colors now. There's also a green. I see brown, especially Aristarchus and north toward the north pole. As you move up towards Pythagoras, that just gets

> browner and browner. And there's a, there's a line that just appears to demarcate the kind of gray to a brown, where most of it is brown. Most of the ground-covering is brown. And it looks like it wisps maybe down from the north. I don't know why, I just feel like it kind of flows down from the north in brown streaks, maybe three very distinct streaks into the darker mare, which looks like it's lying on top of the darker [materials]. Also in the southern portion, kind of around -- if you were to go just parallel to Grimaldi into the [maria], that is another area where it starts to get brown and it appears that there's just brown kind of scattered on top of the darker gray. (V. Glover, camera, PCD crew audio, art002a000034, 20:10:19 UTC)

The crew contrasted those yellow/greens to the grays of the maria proximal to Aristarchus and to the brown hues of the maria to the northwest, as discussed in **Section 5.9.1**. Brown and green hues could be associated with orange (titanium-rich) and green (magnesium-rich) glass beads respectively, akin to Apollo 17 and 15 glass beads that were produced by fire fountain volcanic eruptions on the Moon (Heiken & McKay, 1978). Crew observations also indicated that the greenish hues observed on Aristarchus Plateau extended beyond the plateau, into the Prinz crater region to the east. These crew observations are consistent with orbital spectral signatures detected in M^3 data. Specifically, M^3 data indicates a concentration of material consistent with absorption features at the 1-µm band center,

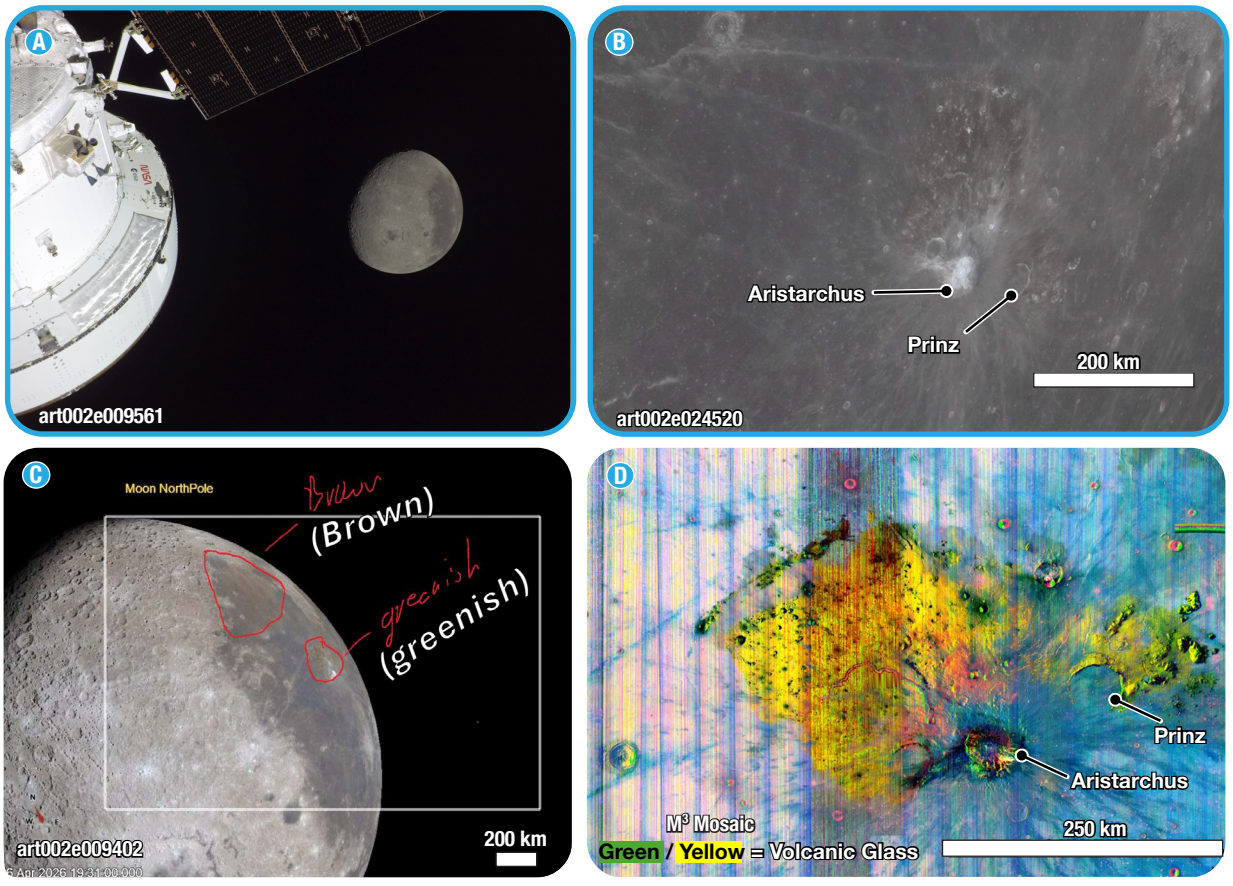


Figure 5.40: Aristarchus Mineralogy. (**A**) Vehicle image art002e009561, acquired 18:46:24 UTC, shows the scale of Aristarchus in context of the entire lunar view. (**B**) Crew image art002e024520 is compared to crew annotations of the color hue occurrences (**C**), and to volcanic glass identified via spectral reflectance by McBride et al (2016). (**D**) M3 composite mosaic of the region overlaid on an LROC WAC mosaic (Red = Glass Band Depth Parameter, Green = 1 µm band center position, Blue = 2 µm band center position); Credit: NASA/GSFC/Intuitive Machines.

interpreted to represent pyroclastic glass. This signature extends from Aristarchus to the Prinz crater region to the east (McBride et al., 2016) (yellow surfaces in **Figure 5.40B**).

During their Aristarchus observations, the crew also described a curvilinear feature on the plateau, which the LST confirmed is Vallis Schröteri, a sinuous rille likely produced by a large, ancient lava flow (Moore, 1965; Hurwitz et al., 2013). In addition to observations of volcanic terrain, the crew consistently identified the Aristarchus Plateau as amongst the highest-albedo features visible to their eyes, describing it as a ten out of ten on their albedo scale (**Section 5.2.2**). While the crew did not directly comment on the brightness of the southern ejecta extending from Aristarchus crater, the ejecta is hypothesized to include exposures of rarer silicic volcanic materials (Glotch et al., 2010; Mustard et al., 2011).

In addition to observing Aristarchus Plateau, the crew made several observations of the annular ring of Orientale, the origin of which has been a subject of scientific interest for several decades (e.g., Hartmann & Wood, 1971; Schultz & Spudis, 1978; Wilhelms et al., 1987; Head et al., 1993; Weitz et al., 1998; Henderson & Petro, 2023). During the flyby, the crew described the shape of the ring:

> The annular ring, which I think everybody kind of describes as like a pair of lips or a kiss on the farside of the Moon from here, is very circular in nature. The northern part of [the annular ring] is wider, darker. The southern part is much lighter. (R. Wiseman, unaided eye, O/E-1 voice loop, 20:16:08 UTC)

J. Hansen was struck by the topographic relief of Orientale's rings and correlated a collapsed section of the southern Rook ring walls to the annular ring, while positing its origin (**Figure 5.41C, D**):

> Okay, so if I look at the ring, the annular ring, you know what's going on there is you've got that wall [of the Inner Rook] that I've been talking about is definitely collapsed in that area. And you've got some of the -- let me see -- […] inside the annular ring is collapsed wall. […] And so, what causes the dark [material] around to make the annular ring? Because it looks like it's in collapsed-wall debris. […] It makes you wonder how that [dark material of the annular ring] got clearly uphill. So […] maybe this was a bit of a, you know, magma came up here, flowed up, through the cracks up to that elevation and then ran down the slope. It's interesting to contemplate why the dark [annular ring] is there, the darkness is there in the southern part of the annular ring. Actually, I wish I could explain that. (J. Hansen, camera, PCD crew audio, art002a000039, 21:22:10 UTC)

Related to color, R. Wiseman reported:

> I would say the color of the annular ring is distinctly different than the color of the [maria] in Orientale. […] This annular ring is -- this is a different shade of gray. I'd almost say this has more brown tones and this has more gray tones [than the mare]. (R. Wiseman, unaided eye, PCD crew audio, art002a000024, 21:20:10 UTC)

The reported brown tones within the annular ring can be correlated to compositional signatures measured from orbit. For example, analysis of M^3 spectral data indicates that the annular ring has orthopyroxene signatures that are distinct from the mineralogy of Orientale maria (**Figure 5.41B**; Henderson & Petro, 2023), consistent with crew observations and interpretations that the brownish tones of the annular ring are distinct from the gray tones of the maria within Orientale or the glassier signatures associated with most pyroclastic deposits. This observation underscores that human eyes can be effective sensors for qualitatively identifying compositionally distinct units on the lunar surface. The crew's observations that associate the annular ring with the collapsed section of the Orientale ring wall, in

conjunction with spectral data that indicate the annular ring and mare basalts have distinct compositions, may contribute to ongoing analyses investigating the formation of this enigmatic feature.

5.9.3 Signs of Cryptomaria

The flyby trajectory did not afford favorable viewing opportunities of cryptomaria, and thus none was included in the LTP as an observation target. Over the course of the flyby, images indicate a variety of albedo variations surrounding small fresh craters in the northern ejecta of Orientale basin. Some, like Sundman J and Mees Y to the northwest, have low-albedo characteristics, whereas other nearby unnamed small craters have high-albedo properties associated with fresh ejecta. Given the low-albedo signatures in otherwise high-albedo highlands terrain, a cryptomare origin represents one hypothesis for the source of these low-albedo deposits. For further discussion, see **Section 5.4.4.4**.

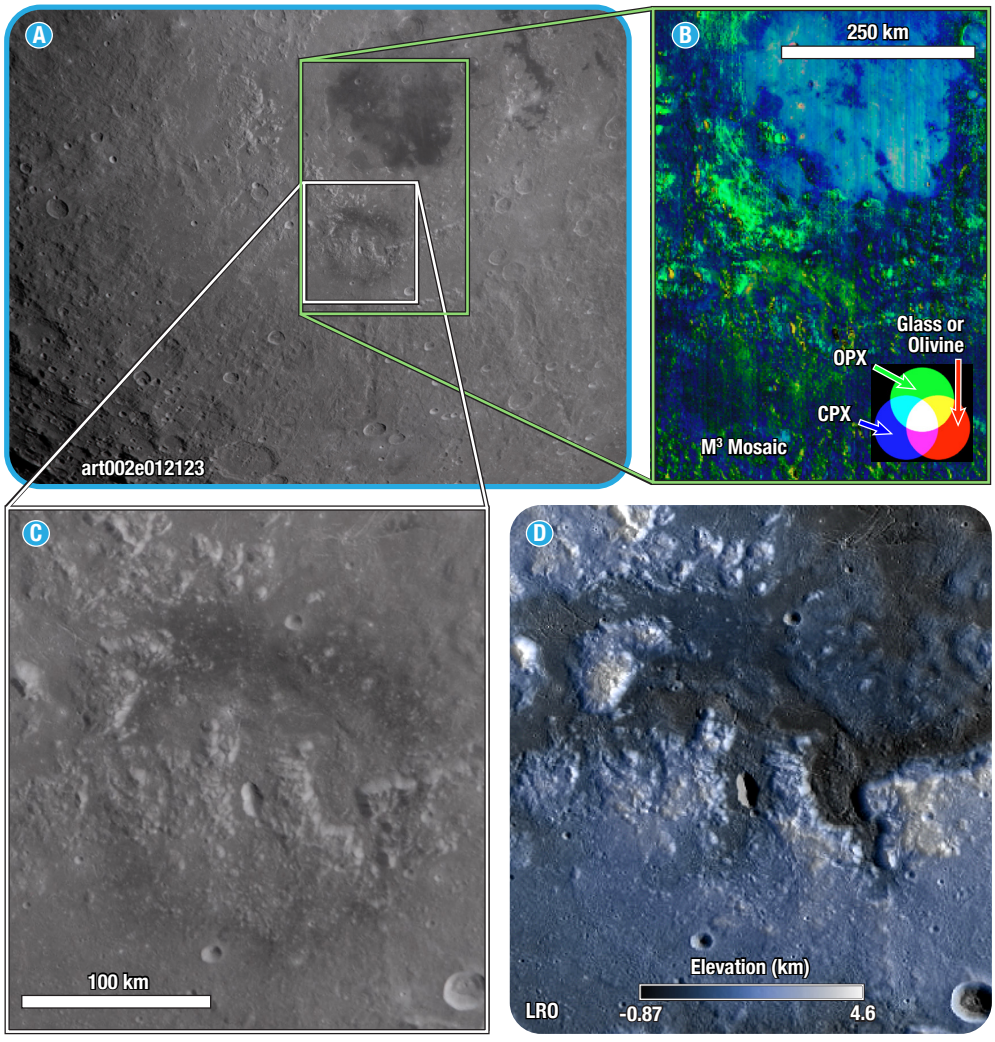


Figure 5.41: Orientale Annular Ring. (**A**) Crew image art002e012123 of Orientale basin and its annular ring. (**B**) M^3 mafic composition map from Henderson & Petro (2023). Red, orange, and yellow pixels denote detections of mafic minerals (pyroxene) in the central mare region of Orientale that are absent in the annular ring. (**C**) Enlarged view of crew image art002e12123 showing the annular ring. (**D**) Shaded relief (colorized by elevation) of the same area shown in (**C**) produced using LRO LOLA-derived topography.

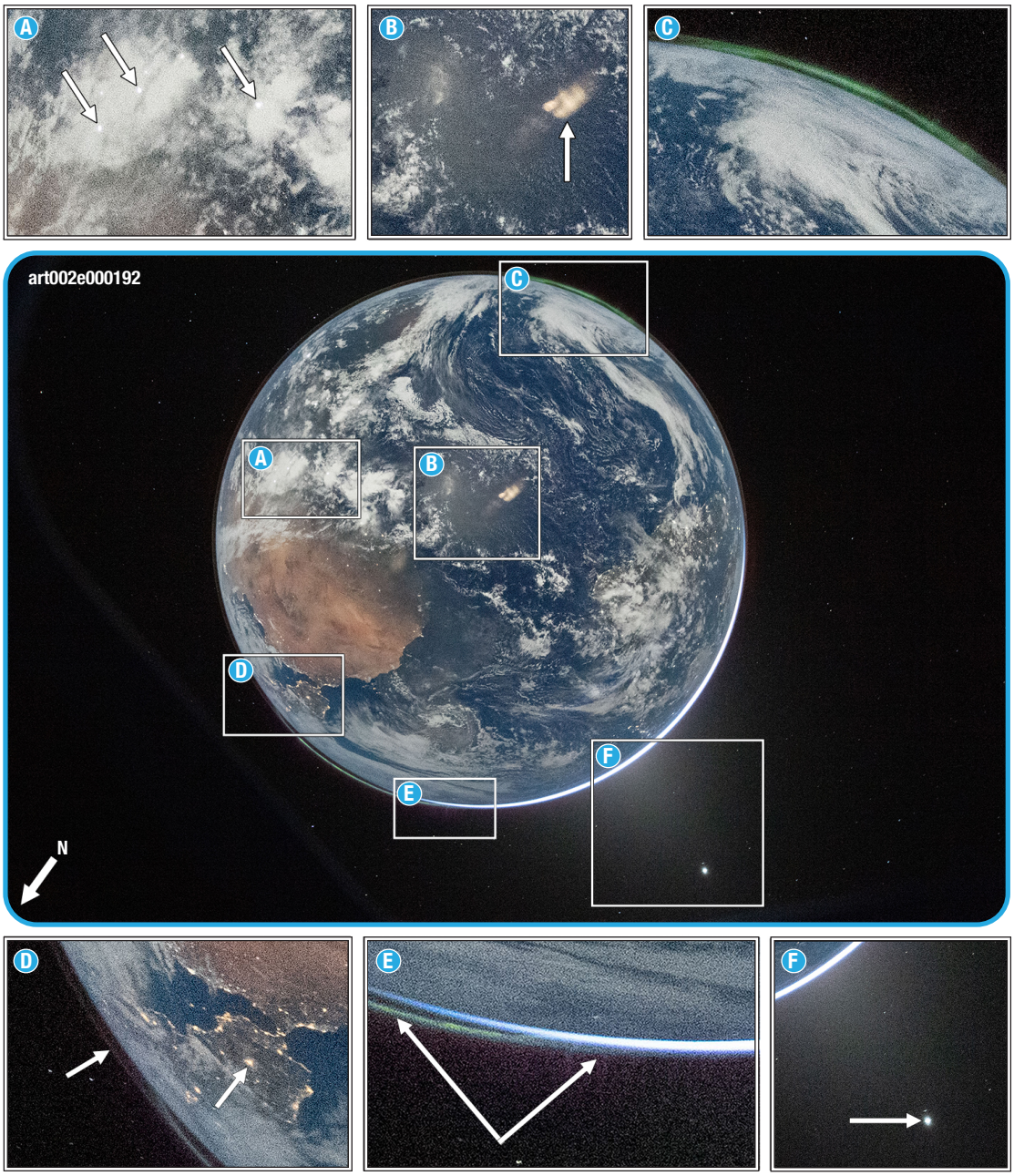


Figure 5.42: Hello, World. "Hello, World" image acquired on Flight Day 02 at 00:27:39 UTC. Earth was illuminated at night by the Moon (crew image art002e000192). Breakout boxes provide details of (**A**) lightning flashes over the Congo basin in central Africa, (**B**) moonshine reflecting off the mid-Atlantic and a window reflection (arrow), (**C**) Aurora Australis near the South Pole, (**D**) city lights on the Iberian peninsula (arrow over land points to Madrid) and Northern Africa, with airglow defining the Earth's atmosphere above the horizon (leftmost arrow), (**E**) northern aurora (leftmost arrow) and sliver of sunlit Earth (rightmost arrow) where the Sun is setting in the western hemisphere, and (**F**) zodiacal light and Venus (arrow). Note: The image in (**F**) is stretched to enhance contrast.

5.10 Earth Observations from Deep Space

The Artemis II flight plan afforded the crew the opportunity to collect Earth observations throughout the mission. Earth was observed during the outbound transit to the Moon, during the lunar flyby

corresponding to LTP earthset and earthrise targets, and during the return journey to Earth. During the outbound leg, nighttime views of Earth illuminated only by moonlight provided exceptional perspectives, revealing city lights, polar aurora, airglow (the visible layer of the atmosphere around Earth), lightning flashes, and zodiacal light (also discussed in **Section 5.5.2**). During the flyby, several crew descriptions noted how Earth's brightness, which was significantly greater than the Moon's, affected their observations of the lunar surface. This was especially evident during the eclipse, when the lunar surface was illuminated only by reflected earthshine (**Section 5.2.3**). The crew also described how their perceived colors of both Earth and the Moon changed throughout the mission, as well as how each body's colors influenced the appearance of the other when both were in view (**Section 5.2.4**).

5.10.1 Earth's Atmosphere

One of the most iconic Earth images taken by the Artemis II crew was the moonglow image titled "Hello, World" (**Figure 5.42**). This image was captured on Flight Day 02 (April 2, 2026, 00:27:39 UTC), just after the TLI burn, as the crew headed toward the Moon at a distance of ~10,100 km away from the Earth. In a post-mission debrief, the crew were asked about their ability to resolve features on Earth during the time period this image was taken. The crew reported they could distinguish several features on Earth, including: lightning flashes (visible over the Congo basin in central Africa in **Figure 5.42A**); the aurora and auroral motion (**Figure 5.42C**); city lights across Europe and northern Africa (**Figure 5.42D**); airglow (i.e., the visible layer of the atmosphere around Earth); what they interpreted as noctilucent clouds (i.e., Earth's highest layer of atmospheric clouds that form in the mesosphere); and zodiacal light (i.e., diffuse sunlight scattered by interplanetary dust in **Figure 5.42F**).

When the post-TLI-burn Earth images were released publicly, the sequence was stacked and animated, revealing dynamic movement of the aurora, lightning, and bright dots above the Earth interpreted as satellites reflecting sunlight. The Artemis II images and crew descriptions captured real-time atmospheric events and unmistakable indicators of an inhabited, dynamic Earth. This perspective compares well with the iconic "Blue Marble" image of Earth taken by the Apollo 17 crew when they were returning from the Moon in 1972 (discussed further in **Section 7.4**).

Collecting images of Earth's full disk enables the visualization of meso-, synoptic-, and global-scale meteorological systems and processes. Notably, the Artemis II data recorded these dynamic systems in a full disk view during the Earth's night, which many visible-light sensors from meteorological satellites generally cannot do. Lightning over the Congo River basin, Africa, and the Amazon River, South America, was associated with regional equatorial thunderstorms. Cloud patterns across "Hello, World" were consistent with the formations associated with the Coriolis effect and the Intertropical Convergence Zone (ITCZ). The cloud accumulations in equatorial regions and circulation patterns in the northern and southern reaches of the image (**Figure 5.42**) are consistent with expected hemispheric prevailing winds. **Figure 5.43** highlights the cloud patterns of tropical cyclones and low-pressure systems. In addition, Saharan dust from northern Africa was captured traveling across the mid-Atlantic Ocean (**Figure 5.44**). The circulation of the clouds (**Figure 5.43**) and the observed dust (**Figure 5.44**) obscures views of the ocean and city lights of the Canary Islands.

Even from the vantage point of the Moon's farside at a distance of 413,041 km away, the crew could observe structures of large-scale weather systems on Earth while using a long lens on the Nikon cameras. **Figure 5.43** shows two weather systems that were captured in crew images from the lunar farside and simultaneously tracked by Moderate Resolution Imaging Spectroradiometer (MODIS) instruments onboard the Terra and Aqua weather satellites.

One of these systems was a low-pressure system moving northward from the circum-Antarctic region over southeastern Australia, with cloud shadowing indicating substantial vertical structure. The second system, Cyclone Maila, had been building for days leading up to the lunar flyby. By the time earthset occurred for the Artemis II crew, the storm had strengthened substantially, and its development continued to be tracked by meteorological agencies on Earth. The severity of the storm was highlighted in a

public update from the World Meteorological Organization (WMO) on April 9, 2026, which featured an image taken by the Artemis II crew from inside the cabin on Flight Day 02 (April 2, 2026, 22:42:35 UTC). Satellite composite images contextualized the crew's images of the storm: corrected-reflectance and true-color data from MODIS mapped the exact cloud structures in both the low-pressure system over southeastern Australia and also Cyclone Maila, which crew images captured.

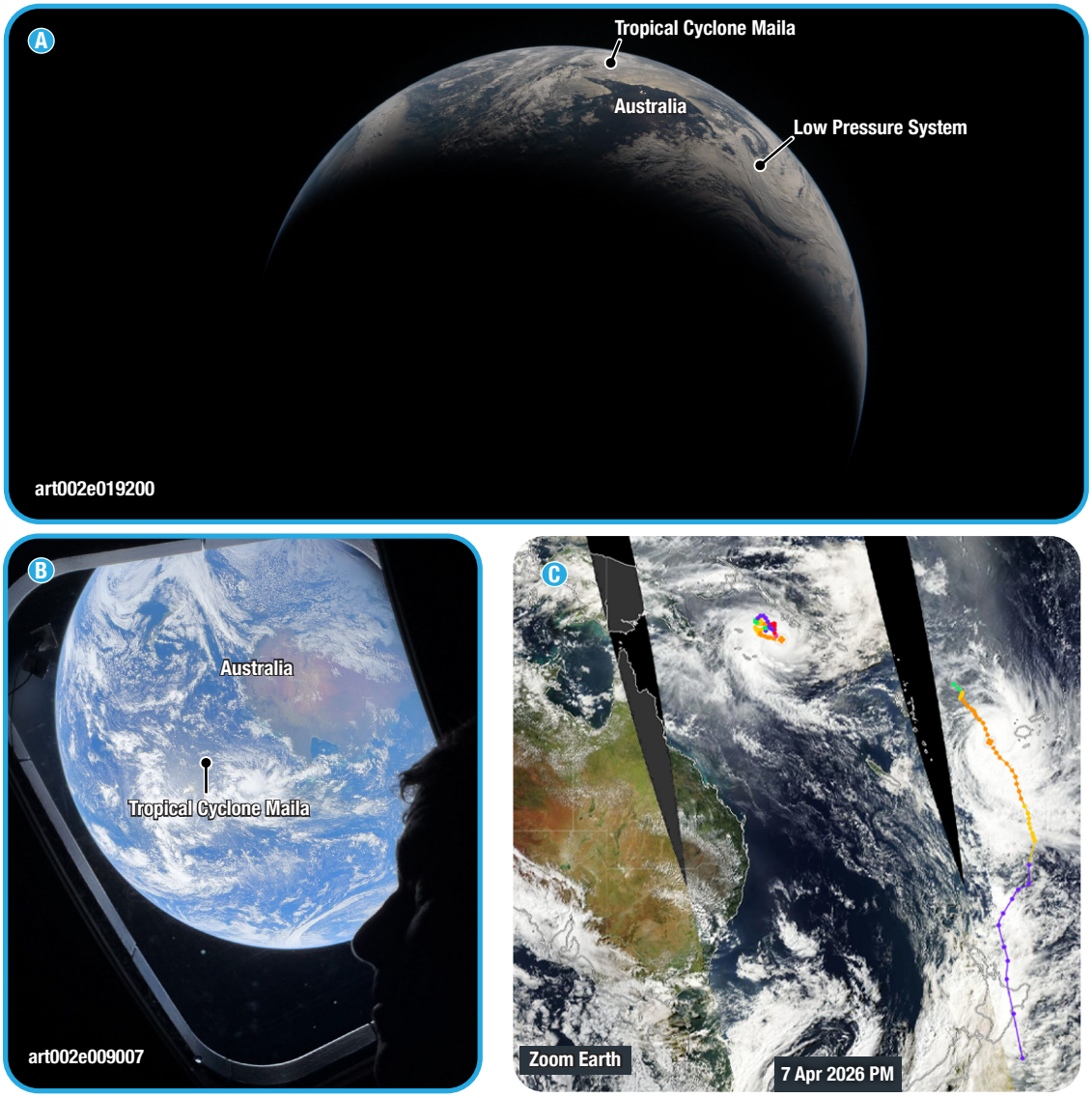


Figure 5.43: Earth's Storms. (**A**) The crescent Earth just before setting behind the Moon during the lunar flyby (crew image art002e019200) on April 6, 2026. This image highlights a significant low-pressure system moving into southeastern Australia from the circum-Antarctic circulation system. The shadowing from the local morning Sun highlights some of the vertical structure in that frontal system. The image also captures Tropical Cyclone Maila as it was churning near Papua New Guinea. (**B**) R. Wiseman observing Earth on April 2, 2026 (crew image art002e009007), as Tropical Cyclone Maila is visible out Orion's window. (**C**) An image acquired from Zoom Earth. Data are corrected reflectance/true color from the MODIS instrument on NASA's Terra and Aqua satellites.

The "Hello, World" image acquired on Flight Day 03 also captured a dust plume aloft over the Sahara Desert that was migrating westward (**Figure 5.44**). The Artemis II vantage point provided a unique

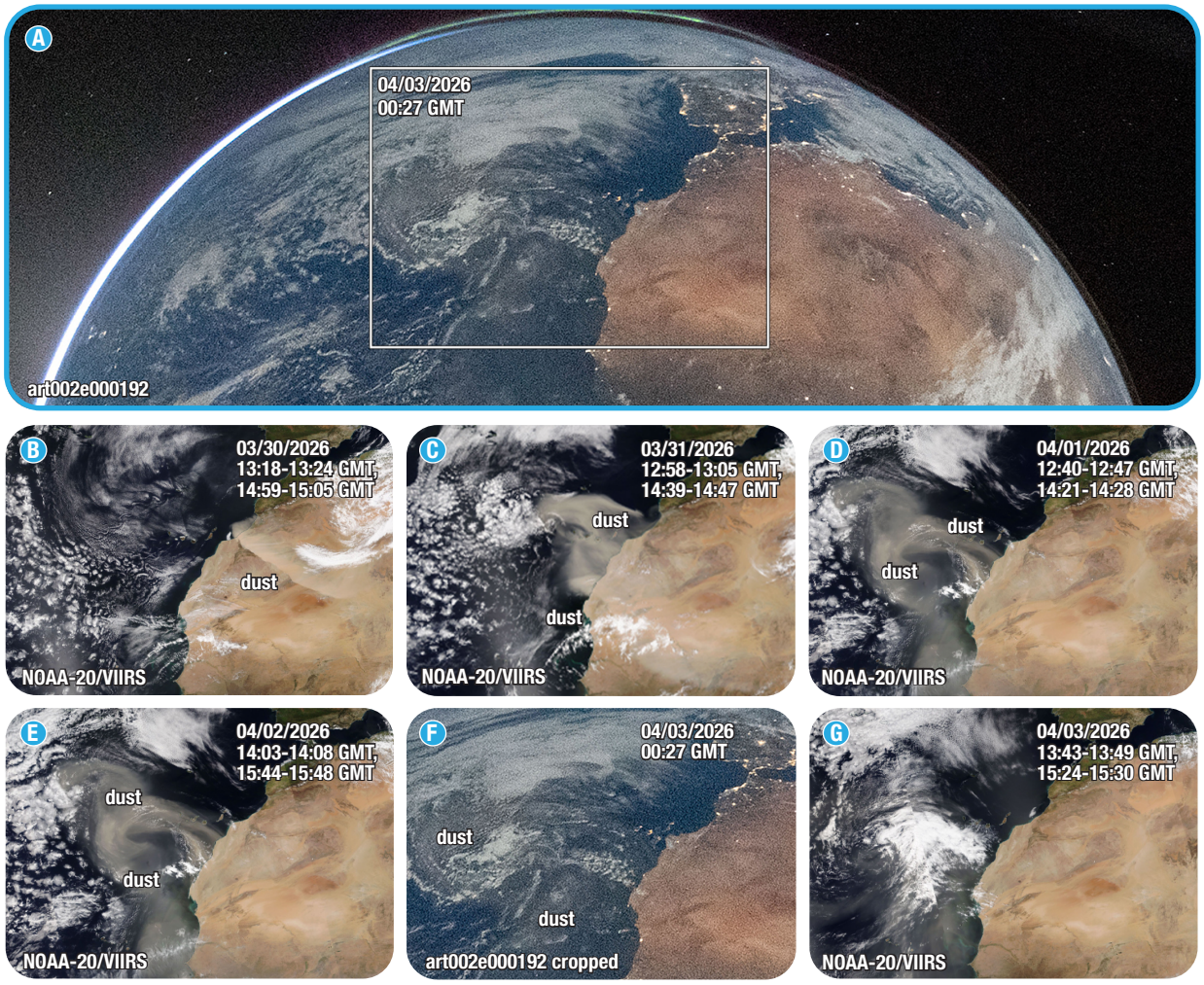


Figure 5.44: Saharan Dust. "Hello, World" image (crew image art002e000192, cropped) shows dust from the Saharan Desert traveling across the Atlantic Ocean. Each lower panel (**B-G**) highlights the dust plume's traverse across the various days, with data collection timestamps and sources indicated on the individual panels.

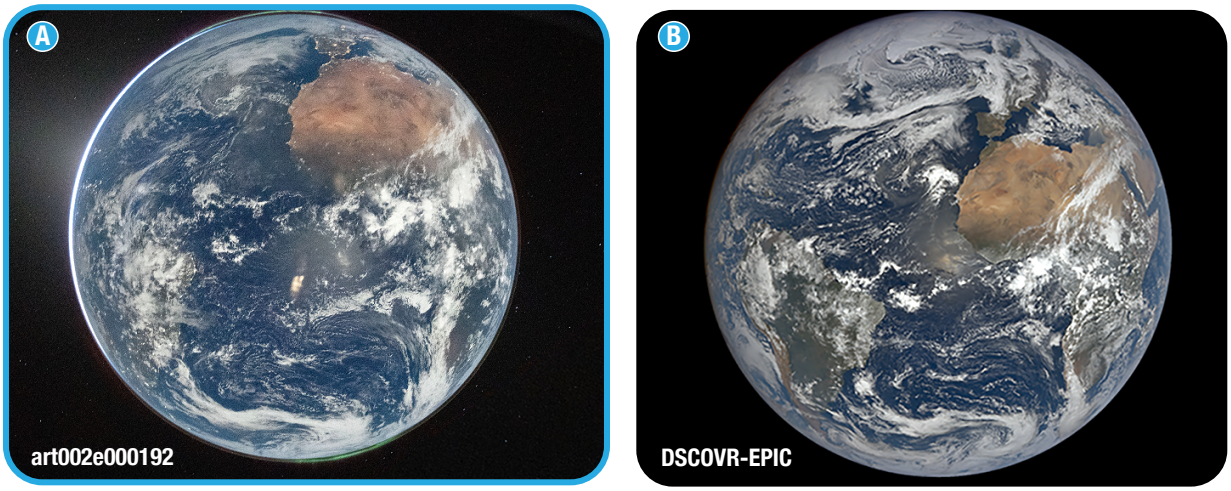


Figure 5.45: Cloud Migration. (**A**) Artemis II crew image captured on Flight Day 03 (April 3, 2026) at 00:27:39 UTC. Crew image art002e000192, rotated, was taken as an over-exposure of an unilluminated Earth. (**B**) DSCOVR EPIC natural color image of the sunlit Earth taken on the same day at 13:03:27 UTC (image ID epic_1b_20260403130327).

perspective on the plume, as it was far beyond low Earth orbit and not limited by the fixed space station orbital track or a fixed, Sun-synchronous orbital track characteristic of Earth-observing satellites.

As Earth's largest dust source, North Africa is a key focus for research on dust plumes, with satellite tracking used to study their emission, transport, and downstream impacts on weather, climate, and human health (e.g., Harr et. al, 2024). Remotely sensed images and aerosol compositional measurements acquired by the Visible Infrared Imaging Radiometer Suite (VIIRS) onboard the National Oceanic and Atmospheric Administration-20 (NOAA-20) platform supports such ongoing research.

The North African dust plume that occurred during the mission was first captured by VIIRS on March 30, 2026. On April 2, 2026, VIIRS imaged the dust plume ~10 hours before the crew captured images of the same plume. VIIRS acquired another image ~13 hours later on Flight Day 03. The combination of nadir VIIRS observations and the oblique crew images provides complementary perspectives of the same event. **Figure 5.44** shows these datasets together, with the lower panels showing the plume progressing from the northwest African coast toward the Atlantic Ocean by Flight Day 03, when it began mixing with ocean atmospherics. Additionally, the VIIRS Deep Blue Aerosol Type algorithm classified the pixels of aerosol composition over land and ocean surfaces as dust. All VIIRS data for this report are derived from and accessible on NASA Worldview.

Finally, Artemis II observations of a dynamic Earth were complemented by Deep Space Climate Observatory (DSCOVR) Earth Polychromatic Imaging Camera (EPIC) images of Earth collected at similar times. For example, **Figure 5.45** shows cloud fields that shifted over the ~12 hours separating Artemis II and EPIC observations. Features associated with nighttime illumination, such as aurora and city lights (**Figure 5.42**), are no longer present in the DSCOVR image.

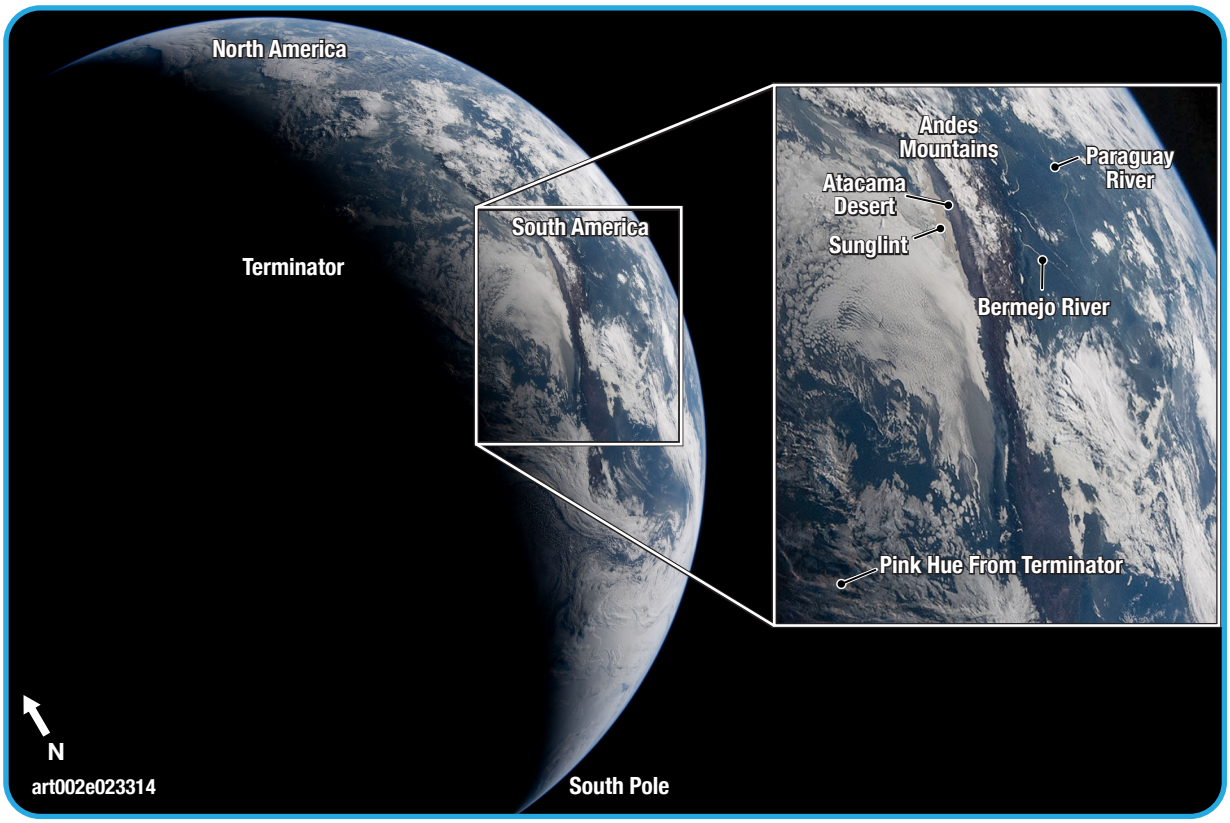


Figure 5.46: Earth's Terminator. Crew image art002e023314 (cropped) shows the Earth visible to the crew on Flight Day 02 from ~70,000 km away.

5.10.2 Earth's Surface

The crew made observational descriptions of the Earth's colors and major features during the transit to the Moon on Flight Day 02, lunar flyby on Flight Day 06, and transit back to Earth on Flight Day 07. During the transit to the Moon on April 2, 2026, when Orion was ~70,000 kilometers from Earth, C. Koch observed Earth's coloration and feature visibility:

> Yeah, I just wanted to describe for you guys the beauty that we're seeing. You can actually make out the coastline of the continent. You can make out rivers because of the Sun glare. You can see high thunder clouds. And all the while, you can see the entire terminator. And you can see the South Pole lit up. It's just phenomenal. […] And even from this far, you can make out a slight pink hue along the terminator. It is just absolutely phenomenal. You guys look great. (C. Koch, O/E-1 voice loop, 12:34:19 UTC, Flight Day 02)

Figure 5.46 shows one of the images with timestamps that correlate to this observation of a full Earth disk centered on the terminator. The image spans pole-to-pole, but the visible land details are focused on South America: the Atacama Desert lining the South American coastline, the Andes Mountains trapping clouds between the coast and inland Bolivia, Peru, and Argentina, and sunglinted tributaries of the Paraguay and Ichilo Rivers. The local sunrise casts pinkish hues on the nearby clouds near the terminator.

At farther distances from Earth, the crew noted the clouds on the planet were so bright that the features of Earth were difficult to distinguish. During the lunar flyby on April 6, C. Koch recorded the following observation while looking through the camera viewfinder:

> The Earth, I will say, this whole time when we've seen it from far away, has not quite looked like the pictures. You really can't make out the deep royal blue [that is captured in the images]. It's just a bright, bright, light blue. […] And then the continents are like a dark, dark bluish green. But overall, the whole thing is just like, electric blue. (C. Koch, camera, PCD crew audio, art002a000011, 22:44:09 UTC)

Additionally, on April 7, after the lunar flyby, R. Wiseman noted:

> But when we're looking at Earth, just a normal Earth lit up by the Sun, I'm used to seeing these deep blue pictures of like Earth Day photos, Apollo 8 photos, but when we look out, the cloud cover is so bright, it is almost blindingly bright, and you really cannot make out significant detail in the Earth when we're at long distance on a sunlit Earth. So, it was very interesting to me that the Earth is so bright from the clouds that it is actually hard to look at. (R. Wiseman, O/E-1 voice loop, 19:19:32 UTC, Flight Day 07)

6.0 COORDINATED OBSERVATIONS

During the Artemis II flight, active spacecraft and Earth-based science teams collected data that aligned with Artemis II science objectives. Two of these data-collection efforts, led by LRO (**Section 6.1**) and NASA's MEO and SMD citizen science office (**Section 6.2**), involved coordination with the LST before the mission. Included are details of these activities, as well as of other coincident lunar science investigations (**Section 6.3**) that took place during the mission.

6.1 Lunar Reconnaissance Orbiter

Data from LRO played a vital role in the preparation and live execution of the Artemis II mission. LRO has provided NASA with nearly 17 years of lunar imaging and measurements of surface temperature, albedo, and topography, and the radiation environment, all of which were used to identify scientifically interesting features and plan the LTP. These data also actively support ongoing efforts to

identify and assess safe landing sites for future Artemis missions. Additionally, LRO's high-resolution images and DEMs were transformed into realistic simulations that were crucial for training the Artemis II crew to identify surface features during the flyby. The crew also used LRO-derived maps of the lunar surface to assist in their real-time observations.

The LRO team provided support for the Artemis II lunar flyby via: (1) the creation of data products of select crew-targeted features from pre-existing LRO observations (**Section 6.1.1**); (2) real-time imaging of Orion (**Section 6.1.2**); and (3) the acquisition of new LRO observations during the time surrounding the Artemis II lunar flyby to complement crew observations (**Section 6.1.3**). This effort served as a demonstration of how NASA mission teams and assets can operate collaboratively during active spaceflight missions. Artemis II presented an opportunity to develop and implement processes for coordination, real-time communication, and execution of operations across missions, including synchronizing spacecraft in lunar orbit/trajectory. Such efforts result in a diversity of information from a range of instruments that enhance overall science return from all missions involved.

6.1.1 LRO Data Products of Select Crew-Targeted Features from Pre-Existing LRO Observations

The LRO team generated data products and maps of select Artemis II lunar features of interest utilizing existing LRO data. These data products provided depictions of the surface that complemented crew observations with information including predicted surface temperatures at the time of the flyby, mineral composition, surface maturity, rock abundance, and structures on and below the surface (**Figure 6.1**). LRO instruments were used to derive the following data products:

- LROC wide-angle camera (WAC) (e.g., Robinson et al., 2010): visible-light mosaics.
- Diviner Lunar Radiometer Experiment (Diviner) (e.g., Powell et al., 2023): thermal maps showing predicted temperatures at the time of the lunar flyby.
- Mini-RF radar instrument (e.g., Raney et al., 2010; Patterson et al., 2017; Fassett et al., 2024): maps showing details of surface and subsurface rock density, surface material maturity, potential future landing hazards, and radar reflectivity.
- Lyman Alpha Mapping Project (LAMP) (e.g., Gladstone et al., 2010; Byron et al., 2020): far ultraviolet light off-band albedo maps and off-band/on-band albedo ratio maps revealing details in composition, maturity, and physical properties of the surface.
- Lunar Orbiter Laser Altimeter (LOLA) (e.g., Smith et al, 2010; Barker et al., 2016; Walker, 2026): maps revealing changes in elevation, slope, and surface roughness, as well as composition and surface maturity.

LRO data products were created for three crew targets that were, at the time, potential targets: Orientale basin (**Figure 6.1**), Ohm crater, and Aristarchus Plateau. These products help contextualize the Artemis II crew observations and images, demonstrating how different views and measurements of targets support interpreting scientific observations made by the crew. Additionally, the LRO data products were incorporated into Artemis and LRO social-media materials and posts for educational public outreach and engagement.

6.1.2 LRO Real-Time Imaging of Orion During the Lunar Flyby

On April 6, 2026, LRO performed two complicated and high-priority slews to observe the Artemis II Orion vehicle during the lunar flyby. These observations included LROC imaging and LAMP imaging to detect gas trails or exhaust from Orion. The observations required several weeks of preparations, simulations, and analysis and required extensive coordination across multiple organizations and teams, including the LRO Mission Operations team, Space Science Mission Operations Systems Engineering team, NASA's Goddard Space Flight Center Flight Dynamics team, LRO science instrument teams (e.g., LROC, LAMP), the Naval Postgraduate School, and the Artemis II Flight Dynamics team.

Coordination activities included several weeks of modeling and simulations (i.e., trajectory/lunar orbit for both spacecraft for different launch dates; illumination and viewing geometries for different launch dates to identify common targets) and planning (i.e., precise imaging maneuvers, observation targeting). For these activities, LRO accounted for technical constraints, including LRO's disabled reaction wheel #4 and the lack of regularly scheduled Deep Space Network passes. All teams collaborated to coordinate real-time and last-minute adjustments to LRO's observation slew maneuvers and imaging times due to Orion's outbound trajectory correction as it traveled to the Moon. This level of coordination was necessary to synchronize two spacecraft in lunar orbit/trajectory, execute precise imaging maneuvers with existing hardware capability, and integrate data across multiple teams and missions.

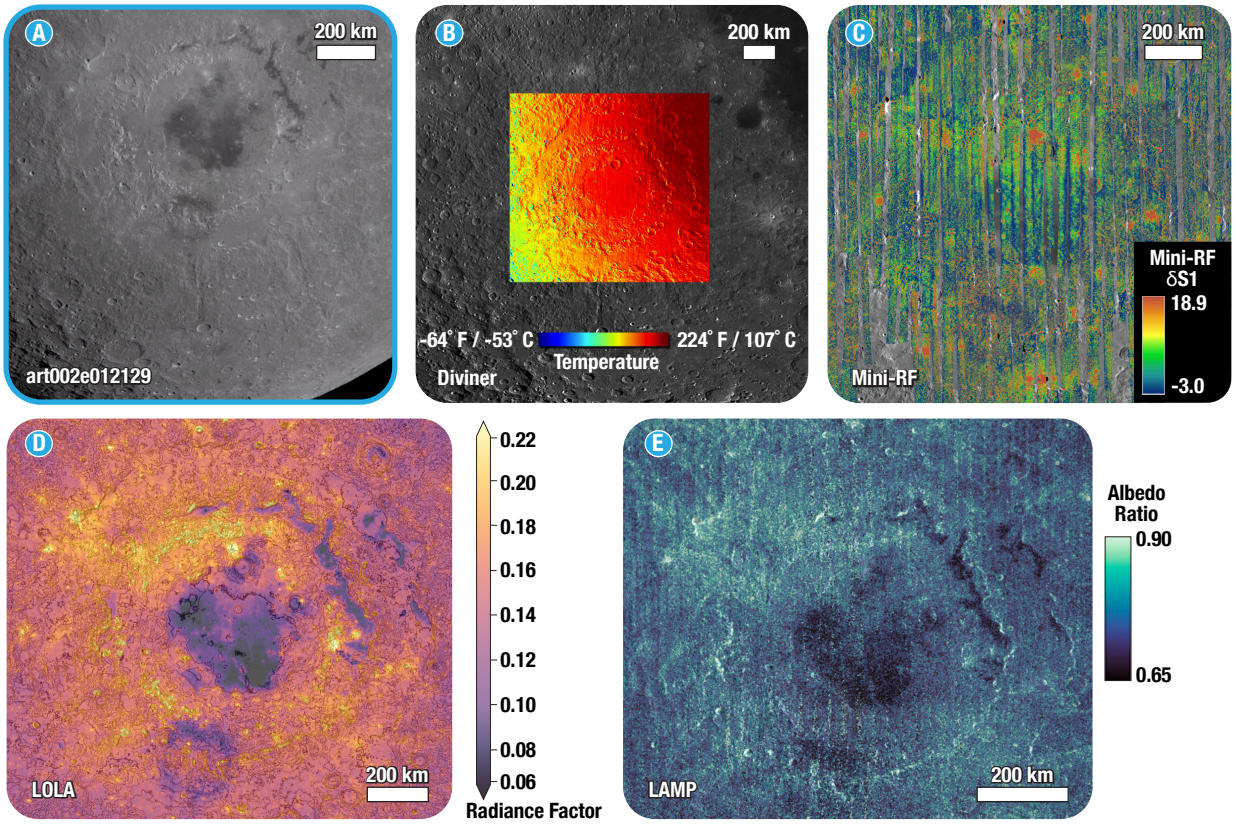


Figure 6.1: LRO Views of Orientale. (**A**) Crew image art002e012129 of Orientale basin. (**B**) Diviner map showing predicted surface temperatures in Orientale basin during the Artemis II lunar flyby. Red areas are the hottest (>100°C). A red-to-yellow gradient shows that one side of the basin is hotter than the other. (**C**) Mini-RF radar instrument map depicting rock abundance from the surface down to 1 meter depth. The darker red colors represent higher rock abundance and the green colors indicate fewer rocks. (**D**) Map of Orientale as seen by both operating modes of LOLA. The reflectance of sunlight from the Moon's surface in the near infrared (shown in false color) is overlaid on a topographic map created from measurements of surface elevation using LOLA's lasers. Areas with more iron and/or titanium in the top layer of lunar regolith are relatively dark, as are areas that have been more strongly weathered by exposure to radiation and micrometeoroids at the surface. Brighter areas surrounding craters may indicate fresher material brought to the surface by the crater-forming impact. Dark lines are topographic contours spaced 100 meters apart. (**E**) LAMP map derived from far-ultraviolet light sensitive to composition, texture, and maturity of surface materials. This map shows the Off-band (155–190 nm)/On-band (130–155 nm) albedo ratio, overlaid on an LROC WAC basemap (Credit: NASA/GSFC/Intuitive Machines). Mare deposits in the center and along the northeastern edge of Orientale have low ratios due to their relatively high iron abundance, and fresh ejecta materials (e.g., along the northwestern edge of the basin) have high ratio due to the relative lack of space weathering.

The LROC team confirmed that the LRO maneuvers and imaging were executed as planned based on the targeting information provided by the Artemis II Flight Dynamics team. From the preliminary Orion orbit determination, the ephemeris predictions matched reality, and Orion passed through the LROC NAC FOV while its cameras were imaging. Since pointing is the same for LRO's LAMP instrument, Orion also passed through the FOV of the LAMP observations, resulting in successful observing attempts by both instruments.

Due to the large distance between the two spacecraft, the Orion capsule and European Service Module filled <1% of an LROC NAC pixel and, despite planning timing of two observations to maximize favorable illumination and imaging conditions, Orion was too faint to be detected in the images. Likewise, LAMP was unable to detect faint emissions from Orion. These results were predicted and expected by the LRO teams, but the observation activities were pursued to refine this collaborative process for applications to future missions. The distance between LRO and Orion was >7,600 km during the first observation and >8,900 km during the second observation. To confidently detect Orion in an LROC NAC image, the two spacecraft would need to have been within ~2,000 km of each other (in optimal conditions), and within <500 m for detailed views. Although Orion was not detected in the LROC or LAMP observations, this observation sequence was still a successful collaboration between the two mission teams and a productive test of the processes to strengthen future mission-support efforts between the Artemis and LRO teams.

6.1.3 LRO Observations Acquired During the Time Surrounding the Artemis II Lunar Flyby to Complement Crew Science Observations

Observations of high-priority Artemis II crew targets were acquired by LROC and Mini-RF during the time surrounding the lunar flyby (within ~24 hours before and after the flyby). Regular communication between the LST and the LRO teams helped to identify high-priority crew targets for LRO targeting in the months before launch. The Goddard Flight Dynamics team utilized Artemis II and LRO ephemerides to model illumination of the lunar surface in combination with the crew FOV and the LRO orbit path for the time period of the flyby for each launch scenario. These model results were used to identify key targets that were illuminated and visible to both the crew and LRO. The LRO targets were designed to capture observations of features under illumination conditions similar to those observed by the crew to provide complementary data from LRO's position in orbit for comparison to crew observations.

For example, comparisons of crew observations with LRO data captured under similar viewing conditions can potentially add insight to our understanding and interpretation of existing LRO and other orbital data. Such comparisons potentially enable feature characteristics that stood out to the crew (e.g., crew descriptions of high/low albedo, colors) to be identified in LRO data in additional locations across the lunar surface (including locations not visible to the crew during flyby). Within roughly 24 hours of the Artemis II lunar flyby, Mini-RF acquired observations of Aristarchus Plateau, Oceanus Procellarum, and Mare Imbrium, and LROC acquired 74 WAC images and 245 NAC images within the crew's illuminated FOV.

Additionally, the Cosmic Ray Telescope for the Effects of Radiation (CRaTER) instrument was continuously acquiring data to characterize the deep-space radiation environment around the Moon throughout the flyby and the entirety of the Artemis II mission. With a minimum separation of roughly 8,000 km, the radiation environment enveloping LRO and Orion was likely the same during the lunar flyby. CRaTER is designed to measure linear energy transfer (LET), which is the energy deposited per unit distance traveled through the Tissue Equivalent Plastic. Due to this, as well as LRO's closer proximity to the Moon (which will block some energetic particles), the data from CRaTER is expected to differ but provide complementary measurements to those acquired by the radiation monitoring instruments on Orion throughout the Artemis II mission.

At the time of this writing, comparative analyses with LRO and Artemis II data are ongoing. LRO data are publicly accessible in the PDS and available for future studies, comparative analyses, calibration efforts, and other investigations that will enhance the overall science return of the Artemis II mission into the future.

6.2 Impact Flash Citizen Science Campaign

To complement the observations of impact flashes made by the Artemis II crew during their lunar flyby (**Section 5.1**), the NASA Artemis II LST collaborated with NASA's Citizen Science Program encouraging observers with a suitable telescope and camera to observe the Moon to search for impact flashes. The LST coordinated with several amateur astronomer groups, including the NASA-funded Kilo-nova Catchers, Exoplanet Watch, Unistellar Network Investigating TESS Exoplanets (UNITE), Association of Lunar and Planetary Observers (ALPO), and Night Sky Network teams, as well as the Lunar Impact Flashes project based at the National Research Council of Italy (IMATI-CNR).

As part of this project, named *Impact Flash!*, NASA's Solar System Exploration Research Virtual Institute (SSERVI) Geophysical Exploration of the Dynamics and Evolution of the Solar System (GEODES) team, in collaboration with Los Alamos National Laboratory, published a website with information for observers regarding impact flash science, the Artemis II mission, and recommendations about how to observe. Participants were encouraged to use a telescope (ideally equipped with automated tracking to keep the Moon in field) and a camera with a recording frame rate of at least 25–30 frames per second and accurate timestamps. Participants were also asked to record and report their observing location (e.g., from a phone's GPS).

Observers were instructed to upload video taken (ideally in RAW monochrome format) to the Lunar Impact Flashes database. Data were then analyzed by researchers at Johns Hopkins University. Understanding that the lunar phase as viewed from Earth was not ideal for ground-based observations during the Artemis II lunar flyby, no definitive impact flashes from ground-based assets have yet been reported. However, teams are still encouraged to submit observations to the Lunar Impact Flashes database (LIF database) to aid with ongoing efforts in characterizing the lunar impact flux at different times of the year (e.g., Cudnik, 2009).

6.3 Additional Coincident Lunar Data Collection

Beyond the data-collection collaborations between the LST, LRO, and citizen scientists, several other Earth- and Moon-observing teams collected coincident data supportive of Artemis II science.

DSCOVR captured images of the Moon using its EPIC camera across ten spectral bands, from ultraviolet to near-infrared. These observations were used to help verify EPIC's calibration, since the Moon provides a relatively stable, bright reference target. Natural-color composite images were also generated from selected visible bands. The full-disk lunar images in calibrated color bands are available on the DSCOVR site. This dataset may also help calibrate the Artemis II Nikon images by providing calibrated color and white-balance information.

During the Artemis II lunar flyby, the Time History of Events and Macroscale Interactions during Substorms—Acceleration, Reconnection, Turbulence and Electrodynamics of Moon's Interaction with the Sun (THEMIS-ARTEMIS) probes collected simultaneous plasma and field data. Positioned at the Earth-Moon Lagrange points (L1 and L2), these probes characterized interactions between the lunar surface, its downstream wake cavity, and the solar wind and radiation environment. The data acquired by the THEMIS-ARTEMIS probes during the flyby are publicly archived and accessible through the UC Berkeley Space Sciences Laboratory THEMIS website or PDS Planetary Plasma Interactions Node.

NASA and NOAA provided continuous space weather awareness during the Artemis II mission by monitoring the Sun and supplying real-time decision support to NASA's Space Radiation Analysis Group. Multiple spacecraft continuously measured the solar wind, magnetic field orientation, and hazardous particle radiation. Mission teams created real-time models capable of forecasting hazardous

solar particle radiation up to 24 hours into the future. NOAA's Space Weather Prediction Center (SWPC) evaluated active solar flares and coronal mass ejections in real time, with direct communication to NASA's MCC. Products from the Artemis II mission period can be found by searching the NOAA SWPC website by date.

As a part of the Space Communication and Navigation (SCaN) program, a coordinated effort was organized for community members to monitor the Orion spacecraft through passive doppler radar. For more information, see communications posts: NASA Selects Participants to Track Artemis II Mission and NASA's Artemis II Orion One-Way Doppler Measurements Tracking.

In addition to Earth and satellite-based monitoring of the Moon, the Expedition 74 crew onboard the space station also took handheld images of the Moon during Artemis II, providing a complementary low Earth orbit perspective on the mission and capturing the Moon's changing phase over the mission's duration. For example, image iss074e0431864 (**Figure 6.2A**), acquired at 20:53:26 UTC on Artemis II's Flight Day 01 from the space station Cupola window, shows a full Moon at moonset, just a few hours after the Artemis II launch. The oblique viewing angle captures the Moon and Earth's atmosphere in the same shot. Image iss074e0432036 (**Figure 6.2B**), taken later the same day at 21:30:50 UTC from the same window, shows the Moon framed by the station's Canadarm (the shuttle remote manipulator system). The image also shows a cross-section of Earth's atmosphere, beneath which northern Canada is visible, including several icy rivers and the Manicouagan Reservoir, partially obscured by high-altitude clouds. Image iss074e0448009 (**Figure 6.2C**) was captured on Flight Day 05 and shows an oblique view of a waning gibbous Moon and cross-section of Earth's atmosphere in the foreground. Finally, captured on Flight Day 10, image iss074e0460378 (**Figure 6.2D**) shows a third quarter Moon with the terminator running from Mare Imbrium in the north to Mare Nubium in the south.

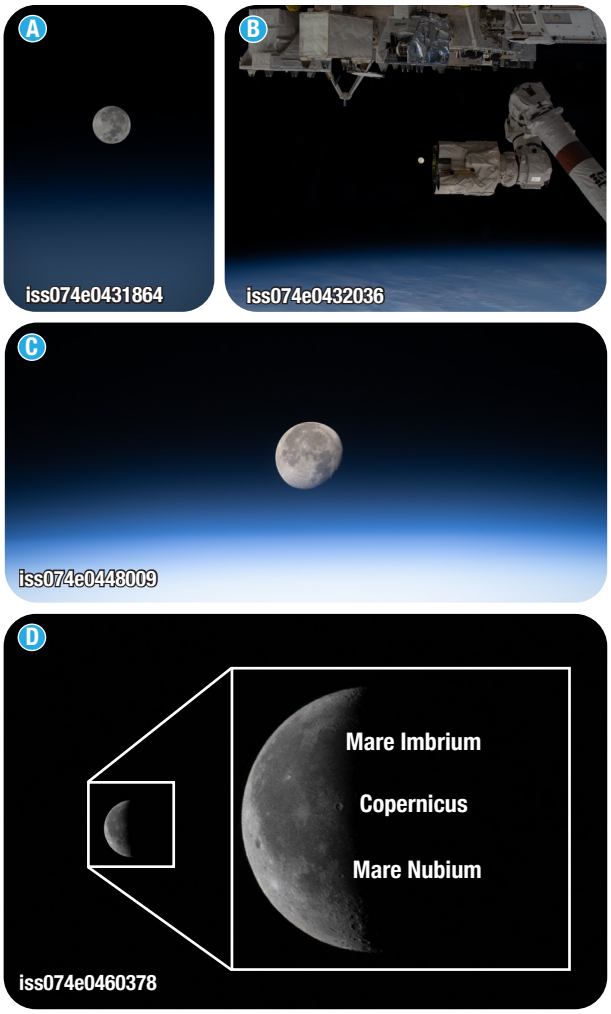


Figure 6.2: Space Station Views of the Moon. (**A**) NASA image iss074e0431864 showing the Moon on Flight Day 01, shortly after launch. (**B**) NASA image iss074e0432036 shows the Moon, with Canadarm and a cross-section of Earth's atmosphere in the foreground, also on Flight Day 01. (**C**) NASA image iss074e0448009 (cropped) shows an oblique view of the Moon and a cross-section of Earth's atmosphere on Flight Day 05. (**D**) NASA image iss074e0460378 shows the Moon on splashdown day (Flight Day 10).

7.0 CONSTRAINTS ON SCIENCE IMAGES AND OBSERVATIONS

7.1 Window Quality Observations

As discussed in **Section 3.2.3**, a DFTO activity was conducted on Flight Day 03 to assess window quality for science observations. The in-flight evaluation produced three major findings: (1) the

docking-hatch window was optically superior to the forward windows (but not recommended for observations during the flyby because it would prevent the crew from working in pairs); (2) of the forward windows, Window 2 was the best for imaging; and (3) images acquired flush to the windowpane could be collected at all planned zoom levels (i.e., up to 400mm focal length), whereas oblique-angle images should be limited to 200mm to reduce distortion. Based on this evaluation, vehicle pointing was directed to center the lunar disk in Window 2 and crew actions were recommended to take images from the left side of Window 2 with the lens flush against the windowpane.

After splashdown, the ISAG and LST analyzed additional mission data to complement the window-quality DFTO dataset to search for and evaluate distortions introduced by the window. This post-flight analysis confirmed that window characteristics influenced science quality and science return. First, the optical advantage of the docking-hatch window was confirmed, and the differences in quality of images collected from the docking-hatch window and the forward windows were also more clearly characterized. The crew also reported during the mission that glare and internal reflections from the multiple panes in the forward windows interfered with iPhone imaging, leading them to rely primarily on the docking-hatch window for iPhone use. Second, analysis of the forward windows reinforced that Window 2 enabled the most reliable imaging. Third, the post-flight dataset demonstrated that window characteristics affected image quality at different focal lengths: some lunar images acquired at 400mm were clear, while others showed distortion at the same zoom level. Refer to the *Artemis II Lunar Science Data User Guide Appendix E* for more details on the window-quality DFTO.

7.2 Effects of the Orion Cabin Environment on Science Observations

Because the crew conducted science activities during IVAs, their observations were influenced by various aspects of the Orion cabin environment. For observing and imaging, this included illumination from interior light sources and external light entering through the windows. For recording audio, the ambient cabin noise was the primary environmental factor. Across all operations, the crew's close proximity to one another, combined with the simultaneous execution of non-science activities, were important additional considerations in the noise environment (for example, exercise for the non-observing pair was intentionally scheduled outside of science observation periods to help maintain a quiet cabin environment for audio recording during the flyby).

An initial assessment of cabin window quality for science observations was performed with the DFTO activity on Flight Day 03 (**Section 3.2.3**, **Section 7.1**). During the flyby, the vehicle was intentionally oriented so that the forward windows designated for science observations were pointed toward the Moon. Cabin lighting during these observations was controlled by dimming (or entirely turning off) the cabin interior lights. Other sources of interior illumination included, but were not limited to, the Orion flight control system display units, which were dimmed as much as possible, and various colored LEDs in the cabin, many of which could not be turned off and required physical coverings. Exterior light entering the cabin was controlled using window shades, including a shroud around the window that was used by the crew for imaging.

The crew reported that the sunlight entering through the windows was extremely bright. For example, R. Wiseman reported: "I gotta shield my eyes from the sunlight coming in the cabin. I'm gonna actually close my right eye completely" (R. Wiseman, camera, PCD crew audio, art002a000025, 21:46:19 UTC). Even with the interior lights turned down as much as possible and the window shroud installed, the crew reported residual and noticeable glare in the cabin: "The glare coming in from the Sun is getting past the side of the window and it's making it difficult to shroud. It's not protecting from the reflections coming from the outside" (V. Glover, camera, PCD crew audio, art002a000049, 23:19:05 UTC). During portions of the flyby just before and after the eclipse, the effect of overpowering illumination from the Sun was particularly challenging since the unilluminated disk of the Moon and the Sun were in view simultaneously.

The interference from solar brightness was more significant than anticipated, and the crew commented repeatedly on the intensity of the direct sunlight and its reflections within the cabin. Indirect illumination arose from a variety of reflective surfaces, including white headset cables, windowpanes, the windows themselves, and portions of the vehicle exterior. In response to the limitations of the illumination shrouds they were provided, the crew improvised additional light-blocking solutions using a black t-shirt and bungee cords.

Additionally, when the daytime Earth was visible, its imaging remained challenging: SAW GoPro imaging of the Earth was limited by spatial resolution and dynamic range constraints, while the Artemis II crew described difficulty imaging the Earth with their iPhones. R. Wiseman commented:

> Everything is just very white, bright, and washed out. The iPhones, you have to manually go in and bring the gain down, and even at that, it's very difficult. It's like walking out back at your house and trying to take a picture of the Moon. That's what it feels like right now, trying to take a picture of Earth. (R. Wiseman, O/E-1 voice loop, 12:32:02 UTC, Flight Day 02)

The crew found that the Nikon D5 and Nikon Z9 did not have the same issues.

Overall, the combined effects of direct and indirect solar illumination affected the crew's perception of and sensitivity to the brightness and color of science targets. For example, at one point during the flyby V. Glover reported: "from this angle, it's hard to really pick out color and albedo variations. My eyes are gaining down because of the brightness of the Sun and I'm not picking up a whole lot of subtlety" (V. Glover, unaided eye, PCD crew audio, art002a000046, 22:47:59 UTC).

The crew's ability to easily discern color was affected not only by the illumination environment, but also by the presence of other colored objects in their FOV. In one instance, V. Glover was asked by the Science Officers during a SitRep if he could actively resolve the color variations in Orientale that R. Wiseman had seen, and V. Glover reported back:

> The way that I'm looking at Orientale, again I'm still in the docking-hatch window, there's like a thermocouple right here in the center of the window and it is the orange Kapton tape color and so it is unfortunately -- it's like trying to look at stars, you know, next to a metropolis. I think it's drowning out any color that I could pick up from the Moon. I am not able to see that color, but I have not looked at it from one of the windows one through four. I think when I get away from this Kapton tape strip that I would be able to see the [color] variation that Reid's talking about. (V. Glover, unaided eye, O/E-1 voice loop, 21:32:57 UTC)

Without sufficient time for dark adaptation, the crew reported initial difficulty seeing subtle variations in brightness and color on the lunar surface.

> I see brown in the south. I definitely -- I didn't in the beginning, and as my eyes adjusted, I see brown in the south of the [maria]. (V. Glover, camera, PCD crew audio, art002a000037, 20:41:20 UTC)

> The Moon is so bright. And uhm it's like a half-Moon right now. I'm just going to let my eyes adjust and talk about some of the areas that I annotated for color, albedo, variations before. (J. Hansen, camera, PCD crew audio, art002a000041, 21:44:27 UTC)

> I'd say probably 20% of the left side of the Moon is lit up in earthshine. I still, my eyes have not adjusted enough to be able to see any landmarks. (R. Wiseman, camera, PCD crew audio, art002a000052, 01:10:48 UTC)

These observations provide important insights into how to optimize the observing environment to maximize science return on future missions. By characterizing constraints such as window orientation, illumination impacts, and color interferences, future missions can better mitigate similar challenges going forward.

7.3 Spatial Resolution of Surface Features with Unaided Human Eyes

During Orion's approach to the Moon and throughout the flyby, the LST collected data on how the crew used landmarks as key navigational markers. The crew's ability to confidently recognize different landmarks varied in response to several factors, including their proximity to the Moon, their viewing angle of the surface, the local illumination conditions, and the presence of other illuminated or colored objects in their field of regard (e.g., the Earth, cabin equipment). Evaluation of landmark recognition in correlation with these various factors will provide valuable insight for future crew activities in lunar orbit and on the surface.

Related to discerning feature size, one of the Artemis II lunar science objectives was to characterize the smallest lunar feature that could be identified by observers with and without camera assistance. During one flyby observation period, J. Hansen described a linear feature he could see with the camera zoom lens near Lacus Excellentiae and north of Byrgius A, a feature that was not visible to R. Wiseman's unaided eye:

J. Hansen	So, those really dark spots we're talking about between our handprint and Grimaldi, a little bit further west than that line. What'd you call that Byrgius Alpha that bright spot, right? Just north of Byrgius Alpha. They are linear. The one in the middle, the dark spot in the middle is very linear, like a canyon of dark. It does not look like a circular feature.
R. Wiseman	Oh, cool! I cannot see that with the naked eye. That is awesome.
J. Hansen	There's like a gouge, and it's not all dark. It's dark, and then the top of the gouge, if we call that a canyon or a gorge, it's got high albedo.

(J. Hansen, camera, PCD crew audio, art002a000028, 18:59:53 UTC; R. Wiseman, unaided eye, PCD crew audio, art002a000018, 19:00:18 UTC)

The LST identified this feature to likely be Rimae Sirsalis, the longest rille on the Moon. It stretches ~426 km from the edge of Oceanus Procellarum, southwest across predominately highlands terrain, terminating in the fractured interior of Darwin crater north of Byrgius Alpha crater (**Figure 7.1**). The high-albedo feature near "the top of the gouge" (J. Hansen, camera, PCD crew audio, art002a000028, 18:59:53 UTC) is likely to be Sirsalis F crater (**Figure 7.1**). These features were further analyzed using Lunar QuickMap data, in light of J. Hansen's and R. Wiseman's commentary, to help constrain the limits of the spatial resolution of the crew's observations.

Along its extent, Rimae Sirsalis is consistently ~2.5 km wide. At the time of the quoted observation, the slant range to the center of its extent was ~16,700 km, and, given the view angle and the orientation of the linear rille, its width at this location subtended an angle of 32.3 arcseconds, roughly half the linear rille's width if viewed at nadir. Since this was not resolvable by the unaided eye but could be seen through a 400mm lens, the observation constrains the minimum size feature visible on the lunar surface at this distance. In the diffraction-limited case, the angular spatial resolution q of an optical system is found by the Rayleigh criterion:

$$q = 1.22\ (l / D)$$

where l is the wavelength of observed light and D is the diameter of the circular aperture of the optics.

Given l = 550 nm (peak human sensitivity in daylight) and D = *2* mm (approximate diameter of the pupil in bright light), q = 69.2 arcseconds, roughly the 1-arcminute rule of thumb for normal human vision and about twice the angle subtended by the width of Rimae Sirsalis. The inability to resolve the linear rille with the unaided eye is therefore unsurprising. However, the linear rille was visible through the 400mm lens of the Nikon D5 camera. Unlike telescope and microscope optics, the concept of magnification for camera lenses used visually is not well-defined except as "magnifying power" relative to a baseline focal length, usually 50mm. Optical viewfinder magnification is also expressed relative to a 50mm lens focused at infinity. The approximate magnification of the view through the viewfinder is:

$$M = v\,f\,/\,(50\text{mm})$$

where v is the viewfinder magnification, f is the lens focal length, and the baseline, 50mm, is considered comparable to the eye for a full-frame, 35mm camera. On the Nikon D5, v = 0.72 and f = 400, which yields M = 5.8x for the camera observation. This is equivalent to a resolution of q / M = 12 arcseconds. For comparison, the pixel scale of the D5 with a 400mm lens is 3.3 arcseconds.

Viewed with the unaided eye from the unique environment of the Orion spacecraft, the combined observations place the resolvability of lunar features at subtended angles >0.5 and <3 arcminutes, or between 1.0 and 6.0 km nadir at pericynthion.

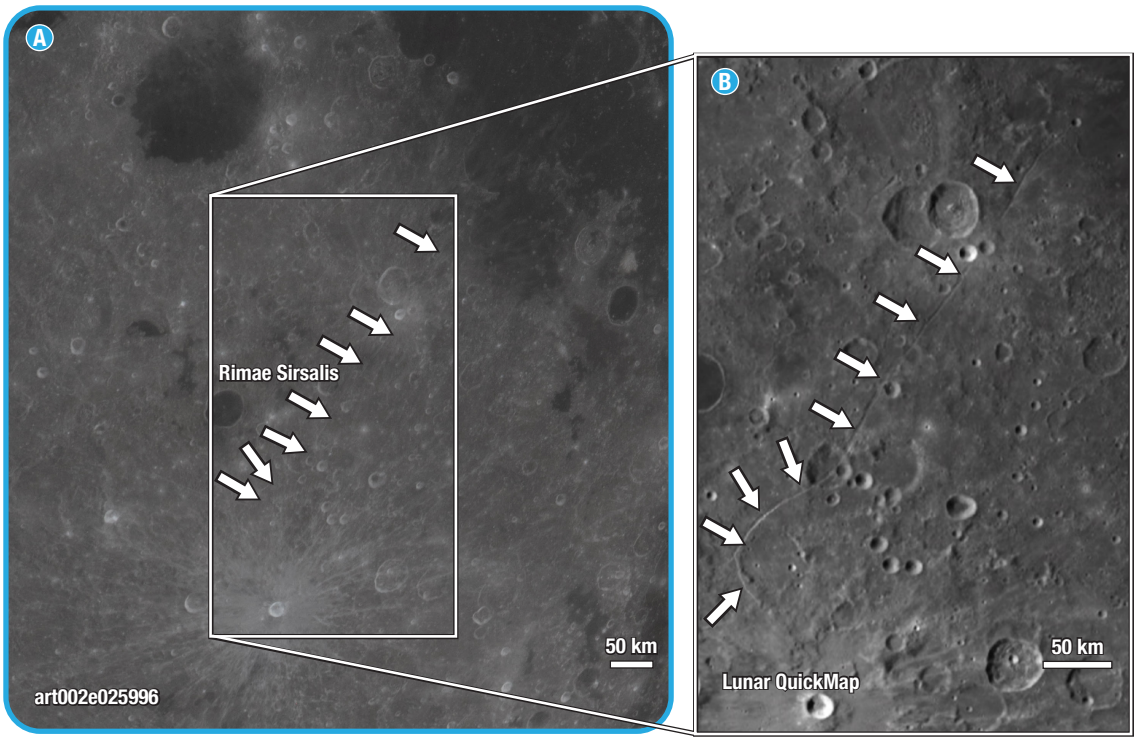


Figure 7.1: Rimae Sirsalis. (A) Crew image art002e025996 of Rimae Sirsalis spanning from the edge of Oceanus Procellarum (northeast) to Darwin Crater (southwest). (B) LROC WAC+NAC regional mosaic better reveals the Rimae Sirsalis with arrows pointing to the linear feature (Credit: NASA/GSFC/Intuitive Machines).

7.4 Comparison of Handheld Cameras as Science Tools

ISO is the setting that controls a camera's sensitivity to light. The Nikon D5, with its expanded ISO range (100–102,400), enabled the crew to capture the instantly iconic "Hello, World" image (**Figure 7.2**) commemorating the first human mission beyond low Earth orbit in more than 50 years. As described in **Section 5.10**, many images of Earth taken during the early flight days, including "Hello,

World," show Earth in nighttime illumination. In these images, the Earth is dimly illuminated only by moonshine with a high ISO setting (~51,000) used on the Nikon D5. This increased light sensitivity enabled better images of the low-light scenes but also led to the perceived muted colors relative to the "Blue Marble" image collected with film cameras during Apollo 17 when Earth was fully illuminated by the Sun (**Figure 7.2**). The ~51,000 ISO used with the Nikon D5 in low-light conditions exceeds the native ISO range of the Nikon Z9 and thus the Nikon Z9 was not employed in such cases.



Figure 7.2: An Apollo and an Artemis Earth. (A) The famous Blue Marble image acquired by the Apollo 17 crew after their trans-lunar injection burn on December 7, 1972. This image was obtained with a modified Hasselblad 500 EL camera with an 80mm Zeiss Sonnar planar lens using 70mm Kodak Ektachrome color-reversal (transparency) film with an ASA/ISO of 64. (B) The "Hello, World" image (crew image art002e000192) taken by the Artemis II crew after their TLI burn on Flight Day 02 (April 3, 2026). This image was obtained with a Nikon D5 DSLR camera with a 14–24mm lens and an ISO setting of 51,200.

Beyond ISO performance, the optical architecture of the Nikon D5 and Nikon Z9 resulted in distinct operational differences during Artemis II. The D5's optical viewfinder provides the photographer with a mirrored reflection of the actual view through the camera's lens. In contrast, the Z9 is a mirrorless camera without a mechanical shutter or optical viewfinder; instead, the photographer has an electronic preview of the view through the camera lens. These fundamental optical differences between the D5 and Z9 were apparent in three primary ways during Artemis II: (1) the D5 offered a more natural visual experience; (2) the D5 offered capabilities of a handheld monocular; and (3) the Z9's electronic viewfinder provided safety advantages during extreme illumination events.

In the first way, the D5's optical viewfinder enabled the crew to leverage the benefits of observing with human eyes when composing photographs. C. Koch, for example, commented:

> I just wanted to mention, great call from the Science Team on sticking with the D5 for our observations, the real science observations during the flyby, because I can confirm that the Z9 imagery, even through the viewfinder, because it's digital, was very different. It was much higher contrast than the naked-eye view through the D5 viewfinder. (C. Koch, O/E-1 voice loop, 04:13:02 UTC, Flight Day 04 opportunistic imaging)

Second, when combined with the zoom lens, the D5 optical viewfinder effectively provided the crew with a small monocular for visual observations, even without the need to have the camera powered on



Figure 7.3: Vehicle Lunar Views. Individual frames from SAW Cam 3 streamed video. (**A**) Vehicle camera images art002m1010962338 and (**B**) art002m1010962338 compared to corresponding still images from (**C**) vehicle camera images art002e00957 and (**D**) art002e009571. These enhanced observations were made possible by the scripts developed by the INCO to capture multi-shot sequences with varying exposure times. During the eclipse period, these sequences consisted of sets of four images with exposure times of 2, 5, 10, and 15 seconds, taken at 15-minute intervals to capture dynamic visual phenomena.

or to capture images. In contrast, using the Z9 for observing requires having the camera powered on and using a sensor-generated view.

Third, due to safety advantages of the electronic viewfinder, the Z9 enabled imaging scenes even where the Sun was in the FOV (e.g., at earthrise, earthset, and on either end of the eclipse period). Viewing the scene through the Z9's electronic viewfinder offered an added layer of eye safety by preventing inadvertent direct exposure to the Sun through camera optics. Additional discussion of this comparison is present in the crew perspectives section (**Section 2.0**).

7.5 Comparison of Image Quality Between SAW Camera Stills and Video Frames

In planning prior to launch, the vehicle cameras were initially scheduled to only stream videos during the lunar flyby. To better support science objectives, the LST collaborated with ISAG and the Integrated Communications Officer (INCO) to add a higher-resolution still-image acquisition to the vehicle imaging plan (**Section 3.3**).

After splashdown, the LST compared individual frames extracted from the SAW Cam 3 video with still images captured simultaneously by the same camera. As shown in **Figure 7.3**, the extracted video frames have a lower spatial resolution and are constrained by fixed exposure settings, whereas the still images provide the spatial resolution and exposure needed to resolve the solar corona, earthshine, and details of the spacecraft's exterior. By maximizing data acquisition to align with science needs (i.e., capturing high-resolution stills in addition to continuous video), the SAW cameras produced observations of enhanced scientific value.

7.6 Photogrammetric Analysis

To quantify and validate image-related constraints, the LST used 3-dimensional (3D) animation software to precisely reproduce the geometry of Artemis II images. This method simultaneously tests potential sources that can influence science analyses: the camera timestamp accuracy, geometry of the camera optics, accuracy of the spacecraft ephemeris, potential geometric distortion introduced by the cabin windows, and georeferencing of LRO mapping. Images acquired around the times of earthrise and earthset are particularly sensitive tests because any discrepancy in the obscuration of the Earth between the crew image and the 3D rendered image is visually obvious.

The LST initially undertook 3D render matching (a form of photogrammetry) to identify features along the lunar limb. The trial-and-error process of dialing in the precise timing, view direction, and focal length of the virtual camera to match the crew images revealed discrepancies that may be relevant for future analyses of the images. The discussion that follows is based on the preliminary spacecraft ephemeris generated one day after the flyby (April 7, 2026, 17:30:05 UTC) and published on NASA's website. This ephemeris comprises state vectors at four-minute intervals during the period of the flyby images. The animation software (Autodesk's Maya) was scripted to interpolate the ephemeris positions using Catmull-Rom cubic splines applied separately to each vector component, with the result used

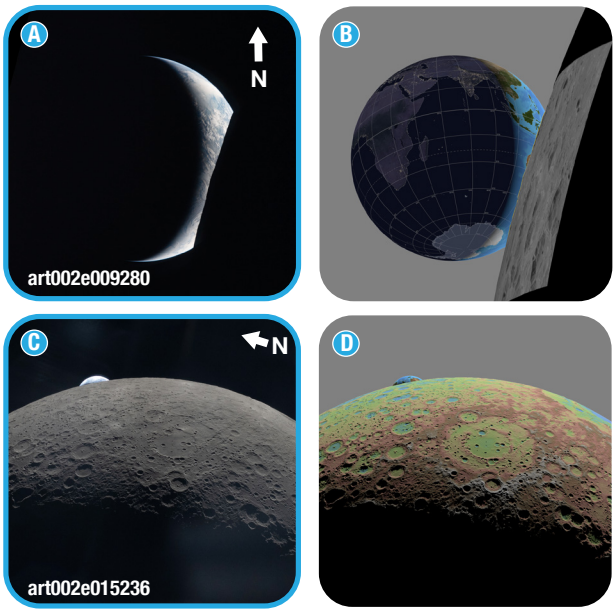


Figure 7.4: Photogrammetry Renders. Side-by-side comparisons of crew images and computer simulations. (**A**) Earthrise, crew image art002e009280, (slightly rotated to lunar north up). (**B**) The matching digital recreation of the geometry of the photograph, used to verify that limb points (thin yellow line where the limb intersects Earth) had been correctly identified (see **Figure 5.33**). (**C**) Earthset, crew image art002e015236, (original orientation). (**D**) The matching digital recreation of the geometry of the photograph. The large impact features are Hertzsprung (center) and Orientale (on the limb, at right). The colors encode elevation (red high, blue low).

to position the virtual camera. The aim of the camera was found by iteratively rendering images (using Pixar's RenderMan) and overlaying them onto the Artemis II images until they matched.

Earthrise photo art002e009280 (**Figure 7.4**) was taken by the crew with one of the Nikon D5 cameras at a 400mm focal length. A pixel-accurate matching render was created by setting the time in the animation software to 23:22:44.5 UTC, 14.2 seconds later than the 23:22:30.29 UTC timestamp recorded by the D5. The selenographic coordinates of points on the lunar limb's intersection with Earth in this image (**Figure 5.33**) were found by creating a version of the matching render in which latitude is rendered as varying levels of red and longitude as levels of green. The values at limb pixels, defined as the outermost pixels at which the render's alpha channel showed full opacity, were then transformed from linear floating-point red and green to selenographic latitude and longitude.

Earthset photo art002e015236, taken by the crew on the Nikon Z9 at 35mm, was matched at 22:42:50 UTC, 24.5 seconds before the 22:43:14.51 UTC camera timestamp. To match the Z9's image scale, it was also necessary to set the virtual camera's focal length to 35.71mm, likely due to slight barrel distortion in the lens on the Z9.

The magnitudes and opposite signs of the timestamp discrepancies might tend to point toward inaccuracy of the camera clocks rather than the ephemeris, but the true contributions of each factor await future analysis. No discrepancies attributable to window distortion or the georeferencing of LRO data were observed in these two cases.

This photogrammetric approach provides a rigorous, image-by-image method to quantify timing offsets, focal length differences, and geometric distortions that can constrain scientific interpretation. By identifying and bounding these factors, future missions can improve calibration practices, refine imaging timelines, and mitigate geometry-related uncertainties in science observations.

8.0 HUMANS IN LUNAR SCIENCE AND EXPLORATION

The Artemis II mission demonstrated the exceptional value of human observation and cognition as scientific assets in planetary exploration. Unlike cameras, which capture isolated moments and often narrow subsets of a scene, human observers continuously interpret their surroundings, integrating real-time visual perception with contextual understanding. With an understanding of the mission's science objectives, the Artemis II crew dynamically assessed color, texture, and geologic relationships, and then applied that understanding to target, frame, and acquire images that directly advanced those objectives.

Stand-alone instrumentation measures exactly what it is designed to measure in a systematic, quantitative, and calibrated way, while trained human observers can detect the unexpected and adapt accordingly. In this way, trained human observers do not replace robotic instruments, but augment them;

humans contextualize what they observe, integrate observations with their knowledge and experience, and exercise real-time judgement to recognize anomalies, refine interpretations, and prioritize how to respond—all of which enable discovery.

Capitalizing on these attributes of human explorers, the LTP was intentionally designed to enable crew discovery in numerous ways (**Sections 3.6**, **3.7**). Its timeline of targets provided structure to the flyby observations, while preserving sufficient time within each observation block for target identification, interpretation, and reflection by the crew, as determined through iterative training with and feedback from the crew (**Section 3.4**). The LST recognized the importance of providing the crew with the ability to exercise their discretion in documenting their observations and the intent behind the observational plans, a principle reinforced throughout crew training activities and embodied in the LTP's dedicated Crew Choice targets. As a result, the Artemis II crew data were collected within a more flexible and responsive observational framework, different than the highly scripted plans typical of robotic missions, allowing human adaptability to enhance scientific return.

The color sensitivity and dynamic range of the human eye are particularly suited to continuous observations under changing conditions, including illumination and viewing geometry. In addition, the human visual system benefits from an enormous range in FOV, enabling multi-scale perception from broader regional context to fine-scale details which can be difficult to achieve with instrumentation. Without the need for data post-processing, human observers can immediately discern color, tone, brightness, and shape, among other characteristics, that are difficult to immediately reconstruct from remotely sensed data. Although remotely sensed data can provide these properties more quantitatively, human interpretations offer an instantaneous, qualitative complement.

During the Artemis II flight, the crew applied these capabilities while dynamically operating their handheld Nikon cameras to collect images with bracketed exposures, capture mosaics of the entire lunar disk as well as targeted areas on the Moon, and capture details of a solar eclipse and deep space by adjusting camera settings. A key advantage of human-operated imaging is the ability to perceive subtle color and tonal variations, capture these details in verbal descriptions, and adjust camera settings to capture these variations in images. Because cameras do not always fully capture such subtleties (or require sophisticated hardware with numerous filters to do so), the verbal descriptions of color made by the Artemis II crew are a critically complementary and unique dataset, as described in **Section 5.2**. Crew images and descriptions also complement the wealth of existing orbital datasets of the Moon.

8.1 Science Synergies of Data Types

The combination of crew images, recorded verbal observations, annotations, and vehicle images provide a rich scientific dataset for the planetary science community. Since much of the data was collected by human observers and camera operators, an important piece of the Artemis II metadata is an understanding of collection intent, which was captured in crew verbal observations and crew annotations. The verbal descriptions can be placed into context by associating them with crew and vehicle images taken at the same time.

The imaging plan for the vehicle cameras (**Section 3.3**) ensured the collection of a diverse dataset to enable comparisons of images taken by Orion's interior and exterior cameras, images taken by the crew, and verbal descriptions recorded by the crew. The exterior camera datasets enabled the regional-scale assessments of the lunar surface without the influence of vehicle windows, which can alter and degrade image quality (**Section 7.1**). While the crew images have higher spatial resolutions than the images obtained by the vehicle, the vehicle cameras provided valuable context to the science observations made by the crew.

Throughout the flyby, the LST coordinated data collection from the multiple vehicle cameras (**Section 3.3**), including from through the cabin windows and outside the vehicle. This coordination enabled images acquired by different cameras at the same time and thus the same illumination conditions. These images should not be used for direct quantitative comparison of surface properties,

as differences in camera settings (e.g., color temperature, white balance, exposure settings) and data compression can influence apparent color and brightness (**Figure 8.1**). Refer to the *Artemis II Lunar Science Data User Guide* for a detailed description of each camera system.

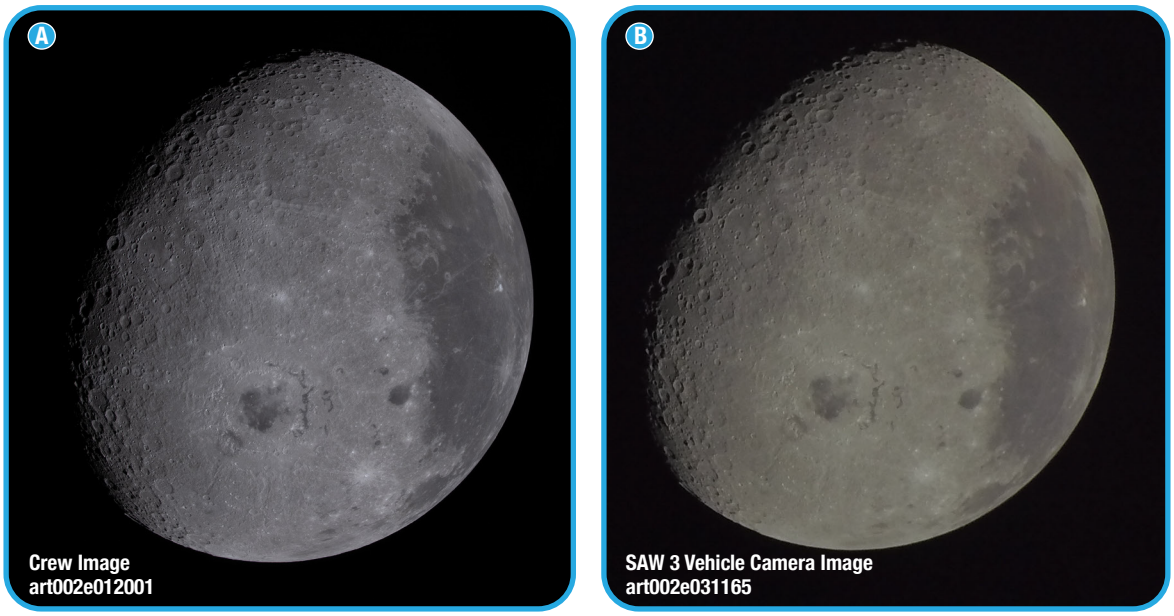


Figure 8.1: Camera Comparisons. (**A**) Crew image art002e012001 (acquired at 2026:04:06 19:01:18 UTC) and (**B**) exterior vehicle camera image art002e031165 (acquired at 2026:04:06 19:10:24 UTC) provide a full Moon view acquired only roughly nine minutes apart.

Timestamps associated with vehicle images, crew images, and crew audio recordings are used to connect different datasets. An additional cue helpful for aligning crew images with science intent is the sound of camera shutter clicks, which are easily audible above the ambient cabin noise in the audio recordings. Although the crew annotations are not time-stamped, they were collected as OneNote pages linked to specific LTP observation blocks. Each observation block is associated with a defined time period, and a capture time can be identified by listening to the crew audio as the crew frequently called out when, why, and the topic of an annotation.

Accurate time correlations required Nikon camera clocks, PCD clocks, and mission clocks to be synchronized. Cameras and PCD clocks were automatically set and manually verified and reset, if needed, to the mission clock. This process allowed for correct and consistent timestamps within image metadata. Any additional correlation effort occurred post-downlink and was focused on the PCD audio files, as the files were timestamped with the time and date of the audio file save. This process required interpolation of utterance times based on each recording's end time. These times were then validated by cross-referencing O/E 1 communications captured in the background audio, successfully reconciling the time the transmissions left Earth with when they were heard in the capsule.

Figure 8.2 illustrates the synergy within the Artemis II multi-modal dataset. While observing the geologic setting of Aristarchus Plateau, C. Koch observed a color boundary in the maria separating "brownish" and "grayish" terrains (citation, PCD crew audio, 20:13:18 UTC). In response to this observation, she initiated cross-tool data collection by capturing a handheld image and annotating the perceived contact. A vehicle image acquired at the same time provides complementary context, showing the crew's view from Orion and providing insight into the spatial scale at which these colors were discernable to the human eye. The combination of data—from verbal descriptions, handheld images,

annotations, and vehicle images—allows users to examine relative tonal and brightness characteristics from different cameras, link them to human perceptions in verbal descriptions, verify the location of the contact from the annotation, and pursue follow-on investigations of these colored terrains with orbital datasets. The integration of datasets produces a more complete scientific picture than any dataset could provide alone.

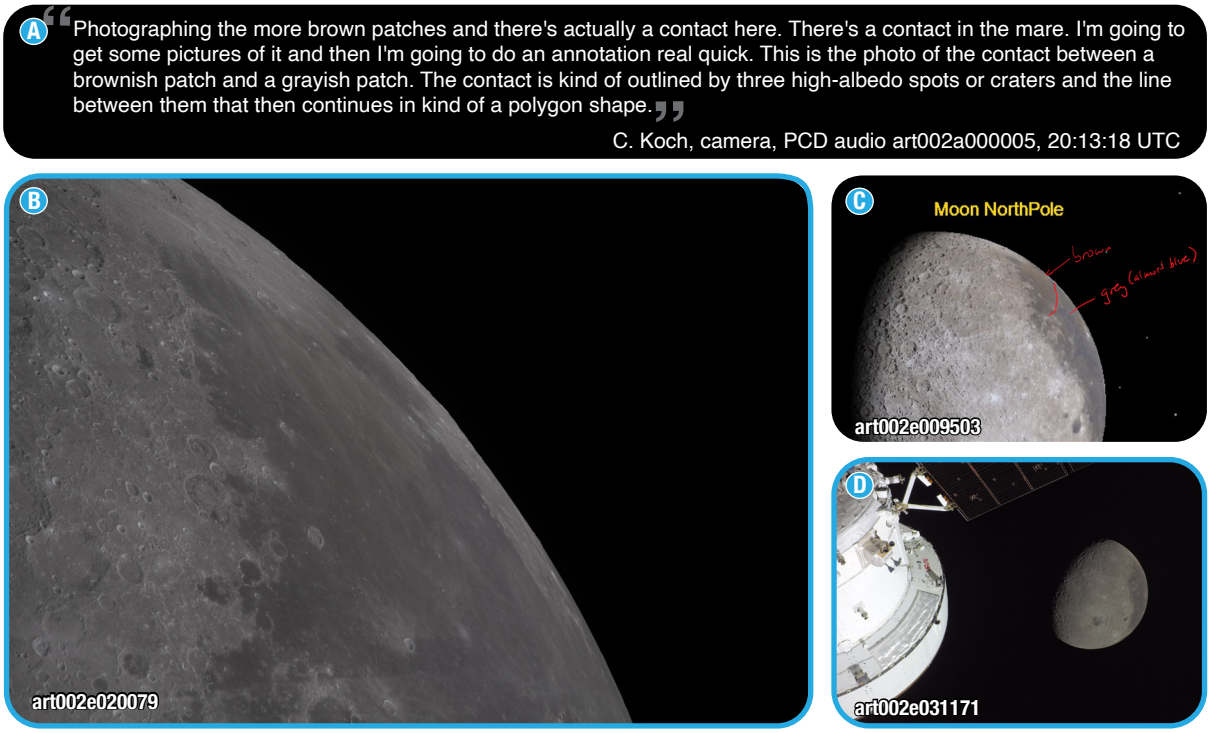


Figure 8.2: Synergistic Data. An illustrative example of the synergies between Artemis II data types acquired during a single observation block, including (**A**) crew verbal description, (**B**) crew image art002e020079, (**C**) crew annotation art002e009503, and (**D**) vehicle image art002e031171.

8.2 Importance of Crew Science Discussions

As discussed in **Sections 3.6**, **3.7**, the LTP included several structured crew discussion periods where all available crew were asked to come together for scientific discourse, prompted by different discussion topics and questions. These discussion periods emerged from the LST's close, iterative collaboration with the Artemis II crew, reflecting an understanding of how the crew's teamwork strengthened their collective observations and interpretations.

For example, C. Koch and V. Glover discussed their perception of color during the Farside Albedo/Color Discussion, in which the crew were prompted to describe any regional-scale variations in color and albedo. In this discussion, C. Koch and V. Glover shared perspectives and expressed concurrence on color and albedo variations in Oceanus Procellarum.

C. Koch	Like the color albedo, I mean, I am just obsessed with the different colors in the [maria] on the eastern side.
V. Glover	Same. Same. Some seriously interesting colors.
C. Koch	I don't know about you, but I see like a very distinctive contact in the north -- that's like brownish tan to the middle which I see is definitely more gray.
V. Glover	Brown and tan and gray. Yes, and I even saw some green in there.
C. Koch	Yes. I saw a lot of green.
V. Glover	What I thought was gray, but was green and gray. You know, green over the gray or under the gray. Yes, and we're both talking about the [maria] off in the east.
C. Koch	Yes. And then, so I wanted to see if you see the same boundary

(C. Koch, unaided eye, PCD audio art002a000008, 20:39:09 UTC; V. Glover camera, PCD audio art002a000037, 20:39:14 UTC)

The crew underscored the value of these discussions, even pausing during the flyby to acknowledge their impact directly to the Science Officer:

> As we continue to explore, when we actually do go down there to the surface, I know for safety reasons that we would never send someone alone, but I just want to really emphasize how important the discussion time was. When we started to talk, we not only got better science discussion, we got better human connection. Doing this as a pair we just learn and grow together and that's just super important, so thank you for adding that to this plan. (V. Glover, O/E-1 voice loop, 21:21:35 UTC)

The crew also applied discussion skills outside the scheduled discussion periods, treating their observation partner as an active scientific collaborator while working in the windows. For example, the following exchange between J. Hansen and R. Wiseman, captured as they transitioned from observations of Glushko to observations of Ohm, illustrates how real-time dialogue enabled the exchange of perspectives, debate, and refinement of scientific interpretations:

(J. Hansen, camera, PCD crew audio art002a000029, 19:21:37 UTC; R. Wiseman, unaided eye, PCD crew audio art002a000020, 19:21:58 UTC)

J. Hansen	There's that huge crater at the north of the Moon that has dumping rays on there [of the northwest boundary of the maria].
R. Wiseman	Yep.
J. Hansen	That -- I mean, sort of what I'm thinking is when these rays land, they're sort of the finer, when it's not thick enough to see it as a ray, it's creating the brown. And that whole region seems like that is covered in ray that created the brown.
R. Wiseman	Dude, that, I do not agree with you, but let me think about that. That is blowing my mind right there. Because if you come back down to Glushko now, I could actually convince myself that I could agree with that at Glushko. On the nearside mare of Glushko, I see some of those browns.
J. Hansen	Yeah.
R. Wiseman	And it could be a blanket of fine ejecta. I don't think it is, but it could be. You, you could absolutely be right there, Jeremy.
J. Hansen	Now, it doesn't, where it kind of falls down a little bit is the, um, Aristarchus Plateau is different.
R. Wiseman	Yeah, that is decidedly different.

J. Hansen	Um, what if we go back and look at Ohm through that lens?
R. Wiseman	[…] Ohm is like, it's a little bit of a messy crater system right there. And you get those prominent rays out the 2:30 that streak across to the nearside.
J. Hansen	Yeah.
R. Wiseman	The double rays --
J. Hansen	They're laying on top of what we're calling the brownish.

Through this exchange, the crew actively compared perspectives on geologic features, superpositional relationships, and color provinces. Their collaborative analysis of crater rays and ejecta prompted them to revisit earlier descriptions of Glushko crater and the Aristarchus Plateau, demonstrating how paired exploration and scientific dialogue during the flyby strengthened scientific insight and enriched the mission's observational return.

9.0 RECOMMENDATIONS

The Artemis II lunar science campaign was proof of concept in demonstrating what human-tended lunar science can contribute to our understanding of the Moon and a first step toward the sustained scientific exploration that the Artemis program promises. As with any first attempt at something new, the LST's experience executing this mission yielded not only a scientific dataset, but also a body of insight into how future lunar science campaigns might be improved. This section presents feed-forward recommendations developed from the Artemis II science experience, offered here in the same spirit of transparency and continued discovery that has guided this report.

These recommendations are distinct from the ground-based operational recommendations captured the *Artemis II Lunar Science Operations Report*, which addresses topics such as facility design, team staffing, and communication protocols. Several of the operational recommendations, however, are themselves informed by the science data discussed in this document, and are worth noting as cross-cutting considerations for future missions:

1. The importance of science discussions with crew immediately after splashdown;
2. The value of prior crew experience in making scientific observations from space;
3. The additional value of the D5 as a monocular;
4. The importance of enabling high-quality observational sketches and annotations;
5. The need to correctly scope time-critical science activities to the mission;
6. The need to be flexible with the amount of data actually downlinked from the lunar vicinity; and
7. The importance of tracing vehicle camera images to science objectives.

The recommendations that follow in this section reflect what the Artemis II lunar science data have taught us and are offered in service of the next generation of lunar explorers who will build upon this work.

9.1 Science as a Key Mission Component and Outcome

Artemis II was a test flight, not only for the Orion vehicle and for crewed mission operations, but also for science. An overarching outcome of that test flight was a demonstration of how science can successfully be integrated into a crewed lunar mission and the benefits that were often gained in doing so. The inclusion of science into Artemis II is directly in line with the current direction from NASA leadership to incorporate science into missions wherever possible. Doing so for Artemis II was challenging, and it was accomplished with the continual understanding that science was not the primary objective for this mission. Nevertheless, the Artemis II experience demonstrated that science can be a benefit to a crewed mission, with outcomes that arguably outweigh its priority in the mission.

To place these other recommendations into context, it is instructive to acknowledge that the considerable investment of time and effort to include science in Artemis II was worthwhile:

- Direct interaction between the crew and the science team, starting in training, through the mission itself, and continuing into the post-mission data curation phase, has been vital to achieving the science return reported here. More generally, this direct interaction has engendered and intensified interest amongst the astronaut and operations communities to incorporate science even more closely and deeply for future Artemis missions. This positive response to science as a key component of the myriad activities the crew engages in during a lunar spaceflight is well aligned with science discovery as a stated motivation for future Artemis missions.
- Artemis II was the inaugural mission for the new Science Officer position in mission control. The years of relationship- and trust-building amongst the science and operations communities culminated in Artemis II, especially the unprecedented direct dialogue between the Science Officer and the crew during the flyby. Science as an operational discipline was exercised and legitimized by Artemis II, leading to a richer mission because of the science outcomes. Future Artemis missions will directly benefit from the science-operations relationships built and tested for Artemis II.
- Crew science training for Artemis II, including field work, classroom instruction, and mission simulations, established a foundation of experience and knowledge that empowered the Artemis II crew to operate with confidence as science team members. The familiarity the crew had with the science objectives and fundamentals enabled successful science plan execution, and it also established science activities as an integrated, unobtrusive part of the mission that could be executed with confidence. Future Artemis missions will similarly benefit from sustaining, if not expanding, the science component of crew training.
- The data the astronauts collected on Artemis II, and the discoveries that the community will be able to make as a result, is a testament to the science output achievable when a science team, astronaut crew, and operations partners are all invested in and aligned with including science as a part of mission success. Artemis II did so even under the constraints of a test flight where science was not the top priority and where science assets (instruments, cameras, etc.) were limited in scope. Even more can be possible on future Artemis missions with increased science capability and scope.
- The NASA team and media partners did an outstanding job showcasing Artemis II to the world, and it was gratifying that a piece of the massive public engagement response was due to the attention that science attracted. Between the joyful yet focused way the LST did their work, and the genuine and professional way the crew did theirs, Artemis II showed everyone the approachable humanity of science and exploration. Future Artemis missions will benefit from the support and good will that science and exploration generate.

Recommendation: Science is a worthwhile activity for crewed missions that establishes a foundation for crew activities, yields valuable outcomes and tangible deliverables, and positively feeds into public engagement and interest. As such, future Artemis missions should continue to integrate science into training, mission planning, mission operations, and post-mission activities, to include commensurate investments in time, personnel, and resources.

9.2 LST-Crew Collaboration

Artemis II demonstrated that strong collaboration between the crew and the LST is central to maximizing scientific return from human lunar missions. Throughout training, during flight, and after splashdown, the crew operated as members of the LST. They trained in lunar science, practiced observation techniques, and provided critical feedback on LST products and procedures. Following splashdown, their continued involvement remained critical since the crew members were the mission scientists who collected the data and were uniquely positioned to review, clarify, and interpret the Artemis II datasets.

Furthermore, the mission showed the value of encouraging and supporting the crew to be exploratory as they look, observe, and describe to collect their scientific observations. The crew were trained

as mission scientists, not scripted data collectors. The crew's developed ability to react to what they saw, compare observations in real time, and refine interpretations together directly enhanced the scientific return of the flyby. Maintaining this collaborative, curiosity-driven approach should be a priority across all phases of future Artemis missions.

Recommendation: Future Artemis missions should continue to engage crew as embedded members of the science team across all phases of mission development (including pre-flight training, in-flight execution, and post-mission analysis) to strengthen observation accuracy, enhance scientific return, and ensure the fullest use of human-acquired datasets.

9.3 Scientific Crew Training

Based on crew feedback and mission results, the lunar science and geology training team was successful in developing and delivering training content for the Artemis II crew that enabled them to engage their scientific curiosity and perform their lunar observations as mission scientists. The training plan evolved over the approximately 2.5 years that the crew trained, and both the crew and the training team benefited from extra training time and diverse training environments, including classroom instruction, field deployments, simulations, and one-on-one tutorials. Throughout this process, the crew provided specific feedback about their training experience, informing the recommendations below for science and science operations training in future Artemis crews.

Among this feedback, the crew feedback emphasized the value of establishing a strong scientific foundation early in the training flow, alongside hands-on field experience that grounded classroom concepts in real geological processes. Field training in particular was identified as critical to learning how to observe and interpret geological features firsthand, in ways classroom instruction alone cannot replicate.

The crew also pointed to the importance of training that could flex to meet evolving mission needs, while still building skills in a structured, repeatable way. This included hands-on practice designed to progressively build both scientific "stamina" and final required skills, scenario-based exercises requiring collaborative problem-solving, and opportunities for real-time scientific feedback during simulations and one-on-one mentoring.

Finally, the crew underscored the value of self-directed learning tools that reinforced material between formal training sessions. Frequent, low-effort exposure to lunar science content with rapid turnaround feedback helped the crew retain critical knowledge over the course of a multi-year training flow. This self-directed and curiosity-driven training even extended into the mission itself. In addition to the LGR provided by the LST, the crew brought self-selected reference materials to the mission to continue reading and learning on their way to the Moon.

Taken together, this feedback provides the following recommendations to support future Artemis crew training:

Recommendation: Future Artemis crew training should maintain an early, introductory learning experience that provides foundational and contextual information about the Moon and the Artemis campaigns and should continue to prioritize field training as a critical tool for learning geological processes.

Recommendation: Future Artemis crew training should develop flexible training modules that address just-in-time training needs for the crew and for science; build training opportunities into simulations, with scientists providing real-time feedback: assign geology mentors to individual crew members to extend this real-time mentoring and feedback availability beyond simulation events; and build and train to standardized procedures that can be practiced consistently across training environments.

Recommendation: Future Artemis crew training should create a robust, regularly updated portfolio of digital training products and short homework assignments that the crew and FCTs can access independently, providing frequent exposure to lunar science material with assessment and feedback delivered within one day to support knowledge retention.

9.4 In-Mission LST to Crew Communications

Real time, bidirectional communication between the LST and the crew proved to be a valuable asset throughout the mission, enabling the LST to respond to crew questions as they arose, request clarification during time-critical science events, and directly support science interpretation while data were being collected.

Several times during the lunar flyby, the crew requested scientific information from the LST. For example, the crew asked for assistance with identifying surface features they were observing on the Moon in real time or determining relative ages of observed targets. Because the LST staffed in the SER had direct communication with the Science Officer, and because the Science Officer had direct communication with the crew, these requests received immediate, in-mission responses.

During the solar eclipse period, the crew reported seeing several impact flashes. With direct voice communication, the LST was able to immediately solicit information on the timing and locations of the flashes, allowing the team to determine with greater confidence the number of flashes observed, which flashes were observed by multiple crew members, and where on the lunar surface the flashes were located. This additional data collection that was enabled through real-time communication between the LST and crew at the Moon proved critical for subsequent scientific analysis of these impact flash data.

Direct communication also strengthened the scheduled post-flyby crew debrief on Flight Day 04. Because the LST could ask questions in real time, rather than relying solely on post-mission recollection, this enabled more accurate reconstruction of observational context and improved the overall fidelity of the science record.

Recommendation: Future Artemis missions should maintain a dedicated science team presence with direct, real-time voice communication to the crew in relevant mission phases. This capability enables higher fidelity data interpretation, timely clarification of crew observations, and more effective follow-up during time-critical science events.

9.5 Science Planning and Preparation

The LST spent months prior to the Artemis II launch building and refining the processes and tools for creating and implementing a science observation campaign for a crewed Artemis mission. The resulting workflow and tools that led to the Artemis II LTP can be used to enable orbital science observations on future Artemis missions. The pre-mission time and intellectual investment also prepared the LST to effectively and efficiently support the Artemis II crew during the mission as the astronauts performed the science activities, a model for how extensive pre-mission work will set up future Artemis missions for success. The Artemis II lunar science planning and preparation experience offers additional lessons learned that can be generally applied to conducting science on future Artemis missions.

The final version of the Artemis II LTP was created after launch because the LST required knowledge of the launch timing and TLI burn to determine what features would be in view on the surface of the Moon based on the spacecraft trajectory and illumination conditions. However, the process of creating the LTP benefited from having a starting point in the form of the pre-mission LTP uploaded prior to launch, rather than starting from a clean slate. An enabling strategy for this approach was including "view-agnostic" targets in the almanac of potential targets from which the LTP was built. These would be minimally affected by the exact trajectory or illumination conditions and established a stable set of potential targets that most iterations of an operational LTP could include. In this way, a substantial portion of the science plan could be built without specific knowledge of the mission parameters, allowing more time and resources to be allocated to planning those parts that would have to be tailored to a particular mission profile.

Mission profile-specific mission planning benefited from the extensive set of pre-mission simulations the LST participated in, including integrated simulations, as well as LST-internal activities. Not only did these events exercise LST personnel, processes, and tools, they also explored a wide range of possible

mission scenarios, each of which necessitated an LTP tailored to that mission profile. Doing so in the months leading up to the mission enabled the LST to build a repertoire of science targets and observation tasks to draw from, with some modification, enabling quick response to actual mission requirements. In this way, mission simulation work not only built individual and team readiness, but also built subject matter expertise and science content that could be rapidly brought to bear during the mission.

The framework the LST relied upon throughout the science planning process and into mission execution was the STM. By intentionally linking every aspect of the planning effort to the STM, the Artemis II LST established a rigorous, yet flexible, system for enabling effective decision making throughout the mission. Pre-prioritization of targets and tasks relative to the STM enabled the LST to efficiently create the final LTP in the first days after launch; empowered the Science Officers and their support staff in the SER and SMOR to respond to replanning requests, unanticipated science opportunities, and crew questions throughout the mission; and linked mission accomplishments and acquired data to objectives during and after the mission. In this way, the effort made in building and following a robust STM from the start of science planning yielded consistency and efficiency in science decision making, in addition to serving as a guide for those outside of the science team to understand science priorities and decisions.

Recommendation: Future Artemis missions should carry landing site- and/or time-agnostic science objectives, tasks, and targets, as well as those that are site- and/or time-specific, all of which are tied to an STM. This will enable efficient mission science planning when the exact mission profile may not be known until a short time before launch or until after launch.

Recommendation: Future Artemis missions should include extensive pre-mission preparation in the form of mission simulations focused on planning and doing science in the context of a wide range of plausible mission scenarios. This will best exercise the expertise, confidence, and flexibility needed in a well-prepared science team and also result in STM-responsive products that provide the science team with early progress on actual mission planning and execution.

9.6 Calibration of Cameras

Camera calibration will be essential for future missions to independently contextualize crew observations and enable quantitative analyses. Within the Artemis II mission architecture, the LST was not afforded the opportunity to select instrumentation or specify calibration needs in support of science. As discussed in **Section 3.2.2**, the cameras used during Artemis II were COTS systems with only partial pre-flight characterization, and no geometric, radiometric, or spectral calibration were completed on any of the included imaging systems.

To enable quantitative use of images in future missions, it will be important to specify the minimum required calibration level needed to support science objectives. Camera characterization and calibration are needed to understand internal parameters (e.g., sensor response) and external factors (e.g., window effects; **Section 7.2**), as both influence image quality and the interpretation of color, brightness, and shape. Additionally, the performance of manifested camera systems, including handheld, vehicle-mounted, and EVA tools, should be characterized in the unique lighting, thermal, and viewing environments in which they will be utilized.

Recommendation: Future Artemis missions should define minimum camera calibration requirements and characterize camera performance inside and outside the spacecraft to enable quantitative and independently verified crew observations.

9.7 Instrumentation for Enhanced Science Return

Artemis II highlighted several areas where dedicated science instrumentation would substantially improve the quality, interpretability, and diversity of lunar observations. Many of the lunar science objectives, particularly those associated with the characterization of impact flashes, color and albedo, photometry, dust detection, and deep-sky imaging, would have benefited from instruments specifically designed to address the unique observational challenges of cislunar space. Several illustrative examples

of instruments for enhanced science return are outlined below. Missions to the surface of the Moon may have different instrument needs based on science objectives and the nature of in situ versus remote measurements (e.g., surface missions would benefit from strategically selected handheld field instruments for crew members).

Although the crew observed and described several impact flashes during the solar eclipse, a dedicated impact-flash sensor that is capable of high-frame-rate, high-dynamic-range imaging would allow systematic monitoring of impact events, enable quantitative flash brightness measurements, improve temporal precision and location identification, and enable direct comparison with human observations.

Calibrated and more capable imaging and/or spectrometer systems would improve collection of color and albedo data. The Artemis II crew frequently described subtle color variations across the lunar surface, but camera limitations prevented quantitative characterization. A calibrated multispectral camera and/or dedicated spectrometer system(s) would provide independent measurements of spectral variations and allow direct comparison between crew perception and instrument-derived reflectance and spectral properties, strengthening scientific interpretation of surface composition and photometric behavior.

Relatedly, a physical onboard color wheel would provide the crew with a stable, standardized reference for color hue and value, improving consistency and reproducibility in real-time descriptions of lunar color and albedo. A color wheel proved to be a highly effective tool for supporting visual observations during the Apollo-Soyuz mission (El-Baz, 1977, 2011).

For investigations of the lunar dust environment, future missions would benefit from a dedicated low-light camera optimized for limb and horizon observations. Such a system would provide quantifiable measurements of extended faint sources and enable confident detection or non-detection of lofted dust.

Deep-sky imaging revealed optical constraints of general-purpose lenses. Coma and corner distortions were evident in wide-field images, which is expected for fast lenses not optimized for astronomical use. For future missions, particularly those spending longer durations in lunar orbit, a dedicated prime lens for deep-sky imaging would provide higher-quality stellar data and support investigations of zodiacal light and other faint phenomena.

As instrumentation needs will vary by science objectives and priorities, future development should be responsive to each mission profile, as well as community priorities, while maintaining compatibility with human-driven observation workflows.

Recommendation: Future Artemis missions should manifest dedicated science instruments that meaningfully support the science objectives of the mission, to include IVA instrumentation to support orbital observations similar to the Artemis II flyby observations, as well as EVA-specific instrumentation for use by astronauts on the lunar surface.

9.8 Window Design for Science Observations

For Artemis II, lunar images collected through Orion's windows were a cornerstone of the lunar science dataset. These images enabled cross-regional comparisons, supported interpretation and contextualization of the crew's verbal observations, and anchored the LST's ability to map observations to specific lunar features. These images were also affected by the vehicle window design, including window size, pane design, and optical quality, and thus window design is a critical component in enabling high-fidelity science observations.

The Artemis II window-quality DFTO results underscore the need to continue to characterize vehicle window designs. Windowpanes should be characterized individually and as an installed stack. This should be included for any updates to Orion's windows that may be implemented for future Artemis flight missions and also the windows for the Human Landing System vehicles that will deliver subsequent Artemis crews to the lunar surface. Lower quality windows and/or incomplete characterization of windows for imaging will have a detrimental effect on the science return from human observations and images, particularly regarding phenomena that Artemis II demonstrated humans are adept at observing and describing, such as impact flashes, nuanced color patterns, and regional comparisons.

Recommendation: Future Artemis missions should rigorously characterize and prioritize window optical performance of windowpanes and the assembled window stack (for Orion and Human Landing System vehicles) to maximize the quality of science return from crew observations and images.

9.9 Crew-Audio Recording Capabilities and Time Synchronization of Multi-Modal Datasets

This report highlights the importance of crew observations to the mission's science return. This highest-priority dataset was enabled on Artemis II via manual audio recordings captured by the crew on their PCDs. However, using PCDs for this critical scientific purpose introduced risks and challenges in several ways. First, the tablets were at significant risk of data loss due to radiation strikes. Without downlink capability, these critical data could have been permanently lost, as no backup solution existed. Second, each observation required the crew to manually start and stop the audio recordings on their PCDs. This added operational burden and increased the likelihood of missed activations or incomplete recordings, potentially compromising the dataset. Third, managing the PELTOR headsets, which were attached to the PCDs by lengthy cables floating in microgravity, proved cumbersome. By contrast, Apollo missions benefited from in-cabin recording devices that did not require any action from the crew. These passive audio recordings have been used for decades as an indispensable historical record of the mission, as well as a valuable scientific record (e.g., recordings of the Apollo 11 crew making lunar observations in LOS before landing).

Further related to the value of audio recordings, the LST often relied on the sounds of camera shutter clicks as a useful audio cue for aligning multi-modal crew data (i.e., images, audio files, and annotations) with science intent during Artemis II (**Section 8.1**). This in-cabin cue worked well for IVA operations, where handheld images and voice-loop recordings were collected within the same acoustic environment and could be cross-referenced by listening for shutter sounds in the audio. For future surface missions, however, this approach will not always be viable. The sound of a Nikon D5 camera shutter or the simulated shutter sound of the Nikon Z9 will not reliably propagate to microphones embedded in EVA suits. Additionally, crew members on a surface EVA will not use PCDs for real-time annotations as IVA crews do, and will instead rely more heavily on verbal communication. As a result, correlating multi-modal science observations, including images, verbal descriptions, and other data streams during EVAs, will be even more dependent on precise and consistent timestamps across all devices.

Recommendation: Subsequent Artemis missions should incorporate a passive audio-recording capability to support the collection of crew observations. A continuous, timestamped onboard audio record would also provide an independent means of establishing the timing of activities not captured by other onboard systems, substantially improving post-mission reconstruction and interpretation of the sequence of mission events. This capability would be particularly beneficial during highly dynamic science mission phases, such as the Artemis II lunar flyby. Passive audio recording would reduce crew workload by eliminating the need to manage additional hardware during high-priority and time-critical periods. Additionally, passive audio would capture valuable scientific context by recording crew perception during mission phases where opportunistic or serendipitous science data is collected. This recommendation aligns with crew feedback in the crew perspectives section (**Section 2.0**).

Recommendation: Subsequent Artemis missions should maintain coordinated and correct timestamp synchronization across all science-relevant systems, including cameras, crew suits, PCDs, voice loops, any additional manifested science payloads, and the spacecraft, to ensure accurate alignment of multi-modal datasets during orbital and surface mission phases.

10.0 CONCLUSIONS

The Artemis II mission was a crucial advancement in humanity's forward journey to the Moon, marking the first time in more than fifty years that a human crew conducted dedicated scientific observations in cislunar space. Ten lunar science themes were selected in response to community-driven science priorities and shaped by the unique constraints afforded by the Artemis II flight profile. These themes were addressed with coordinated crew activity and dedicated data collections during a several-hour lunar flyby. The crew recorded detailed verbal descriptions, executed targeted imaging, and made thoughtful annotations, capturing a scientifically rich record of lunar and terrestrial color, morphology, illumination conditions, as well as impact flashes, transient solar phenomena, and human perception in space. Together with data acquired by Orion's vehicle-mounted cameras, these observations stand as the most comprehensive human-acquired orbital dataset of the Moon since Apollo, enriching our scientific understanding of the Moon built over decades of robotic exploration.

The datasets presented in this report and in its companion documents serve not only as a legacy on Artemis II, but also as a launchpad for continued discovery. The information within these reports provides immediate opportunities for the broader science community to engage with these new observations and refine our understanding of the Moon and Solar System evolution. The findings presented here will help shape future Artemis mission architectures via recommendations related to crew training, science instrument manifests and calibration standards, window design requirements, and science operations. The LST substantiated the value of integrating lunar science into the Artemis mission operations environment, demonstrating that real-time collaborations between crew and scientists can sharpen observational intent, accelerate discovery, and elevate scientific return.

As NASA prepares for continuing the Artemis campaign and conducting the first crewed missions on the lunar surface, the achievements of Artemis II underscore how the integration of humans into exploration unlocks inspiration and scientific discovery. The LST looks forward to the insights, collaborations, and breakthroughs the community will derive from the Artemis II data, and to the expanding frontier that Artemis II has helped open for all explorers.

Copy, Moon Joy!



ACKNOWLEDGEMENTS

The lunar science of Artemis II was made possible through the dedicated efforts and close collaboration of numerous individuals and teams across and beyond NASA. The Lunar Science Team gratefully acknowledges the contributions of our partners, whose expertise and support enabled this team's scientific success, and expanded the scope of Artemis II lunar science beyond its initial objectives. In particular, our team expresses deep gratitude for our field scientists: Reid Wiseman, Victor Glover, Christina Koch, and Jeremy Hansen. The Lunar Science Team is also grateful for the broader lunar and planetary science community for defining lunar science priorities that helped guide this mission's STM, and for future analyses that will continue to advance understanding of the Moon through the Artemis II data.

Data and visualizations from the LRO Team, Lunar QuickMap (a collaboration between NASA, Intuitive Machines, and Applied Coherent Technology Corp.), and the NASA Goddard Science Visualization Studio supported LST work throughout all phases of the mission, including pre-flight planning, real-time mission operations, and post-flight analyses. We are grateful to Charles Arge, Gina DiBraccio, Aleida Higginson, and Nicholeen Viall-kepko for scientific discussions regarding solar eclipse observations. Thoughtful external reviews provided by David Bretz, Brian Day, Erica Miles, David Melenderez, Daniel Moriarty, Amanda Nahm, Elizabeth Rampe, Renee Weber, Shoshana Weider, and Michael Zanetti helped improve this report, as did copyediting, typesetting, and graphics support from Chris Fleming, Ruth Jennings, Brittany Klein, and Heather Ghannadian.

Finally, the Lunar Science Team gratefully thanks their families for their support throughout the pre-mission and mission execution phases. We couldn't have done it without your understanding and support through this incredibly busy time.

REFERENCES

Atlas, H. P. L. (2005). A Survey of the Moon's Near Side. In *The Moon and How to Observe It*. Astronomers' Observing Guides. Springer, London. https://doi.org/10.1007/1-84628-243-8_7

Bandfield, J. L., Hayne, P. O., Williams, J.-P., Greenhagen, B. T., & Paige, D. A. (2015). Lunar surface roughness derived from LRO Diviner Radiometer observations. *Icarus*, 248, 357–372. https://doi.org/10.1016/j.icarus.2014.11.009

Barker, M. K., Mazarico, E., Neumann, G. A., Zuber, M. T., Haruyama, J., & Smith, D. E. (2016). A new lunar digital elevation model from the Lunar Orbiter Laser Altimeter and SELENE Terrain Camera. *Icarus*, 273, 346–355. https://doi.org/10.1016/j.icarus.2015.07.039

Bellot Rubio, L. R., Ortiz, J. L., & Sada, P. V. (1998). Observation and interpretation of meteoroid impact flashes on the Moon. *Earth, Moon, and Planets*, 82(0), 575–598. https://doi.org/10.1023/A:1017097724416

Berg, O. E., Wolf, H., & Rhee, J. (1976). 2.2.4 Lunar Soil Movement Registered by the Apollo 17 Cosmic Dust Experiment. *International Astronomical Union Colloquium*, 31, 233–237. https://doi.org/10.1017/s0252921100051757

Binder, A. B., & Gunga, H. C. (1985). Young thrust fault scarps in the highlands: Evidence for an initially totally molten Moon. *Icarus*, 63, 421–441. https://doi.org/10.1016/0019-1035(85)90055-7

Blewett, D. T., Coman, E. I., Hawke, B. R., Gillis-Davis, J. J., Purucker, M E., & Hughes C. G. (2011). Lunar swirls: Examining crustal magnetic anomalies and space weathering trends. *Journal of Geophysical Research,* 116, E02002. https://doi.org/10.1029/2010JE003656

Blewett, D. T., Halekas, J. S., Ho, G. C., Greenhagen, B. T., Anderson, B. J., Vines, S. K., et al. (2023). PRISM-1 Lunar Vertex: Overview and Status. *AGU Fall Meeting,* P31B-05.

Boardman, J. W., Pieters, C. M., Green, R. O., Lundeen, S. R., Varanasi, P., Nettles, J., et al. (2011). Measuring moonlight: An overview of the spatial properties, lunar coverage, selenolocation, and related Level 1B products of the Moon Mineralogy Mapper. *Journal of Geophysical Research: Planets*, 116(E6). https://doi.org/10.1029/2010je003730

Byrne, C. J. (2005). Orientale Basin Region. In: *Lunar Orbiter Photographic Atlas of the Near Side of the Moon*. Springer, London. https://doi.org/10.1007/978-1-84628-154-9_5.

Byrne, C. J. (2008). The Orientale Limb Region. In: *The Far Side of the Moon*. Springer, New York, NY. https://doi.org/10.1007/978-0-387-73206-0_12.

Byron, B. D., Retherford, K. D., Greathouse, T. K., Wyrick, D., Cahill, J. T. S., Hendrix, A. R., et al. (2020). Far UV Observations of Lunar Rayed Craters with LRO-LAMP. *Journal of Geophysical Research: Planets*, 125(3). https://doi.org/10.1029/2019JE006269

Campbell, B. A. (2016). Planetary geology with imaging radar: insights from earth-based lunar studies, 2001–2015. *Publications of the Astronomical Society of the Pacific*, 128, 062001. https://doi.org/10.1088/1538-3873/128/964/062001

Carter, L. M., Neish, C. D., Bussey, D. B. J., Spudis, P. D., Patterson, G. W., Cahill, J. T., & Raney, R. K. (2012). Initial observations of lunar impact melts and ejecta flows with the Mini-RF radar. *Journal of Geophysical Research: Planets*, 117(E12). https://doi.org/10.1029/2011JE003911

Colwell, J. E., Batiste, S., Horányi, M., Robertson, S., & Sture, S. (2007). Lunar surface: Dust dynamics and regolith mechanics. *Reviews of Geophysics*, 45(2). https://doi.org/10.1029/2005rg000184

Connolly, J. F. (2006). Constellation Program Overview. https://www.lpi.usra.edu/lunar/artemis/Connolly_Constellation_Program_Overview_October%202006.pdf

Coombs, C. R., Hawke, B. R., & Allen, C. C. (2012). Aristarchus Plateau: As a Potential Lunar Base Site. *Space and Robotics*, 98, 608–615. https://doi.org/10.1061/40339(206)70

Coyan, J., Siegler, M., Marinez-Comacho, J., Beyer, R., & Shirley, M. (2025). Propsectivity Modeling of the NASA VIPER Landing Site at Mons Mouton near the Lunar South Pole. *The Planetary Science Journal*, 6(105). https://doi.org/10.3847/PSJ/adbc6c

Criswell, D. R. (1972). Lunar dust motion. *Proceedings of the Lunar Science Conference, 3,* 2671–2680.

Criswell, D. R. (1973). Horizon-glow and the motion of lunar dust. In Photon and Particle Interactions With Surfaces in Space, edited by R. J. L. Grard, pp. 545–556, Springer, New York.

Cudnik, B. (2009). Lunar Meteoroid Impacts and How to Observe Them. New York, NY: Springer, 240 pp.

Cudnik, B. (2023). Opposition Effect. In B. Cudnik (Ed.) Encyclopedia of Lunar Science (pp. 935–943). Springer Cham. https://doi.org/10.1007/978-3-319-14541-9_188

El-Baz, F. (1977). Astronaut Observations from the Apollo-Soyuz Mission (Smithsonian Studies in Air and Space, No. 1). Washington, DC: Smithsonian Institution Press/US Government Printing Office, 400 pp. http://dx.doi.org/10.5479/si.01977245.1.1

El-Baz, F. (2011). Training Apollo astronauts in lunar orbital observations and photography. In W. B. Garry & J. E. Bleacher (Eds.), *Analogs for Planetary Exploration* (GSA Special Paper 483, pp 49–66). Boulder, CO: Geological Society of America. https://doi.org/10.1130/2011.2483(04)

Fassett, C. I., Bramson, A. M., Cahill, J. T., Harris, C. P., Morgan, G. A., Neish, C. D., et al. (2024). Improved orthorectification and empirical reduction of topographic effects in monostatic Mini-RF S-band observations of the Moon. *The Planetary Science Journal*, 5(1), 4. https://doi.org/10.48732/VZJT-1634

Flahaut, J., Blanchette-Guertin, J. F., Jilly, C., Sharma, P., Souchon, A., van Westrenen, W., & Kring, D. A. (2012). Identification and characterization of science-rich landing sites for lunar lander missions using integrated remote sensing observations. *Advances in Space Research*, 50(12), 1647–1665. https://doi.org/10.1016/j.asr.2012.05.020

Gaddis, L. R., Staid, M. I., Tyburczy, J. A., Hawke, B. R., & Petro, N. E. (2003). Compositional analyses of lunar pyroclastic deposits. *Icarus*, 161, 262–280. https://doi.org/10.1016/s0019-1035(02)00036-2

Gladstone, G. R., Stern, S. A., Retherford, K. D., Black, R. K., Slater, D. C., Davis, M. W., et al. (2010). LAMP: The Lyman Alpha Mapping Project on NASA's Lunar Reconnaissance Orbiter Mission. *Space Science Reviews*, 150, 161–181. https://doi.org/10.1007/s11214-009- 9578-6

Glenar, D. A., Stubbs, T. J., Schwieterman, E. W., Robinson, T. D., & Livengood, T. A. (2019). Earthshine as an illumination source at the Moon. *Icarus*, 321, 841–856. https://doi.org/10.1016/j.icarus.2018.12.025

Glotch, T. D., Lucey, P. G., Bandfield, J. L., Greenhagen, B. T., Thomas, I. R., Elphic, R. C., et al. (2010). Highly Silicic Compositions on the Moon. *Science*, 329(5998), 1510–1513. https://doi.org/10.1126/science.1192148

Glotch, T. D., Jawin, E. R., Greenhagen, B. T., Cahill, J. T., Lawrence, D. J., Watkins, R. N., et al. (2021). The scientific value of a sustained exploration program at the Aristarchus Plateau. *The Planetary Science Journal*, 2(4), 136. https://doi.org/10.3847/PSJ/abfec6

Goode, P. R., Pallé, E., Shoumko, A., Shoumko, S., Montañes-Rodriguez, P., & Koonin, S. E. (2021). Earth's albedo 1998–2017 as measured from earthshine. *Geophysical Research Letters*, 48, e2021GL094888. https://doi.org/10.1029/2021GL094888

Goode, P. R., Pallé, E., Yurchyshyn, V., Qiu, J., Hickey, J., Montañes-Rodriguez P., et al. (2003). Sunshine, earthshine and climate change: II. Solar origins of variations in the Earth's albedo. *Journal of the Korean Astronomical Society*, 36, S83–S91.

Guest, J. E., & Fielder, G. (1968). Lunar ring structures and the nature of the maria. *Planetary and Space Sciences*, 16(5), 665–673. https://doi.org/10.1016/0032-0633(68)90105-0

Guo, D., Liu, J., Head, J. W., & Kreslavsky, M. A. (2018). Lunar Orientale impact basin secondary craters: Spatial distribution, size-frequency distribution, and estimation of fragment size. *Journal of Geophysical Research: Planets*, 123(6), 1344–1367. https://doi.org/10.1029/2017JE005446

Harr, B., Pu, B., & Jin, Q. (2024). The emission, transport, and impacts of the extreme Saharan dust storm of 2015. *Atmospheric Chemistry and Physics*, 24, 8625–8651. https://doi.org/10.5194/acp-24-8625-2024

Hartmann, W. K., & Wood, C. A. (1971). Moon: Origin and evolution of multi-ring basins. *The Moon*, 3(1), 3–78. https://doi.org/10.1007/BF00620390

Hawke, B. R., & Head, J. W. (1977). Impact melt on lunar crater rims. In *Impact and explosion cratering: Planetary and terrestrial implications*, pp. 815–841.

Head, J. W., Murchie, S., Mustard, J. F., Pieters, C. M., Neukum, G., McEwen, A., et al. (1993). Lunar impact basins: New data for the western limb and far side (Orientale and South Pole-Aitken basins) from the first Galileo flyby. *Journal of Geophysical Research: Planets*, 98, 17149–17181. https://doi.org/10.1029/93je01278

Head, J. W., Wilson, L., & Weitz, C. M. (2002). Dark ring in southwestern Orientale Basin: Origin as a single pyroclastic eruption. *Journal of Geophysical Research: Planets*, 107(E1). https://doi.org/10.1029/2000JE001438

Heiken, G., & McKay, D. (1978). Petrology of a sequence of pyroclastic rocks from the valley of Taurus-Littrow (Apollo 17 landing site). *Lunar and Planetary Science Conference,* 9, 1933–1943.

Heldmann, J. L., Colaprete, A., Deutsch, A. N., Honniball, C. I., Lemelin, M., Ennico-Smith, K., et al. (2026). The Relevance of the VIPER Mission to NASA's Artemis Human Exploration of the Moon. *The Planetary Science Journal*, 7(4), 95. https://doi.org/10.3847/PSJ/ae4232

Henderson, M. J., & Petro, N. E. (2023). Investigation of Orientale's Dark Annular Ring with Moon Mineralogy Mapper and Lunar Reconnaissance Orbiter Data. *Lunar and Planetary Science Conference,* 54, 2980.

Hiesinger, H., Head, J. W., Wolf, U., & Neukum, G. (2011). Ages and stratigraphy of lunar mare basalts: A synthesis. *Recent Advances and Current Research Issues in Lunar Stratigraphy*, eds. Ambrose, W. A., Williams, D. A. https://doi.org/10.1130/2011.2477(01)

Hiesinger, H., Head, J. W., Wolf, U., Jaumann, R., & Neukum, G. (2003). Ages and stratigraphy of mare basalts in Oceanus Procellarum, Mare Nubium, Mare Cognitum, and Mare Insularum. *Journal of Geophysical Research*, 108(E7), 5065. https://doi.org/10.1029/2002JE001985

Hood, L. L., & Schubert, G. (1980). Lunar magnetic anomalies and surface optical properties. *Science*, 208(4439), 49–51. https://doi.org/10.1126/science.208.4439.49

Hood, L. L., & Williams, C. R. (1989). The lunar swirls: Distribution and possible origins. *Proceedings Lunar and Planetary Science Conference,* 19, 99–113.

Horányi, M., Szalay, J., Kempf, S., Schmidt, J., Grün, E., Srama, R., & Sternovsky, Z. (2015). A permanent, asymmetric dust cloud around the Moon. *Nature*, 522, 324–326. https://doi.org/10.1038/nature14479

Hu, H., Zeng, X., Li, X., & Liu, J. (2025). Lunar Highland Preserves Meteoritic-iron-rich Materials in the Earth–Moon System. *The Astrophysical Journal*, 993(1), 148. https://doi.org/10.3847/1538-4357/ae08b5

Hurlbert, A., & Yu, C. (2025). Seeing the Light: Perception and Discrimination of Illumination Color. *Annual Review of Vision Science*, 11, 267–301. https://doi.org/10.1146/annurev-vision-121423-013755

Hurwitz, D. M., Head, J. W., & Hiesinger, H. (2013). Lunar sinuous rilles: Distribution, characteristics, and implications for their origin. *Planetary and Space Science*, 79–80, 1–38. https://doi.org/10.1016/j.pss.2012.10.019

Jawin, E. R., Valencia, S. N., Watkins, R. N., Crowell, J. M., Neal, C. R., & Schmidt, G. (2019). Lunar science for landed missions workshop findings report. *Earth and Space Science*, 6, 2–40. https://doi.org/10.1029/2018EA000490

Jawin, E., Glotch, T., Watkins, R., Jozwiak, L., Valencia, S., Meyer, H., et al. (2021). Exploring end-member volcanism on the Moon at the Aristarchus Plateau. *Bulletin of the American Astronomical Society,* 53(4), 204. https://doi.org/10.3847/25c2cfeb.2a3096f4

Jozwiak, L. M., Head, J. W., Zuber, M. T., Smith, D. E., & Neumann, G. A. (2012). Lunar floor-fractured craters: Classification, distribution, origin and implications for magmatism and shallow crustal structure, *Journal of Geophysical Research: Planets,* 117, E11005. https://doi.org/10.1029/2012JE004134

Kopal, Z. (1974a). Manned Exploration: Apollo (1969–1972). In *The Moon in the Post-Apollo Era* (Geophysics and Astrophysics Monographs, vol 7). Dordrecht: Springer. https://doi.org/10.1007/978-94-010-2101-2_2

Kopal, Z. (1974b). Stratigraphy and Chronology of the Lunar Surface. In *The Moon in the Post-Apollo Era* (Geophysics and Astrophysics Monographs, vol 7). Dordrecht: Springer. https://doi.org/10.1007/978-94-010-2101-2_8

Lemelin, M., Lucey, P. G., Neumann, G. A., Mazarico, E. M., Barker, M. K., Kakazu, A., et al. (2016). Improved calibration of reflectance data from the LRO Lunar Orbiter Laser Altimeter (LOLA) and implications for space weathering. *Icarus*, 273, 315–328. https://doi.org/10.1016/j.icarus.2016.02.006

Liakos, A., Bonanos, A. Z., Xilouris, E. M., Koschny, D., Bellas-Velidis, I., Boumis, P., et al. (2020). NELIOTA: Methods, statistics, and results for meteoroids impacting the Moon. *Astronomy and Astrophysics*, 633, A112. https://doi.org/10.1051/0004-6361/201936709

Liakos, A., Bonanos, A. Z., Xilouris, E. M., Koschny, D., Bellas-Velidis, I., Boumis, P., et al. (2024). NELIOTA: New results and updated statistics after 6.5 years of lunar impact flashes monitoring. *Astronomy and Astrophysics*, 687, A14. https://doi.org/10.1051/0004-6361/202449542

Lunar Exploration Analysis Group (LEAG) (2016). The Lunar Exploration Roadmap: Exploring the Moon in the 21st Century: Themes, Goals, Objectives, Investigations, and Priorities. https://www.lpi.usra.edu/ leag/roadmap/US-LER_version_1_point_3.pdf

Madiedo, J. M., Ortiz, J. L., Organero, F., Ana-Hernández, L., Fonseca, F., Morales, N., & Cabrera-Caño, J. (2015). Analysis of Moon impact flashes detected during the 2012 and 2013 Perseids. *Astronomy & Astrophysics*, 577, A118. https://doi.org/10.1051/0004-6361/201525656

Madiedo, J. M., Ortiz, J. L., Yanagisawa, M., Aceituno, J., & Aceituno, F. (2019). Impact flashes of meteoroids on the Moon. Meteoroids: *Sources of Meteors on Earth and Beyond*, 25, 136.

McBride, M. J., Horgan, B. H. N., & Gaddis, L. R. (2016). Revisiting the Mineralogy of the Aristarchus Regional Pyroclastic Deposit with New M^3 Analysis Techniques. *Lunar and Planetary Science Conference,* 47, 3052.

McCoy, J. E., & Criswell, D. R. (1974). Evidence for a high altitude distribution of lunar dust. *Lunar and Planetary Science Conference,* 5, 2991–3005.

Meyer, H. M., Denevi, B. W., Boyd, A. K., & Robinson, M. S. (2016). The distribution and origin of lunar light plains around Orientale basin. *Icarus*, 273, 135–145. https://doi.org/10.1016/j.icarus.2016.02.014

Moore, H. J. (1965). Geologic map of the Aristarchus region of the Moon. U.S. Geological Survey IMAP 465, 1 map. https://doi.org/10.3133/i465

Morgan, G. A., Jawin, E. R., Campbell, B. A., Patterson, G. W., Bramson, A. M., Nypaver, C. A., et al. (2023). Radar Perspective of the Aristarchus Pyroclastic Deposit and Implications for Future Missions. *The Planetary Science Journal,* 4(11), 209. https://doi.org/10.3847/PSJ/ad023a

Moriarty III, D. P., & Pieters, C. M. (2016). Complexities in pyroxene compositions derived from absorption band centers: Examples from Apollo samples, HED meteorites, synthetic pure pyroxenes, and remote sensing data. *Meteoritics & Planetary Science*, 51(2), 207–234. https://doi.org/10.1111/maps.12588

Morse, Z. R., Osinski, G. R., & Tornabene, L. L. (2018). New morphological mapping and interpretation of ejecta deposits from Orientale Basin on the Moon. *Icarus*, 299, 253–271. https://doi.org/10.1016/j.icarus.2017.08.010

Moser, D. E., Suggs, R. M., Kupferschmidt, L., & Feldman, J. (2015). Lunar Impact Flash Locations from NASA's Lunar Impact Monitoring Program. *NASA Technical Memorandum* NASA/TM-2015-218213, 56.

Mustard, J. F., Pieters, C. M., Isaacson, P. J., Head, J. W., Besse, S., Clark, R. N., et al. (2011). Compositional diversity and geologic insights of the Aristarchus crater from Moon Mineralogy Mapper data. *Journal of Geophysical Research: Planets,* 116, E00G12. https://doi.org/10.1029/2010JE003726

Nahm, A. L., Öhman, T., & Kring, D. A. (2013). Normal faulting origin for the Cordillera and Outer Rook Rings of Orientale Basin, the Moon. *Journal of Geophysical Research: Planets,* 118(2). https://doi.org/10.1002/jgre.20045

NASA (1969). Apollo 11 Preliminary Science Report. NASA SP-214. https://www.lpi.usra.edu/lunar/documents/NASA-SP-214.pdf.

NASA (1970). Apollo 12 Preliminary Science Report. NASA SP-235. https://www.lpi.usra.edu/lunar/documents/NASA-SP-235.pdf.

NASA (1971). Apollo 14 Preliminary Science Report. NASA SP-272. https://www.lpi.usra.edu/lunar/documents/NASA-SP-272.pdf.

NASA (1972a). Apollo 15 Preliminary Science Report. NASA SP-289. https://www.lpi.usra.edu/lunar/documents/NASA%20SP%20289.pdf.

NASA (1972b). Apollo 16 Preliminary Science Report. NASA SP-315. https://www.lpi.usra.edu/lunar/documents/NASA%20SP%20315.pdf.

NASA (1973). Apollo 17 Preliminary Science Report. NASA SP-330. https://www.lpi.usra.edu/lunar/documents/NASA%20SP%20330.pdf.

NASA (2020). Artemis III Science Definition Team Report. NASA/SP-20205009602. https://www.nasa.gov/wp-content/uploads/2015/01/artemis-iii-science-definition-report-12042020c.pdf?emrc=841cb1

NASA (2022). Moon to Mars Objectives. https://www.nasa.gov/wp-content/uploads/2022/09/m2m-objectives-exec-summary.pdf

National Academies of Sciences, Engineering, and Medicine (2022). Origins, Worlds, and Life: A Decadal Strategy for Planetary Science and Astrobiology 2023–2032. Washington, DC: The National Academies Press. https://doi.org/10.17226/26522

National Research Council (2007). The Scientific Context for Exploration of the Moon. Washington, DC: The National Academies Press. https://doi.org/10.17226/11954

Neish, C. D., Blewett, D. T., Harmon, J. K., Coman, E. I., Cahill, J. T. S., & Ernst, C. M. (2013). A comparison of rayed craters on the Moon and Mercury. *Journal of Geophysical Research: Planets,* 118(10), 2247–2261. https://doi.org/10.1002/jgre.20166

Ortiz, J. L., Aceituno, F. J., Quesada, J. A., Aceituno, J., Fernández, M., Santos-Sanz, P., et al. (2006). Detection of sporadic impact flashes on the Moon: Implications for the luminous efficiency of hypervelocity impacts and derived terrestrial impact rates. *Icarus*, 184(2), 319–326. https://doi.org/10.1016/j.icarus.2006.05.002

Ortiz, J. L., Quesada, J. A., Aceituno, J., Aceituno, F. J., & Rubio, L. B. (2002). Observation and interpretation of Leonid impact flashes on the Moon in 2001. *The Astrophysical Journal,* 576(1), 567–573. https://doi.org/10.1086/341625

Ortiz, J. L., Sada, P. V., Bellot Rubio, L. R., Aceituno, F. J., Aceituno, J., Gutierrez, P. J., & Thiele, U. (2000). Optical detection of meteoroidal impacts on the Moon. *Nature*, 405(6789), 921–923. https:// doi.org/10.1038/35016015

Patel, S., Satyakumar, A. V., El-Maarry, M. R., & Solanki, P. (2023). Compositional variations in Ohm ray crater on the farside of the Moon: Implications for mafic anomaly. *Planetary and Space Science,* 229, 105674. https://doi.org/10.1016/j.pss.2023.105674

Patterson, G. W., Stickle, A. M., Turner, F. S., Jensen, J. R., Bussey, D. B. J., Spudis, et al. (2017). Bistatic radar observations of the Moon using Mini-RF on LRO and the Arecibo Observatory. *Icarus*, 283. https://doi. org/10.1016/j.icarus.2016.05.017

Pieters, C. M. (1978). Mare basalt types on the front side of the Moon: A summary of spectral reflectance data. *Proceedings Lunar Planetary Science Conference,* 9, 2825-2849.

Powell, T. M., Horath, T., Robles, V. L., Williams, J. P., Hayne, P. O., Galliger, C. L., et al. (2023). High-resolution nighttime temperature and rock abundance mapping of the Moon using the Diviner lunar radiometer experiment with a model for topographic removal. *Journal of Geophysical Research: Planets,* 128(2). https://doi.org/10.1029/2022JE007532

Raney, R. K., Cahill, J. T., Patterson, G. W., & Bussey, D. B. J. (2012). The m-chi decomposition of hybrid dual-polarimetric radar data with application to lunar craters. *Journal of Geophysical Research: Planets,* 117(E12). https://doi.org/10.1029/2011je003986

Raney, R. K., Spudis, P. D., Bussey, B., Crusan, J., Jensen, J. R., Marinelli, W., et al. (2010). The lunar mini-RF radars: Hybrid polarimetric architecture and initial results. *Proceedings of the IEEE, 99(5)*, 808–823. https://doi.org/10.1109/jproc.2010.2084970

Rizos, J. L., Lara, L. M., Ortiz, J. L., & Madiedo, J. M. (2026). From flash to crater: Morphological and spectral analysis of the brightest lunar impact on 2013 September 11 using LRO data. *Monthly Notices of the Royal Astronomical Society*, 545(2), staf2068. https://doi.org/10.1093/mnras/staf2068

Robinson, M. S., Brylow, S. M., Tschimmel, M., Humm, D., Lawrence, S. J., Thomas, P. C., et al. (2010). Lunar Reconnaissance Orbiter Camera (LROC) Instrument Overview. *Space Science Reviews*, 150, 81–124. https://doi.org/10.1007/s11214-010-9634-2

Sato, H., Robinson, M. S., Hapke, B., Denevi, B. W., & Boyd, A. K. (2014). Resolved Hapke parameter maps of the Moon. *Journal of Geophysical Research: Planets,* 119(8), 1775–1805. https://doi.org/10.1002/2013JE004580

Schubert, G., Lingenfelter, R. E., & Peale, S. J. (1970). The Morphology, Distribution, and Origin of Lunar Sinuous Rilles. *Reviews of Geophysics and Space Physics,* 8(1), 199–224. https://doi.org/10.1029/RG008i001p00199

Schultz, P. H., & Spudis, P. D. (1978). The dark ring of Orientale: Implications for pre-basin mare volcanism and a clue to the identification of the transient cavity rim. *Proceedings Lunar Planetary Science Conference,* 9, 1033–1035. https://doi.org/10.1029/rg008i001p00199

Schultz, P. H., & Srnka, L. J. (1980). Cometary collisions on the Moon and Mercury. *Nature*, 284(5751), 22–26. https://doi.org/10.1038/284022a0

Scott, D. H., McCauley, J., & West, M. (1977). Geologic map of the west side of the Moon: U.S. Geological Survey IMAP 1034, 1 map. https://doi.org/10.3133/i1034

Sharma, H., Hedman, M. M., Wooden, D. H., Colaprete, A., & Cook, A. M. (2021). Constraining low-altitude lunar dust using the LADEE-UVS data. *Journal of Geophysical Research: Planets,* 126, e2021JE006935. https://doi.org/10.1029/2021JE006935

Sheward, D., Avdellidou, C., Cook, A., Sefton-Nash, E., Delbo, M., Cantarella, B., & Zanatta, L. (2022). PyNAPLE: Lunar surface impact crater detection. *Monthly Notices of the Royal Astronomical Society,* 514(3), 4320–4328. https://doi.org/10.1093/mnras/stac1495

Sheward, D., Delbo, M., Avdellidou, C., Cook, A., & Lognonné, P. (2025). Detection of small fresh craters on the Moon-Linking fresh craters to their lunar impact flash events. *Astronomy & Astrophysics,* 699, L3. https://doi.org/10.1051/0004-6361/202555481

Smith, D. E., Zuber, M. T., Jackson, G. B., Cavanaugh, J. F., Neumann, G. A., Riris, H., et al. (2010). The Lunar Orbiter Laser Altimeter Investigation on the Lunar Reconnaissance Orbiter Mission. *Space Science Reviews,* 150, 209–241. https://doi.org/10.1007/s11214-009-9512-y

Smith, D. E., Zuber, M. T., Neumann, G. A., Lemoine, F. G., Mazarico, E., Torrence, M. H., et al. (2010). Initial observations from the Lunar Orbiter Laser Altimeter (LOLA). *Geophysical Research Letters,* 37, L18204. https://doi.org/10.1029/2010GL043751

Speyerer, E. J., Wagner, R. V., Robinson, M. S., Licht, A., Thomas, P. C., Becker, K., et al. (2016). Pre-flight and On-orbit Geometric Calibration of the Lunar Reconnaissance Orbiter Camera. *Space Science Reviews*, 200(1), 357–392. https://doi.org/10.1007/s11214-014-0073-3

Spudis, P. D. (1993). The Geology of Multi-Ring Impact Basins: *The Moon and Other Planets*. Cambridge, UK: Cambridge University Press, 263 pp. https://doi.org/10.1017/CBO9780511564581

Stockstill, K. R., & Spudis, P. D. (1998). Geology and deposits of the Hertzsprung Basin, Lunar Far Side. *Lunar and Planetary Science Conference,* 29, 1236.

Suggs, R. M., Moser, D. E., Cooke, W. J., & Suggs, R. J. (2014). The flux of kilogram-sized meteoroids from lunar impact monitoring. *Icarus*, 238, 23–36. https://doi.org/10.1016/j.icarus.2014.04.032

Thompson, T. J., Robinson, M. S., Watters, T. R., & Johnson, M.B. (2017). Global Lunar Wrinkle Ridge Identification and Analysis. *Lunar and Planetary Science Conference*, 48, 2665.

Walker, R. (2026). Near-infrared Hapke photometric analysis of the Moon's regolith with passive radiometry from the Lunar Orbiter Laser Altimeter (LOLA) [Data set]. NASA Goddard Space Flight Center Planetary Geodesy Data Archive. https://pgda.gsfc.nasa.gov/products/93

Weitz, C. M., Head, J. W., & Pieters, C. M. (1998). Lunar regional dark mantle deposits: Geologic, multispectral, and modeling studies. *Journal of Geophysical Research: Planets,* 103, 22725–22759. https://doi.org/10.1029/98JE02027.

Whitford-Stark, J. L., & Head, J. W. (1977). The Procellarum volcanic complexes: Contrasting styles of volcanism. *Lunar and Planetary Science Conference,* 8, 2705–2724.

Whitford-Stark, J. L., & Head, J. W. (1980). Stratigraphy of Oceanus Procellarum basalts: Sources and styles of emplacement. *Journal of Geophysical Research,* 85(B11), 6579–6609. https://doi.org/10.1029/jb085ib11p06579

Whitten, J., Head, J. W., Staid, M., Pieters, C. M., Mustard, J., Clark, R., Nettles, J., Klima, R. L., & Taylor, L. (2011). Lunar mare deposits associated with the Orientale impact basin: New insights into mineralogy, history, mode of emplacement, and relation to Orientale Basin evolution from Moon Mineralogy Mapper (M3) data from Chandrayaan-1. *Journal of Geophysical Research: Planets,* 116, E00G09. https://doi.org/10.1029/2010JE003736

Wilhelms, D. E. (1970). *Summary of Lunar Stratigraphy - Telescopic observations* (Contributions to Astrogeology, US Geological Survey Professional Paper 599-F). Washington, DC: US Government Printing Office, 47 pp.

Wilhelms, D. E., McCauley, J. F., & Trask, N. J. (1987). *The Geologic History of the Moon* (US Geological Survey Professional Paper 1348). Washington, DC: US Government Printing Office, 337 pp.

Woolf, N. J., Smith, P. S., Traub, W. A., & Jucks, K. W. (2002). The Spectrum of Earthshine: A Pale Blue Dot Observed from the Ground. *The Astrophysical Journal,* 574(1), 430. https://doi.org/10.1086/340929

Xu, L., Qiao, L., Xie, M., Want, Y., Zhu, M.-H., & Yan, J. (2024). Chronology, Local Stratigraphy, and Foreign Ejecta Materials at the Chang'e-6 Landing Site: Constraints on the Provenance of Samples Returned From the Moon's Farside. *Geophysical Research Letters,* 51(24). https://doi.org/10.1029/2024GL111311

Zhu, M. H., Wünnemann, K., & Potter, R. W. (2015). Numerical modeling of the ejecta distribution and formation of the Orientale basin on the Moon. *Journal of Geophysical Research: Planets, 120(12)*, 2118–2134. https://doi.org/10.1002/2015JE004827

Zisk, S. H., Hodges, C. A., Moore, H. J., Shorthill, R. W., Thompson, T. W., Whitaker, E. A., & Wilhelms, D. E. (1977). The Aristarchus-Harbinger region of the Moon: Surface geology and history from recent remote-sensing observations. *The Moon,* 17, 59–99. https://doi.org/10.1007/BF00566853

Zook, H. A., Potter, A. E., & Cooper, B. L. (1995). The lunar dust exosphere and Clementine lunar horizon glow. *Lunar and Planetary Science Conference*, 26, 1577–1578.

APPENDIX 1: LUNAR TARGETING PLAN

The Artemis II Lunar Targeting Plan provided the timeline and science and operational objectives for the Artemis II crew to execute during the lunar flyby. The guide to the Artemis II Lunar Targeting Plan was published during the mission and a static archived version is available as part of the PDS archive:

Artemis II Lunar Science Team (2026). Artemis II Lunar Targeting Package, Planetary Data System (PDS) Geosciences (GEO) Node. https://doi.org/10.17189/fq8g-6z49

APPENDIX 2: SCIENCE DATA ARCHIVE AND ACCESS

Scientific data used in this report are archived and accessible through NASA's Planetary Data System. The archive is described in detail in the *Artemis II Lunar Science Data User Guide* that is provided as a document alongside the data:

Artemis II Lunar Science Team (2026). *Artemis II Lunar Science Data User Guide*, Planetary Data System (PDS) Geosciences (GEO) Node. https://doi.org/10.17189/dtpt-2857.

The PDS archive is organized into five separate bundles and hosted at different PDS Discipline Nodes according to their area of expertise (**Table A.1**). The PDS Geosciences (GEO) Node hosts the mission bundle of documents (including the *Artemis II OSDMP*, *Artemis II Lunar Science Data User Guide*, static LTP, and OTR database) and Orion environment data (data logger temperature and humidity data), the Cartography and Imaging Sciences (CIS) Node hosts crew handheld camera and Orion camera image and audio bundles, and the Navigation and Ancillary Information Facility (NAIF) Node hosts the SPICE kernels bundle with spacecraft and instrument navigation and ancillary information (e.g., trajectory, attitude, etc.). Each node provides public access to the data via its website and the main PDS website provides a search function across all of PDS. **Table A.1** lists the URLs for the main PDS search function and for the specific websites for each bundle at the various PDS nodes. Also included are recommended citations and DOIs to the data bundles.

Table A.1: PDS Archives. Archive URLs and citations for the PDS-wide search and for individual PDS Nodes.

PDS Archive Bundle	URL and Citation	PDS Node
PDS-Wide Data Search	https://pds.nasa.gov/datasearch/data-search/	–
Links to All Bundles (Artemis II PDS data homepage at GEO Node with links to bundles at other PDS Nodes)	https://pds-geosciences.wustl.edu/missions/artemis2/index.htm	GEO
Crew Camera (Nikon camera images)	https://pds-imaging.jpl.nasa.gov/tools/atlas/archive-explorer?mission=artemis2&bundle=artemis2_crew_camera **Citation:** Artemis II Lunar Science Team (2026). Artemis II Crew Camera Data Bundle, Planetary Data System (PDS) Cartography and Imaging Sciences (CIS) Node. https://doi.org/10.17189/x52v-tb80	CIS
Orion Camera (Orion vehicle camera images and video)	https://pds-imaging.jpl.nasa.gov/tools/atlas/archive-explorer?mission=artemis2&bundle=artemis2_orion_camera **Citation:** Artemis II Lunar Science Team (2026). Artemis II Orion Camera Data Bundle, Planetary Data System (PDS) Cartography and Imaging Sciences (CIS) Node. https://doi.org/10.17189/hzev-nq50	CIS
Mission Audio (PCD and voice loop audio and transcripts)	https://pds-imaging.jpl.nasa.gov/tools/atlas/archive-explorer?mission=artemis2&bundle=artemis2_mission_audio Citation: Artemis II Lunar Science Team (2026). Artemis II Mission Audio Data Bundle, Planetary Daya System (PDS) Cartography and Imaging Sciences (CIS) Node. https://doi.org/10.17189/4a29-dz64	CIS
Mission (Lunar Science Data User Guide, OSDMP, LTP, OTR database, and temperature/ humidity data)	https://pds-geosciences.wustl.edu/artemis2/urn-nasa-pds-artemis2_mission/ **Citation:** Artemis II Lunar Science Team (2026). Artemis II Mission Audio Data Bundle, Planetary Data System (PDS) Geosciences (GEO) Node. https://doi.org/10.17189/36fx-pd80	GEO
SPICE (Orion trajectory and other ancillary data)	https://naif.jpl.nasa.gov/pub/naif/pds/pds4/artemis2/artemis2_spice/	NAIF

APPENDIX 3: ABBREVIATIONS

Abbreviation	Definition	Description
3D	3-Dimensional	Having three spatial dimensions.
ALPO	Association of Lunar and Planetary Observers	International organization of amateur and professional astronomers.
BPS	Biological and Physical Sciences	NASA's Division of Biological and Physical Sciences uses the spaceflight environment to study phenomena in ways that cannot be done on Earth.
Cab Cam #	Cabin camera #	Interior vehicle-mounted camera bundle. GoPros were used for Artemis II.
CBOE	Coherent Backscatter Opposition Effect	A sudden surge in brightness when a rough surface or celestial body is illuminated from directly behind the observer (at a zero phase angle).
CIS	Cartography and Imaging Sciences	PDS Node for archiving digital image and cartographic data.
CLPS	Commercial Lunar Payload Services	NASA's acquisition of lunar delivery services from commercial vendors.
CMA Camera	Crew module adaptor camera	Vehicle-mounted camera.
ConOps	Concept of operations	Mission execution plan and operational workflow.
CMOS	Complementary metal-oxide-semiconductor	Light-sensing chip used in digital imaging.
COTS	Commercial off the shelf	Ready-made commercial products for mission use.
CRaTER	Cosmic Ray Telescope for the Effects of Radiation	A scientific instrument measuring space radiation aboard NASA's Lunar Reconnaissance Orbiter mission.
CSV	Comma-Separated Values format	A plain-text file that stores tabular data.
DEM(s)	Digital elevation model(s)	Elevation model representing surface topography.
DFTO	Developmental flight test objective	A structured in-mission datacollection activity designed to evaluate and characterize system performance.
DN	Digital number	Raw pixel value in digital imagery.
DNG	Digital Negative Format	An open source, lossless, well-defined camera RAW data container.
DSCOVR	Deep Space Climate Observatory	A joint NOAA, NASA, and U.S. Air Force satellite that monitors real-time solar wind and provides early warnings for geomagnetic storms.
DSCOVR EPIC	Deep Space Climate Observatory Earth Polychromatic Imaging Camera	Earth-observing camera on DSCOVR spacecraft.
DSLR camera	Digital single lens reflex camera	Digital camera with interchangeable lenses.
EPIC	Earth Polychromatic Imaging Camera	A 10-channel spectroradiometer (317–780 nm) aboard NOAA's DSCOVR spacecraft.
EVAs	Extravehicular activities	Astronaut activity outside spacecraft.
FB	Forward bay	Front compartment of a vehicle.
FCT	Flight Control Team	Ground-based engineers and specialists who monitor and manage space missions in real time from the MCC.

Abbreviation	Definition	Description
FOD	Flight Operations Directorate	NASA organization responsible for training, planning, directing, and executing all human spaceflight mission operations.
FOV	Field of view	Camera or sensor's visible area.
FX	Full frame	Camera sensor format.
GEO	Geosciences	PDS Node for archiving digital data related to the study of the surfaces and interiors of terrestrial planetary bodies.
GEODES	Geophysical Exploration of the Dynamics and Evolution of the Solar System	A NASA SSERVI research team that uses multidisciplinary geophysics to study the Moon, near-Earth asteroids, Phobos, and Deimos.
GN&C	Guidance Navigation and Control	Orion subsystem and flight control discipline responsible for vehicle attitude, navigation, and trajectory. Staffed at MCC as a GNC flight control position.
HDR	High Dynamic Range	Combined exposures for high-contrast imaging.
HHP Cam #	Human and Health Performance camera #	A camera system used for documenting human-performance-related observations during the mission.
HPD	Heliophysics Division	The Science Mission Directorate Heliophysics Division studies the nature of the Sun and how it influences the very nature of space and the planets and the technology that exists there.
HRP	Human Research Program	HRP uses research to develop methods to protect the health and performance of astronauts in space.
HSMD	Human Spaceflight Mission Directive	The Human Spaceflight Mission Directorate leads NASA's human spaceflight and space-enabling activities across low Earth orbit, the Moon, and beyond.
HULC	Handheld universal lunar camera	A modified Nikon Z9 designed for handheld lunar imaging during Artemis missions, including future EVA use.
INCO	Integrated Communications Officer	Flight controller position responsible for all data, voice, and video communications systems, including monitoring the configuration of in-flight communications and instrumentation systems.
IOT	Imagery Operations Team	Team responsible for image acquisition planning and analysis in support of NASA and commercial space programs.
ISAG	Image Science and Analysis Group	Team dedicated to image acquisition planning and analysis in support of NASA and Commercial Space Programs.
ISO	International Organization for Standardization	Camera setting that controls the sensitivity of the image sensor to light.
IVA	IntraVehicular Activity	Astronaut activity inside spacecraft.
JPEG	Joint Photographic Experts Group	Digital image format.
LADEE	Lunar Atmosphere and Dust Environment Explorer	NASA lunar exploration and technology demonstration mission studying the lunar exosphere and dust in the Moon's vicinity.
LAMP	Lyman Alpha Mapping Project	Instrument onboard NASA's LRO spacecraft.
LED	Light-Emitting Diode	Semiconductor device that emits light when an electric current passes through it.

Abbreviation	Definition	Description
LEG	Live encounters guide	Component to build LTP.
LET	Linear Energy Transfer	The average amount of energy that ionizing radiation deposits or transfers to a material or medium per unit of path length.
LEAM	Lunar Ejecta and Meteorites Experiment	A lunar science experiment that flew to the Moon aboard Apollo 17 in 1972 and collected information on dust particles produced by meteoroid impacts on the lunar surface.
LGR	Lunar geography review	Tool to support crew study of lunar landmarks.
LIF database	Lunar Impact Flash Database	An international repository tracking brief flashes of light produced when high-speed meteoroids strike the surface of the Moon.
LOLA	Lunar Orbiter Laser Altimeter	Instrument onboard NASA's LRO spacecraft.
LOS	Loss of signal	The period when communications between Orion and ground control are interrupted.
LRO	Lunar Reconnaissance Orbiter	NASA mission mapping the Moon's surface.
LROC	Lunar Reconnaissance Orbiter Camera	Camera system onboard NASA's LRO spacecraft.
LST	Lunar science team	Artemis II science team.
LTP	Lunar targeting plan	Trajectory-specific science observation plan executed by the Artemis II crew during the lunar flyby.
M^3	Moon Mineralogy Mapper	Multispectral imager flown on India's Chandrayaan-1 mission.
M4A	MPEG-4 Audio	An audio-only file format.
MCC	Mission Control Center	The primary ground facility located at NASA's Johnson Space Center managing human spaceflight missions.
MEO	Meteoroid Environment Office	NASA organization responsible for meteoroid environments pertaining to spacecraft engineering and operations.
MODIS	Moderate Resolution Imaging Spectroradiometer	Instruments on Earth satellites Terra and Aqua.
MXF	Material eXchange Format	A container format for professional digital video, audio, and rich metadata.
NAC	Narrow Angle Camera	Camera part of the LROC imaging system onboard NASA's LRO spacecraft.
NAIF	Navigation and Ancillary Information Facility	PDS Node for archiving SPICE ancillary data.
NEF	Nikon Electronic Format	Proprietary RAW image file format used exclusively by Nikon digital cameras.
NOAA-20	National Oceanic and Atmospheric Administration-20	Earth-observing spacecraft, part of the Joint Polar Satellite System.
O/E	Orion to Earth	Voice loop between Orion and Houston Mission Control.
OESC	Orion Electronic Still Camera group	A dedicated mission support team and workstation position at NASA's Johnson Space Center responsible for managing, processing, and distributing downlinked photographic imagery during crewed Orion/Artemis spaceflights.
OpNav	Optical navigation	Backup, autonomous navigation system on Orion.

Abbreviation	Definition	Description
OTR	Outgoing target request	Database of target information for inclusion into the LTP.
PCD	Portable computing device	Handheld tablet computer which crew members viewed the LGR and LTP
PDF	Portable Document Format	A universal file format to exchange documents.
PDS	Planetary Data System	NASA's long-term archive for planetary science data.
PNG	Portable Network Graphics	Digital image format.
RAW	Raw (not an acronym, but capitalized in practice)	Descriptor of unprocessed and uncompressed data file.
RGB	Red, Green, Blue	Color mode/model.
SAW	Solar Array Wing	Exterior wing of Orion.
SAW Cam #	Solar Array Wing Camera #	Exterior Orion camera bundle mounted on the vehicle's solar array wings. GoPros were used for Artemis II.
SCAN	Space Communication and Navigation	Program that operates and manages the communications and navigation systems that are critical to every NASA mission.
SER	Science Evaluation Room	Primary backroom for Artemis lunar science and geology; supports the Science Officer.
SHECB	Science in Human Exploration Control Board	NASA board that provides science oversight and guidance for human exploration missions.
SHOE	Shadow Hiding Opposition Effect	Sudden increase in brightness of a rough or particulate surface when a light source shines directly from behind the observer.
SitRep(s)	Situation report(s)	Crew members provided situation reports to the Science Officer during the flyby when not actively observing.
SLS	Space Launch System	Artemis rocket which launches Orion spacecraft.
SMD	Science Mission Directorate	NASA's organizational unit responsible for directing and overseeing space research programs.
SMOR	Science Mission Operations Room	Dedicated support room for the SER and Science Officer, responsible for data analysis.
SOHO	Solar and Heliospheric Observatory	ESA/NASA observatory to study the Sun.
SPICE	Spacecraft, Planet, Instrument, C-matrix, Events	Observation geometry information system to assist in planning and interpreting observations from space-based instruments.
SRAG	Space Radiation Analysis Group	The Space Radiation Analysis Group is responsible for ensuring that the radiation exposure received by astronauts remains below established safety limits.
SSERVI	Solar System Exploration Research Virtual Institute	A tabular tool used to map mission science goals.
STM	Science Traceability Matrix	A tabular tool used to map mission science goals.
SWPC	NOAA's Space Weather Prediction Center	A laboratory that continually monitors and forecasts Earth's space environment, providing solar-terrestrial information.

Abbreviation	Definition	Description
THEMIS-ARTEMIS	Time History of Events and Macroscale Interactions during Substorms - Acceleration, Reconnection, Turbulence and Electrodynamics of Moon's Interaction with the Sun	NASA mission to measure plasma and fields.
TIFF	Tagged Image File Format	Digital image format.
TLI	Translunar injection	Burn to send Orion out of Earth orbit and on a trajectory toward the Moon.
UNITE	Unistellar Network Investigating TESS Exoplanets	NASA citizen science initiative partnered with the SETI Institute that engages amateur astronomers to observe and characterize exoplanet candidates discovered by NASA's Transiting Exoplanet Survey Satellite (TESS).
UTC	Coordinated Universal Time	Time zone used on Orion during mission.
VIIRS	Visible Infrared Imaging Radiometer Suite	Satellite imager for Earth observations onboard NOAA-20.
VIPER	Volatiles Investigating Polar Exploration Rover	NASA landed mission to explore lunar polar volatiles.
WAC	Wide Angle Camera	Camera part of the LROC imaging system onboard NASA's LRO spacecraft.
WAV	Waveform Audio File Format	A standard digital audio file format.
WMO	World Meteorological Organization	A specialized agency of the United Nations whose mandate covers weather, climate and water resources.

National Aeronautics and Space Administration

Goddard Space Flight Center
8800 Greenbelt Road
Greenbelt, MD 20771
https://www.nasa.gov/goddard/

https://www.nasa.gov/

NP-2026-9-641-GSFC